Multi-UAV Operations

Final Report

4005023 E. den Boer
4080610 J.T. Booms
4148649 H.J.A. Engwerda
4023706 A.P. Feenstra
4080602 C.R. Fonville
4017242 L.R.J. Hellenthal
4002571 R.H. Lenssen
4154843 R.C. van 't Veld
1507974 S. Verbist
4140192 J.J. Vroom

Delft University of Technology

Delft University of Technology

Challenge the future

Document History

Version	Changes Made	Date Published
1.0	Created Document	2014-06-22, 01:16
1.1	Added content	2014-06-22, 12:18
1.2	Added content, first review processed	2014-06-23, 22:20
1.3	Added content, second review processed, fixed broken references	2014-06-24, 17:15
2.0	Added content, new report structure, reference fixes, review processed, front-page picture added	2014-06-27, 12:00
2.1	Content review, added list of figures and list of tables, rewrote summary and conclusion, added content	2014-06-27, 21:15
2.2	Content & spelling review, reordered front matter	2014-07-01, 09:20
2.3	Content & spelling review, new cover image, compliance matrix added, minor tweaks	2014-07-01, 16:00
2.4	Minor tweaks	2014-07-01, 16:30

Preface

This report presents the final design of the Soteria unmanned aerial vehicle (UAV) system. Ten students of the Faculty of Aerospace Engineering of the Delft University of Technology (TU Delft) present the results obtained during the design synthesis exercise (DSE) of the final semester of the 2014 academic year. This report is the result of a ten week project in which a UAV was designed to aid in search and rescue (SAR). It will prove itself by winning the international micro aerial vehicle (IMAV) 2014 competition.

Readers who are particularly interested in the project analysis or the selection of a mission scenario can find this information in Chapters 2 and 3 respectively. The payload and propulsion & airframe subsystems are described in Chapters 4 and 5 respectively. Chapter 6 describes the integration of the subsystems in a UAV. In Chapter 7, the characteristics of the final design are analysed. The post-DSE development can be found in Chapter 8.

We would like to express our gratitude to our tutor Ir. C. de Wagter and our coaches Ir. D.B. Deutz and Ir. J. Chu for attending our weekly meetings and for their valuable advice throughout this project. Furthermore, we would like to thank Dr. Ir. G.C.H.E. de Croon, Ir. E.J. van der Horst, L.N.C. Sikkel MSc and the other staff of the Micro Aerial Vehicle Laboratory (MAVLab) for their support and advice. Last we would like to thank the TU Delft and specifically everyone involved with the DSE for providing the logistics and frame within which the Soteria UAV system could be designed. Looking forward, we appreciate the facilities and support as we build the system for the IMAV competition in August.

Contents

List of Figures

List of Tables

Summary

Natural disasters can strike at any time and place. Due to their sudden nature, they often catch local residents unaware, resulting in casualties and extensive damage to the area. In the ensuing chaos, it is often difficult for search and rescue (SAR) teams to coordinate the relief effort and reach survivors quickly. The international micro aerial vehicle (IMAV) Conference and Competition, an annual event taking place in the Netherlands in August 2014, is a combination of a scientific conference with a competition for micro aerial vehicles (MAVs). Competitors are given the opportunity to put their MAVs to the test by completing competition mission objectives to score points. The competition is designed to simulate a SAR mission. For example, unmanned aerial vehicles (UAVs) can score points by identifying human-shaped cardboards as 'survivors', or by creating a photomap of the competition area in less than 40 minutes.

The goal of Design Synthesis Exercise project group 22, was to design a multi-UAV system with autonomous capabilities, which will prove itself to be useful in disaster scenarios in urban areas by winning the IMAV 2014 competition with a budget of €5000. In order to accomplish this task, the project group assessed the time available to complete the design and organised the group as effectively as possible. After the human resource distribution, the strategy to accomplish the task was determined. To optimise the points that the system will score during the competition, the group analysed the individual mission scenarios and identified the ideal combination. Afterwards, the group designed a system of autonomous UAVs to perform this chosen mission strategy. The system is called Soteria, after the ancient Greek goddess of safety. It consists of four UAVs and two computers, together forming the ground station. The UAVs are designed to fly autonomously during its mission; the navigation module consists of an autopilot, a GPS receiver, a nine degree-of-freedom inertial measurement unit (IMU) and a barometer.

It was determined that the best mission strategy consists of taking off from the local command centre (LCC), creating a photomap, identifying blockades on the roads, recognising house numbers, landing on a flat rooftop and finally performing a precision landing at the LCC. After a risk assessment of the various mission elements, it was found that identifying house numbers and landing on a flat rooftop are high risk elements and could possibly result in loss of UAVs due to the increased likelihood of collisions with the environment. Since creating the photomap is done from high altitude, where the UAV environment is free of any obstacles, it was decided to perform this mission first, land in the landing zone, and then proceed to perform the house number inspection and roof landing. After the first landing, the SD card used to store the photographs is removed and inserted into the ground station. The photos are then stitched into one large map of the entire area. The ground station incorporates software that will search the stitched photomap for blockades and mark its findings on the map. Each UAV can attempt a precision landing twice, which is beneficial since a more accurate landing increases the number of points scored for this mission element.

The final design is a three-armed hexacopter, a so-called Y6 configuration. The arms of the UAV are made of carbon fibre, the landing struts and the frame supporting the payload are composed of 3D printed material. The connection between the arms and the payload frame is made of rubber. The payload of the finished UAV will consist of ultrasonic range finders to determine the distance from the UAV to obstacles and the ground. Also among the payload is are one low- and one high-resolution camera. The prior is used for identification of the house numbers, while the latter is used for the photomapping. Along with the SD card it will be removed after the first landing. The decrease in weight will enhance the endurance of the UAVs. The high-resolution camera is stabilised by mounting it on a gimbal. The rangefinder and battery packs are also mounted on the gimbal.

The required sustainability posed an additional problem. Considering the chaos in areas afflicted by natural disasters and the time constraints on SAR missions, there will be no time to search for lost UAVs. Therefore, they are designed to affect the environment as little as possible, so that recovering them in case of a loss can easily be left for a later time.

With the design of the system tailored to scoring the maximum number of points and with the mission strategy of attempting to secure points by performing the safest and most valuable missions first, the task of winning the competition could realistically be achieved.

List of Deliverables

No.	Deliverable	Page
1	DSE work-flow diagrams	MTR*
2	DSE work break-down structure	MTR*
3	DSE Gantt chart	MTR*
4	DSE team organization/organogram & HR allocation	4
5	Functional flow diagram(s)	77
6	Functional breakdown	77
7	Requirements discovery tree	MTR*
8	Resource allocation/Budget breakdown	5
9	Technical risk assessment/risk map	15
10	Design option structuring (tree)	MTR*, 25 , 54
11	Contingency management	5
12	Market analysis	109
13	Interface definition/N^2-charts	MTR*
14	Trade-off method, rationale and organization	14
15	Trade-off criteria	14
16	Criteria weight factors	20
17	Trade-off summary table	21
18	Operations and logistic concept description	117
19	Project design & development logic	112
20	Project Gantt chart	118
21	Cost break-down structure	91
22	H/W, S/W block diagrams (interactions, flows)	84
23	Electrical block diagram	85
24	Data handling block diagram	84
25	Sustainable development strategy	106
26	Compliance matrix	92
27	Sensitivity analysis	107
28	Verification & Validation procedures	Discussed throughout the report
29	Communication flow diagram	84
30	Manufacturing, Assembly, Integration plan (Production plan)	113
32	Reliability, Availability, Maintainability, and Safety (RAMS) characteristics	104
33	Performance analysis	100
34	Configuration/Layout (internal/external)	75
36	Aircraft system characteristics	97
37	Aerodynamic characteristics estimate	99
38	Structural characteristics	102
39	Stability and control characteristics	99
40	Material characteristics	71

*MTR: Mid-term report [1]

Glossary

AC alternating current
AHP analytical hierarchy process

BJT bipolar junction transistor

CAD computer-aided design
CEP circular error probable
COG center of gravity
CTOL conventional take-off and landing

DC direct current
DEM digital elevation model
DOT design option tree
DSE design synthesis exercise

EM electro-magnetic
ESC electronic speed controller

FBS functional breakdown structure
FEM finite element method
FFD functional flow diagram
FTDI Future Technology Devices International

GNSS global navigation satellite system
GPIO general-purpose input/output
GPS global positioning system

HITL hardware-in-the-loop
HWBD hardware block diagram

IMAV international micro aerial vehicle
IMU inertial measurement unit

LCC local command centre

MAV micro aerial vehicle
MAVLab Micro Aerial Vehicle Laboratory
MMOI mass moment of inertia
MNS mission need statement
MTR mid-term report

PLA polylactic acid
POS project objective statement
PWM pulse width modulation

RNMI Royal Netherlands Meteorological Institute
RPM revolutions per minute
RPS revolutions per second

SAR search and rescue
SLAM simultaneous localisation and mapping
SWBD software block diagram

TU Delft Delft University of Technology

UART universal asynchronous receiver/transmitter
UAV unmanned aerial vehicle

VTOL vertical take-off and landing

XML extensible markup language

Nomenclature

a	Acceleration [$\frac{m}{s^2}$]
A	Aspect Ratio [$-$]
A_n	Autonomy level [$-$]
b	Wingspan [m]
C_D	Drag coefficient [$-$]
C_L	Lift coefficient [$-$]
C_P	Power coefficient [$-$]
C_T	Thrust coefficient [$-$]
C_v	Prismatic coefficient [$-$]
D	Drag force [N]
D_p	Propeller diameter [m]
F	Force [N]
$F_{airship}$	Airship slenderness ratio [$-$]
$F_{horizontal}$	Horizontal component of thrust [N]
$F_{vertical}$	Vertical component of thrust [N]
I	Area moment of inertia [mm^4]
L	Lift force[N]
L_n	Largest dimension of UAV [cm]
L_{max}	Length scale for point multiplier [cm]
$L_{airship}$	Length of airship [m]
M	Moment [$N \cdot m$]
M_n	Points associated for mission n [$-$]
n	Propeller rotational speed [RPS]
P	Power [W]
P_{UAV}	Total score per UAV [$-$]
S	Surface area [m^2]
t	Time [s]
T	Thrust force [N]
T_i	Thrust delivered by the ith thruster [N]
T_{max}	Maximum thrust [N]
V	Airspeed [$\frac{m}{s}$]
V_{helium}	Volume of helium [m^3]
α	Angle of attack [°]
Δ_i	Distance between thruster and centre of gravity [m]
ρ	Air density [$\frac{kg}{m^3}$]
θ	Pitch angle [°]

1

Introduction

Natural disasters can strike at any time and place. Due to their sudden nature, they often catch local residents unaware, resulting in casualties and extensive damage to the area. In the ensuing chaos, it is often difficult for search and rescue (SAR) teams to coordinate the relief effort and reach survivors quickly. This leads to the mission need statement (MNS) for this project:

To improve SAR capabilities in the topics of surveillance and recognition in urban areas.

A project objective statement (POS) can be derived from this MNS, that will describe the desired result of this project. It is based on the international micro aerial vehicle (IMAV) 2014 competition. This competition simulates a village in the aftermath of a natural disaster. It is set in a military training village in the Netherlands and challenges competing teams to perform tasks that are common in SAR missions by designing an unmanned aerial vehicle (UAV) system. It is tailored for participation with multiple UAVs, leading to the following POS:

With ten students in ten weeks, design a multi-UAV system with autonomous capabilities, which will prove itself to be useful in disaster scenarios in urban areas by winning the IMAV 2014 competition with a budget of €5000.

The purpose of this report is to present the design process that has eventually led to the final system. The system is called Soteria, after the ancient Greek goddess of safety, since its primary mission boils down to saving lives and generally increasing the safety of victims of natural disasters. The report will describe the process that was used to find a viable conceptual design, which was then optimised through several iterations. Soteria consists of a ground and an aerial segment, with the latter comprised of four UAVs.

1.1. Description of the IMAV Competition

The system shall be used to explore a designated target area during the IMAV 2014 competition, starting at the local command centre (LCC). The competition consists of ten mission elements in four geographic areas, which are depicted in Figure 1.1 [2]. Table 1.1 contains a list of all mission elements, to give the reader an idea of the challenges presented by the competition. It also mentions in which part of the competition area the mission element needs to be performed.

Note that not all mission elements have to be performed, teams are allowed to pick and choose which ones

Table 1.1: Overview of all mission elements and the zone in which they are carried out [2].

Mission element	Description	Zone
1	Take off from ground station position	LCC
2	Create a photomap of the competition area	Zone A
3	Indicate roadblocks on a map	Zone A
4	Perform a quick inspection of house numbers in a specified area	Zone B
5	Scan the rooms in houses for survivors	Zone B
6	Create an overview of the rooms in a building	Zone C
7	Identify items in the rooms of that building	Zone C
8	Land on top of a building with a flat roof	Zone D
9	Read the numbers on a panel across the street from the landing site	Zone D
10	Perform a precision landing	LCC

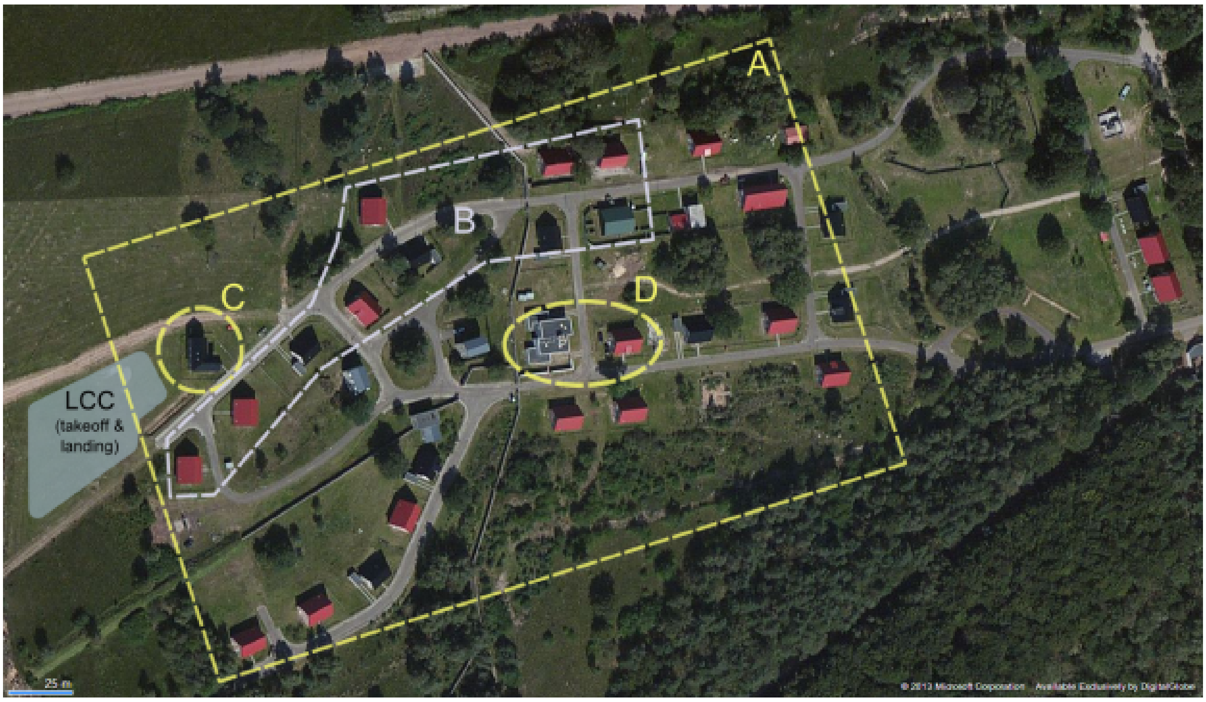

Figure 1.1: Overview of the IMAV 2014 competition area and competition zones [2]

they wish to perform. Any mission element can be performed by multiple UAVs to increase the overall score [2].

1.2. Design Requirements

A requirement analysis of each of the mission elements and stakeholder demands has yielded an extensive list of requirements [3]. Seven top level requirements were identified from the POS and are printed below. If they are not met, the project will be considered unsuccessful. From each top level requirement, more specific requirements were deduced that were used in the design phase. The requirements were all given an identifier that indicates from which top level requirement they are derived.

- The system shall win the IMAV 2014 competition. [*IMAV-CR*] [2]
- The system shall comply with the safety rules and the requirements of the IMAV 2014 competition set by its organisation. [*IMAV-SR*] [4]
- The total cost for production of the system shall not exceed €5,000. [*IMAV-CO*] [5]
- The system shall comprise at least two UAVs. [*IMAV-MU*] [6]
- The design of the system shall be completed within 10 weeks with 10 students. [*IMAV-TU*] [6]
- The system shall demonstrate autonomy. [*IMAV-AU*] [3]
- The system shall be functional in disaster scenarios in urban areas. [*IMAV-SAR*] [3]

The requirements that stem from the safety regulations stipulated by IMAV were found early on in the process, and are listed in Section 6.7. They are not discussed in detail here, but are explained in the baseline report [3]. The design requirements are also listed in Section 6.7. Furthermore, they are introduced as they become relevant throughout the report. Since there is no clear mission scenario, this needs to be defined before the actual design can commence. However, it is important to distinguish between several similar terms that have different meanings. A mission element exclusively refers to the assignments listed in Table 1.1. A mission concept is any generic combination of mission elements. For example, performing mission elements 1, 4, 5 and 10 is a mission concept. There are a total of 2047 possible mission concepts. In Chapter 3, an analysis of all these mission concepts is made, and the best concept is selected. It then becomes the mission scenario, and it specifies exactly what the system shall accomplish.

1.3. REPORT OUTLINE

First, the project management is presented in Chapter 2, detailing the distribution of human, financial and technical resources. A contingency plan is drawn up to cope with potential discrepancies between planned and actual resource distribution. Without these foundations, the work will not be done effectively. After that, Chapter 3 explains the trade-off process used to determine the mission scenario in more detail. The criteria for the trade-off and methods used to arrive at the decision are explained. As explained earlier, a mission scenario needs to be defined before the design process can be initiated. Knowing the mission, the design of the payload will be presented per subsystem in Chapter 4. This yields requirements for the structural components and propulsion system of each UAV, so the design of these is considered next. Chapter 5 lays out the iterative process used to design the propulsion, power supply and airframe subsystems. Subsequently, the interfaces and interactions between the many subsystems are considered in Chapter 6, which deals with the integration of all subsystems into one unit. With the complete system known, its characteristics can be determined, which is done in Chapter 7. More specifically, areas such as performance, materials and structures are discussed to find the limits and capabilities of the system. Chapter 7 also contains sustainability considerations, a market analysis and a sensitivity analysis. The design synthesis exercise (DSE) ends here, as it focuses solely on the design of the system. The actual construction of the system is planned in Chapter 8. This covers both the period leading up to the competition, as well as potential continued development following IMAV 2014. It also features recommendations for future research and testing. Lastly, Chapter 9 provides a conclusion of the report.

2

Project Management

A solid project management is vital in order to complete the project with ten students within ten weeks, as stated in the project objective statement (POS) and requirement *IMAV-TU*. This management will ensure that all resources available are utilised in an optimal fashion. To achieve this, first the team organisation is discussed in Section 2.1. Second, the main project tool used for scheduling, Scrum, which will ensure optimal time planning, is introduced in Section 2.2. Third, by means of self reflection the team constantly tries to improve its efficiency, two events are reviewed and discussed in Section 2.3. Besides human and time resources the project is also bound by other resources. These will be discussed in Section 2.4. This chapter is concluded in Section 2.5.

2.1. Team Organisation

This section describes the team structure and functions used within the team. The team works with a hierarchical structure with a single chairman on top. Every Monday morning the chairman begins the week with a meeting. During this phase of the project the technical manager makes sure an optimal design is reached between all disciplines. The group is divided in a payload and a propulsion group, with both a manager on top. In order to streamline external communication, a single person is chosen for contact with external parties: the external communications officer. The secretary creates minutes of every meeting which are documented for future reading and shared with interested parties. This helps to understand quick decisions taken during meetings and creates involvement and in-depth knowledge of the project for those that read the minutes.

Although the entire team knows the main aspects of every subject, the experts have more in-depth knowledge about specific sub-systems. The technical manager assures quality while the chairman is responsible for the design being finished in time. Finally, the reporting officer creates a platform for documentation. For a more detailed analysis of who wrote what, Appendix B shows a logbook of which team member wrote which part.

2.2. Project Management Tool: Scrum

The 'Scrum' principle creates an overview of what needs to be done and when it is due, thereby optimising the scheduling of tasks [7]. The overview shows what the deliverables are, when they should be finished, who the problem owner is and what the current status is of the deliverables. This is visualised by yellow post-its that can be placed in the following columns: to do, busy, content review, text review and done, shown in Figure 2.1.

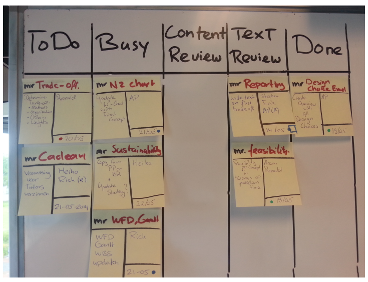

Figure 2.1: Visualisation of the Scrum principle used in the planning for the Multi-UAV Operations project.

Optimisation of scheduling skills is achieved by arranging multiple meetings. Every Monday the schedule is discussed for that specific week, every working day this schedule is checked and resources are redistributed if necessary. Every Friday, the schedule for that week is reviewed and the schedule for the rest of the project gets adapted according to this review.

2.3. Team Optimisation

In order to keep the efficiency of the entire group at a high level, constant evaluation is performed within the group. Besides using the Scrum tool for this evaluation, two other events are highlighted within this section.

As part of the design synthesis exercise (DSE), an on-line peer review has to be filled in [6]. The team decided together that, in order to stimulate personal growth as well as efficiency at group level, an open peer evaluation should be conducted before the official review. First, the team members were asked to write down positive points and points of improvement reflecting on their own work and personality. This personal feedback was reflected upon with the entire group, with the goal of helping the individual create a better understanding of himself.

Secondly, the group process was reviewed. Here, the goal was to find improvements for the current system. The main outcome showed the need for more involvement of the entire group in creating the schedule. This was requested to create a better understanding of the goal and the reason behind certain tasks that needed to be accomplished. This involvement is enlarged by letting the individual team members determine the necessary steps in order to achieve a final goal indicated on yellow post-its.

Before this evaluation, the Scrum system was only updated by the project managers responsible for the scheduling of the project. Now the whole team is involved in the scheduling of tasks. Finally, regular breaks and predefined working hours create structure and overview for all team members. The division between breaks and work time is clear and the entire team strives towards a high productivity level.

2.4. Resource Allocation

This section discusses the analysis of the resources used to design and produce the Soteria unmanned aerial vehicle (UAV) system. The budgets that were used are the cost, mass and power. These budgets will be discussed in sections 2.4.1, 2.4.2 and 2.4.3 respectively. These budgets will ensure the system is feasible and adheres to the requirements. No requirements related to mass, cost and power are therefore generated throughout this report, as these numerical budgets are considered to create a better overview during the iterative design process compared to textual requirements.

For all budgets 5% unforeseen costs are added in order to accommodate any expenses which have not been accounted for.

2.4.1. Cost Budget

The cost budget keeps track of all the costs involved in the design and production of the system. It comes directly from the top-level requirement *IMAV-CO*, which states that the total cost for design and production shall not exceed €5,000.-. This is a maximum which cannot be exceeded. Budgets have the tendency to grow as the design matures and for this a contingency factor was introduced to ensure the costs do not exceed the stated maximum of €5,000.- [8]. The contingency factors and targets for the system are presented in Table 2.1, based on systems engineering experience [9].

2.4.2. Mass Budget

The mass budget keeps track of the mass of all the components used within the UAV. As with the cost budget, the mass budget also has a top-level requirement bounding the maximum allowed mass. Requirement *IMAV-SR-24* states: All UAVs shall have a maximum mass of 5 kilograms. This budget has a contingency factor as well, to ensure the maximum allowed mass is not exceeded even though the mass tends to grow as the design matures (see Table 2.1) [8].

2.4.3. Power Budget

The last budget is the power budget. This keeps track of the power consumption of all the subsystems within the UAV. For the power budget there is no hard upper limit so there is also no contingency factor. Nevertheless it is important to keep track of the power via a budget since this, combined with the required mission time, has a direct influence on the size and mass of the power supply, and thus the UAV.

Table 2.1: Contingency factors at several stages of the design of the Soteria UAV system.

Technical Parameter	Conceptual Design	Halfway Final Design	End Final Design
Mass (< 5 kg)	20% (4 kg)	10% (4.5 kg)	5% (4.75 kg)
Cost (< €5,000.-)	15% (€4,250.-)	8% (€4,600.-)	4% (€4,800.-)

2.5. Project Management Conclusion

It is vital to properly manage a project, in order to assure optimal use of all resources. This is accomplished by the team by adopting a hierarchical structure with a chairman on top. Below him, there is a technical manager who ensures an optimal design is reached that combines all disciplines. Besides this, the team is also split into a payload and a propulsion & airframe group. Several officers were assigned to deal with various aspects of the project. A secretary will ensure all meetings are well documented.

The scheduling of the project is optimised with the use of the Scrum principle. It creates an overview which shows what the deliverables are, when they should be finished, who the problem owner is and what the current status is of the deliverables. Furthermore, every Monday a schedule for the week is made and every day the progress towards that schedule is evaluated and resources are distributed accordingly. On Friday the schedule that was made on Monday is checked and the overall project schedule is adapted accordingly.

The team has been constantly evaluating itself, also outside of the Scrum principle. The outcome of this was that the entire team would benefit from more involvement in planning. This was achieved by including the whole team in scheduling the tasks used in the Scrum overview. Also, a separation between work and break time creates a clear structure which optimises the productivity level of the team.

Besides human and time resources, the project is also bound by several technical resources. These resources are the mass, costs and power of the design. For these, budgets were made and the mass and costs were given contingency factors in order to assure they do not exceed the limits stated by the requirements.

3

Mission Design

The international micro aerial vehicle (IMAV) competition consist of ten mission elements that may be performed. Participants in this competition can choose freely which elements they want to do and in which order. Because the goal of Soteria is to gain the most points within the competition, the most optimal combination of mission elements needs to be chosen. This chapter will discus the method used to find the most optimal combination of mission elements. This follows from the top level requirement that states that the system shall win the IMAV competition of 2014, (*IMAV-CR*) In Section 3.1 all possible mission combinations are found and ranked based on the number of points they can achieve. In Section 3.2, three mission combinations from this ranking are investigated in more detail and from these three the optimal combination of mission elements is chosen by performing a trade-off. In Section 3.3, it is discussed how the mission elements are done and in which order. This is all concluded in Section 3.4.

3.1. Generating Mission Concepts

This section describes the process that is used to find all possible mission element combinations. These combinations are then further analysed and eventually converged to a ranking list of all the mission element combinations based on their points. These mission element combinations are then mission concepts from which the best will be chosen. The input and output of the process are elaborated upon and the process is verified and validated as well. The main functions of the mission concept generation process can be found in Figure 3.1 and will be discussed in more detail in this section.

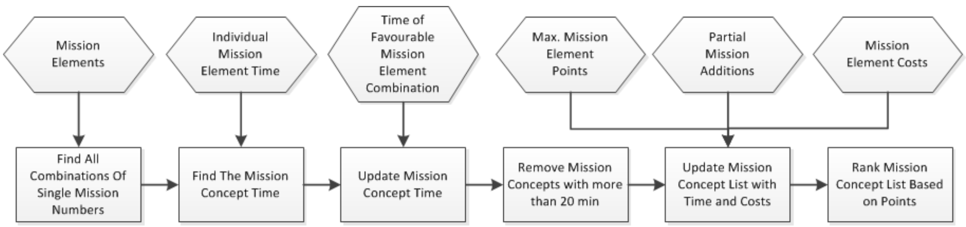

Figure 3.1: Flowchart showing the steps taken within the mission element combination process to find and rank mission concepts.

First, the optimisation process finds all possible individual mission element combinations. Because mission element 1 (take-off) is considered to be part of every mission concept, it is not used to create mission concepts. Mission element 2, is investigated in three ways. 2a is doing the photomap with a single unmanned aerial vehicle (UAV) and orthorectified. 2b is the photomap done with a single UAV without orthorectification and 2c is the photomap with multiple UAVs and with orthorectification. In this way there are 11 possible mission elements considered in the process. Using these 11 mission elements, a list of 2047 mission concepts can be created which consists of all possible mission element combinations.

Some individual mission elements take less time when they are combined. This can result in the situation that the total time required to perform a combination of mission elements is less than the sum of the times of the individual mission elements.

The IMAV competition has a limited time frame of 30 minutes. Within these 30 minutes, the team has to set up its equipment, perform the mission and recover all equipment from the field. Incorporating these set-up and recovery activities, an effective flight time of 20 minutes is taken as a first approximation. This effective mission time is later verified in Section 8.4. Total mission times are calculated for every mission concept and compared with the total allowed mission time. When a mission concept takes more than 20 minutes, it is deleted from the set of mission concept options.

After this, the costs for each mission concept are calculated and the number of points per euro is determined for each mission concept. Also partial mission additions (mission elements that are done partially) are incorporated and together with the maximum number of points and costs, a ranking is created for the mission concepts based on the number of points that can be achieved in the IMAV competition.

3.1.1. Inputs for the Mission Concepts Generation Process

The mission concept generation process uses multiple inputs and outputs. The inputs are discussed in Section 3.1.1 and the outputs in Section 3.1.2. The input encompasses the following for each mission element:

- Time of the mission element
- Maximum number of points of mission elements
- Mission element combinations
- Partial mission element additions
- Mission element costs

Time of the Mission Elements

Because the effective mission time is taken to be 20 minutes, estimations for the time for all mission elements are needed. In order to calculate the time needed for mission elements, the distance between the landing zone and the mission element object is needed. From this distance, the travel time can be derived. When a mission element asks for a distance to be covered (ME4: flying from house to house), this distance is determined as well and with these two distances, a total covered distance can be calculated. Then by studying reference aircraft, flight velocities were estimated at 10 m/s for outdoor near-linear flight (mission element 2), 6 m/s for outdoor flight including non-straight paths (outdoor part of all mission elements except number 1) and 1 m/s for indoor flight (mission elements 5, 6 and 7). With these flight velocities, the time required for outside flight, indoor flight and some extra time for flying to the local command centre (LCC) is determined. When adding these up, a total mission time can be determined. All of these parameters can be found in Table 3.1.

Table 3.1: Estimation of time it takes to perform mission elements and the points awarded for these mission elements.

Mission Element	Total Distance Covered [m]	Mission Time [min]	Points per UAV
1	0	0	12
2a	11670	20	72
2b	7020	12.2	72
2c	1312	2.7	72
3	1220	5.4	48
4	1050	7.9	120
5	755	17.4	180
6	200	5.6	252
7	200	5.3	60
8	340	2.4	36
9	340	19.9	45.6
10	0	1.5	24

Maximum number of points of mission elements

Another input for the mission concept generation process is the maximum number of points that can be obtained with the mission elements. The points that can be obtained with each mission element follow from the IMAV competition guide on competition rules [2]. The equation describing the total points for the entire mission (which may consist of multiple mission elements) is given by Equation (3.1). How the mission elements will be performed is discussed in more detail in Section 3.3. From this equation it can be seen that the mission score depends on the level of autonomy of the system (A_n), the points associated with the mission element (M_n) and the largest dimension of the UAV participating in the mission element (L_n). The summation of n to

N is about the total number of mission elements successfully performed by the UAV. Constants k and L_{max} are given by the IMAV organisation to have a value of 2 and 100 centimetres respectively and $PUAV$ is the number of points.

$$P_{UAV} = \sum_{n=1}^{N} \left(A_n \cdot M_n \cdot \left(2 - \frac{L_n}{L_{max}} \right)^k \right) \tag{3.1}$$

The IMAV competition guide states that points will be awarded to each UAV executing the mission element, so if a mission element is performed by two UAVs, this simply means that the score for this mission element is received twice. This means that the number of UAVs executing a mission element does not influence the relative points that can be obtained for that mission element. Therefore, the number of points obtainable by one UAV is analysed. Also, the most points are gained when the optimal mission concept is chosen. This mission concept is then performed by all the UAVs.

The number of points that is expected to be obtained is determined for each mission element and shown in Table 3.1. As Equation (3.1) states, the largest dimension (L_n) of the UAV performing a mission element influences a factor in the score equation. Since it is not known which value this dimension will take, it is taken equal to the constant L_{max}, namely 100 centimetres. This way, the dimensional factor will have a value of 1, which is a convenient value in the calculations.

The IMAV competition committee has specified three levels of autonomy, each with a corresponding point multiplier (A_n) [2]. If the UAV is controlled by a human, this is given an autonomy multiplier of 1. If flight is controlled autonomously but the operator is still controlling mission aspects, this gives a multiplier of 6. The highest multiplier is obtained when all aspects of the flight and mission are automated, including detection and decision making, yielding a multiplier of 12. For the mission concept generation process, the multiplier is set to 12. This is based on requirement *IMAV-AU-2*, which states that: all UAVs shall perform each mission element autonomously.

The number of items per mission element has been taken into account in the mission element time analysis. Besides time consumption, the number of items per mission element affects the points one can obtain. For mission element 5, points are awarded when the correct number of survivors ('items') in a house is identified. For other mission elements however, namely 3, 4 and 7, each separate correct item localisation and identification yields a specified number of points.

Mission Element Combinations

A mission element combination as input for the mission concept generation process is a series of two or more mission elements that a single UAV can perform consecutively and yield a benefit in mission time, meaning that the combination requires less time to be performed than the sum of its individual elements. Combinations of possible mission elements that are time-wise efficient to be performed together and the method of finding them will be presented in this section.

For example, mission element 4 requires a UAV to go by buildings and recognise their house numbers in area B (see the map in Figure 3.2). It is time-efficient if this same UAV would move to area D as a sidestep and land on the flat roof, which is mission element 8, since it will already get close to it when performing mission element 4. The required mission time for feasible mission element combinations were determined with distance measurements using Google Earth of estimated flight routes between the combined mission elements.

The above discussed mission element combinations in terms of time and points are represented in Figure 3.3. It should be noted that mission element 2 in the figure represents mission element 2a. The red block represents the time-wise infeasible mission element combinations.

What can be concluded from the Figure 3.3 is that mission element 6 and a combination of 6 and 7 yields the most beneficial mission combination with respect to points per time. Moreover there are also restrictions on the time mission elements demand. For example, mission element 5 involves going by ten houses and determining the correct number of survivors. It was estimated that 20 minutes are not sufficient to complete

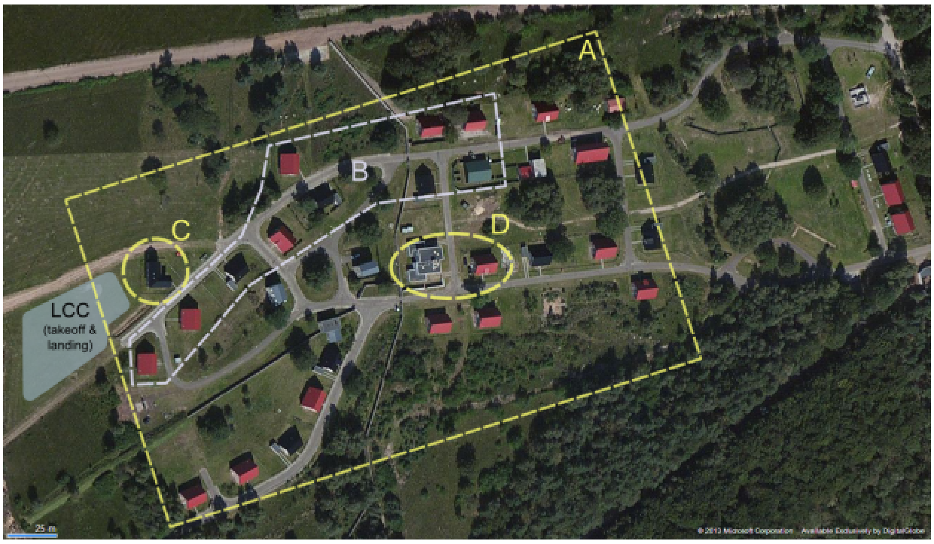

Figure 3.2: Map of the competition area as provided by the IMAV [2].

this mission for all 10 houses. However, it was determined that searching five houses would be possible within this time frame. Therefore, all results of mission element 5 are for the case where only five houses are searched.

Similarly, mission element 9 involves observing digits on a panel, which are shown from the beginning until the end of the 30 minutes time frame. The digit on the panel refreshes every 30 seconds. Using the effective time frame of 20 minutes and the assumptions involving travel time, it was estimated that a sequence of 38 digits can be detected. For this reason, the full mission element 9 can not be time-wise combined with mission elements other then 8.

Partial Mission Element Additions

The partial mission additions as discussed within the previous section only add a part of the full mission element score depicted in Table 3.1. For example, the system receives points for identifying all survivors in a single house for mission element 5. Therefore, the mission can be seen as ten (amount of houses) individual sub-missions, which can be added to mission combinations if the 20 minutes are not yet fully filled.

This analysis has shown that it is feasible for a total of three mission elements to be performed partially, namely mission elements 4, 5 and 9. The time estimation for these partial missions is based on the same assumptions as those made for the full mission elements. These partial mission time additions are incorporated in Table 3.1.

Mission elements 3, 6 and 7 have a partial point scoring system as well. However, the estimated mission times for elements 6 and 7 are quite small and it is not effective to fly into the house and only perform a partial mission. Furthermore, the location of the blockades of mission element 3 are not known, therefore the mission cannot effectively be split up into several partial missions. The points received per partial mission element and the time it takes to complete the partial mission element can be found in Table 3.2.

Table 3.2: Estimation of the time it take and the points award for completing only part of a mission element.

Mission Element	Points	Time [min]
4	12 points per house	0.9
5	36 points per house	3.6
9	1.2 points per consecutive digit	0.5

Payload Cost Estimation

The last input for the generation of mission concepts is the estimation of the cost of the payload per UAV. The following subsystems are considered as payload: location, navigation, data transmission and sense & identify.

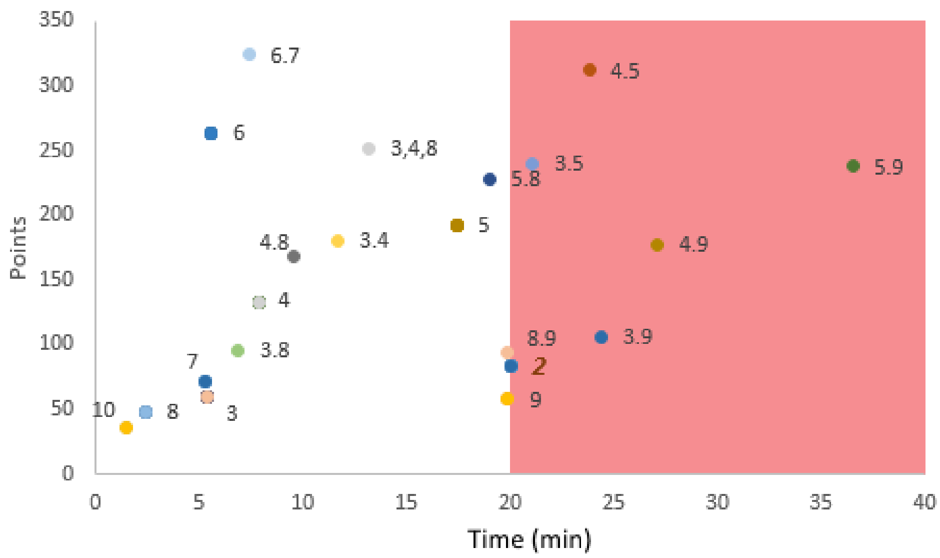

Figure 3.3: Points awarded for mission combinations.

The first step in making an cost estimation was listing the parts needed per function in order to fulfil each mission element. These parts were selected by evaluating design options and looking at reference UAV. For instance: a 20 megapixel high resolution camera was taken as a sensor in order to fulfil the photomap requirements. For the other mission elements where cameras are used, low resolution cameras were used. After the parts had been identified, the cheapest options were taken from the market analysis and literature study. This was done in order to maintain a design with a minimal cost. All the parts needed in the subsystems are listed with their respective price in Table 3.3. Note that RPi means Raspberry Pi. Moreover, this estimation is only a first estimation were the specific parts may vary over the design iterations that are performed in the design process.

Table 3.3: Estimation of the price of several parts which are needed to complete the mission elements.

Part	**Cost [€]**
OpenCV [10]	0
Ultrasonic range finder (range finder) [11]	20
GPS & IMU [12][13]	50
Low-Res Camera [14]	15
UAV transciever [15]	5
High-Res Camera [16]	80
RPi model B [17]	40
Groundstation transciever [18]	60

The total cost for each of the mission elements was calculated as well. This cost of the payload is depicted in Table 3.4.

3.1.2. Outputs for the Mission Concepts Generation Process

Combining the different inputs within the mission concepts generation process, a list of mission combinations is generated and ordered in a way that the mission concepts with the highest points are on top. After determining the number of points per mission per UAV, a total number of points per mission can be found as well. In order to do this, the number of UAVs must be known.

Three mission concepts were taken as output from the process. Concept I consist of mission elements 1, 4, 6, 7, 8 and 10, concept II consist of mission elements 1, 3, 4, 8 and 10 and concept III consists of mission elements

Table 3.4: Estimated costs of the payload needed to complete the mission elements.

Id	Mission Element	Parts	Cost [€]
2	Photomap	GPS, IMU, Dongle, High-Res Camera, RPi Model B	175
3	Blockades	Range finder, GPS, IMU, transciever, RPI Model B	115
4	Quick visual inspection	2x Low-Res Camera, GPS, IMU, transciever, RPI Model B	125
5	Detailed inspection	2x Low-Res Camera, Range finder, transciever, RPi Model B	95
6	Visit rooms	1x Low-Res Camera, Range finder, transciever, RPi Model B	80
7	Locate & identify items	1x Low-Res Camera, Range finder, transciever, RPi Model B	80
8	Land on flat roof	2x Low-Res Camera, Range finder, GPS, IMU, RPi Model B	140
9	Observe panel	2x Low-Res Camera, GPS, IMU, transciever, RPi Model B	125
10	Precision landing	2x Low-Res Camera, Range finder, GPS, IMU, RPi Model B	140
	Ground station	OpenCV , transciever	60

1, 2c, 3, 4, 8 and 10. The reason for these concepts is elaborated upon in Section 3.1.4.

3.1.3. Verification & Validation of the Mission Concepts Generation Process

Within this section verification techniques are used to determine whether the process outputs are correct. Validation is used to check if the program provides the right output.

Software verification is done by checking the correctness of the outcome manually for every function of the program and every type of output, for different numbers or combinations. This shows if the mission concepts that were removed from the list were removed correctly and if the mission concepts that were not removed are valid concepts. The addition of costs was first checked for all mission elements and their combinations. The costs turned out to add up successfully. Furthermore, some verifications on for instance the ranking and the coherence between columns were performed. In this way it was assured that all cells were found in the right column and row and thus representing the correct mission element combination.

The validation consists of checking the outcome of the process with reality. Validation can only be done when the UAV is ready and flying.

3.1.4. Sensitivity of the Mission Concepts Generation Process

When input parameters of the mission concept generation process change, the ranking of concepts changes. A new optimal concept is found when the ranking changes. The sensitivity of this is discussed in this section. The concepts on which the sensitivity analysis are done to maximise the points.

It should be noted that the top concepts all include indoor navigation and object recognition. Since indoor navigation is quite complex, the best mission concepts that only performs outdoor mission elements is considered a concept as well (concept II & concept III). The sensitivity analysis is performed twice, for both the indoor and outdoor only mission concept.

Mission Concepts with Indoor Elements

According to the mission concept generation process, most points can be obtained indoor. The top three concepts all have the mission elements 4, 6 and 7 in them, which involve recognition. Because of this overlap, a more general mission concept, concept I, can be constructed that consists of these three mission elements. This mission concept can be extended by either element 3, 8 or a combination of both 8 and 10 in order to gain a top three position without changing cost per UAV.

The first sensitivity analysis focuses on the costs of the mission. When increasing total costs with a percentage, the ranking stays the same and the points are decreased linearly. When looking at the cost analysis, the biggest uncertainty is located in the systems that do not rely on the mission elements: the basic UAV costs. These costs are the same for all mission concepts and consist, amongst others, of an estimation for battery and propulsion costs. The basic UAV costs are increased by increments of €100 up to €400 and decreased by €50 and €100 to check the impact of this on the ranking.

From the analysis, it can be concluded that mission Concept I remains the best mission concept, even when increasing costs with 400 euros. It can also be seen that the top mission concepts all contain a combination of mission elements 4, 6 and 7.

When the autonomy level of all mission concepts changes, no change in ranking would occur as they all scale linearly with the multiplier. As noticed before, indoor navigation is quite a difficult objective and therefore a change in the autonomy level multiplier has been studied as well. In the next analysis, it is assumed that the flight is still autonomous but the recognition of objects is done by a person.

It might be the case that autonomous indoor navigation and flying is not possible at all, rendering manual controlled flight the only option. In this case a difference can be observed in the ranking. The previous best concept dropped drastically and a new best concept is generated that performs only outdoor mission elements. This mission concept is called mission concept II and consists of elements 3, 4, 8 and 10. Now that this 'outdoors' concept is obtained, a new ranking is made based on only outdoor orientated mission concepts and these are discussed further in the next section.

Mission Concepts without Indoor Elements

When constructing an outdoor mission concept list, concept II is found leading. Almost similar to this concept is a concept that is from now on called concept III. Concept III consists of elements 2, 3, 4, 8 and 10. It should be noted that the only difference between concept II and III is the presence of mission element 2 in concept III. Because the cost per UAV that can perform one of these concepts and thus the number of UAVs available per concept is quite different between concept II and III, these two are considered to be different mission concepts. This is in contrast to concept I, which could be constructed with different mission elements that would lead to the same number of UAVs.

Again the cost deviation for the mission concepts is analysed. As for the previous cost analysis, the ranking does not change significantly for a change in costs of minus €100 through plus €400. As costs become lower for these mission elements, points for mission concept III rise faster than points for mission concept II. For extremely low cost this results in mission concept II becoming a winner, while for high cost mission concept III comes out on top. Therefore this sensitivity analysis only shows that for the cost parameter, mission concepts II and III remain on top of the list, but they are both as good as the other.

The influence of failure of difficult mission elements on the ranking was investigated. The number recognition (mission element 4) is now assumed to be 'broken' and awarded with zero points. When mission element 4 is not successful, mission concept III again surpasses mission concept II. Since this is the second time they interchange places, it is found that a more detailed investigation of those two mission concepts is required.

When autonomous recognition turns out to the be more difficult than expected, non-autonomous recognition can be used as well which will lead to half the points for mission elements 3 and 4. Again mission concept III takes the lead. Since mission element 2 is assumed to be less dependent on the autonomy of design than mission element 3 and 4, mission concept III has an advantage.

Conclusion

Looking at the total number of points, it can be concluded that a UAV that can navigate indoor and also is able to land and recognize numbers (mission concept I), is always the best option. When indoor navigation turns out to be infeasible, mission concepts II and III can be used. It follows from the analysis, that the two interchange rank quite often with differing parameters and therefore both are taken into the trade-off discussed in the next section.

An overview of the different concepts with the estimated points is given in Table 3.5. This table includes both variations for Concept I, i.e. the concept including mission elements 8 & 10 and the concept including mission element 3.

From the concepts it can be concluded that mission elements 4, 8 and 10 are an important part of the mission as they occur in all concepts. Now that a convergence to three concepts is made, a trade-off can be performed of which a sole concept should be the outcome.

Table 3.5: Definition and main parameters of concept I, II and III.

Mission Concept	Mission Numbers						Total Points
Concept I	1	4	6	7	8	10	504
	1	3	4	6	7		492
Concept II	1	3	4	8	10		240
Concept III	1	2c	3	4	8	10	312

3.2. Trade-off between the Mission Concepts

This section presents the trade-off performed to select the final mission concept. The trade-off is based on the conceptual analysis presented in the previous sections. First, Section 3.2.1 elaborates on the methods used to perform the trade-off. Second, Section 3.2.2 discusses the five trade-off criteria used to evaluate each concept. These trade-off criteria are then elaborated upon in Section 3.2.3, 3.2.4, 3.2.5, 3.2.6 and 3.2.7. Section 3.2.8 utilises the discussed methods to determine the criteria weight factors and thus specifies the relevance of each individual criteria used. Finally, Section 3.2.9 utilises the discussed methods to perform the concept trade-off and select the final concept and present the trade-off summary table.

3.2.1. Trade-off Method

The trade-off method used to choose between the three presented concepts is a combination of the analytical hierarchy process (AHP) method and a graphical trade-off. The AHP method is used to determine the weight factors for the trade-off criteria. Afterwards, the graphical trade-off table is used to perform the trade-off itself as discussed in Section 3.2.9.

3.2.2. Trade-off Criteria

A total of five trade-off criteria were selected to compare the three presented concepts. This limited number of trade-off criteria was used, such that concepts that do not fulfil important killer or driving criteria cannot be compensated by a combination of several other criteria [19]. The following trade-off criteria will be discussed in the following sections:

- Point sensitivity
- Operational risks
- Points per euro
- Concept feasibility
- Search and rescue capabilities

3.2.3. Point Sensitivity of the Mission Concepts

This section presents the changes in total points scored by the UAV systems with respect to changes in UAV length, autonomy level and number of UAVs. This is again done with Equation 3.1. All three mission concepts are now evaluated with this formula and the results are plotted in Figure 3.4.

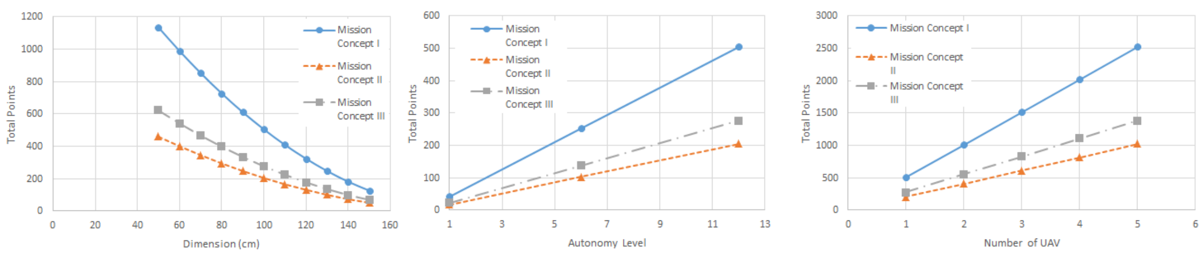

Figure 3.4: Sensitivity analysis of three mission concepts of points with respect to dimensions, autonomy level and number of UAV.

What can be seen in Figure 3.4 is the point variance for each mission concept with the changing parameters. Comparing the point variance of the mission concepts with each other, it can be calculated that the relative change is more or less the same. However, in absolute terms, it can readily be seen that mission concept I has the largest changes due to the higher number of points it can achieve. This means that a mission from concept I could lose a large number of points if a drone does not function. Whereas if the same would happen for concepts II or III, the impact is not as significant. But the impact for concept II is still greater than for concept III.

3.2.4. Operational Risks

In the operational phase of every product certain events can occur that negatively affect the production, operation or disposal of the product. These risks are identified beforehand in this section. This will ensure proper actions can be taken to lower risks and increase the chance of a successful product. The risks in these categories are called environmental risks. The operational risks per mission element are discussed in this section. For each of these events the chance and consequences of occurrence will also be determined.

A mitigation strategy can be developed after the risks are mapped in a risk map and the most critical risks are determined. With this strategy the chance of occurrence and consequences of the most critical risks will be decreased, with the goal of increasing the extent to which the product is successful. The mitigation strategy is described within the last part of this section.

Environmental Risk Identification

The environmental risk identification considers the risks of the design with respect to the environment. These problems may arise once production starts. After that, the product will encounter several operational risks and end of life disposal risks. Possible risks will be identified and divided in different categories. The relevant categories chosen for this product can be found in Table 3.6.

Table 3.6: Risk categorisation of the environmental risks in the multi UAV.

Risk category	**Description**
Production	These are the risks that can occur during the production or risks that are created by the means of production.
Operation	Operational risks are for example subsystem failures or crashes.
Disposal	Disposal risks are for example losing the UAV in the environment.

In each of these risk categories a number of risks is presented in Table 3.7. The operational risks will be evaluated per concept in this section. A short explanation about the exact nature of the risk is also provided. This will make the potential effects of the risks on the production, operation and disposal of the product clear. It should be noted that even though the risks are numbered, these numbers do not indicate a priority. These numbers will be used in the risk analysis section instead.

Table 3.7: Risk identification of the environmental risks in the multi UAV design synthesis exercise (DSE).

Nr.	**Risk**	**Description**
		Production
p.1	Machining inaccuracy	Machines and production are never fully exact.
p.2	Unhealthy/dangerous materials	During production there is a chance that dangerous or unhealthy materials are needed.
p.3	Material costs	The cost of materials is subject to price changes.
p.4	Damage during production	During production, parts may be damaged.
p.5	Delivery times	When producing a system delivery times may take longer than expected.
		Disposal
d.1	Unrecoverable UAV	When the UAV is unrecoverable it will stay in the environment and will be degraded there.
d.2	Environmental hazardous materials	When the end of life of the drone is reached, the environmental hazardous materials can endanger the environment when incorrectly disposed.

Mission Element Risks

For every mission element certain risks are present. These risks need to be identified per mission element. These can later be used to determine the overall risks of the mission. There are several risks that are present for all the different mission elements. These are given in Table 3.8. For example the structure of the UAV might not be able to carry the loads (risk 0.3) also the on-board processor SD card can have a corrupt operation system on it (risk 0.5).

Take-off
During take-off, the UAV is still close to the ground, this results in a relative large influence of potential gusts because it can crash immediately. This is listed in Table 3.9.

Table 3.8: UAV general risks for the different mission elements

Nr.	Risk
0.1	Controllability Failure
0.2	Data Storage Failure
0.3	Structural Failure
0.4	Power Failure

Table 3.9: UAV risks of the take-off mission element

Nr.	Risk
1.1	Gusts / Turbulence

Photomap
Several risks are present when creating a photomap. First of all the UAV should be able to create stable pictures and due to circumstances these could be unclear. Next to that, the different pictures need to be stitched. This is done by software specifically chosen for this task. However, it might occur that the software is unable to stitch pictures together due to possible software problems. This may lead to an unusable photomap not meeting the requirements. The loss of the GPS link will result in that the UAV is not longer able to follow his path. When the photomap is created by means of several different UAVs they have to send and combine the data. This data stream is vulnerable to data loss. This is listed in Table 3.10.

Blockademap
The UAV needs to detect blockades on the road. This will be done by a computer analysis of the photomap provided by the UAVs. In Table 3.11 the risks that come along with the blockade map are identified.

Table 3.10: UAV risks of the photomap mission element

Nr.	Risk
2.1	Camera failure
2.2	Stitching failure
2.3	Inadequate resolution
2.4	Inadequate processing capacity
2.5	GPS failure
2.6	Data link failure

Table 3.11: UAV risks of the blockade map mission element

Nr.	Risk
3.1	Radar failure
3.2	Camera failure
3.3	Inadequate resolution
3.4	Unable to identify blockade
3.5	GPS failure
3.6	Obstacle collision
3.7	Data link failure

Quick Visual Inspection
During the quick visual inspection the UAV has to detect numbers posted on several houses. It might occur that not all the numbers will be recognised properly, by attitude problems or software issues. To perform this mission the UAV should come into close vicinity of buildings, which increases the possibility of turbulent flows or bumping into an obstacle. The loss of the GPS link will result in that the UAV is not longer able to follow his path. The risks are listed in Table 3.12.

Landing on Roof
Mission element 8, which is about landing on a flat roof, has as a major risk that the UAV will be damaged during landing. This damage may result in no longer proper functioning of certain elements or even complete destruction and a no longer functioning UAV. When the UAV is no longer able to depart from the landing location this mission is considered failed and no points will be rewarded. When the UAV is not able to land within the determined boundaries the mission element is failed. Around the landing zone several obstructions are located which pose a possible collision risk for the UAV. The risks are listed in Table 3.13.

Table 3.12: UAV risks of the quick visual inspection mission element

Nr.	Risk
4.1	Camera failure
4.2	Unable to recognise
4.3	Gusts / turbulence
4.4	Not able to locate house
4.5	Not able to locate number
4.6	GPS Failure
4.7	Obstacle collision
4.8	Data link failure

Table 3.13: UAV risks of the detailed inspection mission element

Nr.	Risk
8.1	Unable to Localise
8.2	Crash Landing
8.3	Landing not within boundaries
8.4	Unable to take-off
8.5	Landing spot occupied
8.6	GPS Failure
8.7	Obstacle Collision

Precision Landing
During the precision landing mission element, the UAV should land in a designated area. The risk exists that the UAV will not be able to find the area. The UAV might also (for example due to gusts) not be able to land inside this area. This depends mainly on the controllability and weather conditions. This mission element is comparable with mission element 8 (Roof Landing). The risks are listed in Table 3.14.

Table 3.14: UAV risks of the Panel Inspection mission element

Nr.	Risk
10.1	Unable to Localise
10.2	Crash Landing
10.3	Landing not within Boundaries
10.4	Unable to take-off
10.5	Landing spot occupied
10.6	GPS Failure
10.7	Data Link Failure

Risk Analysis

Different risk categories were determined and in each of these categories several risks were identified. Now these risks need to be analysed. A map of the different risks is shown in Figure 3.5. On the horizontal axis the chance of occurrence is distributed in increasing order. The probability definitions are as follows:

- *very likely*: it is expected to happen multiple times within multiple projects of ten weeks.
- *probable*: it is expected to happen at most once during a project of ten weeks.
- *unlikely*: it is expected not to happen at all during a project of ten weeks.
- *very unlikely*: it is expected not to happen within multiple projects of ten weeks.

On the vertical axis the severity level is distributed in increasing order. The severity level definitions were determined as follows:

- *Catastrophic*: the system will fail if this happens.
- *Critical*: the project results will be damaged significantly but there will be usable results.
- *Marginal*: the project results will be affected slightly but results are still expected to be usable for the larger part.
- *Negligible*: the project results will hardly be affected, if affected at all.

Risk is defined as the chance of occurrence multiplied with the consequences if the event occurs. This means that the most critical risks will be located in the top right corner of Figure 3.5. The lower risks will be located in the lower left corner of the risk map.

The highest risks will be clarified in order to create a better understanding of the risk map.

Highest Risks
The highest risks are a corrupt operating system on the SD card of the Raspberry Pi; during tests it occurred

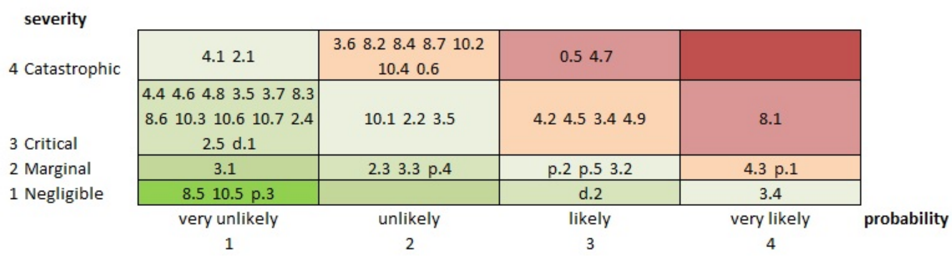

Figure 3.5: Risk map with the identified risks for the multi UAV DSE

multiple times that the card was corrupt and had to be replaced or reinstalled. This can have major consequences on the system. During the roof landing the UAV might not be able to locate the roof and fly above it. This is because of the global positioning system (GPS) location uncertainty further explained in Section 4.4. When the UAV is not above the roof it can not conduct a landing. When detecting the house number the UAV has to approach the house at a very short distance. Because of gusts and GPS inaccuracy there is a chance that the UAV will collide with the building.

Mitigation Strategy

A mitigation strategy is a plan to decrease the influence of the highest risks. Risks can be decreased in two ways. First, the consequences of the event can be made less critical. This will decrease the overall risk of that event. Secondly, the probability of occurrence can be decreased.

Because resources are limited, it is most efficient to first mitigate the highest risks. These are located in the upper right corner of Figure 3.5. The top priority risks for which a mitigation strategy is developed are risks 0.5, 4.7 and 8.1, as introduced in Table 3.7. To overcome the risk of a corrupt operating system (risk 0.5) a spare SD card should be available before the competition to be able to replace a corrupt unit. If the UAV is not able to localise and fly above the roof (risk 8.1) it will reinitialise its mission element. As a mitigation strategy during the building approach and the collision possibility (risk 4.7), a distance measuring device will constantly be obtaining range data. If the UAV is getting too close to the building it may decide to divert its course to avoid a collision.

3.2.5. First Mass and Cost Estimation

During the trade-off, a study was performed to check if a UAV could be build for the three mission concepts and whether it would fulfil the safety requirements. This was done by estimating the mass and cost for a UAV capable of performing one of the mission concepts. A more detailed explanation of the mass and cost estimation can be found in [1].

A multicopter was selected as a platform for this study, since it is capable of flying well in terms of control at low speeds. It was found that the same hardware is needed to complete mission concept I and mission concept II as found in Section 3.1.1. So for these a similar cost and mass was estimated. It was estimated that a hexacopter with a mass of 3.3 kg which costs €810 could fulfil mission concepts I and II. For mission concept III a hexacopter of 3.5 kg which costs €909 was estimated.

The mass for both concept I & II and concept III falls within the 5 kilograms mass requirement *IMAV-SR-24*. Additionally, a momentum restriction of 20 kg*m/s was given by requirement *IMAV-SR-25*. This results in a maximum allowed velocity of 6.0 and 5.7 m/s for concepts I & II and concept III respectively. Furthermore the total costs of €810 and €909 for concept I & II and concept III respectively fall within the budget of €5000 as stated in requirement *IMAV-CO*. When the costs are known, they can be combined in the mission concept generation process with the maximum number of points in order to determine the maximum number of points.

3.2.6. Feasibility of the Mission Concepts

This section will evaluate the feasibility of each of the proposed mission concepts. This will be done by checking whether the necessary hardware, software and methodology is available and whether the individual mission elements have been accomplished by other companies or institutions.

Mission Concept I

Mission concept I mostly consists of indoor navigation and the transition from outdoor to indoor flight, which are also the most challenging abilities to develop in this concept. Several methods may be used in order to be able to navigate indoors. Examples include combinations of simultaneous localisation and mapping (SLAM) algorithms with laser scanners or cameras. The price of laser scanners is at least €1000,- and cameras, which may be used for visual navigation, have a cost as low as €15,- a piece. However, indoor navigation with the use of cameras is currently still a field of research. A proof of concept was, for example, given by a collaboration between MD Robotics and the University of British Columbia in 2002 [20]. With regards to the transition from outdoor to indoor flight, it was obtained from a technical consultation by Christophe De Wagter of the TU Delft that this transition will also be challenging to accomplish. It is expected that 9 out of 10 UAVs will not be able to enter a building [21]. More research and development should therefore be done before the system may be incorporated on the UAV which will compete in the IMAV Competition 2014.

As mission concept I is the most challenging concept to complete within the allocated time, it will have the highest development risk. The reason for this increased development time is the high amount extra research and testing that needs to be done in order to be able to fly indoors

Mission Concept II

Mission concept II has mission 3 and 9 as extra missions besides missions 1, 4, 8 & 10, the three missions which are present in each of the three mission concepts.

Mission concept II is the most straightforward concept, and less development time is therefore required in comparison to the other two concepts. Due to this straightforwardness, the need for human resources to develop concept II is the lowest of the three mission concepts. This therefore lowers the development risks of this mission concept.

Mission Concept III

Mission concept III may be seen as a middle ground between concepts I and II; research has already been done, but some more research may be required. Aside from the standard 1, 4, 8 & 10 combination, mission concept III also contains mission elements 2 and 3. As discussed earlier, mission element 2 may require for example, a 20 megapixel camera as hardware and a photo stitching program as software. Both of these were found to be readily available [17] [22].

With regards to research that still needs to be done, it was mentioned in Section 3.2.5 that the current thrust to weight ratio is 1.7 and that this may be increased in order to improve controllability. Two other points of research are the time required to stitch the photos and the optimum altitude at which the system will need fly, as these have not yet been determined.

Concept III contains the same mission elements as Concept II, but has the photomap as an extra mission. Due to the extra research that needs to be done with regards to the photomap and the higher complexity of the UAV, the likeliness of the development risks is higher than those of Concept II.

Even though further research needs to be done, the concept may still be considered to be feasible up to an acceptable degree. As mentioned earlier, the software and hardware is readily available. This will decrease the production time considerably. Next to that, the risks of concept III are acceptable and may be mitigated as discussed.

3.2.7. SAR Mission Capabilities

This section will discuss the actual benefit of the system in terms of search and rescue (SAR) mission capabilities. This follows from the top level requirement *IMAV-SAR*. This requirement states that: The system shall be functional in disaster scenarios in urban areas. When looking at the impact of each specific mission element on these capabilities, the mission concepts can be compared as well.

One of the most useful mission elements in terms of assistance supplied to a rescue team is the photomapping mission element. An immediate photomap can be created by the system. This photomap gives an overview of the severity of the disaster and about situation and accessibility of the area. In combination with the blockade detection, even more information can be drawn from this photomap. Rescue workers now know which houses can be reached and what areas are impenetrable. However, when only the blockades are detected, while the map is not up to date, this mission element loses some worth. Mission element 4 covers the recognition of the house numbers. With these numbers, the individual houses can be recognised and additional information from other elements such as the amount of survivors can be added. This last piece of information follows from mission elements 5, 6 and 7. Going into a house and inspecting the rooms on survivors, items and rooms gives very detailed information which would decrease the time needed by rescue teams to investigate houses and retrieve survivors. This information increases the effectiveness of the SAR capabilities.

In conclusion it can be said that the most important mission elements are element 2 and 3, namely the photomap and the blockade detection. Those two provide quick and general information of the area. Mission element 4 provides a more detailed inspection which can be used in a later stage of rescue.

If a UAV system does not offer clear advantages for SAR missions, the design has failed to comply with the project objective statement (POS). Thus, misusing potential loopholes in the rules of the IMAV Competition 2014 in order to win would fulfil some top level requirements, but not the POS.

3.2.8. Trade-off Criteria Weight Factors

The trade-off criteria weight factors are determined by the AHP as discussed before. The AHP is based on a pair-wise comparison of all criteria, i.e. for the five criteria selected for the concept trade-off, all ten criteria combination are evaluated. The pairs of criteria are evaluated on relative importance using a numerical scoring scheme from 1 to 9. Afterwards, these numerical scores are used to compute the final criteria weight factors used for the trade-off [23].

The AHP was executed using a pre-developed tool, which includes options to have multiple participants [24]. The output of this tool was successfully verified once, using the described AHP computation process [23]. Furthermore, the tool includes a consistency check, which checks the consistency of the individual input of each participant. Thus, the tool checks when criterion A is more important than criterion B and criterion B is more important than C, then criterion A is more important than criterion C. Moreover, the tool includes a consensus check, which checks the consensus between the input of different participants.

The process described above resulted in the criteria weight factors as listed in Table 3.15. This table also presents the most common reasons of the three participants to determine the importance of each criterion. Note that the AHP input to generate the criteria weight factors has a 99% consistency for the different criteria and a 88% consensus between the three participants. Additional details on the individual inputs and rationale can be found in the mid-term report [1].

Table 3.15: The criteria weight factors including rationale for mission design trade-off

Criterion	Weight factor	Rationale
Point Sensitivity	0.06	The expected amount of points can be estimated with a higher accuracy with a lower sensitivity.
Operational Risks	0.19	Low-risk systems have a higher chance of actually executing the mission for which it is designed.
Points per Euro	0.05	The points per Euro give an indication of the amount of points received, but only if the concept can be produced and does not fail during the competition.
Feasibility	0.46	The concept can only score points and win IMAV, if the concept is feasible and can be produced before the competition day.
SAR Capabilities	0.25	The POS indicates that good SAR capabilities is one of the main objectives of the project.

3.2.9. Trade-off Results

The concept trade-off is performed using the graphical trade-off table combined with the criteria weight factors presented in the previous section. The graphical trade-off table uses a total of four different categories defined as excellent, good, fair and poor. The scoring definition that define each category are defined as follows:

- **Excellent**: The concept has an excellent score for the given criterion, completely fulfilling the criterion or significantly outperforming other concepts.
- **Good**: The concept has a good score for the given criterion, having slight deficiencies in fulfilling the criterion.
- **Fair**: The concept has a fair score for the given criterion, having significant but correctable deficiencies in fulfilling the criterion.
- **Poor**: The concept has a poor score for the given criterion, having unacceptable deficiencies in fulfilling the criterion or significantly under-performing with respect to other concepts.

The trade summary combining the concept analysis of this chapter as well as the trade-off methods of this section is shown in Table 3.16. The trade table presents all criteria in the top row and all concepts in the left-hand column. The reason for the judgement, as discussed in this chapter, are summarised within the trade-off table. The table also presents the criteria weight factors with the column width for each criteria corresponding to the criteria weight factors presented in Section 3.2.8.

Table 3.16: Trade-off Summary Table; Converging from 3 to 1 concepts by selecting Concept III

Options\Criteria	Feasibility	Points/€	Operational Risks	Point Sensitivity	SAR Capabilities
Concept I	Fair Indoor navigation, Highest development/testing time & most complex	Excel-lent 0.59	Poor Many indoor risks	Fair Much variation	Excellent Near-real time information on situation inside houses allows major increase in SAR ops effectiveness
Concept II	Excellent Shortest development and testing time, lowest technical complexity	Fair 0.29	Good No critical risks	Good Some Variation	Fair Most valuable info is blockade locations, but this is nearly worthless without an up-to-date map
Concept III	Good Photomap, stitching & impulse still need detailed analysis.	Good 0.32	Fair Additional photomap risks	Excellent Little variation	Excellent Gives SAR teams required information to move around the afflicted area quickly instead of by trial-and-error

The final concept selected based on the trade-off shown in Table 3.16 is Concept III. Concept I was not chosen based on the fair and poor score for feasibility and operational risks. The combination of both scores was considered unacceptable compared to the other concepts. Concept II and Concept III are both valid options to be chosen as final concepts. Concept III was selected mainly based on the excellent SAR capabilities of this concept as all the other criteria have small deviations between Concepts II and III.

3.3. Mission Strategy

To attain an optimal performance at the IMAV, a proper mission strategy is needed. In the mission strategy the order of the mission elements is determined. Because of the fact that most mission elements can be performed in a number of partials, a route optimisation in combination with partial mission element order can be constructed. In Section 3.3.1 the take-off, photomap mission and blockade mapping elements is combined. After that a strategy for the remainder of the mission, consisting of the roof landing, quick visual inspection and precision landing is constructed in Section 3.3.2.

3.3.1. Photomap

First, the take-off has to be performed at the LCC before all the other mission elements can start. This happens in the area to the left of the map, as shown in Figure 3.6. Every different line type represents a different UAV. When the take-off is performed, each UAV will follow its own route according to the map in Figure 3.6. This route will be followed by means of different waypoints that are to be pre-programmed. The routes were chosen in such a fashion that the distance to be flown per UAV will differ but the total route length is as low as possible. The creation of different route lengths was done so drones will not hinder each other in following mission elements. Aside from that, as a mitigation strategy the routes were constructed in parallel so a UAV can take over the route of another UAV while wasting as little time as possible, in case one of the UAVs would fail.

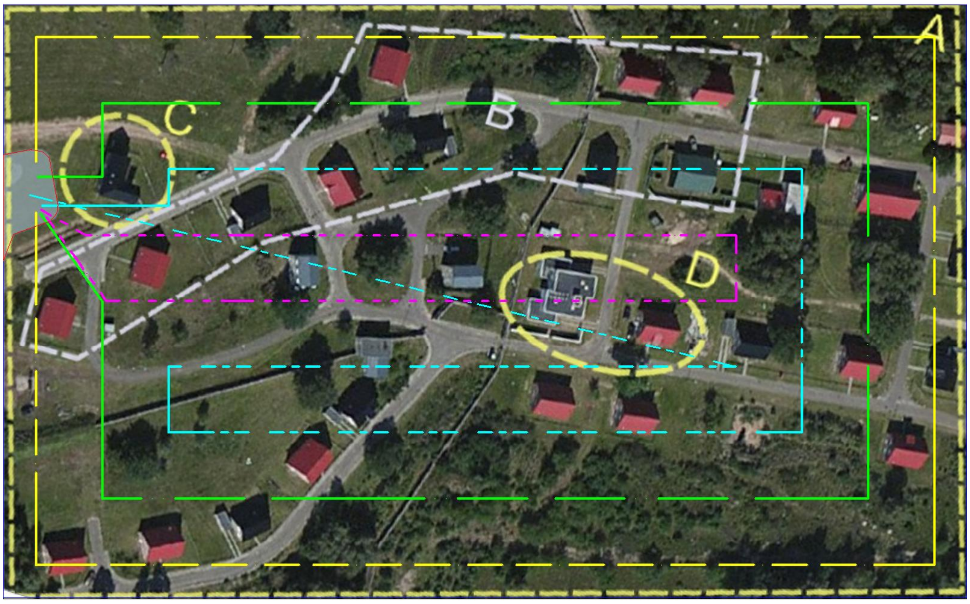

Figure 3.6: The route to be flown for the photomap mission element, every line type indicates a different UAV.

The size of area A is known via the competition rules [2]. With the use of Google Earth it was determined [25] to be 277.3 [m] by 170.6 [m]. When the photomap is finished the UAVs will return to the LCC. At the LCC they will perform the precision landing mission element. When a UAV has landed, its Sony Cybershot camera will be detached by a team member. The UAV will be able to take off again and will continue with the remainder of the mission elements described in Section 3.3.2. The SD cards will be taken out of the cameras and will be inserted into the ground station. This will first run the photo stitching software. When the stitching is completed, an analysis of the map will be made to detect the blockades. This generates a new requirement. Requirement *IMAV-CR-ME2-7*states that: the system shall stitch the photomap and analyse the blockades within 30 minutes. When the software has finished and the blockade map is provided, the team will make a consideration whether it is more favourable to indicate the blockades by hand than to let software do the recognition. This can only be decided on the day itself depending on how the software performed during the competition.

3.3.2. Mission Remainder

When the camera is taken from the UAVs, the UAVs will take off from the LCC. The time at which they will depart from the LCC will differ as described in Section 3.3.1. Based on the different mission element risks first the UAV will perform the roof landing mission element. In Figure 3.7 the route it will fly to the roof landing spot is given. The flight will be performed above house level height evading trees on the route. Upon arrival at the building where the roof landing should be performed, the UAV will land. This might require several tries. The dimensions of the roof are 11 by 6 metres and there is an uncertainty about the exact location as described in Section 4.4. With the use of the ultrasonic range finder the UAV will be able to determine if it is above the roof, if not it will will try the element again from a pre-set starting waypoint. When the roof landing is successfully performed the UAV will conduct the quick visual inspections on its route back to the LCC. It is possible to see the route on the map in Figure 3.7. The squares indicate the houses that need to be inspected, the LCC is again located at the left in the figure. After the roof landing the UAV will take off again, increase altitude to pass over the houses and fly to the first house to be inspected. It will descend there and the circle on the map in the figure indicates the uncertainty of the location. These circles where chosen so that no known obstructions will be present and are located at the house number side of the buildings. This fulfils requirement *IMAV-AU-11*: Navigational waypoints shall be chosen with a 5 metres clear-of-obstacles radius in the horizontal plane.

Not knowing all possible obstructions makes this the mission element with highest risk. When all houses are inspected the UAV will return to the LCC where another precise landing may be performed.

Figure 3.7: The route to be flown for mission element 3, 4, 8 and 10 by the UAVs during the IMAV competition.

From the routes that were determined all the needed waypoints can be deduced. Now the full mission route and order of all the different operations are known.

3.4. Mission Design Conclusion

In this chapter a list of mission element combinations was made and ranked based on the points they can achieve in the IMAV competition. From this list three mission concepts were made. One may think that in order to have a higher certainty of scoring the maximum number of points, first the missions with the highest number of points should be performed. It should be noted that this risk analysis shows that mission elements 5, 6 and 7, all performed indoors, induce the highest risks.

From the feasibility study followed that the UAVs complying with the safety rules set by the IMAV 2014 jury are capable of performing the mission concepts. It may also be concluded from a literature research that concept II has the highest feasibility, after which concept III has a reasonable feasibility and mission concept I has the lowest feasibility. The reason for this difference in feasibility is the availability of the necessary software and hardware and the likeliness and impact of development risks for each of the mission concepts.

The SAR capabilities of the UAV system were identified as being of great importance. In this chapter it was discussed that if a UAV system does not offer clear advantages for SAR missions, the design has failed to comply with the *IMAV-SAR* requirement and therefore with the POS. Thus, misusing potential loopholes in the rules of the IMAV Competition 2014 in order to win would fulfil some top level requirements, but not the POS.

Finally, using the trade-off criteria feasibility, operational risks, points risks and SAR capabilities, concept III is chosen. The main specifications of concept III can be found in Table 3.17. Note that the speed and weight are related by the momentum requirement set by IMAV [2].

After determining which mission elements are done, a strategy was determined stating in which order the mission elements are done. First a take-off is performed, and second, the photomap is made. When the photomap is done, the UAV is going back to the LCC. Here the photos are taken from the UAV and the map is stitched while the UAV takes off again to perform the roof landing and the recognition of house numbers.

Table 3.17: The main prelimanary estimations of mission concept III

Element	**Value**
Mission elements	Take-off (1), Mapping (2), Blockade Map (3), Quick Inspection (4), Roof (8) and Precision Landing (10)
First order weight estimation	3.5 kg
Speed (derived from inertia constraint)	5.7 m/s
First order cost estimation	€ 1120
Number of UAV (derived from cost constraint)	4

Now that the mission concept is chosen, the requirements accompanying the mission elements can be listed. These requirements follow from the IMAV rules and the fact that the team chose to have the mission be performed autonomously by the design [2]. The requirements and their identifier are listed in Table 3.18.

Table 3.18: Requirements following the chosen mission concept

ID	**Requirement**
IMAV-CR-ME1	All UAVs shall take off from the designated take-off area in the LCC
IMAV-CR-ME2	The system shall create a photomap of zone A within 10 minutes after the end of the mission
IMAV-CR-ME3	The system shall indicates all blockades in zone A on the photomap of mission element 2
IMAV-CR-ME4	All UAVs shall identify the building numbers of buildings in zone B
IMAV-CR-ME8-1	All UAVs shall land on the building with the flat roof in zone D
IMAV-CR-ME8-2	All UAVs shall remain at their position on the flat roof in zone D for at least 10 seconds
IMAV-CR-ME8-3	All UAVs shall take off from the building with the flat roof in zone D
IMAV-CR-ME10-1	All UAVs shall make a precision landing in the designated landing area in the LCC
IMAV-CR-ME10-2	All UAVs shall demonstrate airworthiness in case of rough landing
IMAV-AU-01	All UAVs shall fly towards mission elements autonomously
IMAV-AU-02	All UAVs shall perform each mission element autonomously

4

Payload Design

In Chapter 3, the mission elements that will be performed during the competition have been chosen. It was decided that the system will be designed to create a photomap of the competition ground, to find any road blockades and mark them on the photomap, to visually inspect and identify house numbers, to land on a flat rooftop as well as to take off and to land at the local command centre (LCC).

Now that the mission is clear, it is necessary to identify the various hardware components required to successfully complete the mission. The unmanned aerial vehicle (UAV) subsystems will be presented in this chapter and the selection process for the hardware will be shown as well.

Each section within this chapter presents the requirements on which the subsystem design is based, followed by all the design options. Afterwards, the selection process is explained and any necessary verification and validation done is presented. Finally, all sections end with a small discussion on the requirements generated or discarded during the section. Furthermore, it is noted that all payload is designed such that requirement *IMAV-AU-2* is satisfied, which states that: all UAVs shall perform each mission element autonomously.

This chapter begins with Section 4.1 discussing the on-board computer used to process any data collected by the payload subsystem. Next, Section 4.2 describes the object detection methods used to complete mission elements 4 and 8. Section 4.3 continues with an elaboration on the navigation subsystem, which involves the strategy with which a UAV moves from one location to another. This is followed by Section 4.4, which introduces the subsystem used to determine the location of the UAV. Section 4.5 investigates the subsystem needed to recognise numbers, which is important for the execution of mission element 4. Afterwards, Section 4.7 selects a data transmission system to transfer data between the ground station and the UAVs. Next, Section 4.6 describes all elements required to stitch the photomap. This is followed by Section 4.8 discussing the blockade mapping strategy and subsystem. Section 4.9 generates all requirements relating to the translational and rotational control accuracy required for each mission element. The ground station needed to support the UAVs is described in Section 4.10. Finally, Section 4.11 presents an overview of the chosen payload.

4.1. On-board Computer

The on-board computer will be used to process any data collected by the payload subsystem. This data may contain the numbers to be recognised, the command to take a picture for the photomap, the detection of an object or a check whether the UAV has landed. The on-board computer will thus act as a processor for the payload system. A multitude of options may be seen in Figure 4.1.

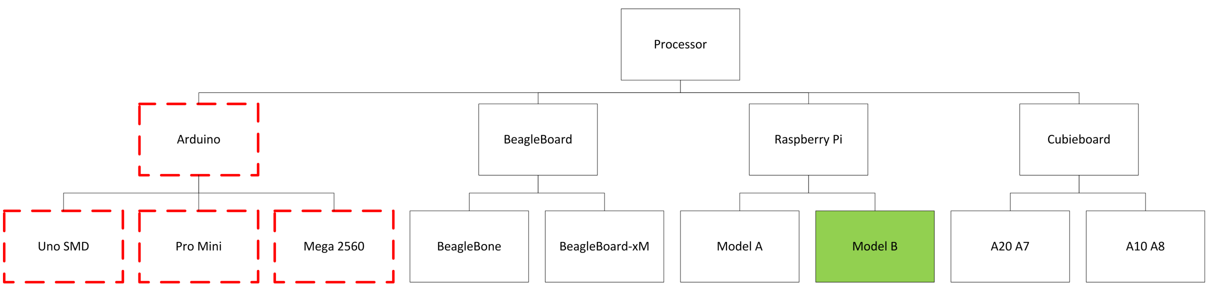

Figure 4.1: Design option tree for on-board computer hardware selection. The (red) dashed line indicates infeasible concepts, the (green) filled block indicates the selected concept.

4.1.1. Requirement Analysis

In order to decide on an on-board computer, the relevant requirements need to be analysed first. These relevant requirements may be seen in Table 4.1.

Table 4.1: The relevant requirements for the on-board processor subsystem

ID	Requirement
IMAV-CR-ME4	All UAVs shall identify the building numbers of buildings in zone B
IMAV-CR-ME8-1	All UAVs shall land on the building with the flat roof in zone D
IMAV-CR-ME8-2	All UAVs shall remain at their position on the flat roof in zone D for at least 10 seconds
IMAV-CR-ME10-1	All UAVs shall make a precision landing in the LCC

In the mid-term report (MTR) it was decided that the processing of the number recognition shall be done on board the UAV [1]. One of the consequences of this decision, is that the first requirement thus indicates that the on-board computer should be able to process obtained data, containing a building number. Furthermore, it is stated in the international micro aerial vehicle (IMAV) 2014 competition rules that the UAV should remain at the flat roof of mission element 8 for ten seconds [2]. In order to know when the ten second count should start, the system should be able to detect that it has landed. The second and fourth requirement of Table 4.1 therefore indirectly state that the on-board computer should be able to process the data of a sensor which detects a successful landing.

4.1.2. Design Option Selection

A number of the proposed design options may be found to be infeasible, by evaluating the design options and and the aforementioned requirements. Hardware specifications of the proposed design options may be found in Table 4.2.

Table 4.2: A multitude of hardware options for the on-board computer

Feature	Voltage (V)	Current (A)	Power (W)	RAM (MB)	Clock rate (MHz)	Mass (g)	Cost (€)
Raspberry Pi Model A [26]	5	0.46	1.75	256	700	45	35.99
Raspberry Pi Model B [27]	5	1.0	5	512	700	39	30
Cubieboard A10 A8 1GB [28]	5	2.0	10	1000	480	45	74.99
Cubieboard A20 A7 1GB [29]	5	2.0	10	1000	480	44	79.99
BeagleBone Black (rev C) [30]	5	2.0	10	512	1000	40	47.5
Arduino Uno SMD [31]	5	0.1	0.25	0.032	16	32	29.99
Arduino Mega 2560 [32]	5	0.0	0.2	0.25	16	41	24.99
Arduino Pro Mini 3.3V/8MHz [33]	3.3	0.15	1.8	0.001	8	2	7.15

It may first of all be noticed that the Arduino Uno SMD, Mega 2560 and Pro Mini barely have any random-access memory and that their clock rates are relatively low. As the system shall be able to process the measured data, containing a building number, it may be noted that the Arduino Uno SMD, Mega 2560 and Pro Mini are infeasible design options, as their random-access memory and clock rate are too little and too low for computer vision processing.

It may furthermore be noticed that the Cubieboard A10 and A20 are the most expensive single-board computers and that, amongst the remaining design options, the Raspberry Pi Model B is the cheapest option. With regards to the amount of Random-acces memory, the Cubieboard is the best option. The second best options are the Raspberry Pi Model B and the BeagleBone Black. However, the BeagleBone Black has a power consumption of 10 Watts due to its high clock rate of 1000 megahertz, whereas the Raspberry Pi uses only 5 Watts for a clock rate of 700 megahertz.

Lastly, it should be noted that the community of the Raspberry Pi Model B is the largest of the proposed design options [34]. This has as a result that the Raspberry Pi Model B is a very well documented option. Together with being the cheapest and lightest option, while still having a decent clock rate and amount of random-access memory, it may be concluded that the Raspberry Pi Model B is the best hardware design option for the on-board computer. The chosen- and infeasible options may also be found in Figure 4.1.

4.1.3. Verification & Validation

To validate the choice of using a Raspberry Pi Model B as the on-board computer, it was tested whether the Raspberry Pi could be configured and programmed from another computer and whether the single-board computer functioned accordingly. A Raspberry Pi was obtained and after installing several software packages it was successfully connected to and accessed by a computer running Windows 7. This indicates that the Raspberry Pi may be programmed and configured with the use of another computer and that the on-board computer does indeed function accordingly.

4.1.4. Additional Requirements

One additional requirement may be obtained from the design choice that was made with respect to the on-board computer. Requirement *IMAV-CR-ME4-1* states that: the hardware used as payload shall be compatible with the Raspberry Pi Model B. This will pose limitations on the payload selected in the remainder of this chapter.

4.2. Object Detection

Object detection will be needed to complete mission elements 4 and 8, which are the house number recognition and roof landing respectively. The system should be able to detect the roof for mission element 8, while it should also be able to detect the house numbers for mission element 4. Furthermore, the system should also detect any obstacles which may block the path of the UAV. Multiple options are available to fulfil this task. These options may be seen in Figure 4.2.

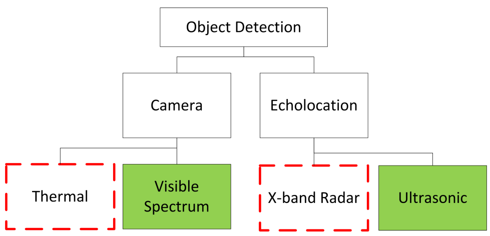

Figure 4.2: Design option tree for detection of objects. The (red) dashed line indicates infeasible concepts, the (green) filled block indicates the selected concept.

4.2.1. Requirement Analysis

In order to develop a detection subsystem, the relevant requirements need to be analysed first. These three relevant requirements may be seen in Table 4.3.

Table 4.3: The relevant requirements for the detection subsystem.

ID	**Requirement**
IMAV-CR-ME4	All UAVs shall identify the building numbers of buildings in zone B
IMAV-CR-ME4-1	The hardware used as payload shall be compatible with the Raspberry Pi Model B
IMAV-CR-ME8-1	All UAVs shall land on the building with the flat roof in zone D

Next to the requirements listed above, requirements may be found for each of the design options. These requirements may be found in Table 4.4.

4.2.2. Design Option Selection

With the use of the aforementioned requirements, several design options may be found to be infeasible. A thermal camera for example, requires an object and its surroundings to have a temperature difference of at least 1.5 degrees Celsius [35]. However, the IMAV competition has a training day two days before the match [36]. The objects will therefore be standing in the competition field for at least two days, which will result in

Table 4.4: The requirements that have been found for each of the possible design options.

Design Option	Requirement
Thermal Camera	The temperature difference between the object and its surroundings shall be at least 1.5 ° C .
Visible Spectrum Camera	The on-board computer shall be able to recognise objects using images with a resolution of TBD by TBD pixels
Radar	The self-developed software shall be completed before the IMAV 2014 competition.
Ultrasonic	The ultrasonic rangefinder shall only be used within a range of TBD metres from an object

an object and its surroundings to have approximately the same temperature. The use of a thermal camera is therefore infeasible.

Secondly, a radar does not have any pre-developed software. The software therefore should be developed before the IMAV 2014 competition. As the allocated development time is five weeks, it is deemed to be infeasible to develop the software in time. The use of an x-band radar is thus not possible.

A camera using the visible EM spectrum and echolocation with the use of an ultrasonic rangefinder remain as feasible design options. For identification of A4-sized sheets or numbers on such a sheet, a rangefinder is inadequate since it can only detect the presence of an object. The detection of numbers and sheets of A4 paper will therefore be done with the use of a camera.

The detection and localisation of an obstacle may be done with either stereo vision or an ultrasonic rangefinder. As stereo vision is computationally intense and requires adding a second camera, an ultrasonic rangefinder will be used to detect obstacles. The chosen- and infeasible options may also be seen in Figure 4.2.

4.2.3. Hardware Selection

Shown in table 4.5 are the specifications of a number of options for the camera. It may be noticed that there is a wide variety of masses, power consumptions and costs available.

Table 4.5: The specifications of a number of options for the on-board camera.

Device	Voltage (V)	Current (A)	Power (W)	Mass (g)	Resolution (-)	Fps (s^{-1})	Cost (€)
KX-171 FPV camera 420TVL [37]	12	0.1	1.2	52	500 x 582	50	75
Trust spotlight webcam [14]	5	0.5	2.5	91	1280 x 1024	30	13.11
Raspberry Pi Camera Module [38]	3.3	0.25	0.825	3	2592 x 1944	30	21

When comparing the power consumption, cost and resolution, the following may be noted: the Raspberry Pi Camera Module uses the second least amount of power and has a price of 21 euros. The Trust Spotlight webcam is the cheapest option, but it uses the most amount of power. With regards to the resolution, the Raspberry Pi camera module has by far the highest resolution. As a higher resolution improves the overview and the area the camera can cover [39], this is a desired characteristic. Furthermore, when noting that the Raspberry Pi camera module has specifically been developed for the on-board computer, the Raspberry Pi, combined with the second lowest power consumption, the highest resolution and the second lowest price, it may be concluded that it is the best hardware design option for the camera.

Several options may be found for the ultrasonic range finder. Specifications of these options may be seen in Table 4.6.

Table 4.6: A number of options for ultrasonic rangefinder and their specifications.

Device	Voltage (V)	Current (A)	Power (W)	Mass (g)	Accuracy (m)	Maximum Range [m]	Cost [€]
Maxbotix HRLV-EZ0 [40]	5.5	0.003	0.017	4.3	0.01	5.0	25.62
Maxbotix LV-EZ1 [41]	5.5	0.002	0.011	4.3	0.025	6.45	19.04
HC - SR04 [42]	5.5	0.015	0.083	15	0.003	4.0	2.57
XL-Maxsonar EZ1 [43]	5	0.003	0017	5.9	0.01	7.65	36.61

From these specifications the following may be noted: the HC-SR04 has the highest power consumption and mass. However, it is by far the most accurate and least expensive rangefinder. A pre-developed script and guide was found on how to attach the HC-SR04 ultrasonic rangefinder module to a Raspberry Pi Model B. This greatly decreases the development time and the development risks. Together with the high accuracy and low cost, the HC-SR04 Ultrasonic rangefinder module may thus be found to be the best design choice for the ultrasonic rangefinder.

4.2.4. Verification and Validation

Raspberry Pi Camera Module
The Raspberry Pi camera module may be validated with the use of literature. As mentioned earlier, it was found that the Raspberry Pi camera module has specifically been developed for the Raspberry Pi single-board processor. Furthermore, on-board computer, the Raspberry Pi Model B, has a dedicated port for this camera module [44]. As a detailed set-up guide has been found for the Raspberry Pi camera module, it may be confirmed that the module works with the Raspberry Pi Model B on-board computer [45].

HC-SR04 Ultrasonic RangeFinder Module
The HC-SR04 ultrasonic rangefinder module has been validated with a test. First, the rangefinder module was attached to a Raspberry Pi Model B. Then, a Python script developed by Raspberry Pi Spy was used to measure the distance to an object [46]. The script had the ultrasonic rangefinder do three measurements and return the average measured distance of these three measurements. The test set-up used in order to do the distance measurements may be seen in Figure 4.3.

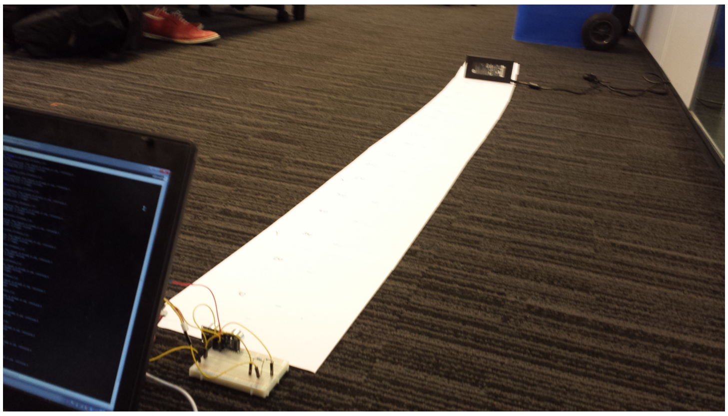

Figure 4.3: The set-up used for the verification and validaiton of the ultrasonic rangefinder.

Two measurement series were performed. The first measurement series resulted in the absolute error over a distance of 10 to 240 centimetres. The result of these measurements and their moving average may be seen in Figure 4.4. It may be noted that the error increases from 0.3 to 12 centimetres. This maximum error of 12 centimetres was measured at a distance of 230 centimetres, thus resulting in an error of 5.3 percent. It can also be seen that there is a decrease in the absolute error at a distance of 210 centimetres. It is recommended to further identify the cause of this decrease in the post-DSE phase of the development.

A second measurement series was performed to measure the measurement error over time. The results of these measurements and their moving average may be seen in Figure 4.5. The error in the measured distance was measured with respect to the actual distance of 190 centimetres to an object. It may be noted that there are three outliers. These outliers might have occurred due to a vibration of the rangefinder or due to environmental noise. The precise cause of these outliers may be investigated in the development stage of the system. It may also be seen that the average measurement error is approximately -2 centimetres. The minus sign indicates that the ultrasonic rangefinder measured a distance smaller than the actual distance.

It should be noted that the accuracy of the ultrasonic rangefinder may be improved in the development stage of the system. These tests validate that the ultrasonic rangefinder works correctly in combination with the Raspberry Pi Model B.

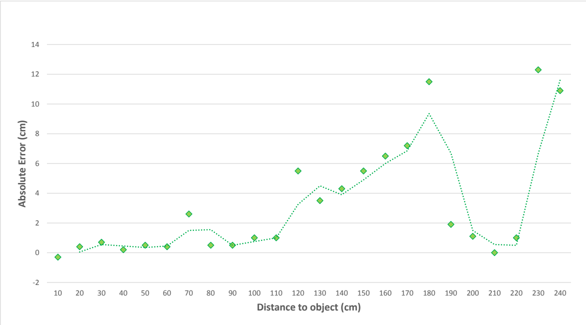

Figure 4.4: The results of the first measurement series, measuring the absolute error over a distance of 10 to 240 centimetres.

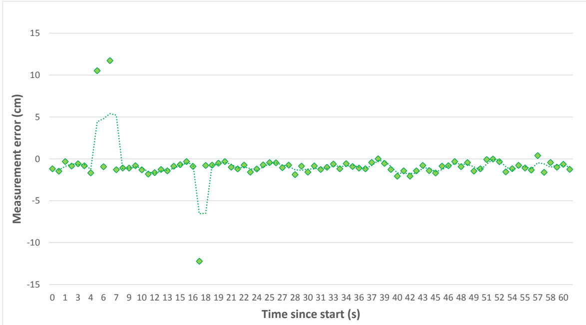

Figure 4.5: The results of the second measurement series, measuring the absolute measuring error over time.

4.2.5. Additional Requirements

Additional requirements may be obtained from the design choices that have been made in this section. Requirement *IMAV-CR-ME4-3* states that: the ultrasonic range finder shall only be used within a range of 4 meters from an object. Requirement *IMAV-CR-ME4-4* states that: The on-board computer shall be able to recognise objects using images with a resolution of 2592 by 1944 pixels.

4.3. Navigation

Navigation involves the strategy with which a UAV moves from one location to another. It is an aspect of the design relevant to every mission element, as every mission element requires the UAV to move to a certain location. Failure to get to a target destination can result in failure of a mission element, which will decrease the total score.

Section 4.3.1 shows the design option tree (DOT) for navigational strategies. Section 4.3.2 describes the requirements relevant to the topic of navigation and shows design options to meet these requirements. Section 4.3.3 elaborates on the choices made with respect to these options. Following from the navigational choices, the required autopilot system is elaborated upon in Section 4.3.4, followed by the manual control system in Section 4.3.5.

4.3.1. Design Option Tree

Various strategies can be used to get a UAV from one location to another. A multitude of options is depicted in Figure 4.6. For autonomous flight, two options are present. One is that the UAV-system itself determines in which direction it will fly at each moment. This is denoted as System-Set Waypoints. The other is that the flight directions are pre-programmed in a so-called flight plan. This option is denoted with Pre-Set Waypoints. Requirements associated with specific design options are given in the following section.

4.3.2. Requirement Analysis

In order to develop a navigational subsystem suited for the mission of this project, a requirement analysis is made. Requirements relevant to the navigation capability of the UAV system that have been generated during the project are listed in Table 4.7. Next to these requirements, each design option as shown in Figure 4.6 has characteristics that influence the design once such an option is chosen. In order to understand the effect of a design option choice, an overview of the most relevant design option characteristics is given in Table 4.8.

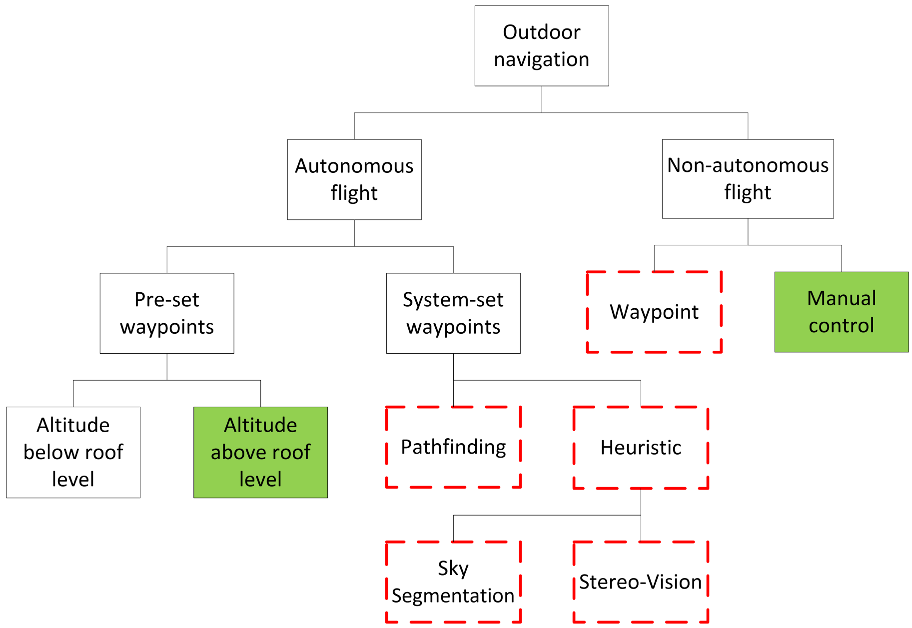

Figure 4.6: Design option tree for strategies of navigation. The (red) dashed line indicates infeasible concepts, the (green) filled block indicates the selected concept.

Table 4.7: The requirements related to the topic of navigation.

Requirement ID	**Description**
IMAV-AU-01	All UAVs shall fly towards mission elements autonomously
IMAV-AU-02	All UAVs shall perform each mission element autonomously
IMAV-CR-ME4-1	The hardware used as payload shall be compatible with the Raspberry Pi Model B
IMAV-CR-ME8-1	All UAVs shall land on the building with the flat roof in zone D
IMAV-CR-ME8-3	All UAVs shall take off from the building with the flat roof in zone D
IMAV-CR-ME10-1	All UAVs shall make a precision landing in the designated landing area in the LCC
IMAV-SR-07	The system shall store the last reliable position of all UAVs
IMAV-SR-12	The UAV shall return to the center waypoint after entering the orange zone
IMAV-SR-13	All UAVs shall never enter the red zone
IMAV-SR-14	The UAV shall perform an emergency landing after entering the red zone
IMAV-SR-15	The UAV shall perform an emergency landing in case of a navigational loss
IMAV-SR-20	The team shall be able to manually take over control of all UAVs
IMAV-SR-29	The GPS coordinates of all UAVs shall be shown on the ground station during the mission, when GPS is used

4.3.3. Design Option Selection

Now that multiple options have been identified, research is performed on the various strategies and their characteristics in order to see which ones are feasible for this design project. Ultimately a choice is made for the option that meets the requirements best.

Stereo vision is a processor-intensive process [47]. This is not beneficial, as this process should run continuously, being the main method of navigation. It could leave little processing capabilities for other functionalities like on-board number recognition and any delay in the process poses the risk of collision with the environment. Therefore the option of stereo vision is deemed infeasible for this design.

The sky segmentation method is deemed not usable as sole navigational method for activity below the skyline. This is because this method is based on distinguishing sky from non-sky, allowing for movement towards objects contrasting with the sky-region [48]. Activity below the skyline is however aimed for, for example for

Table 4.8: Characteristics of design options for the navigation strategy.

Design Option	Characteristics
Waypoints below roof level	Autopilot, knowledge of safe flight paths at low (sub-skyline) altitude, in-horizontal-plane obstacle detection, location determination system applicable at low altitude, ground station.
Waypoints above roof level	Autopilot, knowledge of safe flight paths at object-sparse or -free altitude, ground station.
Pathfinding	Autopilot, pathfinding software compatible with or convertible to autopilot input, software-compatible map with correct fly/non fly regions.
Heuristic* stereo vision	Autopilot, two cameras, computational software to determine distance to objects and recommended flight path, additional system to get to specific target location.
Heuristic* sky segmentation	Autopilot, computational software, navigational target contrasts with sky above horizon. For sub-skyline target location: additional system to get to specific target location.
Non-autonomous waypoint	Autopilot. Ground station able to instruct autopilot, with user input capability
Manual control	Transmitter and receiver, UAV in line-of-sight or telemetry feed at sufficient update frequency.

*Heuristics is the name given to the strategy that the UAV flies in the general direction of the target location and uses situational awareness to detect and avoid obstacles in its way.

approaching correct houses and their house numbers. It would therefore need another system that allows navigation towards mission elements that have target positions below the skyline. This makes the sky segmentation method too complex for the available resources.

The pathfinding method is crossed out as it requires the combination of an efficient pathfinding algorithm with correct fly-/no-fly region information, which must be put in a format usable by the algorithm. This input should also include mission element locations and required UAV orientation at those locations. The result of the pathfinding process should then be converted to information that an autopilot can work with. These steps require software that is not pre-developed, of which the development is expected to exceed available resources.

Waypoint navigation is deemed a viable option, as autopilot systems are known to exist that are able to perform this functionality autonomously using a global navigation satellite system (GNSS). A map with coordinates of the competition area is available, which gives the system operator the required information to determine mission waypoints for a flight plan. Furthermore, following a flight plan requires less processing power on the UAV than the other options, like computer vision. These considerations make pre-set waypoints the most feasible navigation option for this mission. The related choice for an autopilot system is described in Section 4.3.4.

Flight Below Roof Level versus Above Roof Level

As the DOT in Figure 4.6 shows, waypoints allow for two strategies, being flight below roof level and flight above roof level. First the possibility of flight below rooftop level, flying a few metres above the roads, is researched. This flight level has great potential for the achievement of mission elements: it allows for blockade mapping (mission element 3) to be performed on location, using the forward oriented range finder. Furthermore, this flight level allows for a more straightforward strategy for finding house numbers (mission element 4) than flying at high altitudes, as these numbers are located at a low altitude.

However, two main reasons were found to why sub-skyline flight is infeasible. Firstly, the accuracy of a satellite system required for waypoint navigation is inadequate at sub-skyline level. This is due to multipath effects and a decreased satellite coverage. Satellite signals are refracted by objects like houses, which negatively affects the accuracy of location determination by a satellite system. Furthermore, these objects result in a diminished satellite coverage, due to them blocking the UAVs view of the sky. Research into global positioning system (GPS) accuracies in urban areas has shown that location readings may be off by 20 metres or worse [49]. This

level of inaccuracy is unacceptable when a UAV is to fly over roads with buildings nearby.
Secondly, wind around objects creates turbulent flows at sub-skyline altitude. The risk of a UAV drifting into objects like trees and thereby crashing is unacceptable, as it results in loss of points and valuable hardware. Because of the reasons stated, the autonomous navigation method chosen is the use of pre-set waypoints at high altitude, that is: above house tops.

Next to autonomous flight, it is chosen to enable manual control of a UAV by an operator on the ground. This is because requirement IMAV-SR-20 (see Table 4.7) states this need, which is based on safety considerations. Because the possibility that an autonomous system malfunctions is present, one wants to be able to take over control once it does. For example, requirements state that the UAV is not allowed to enter the red zone and should make an immediate emergency landing once it does. If the autonomous system seems not to do so, control will be taken over and it will be done manually. Furthermore, manual control allows for testing of the design during the assembly phase. The hardware involved with manual control is described in Section 4.3.5.

4.3.4. AUTOPILOT

Multiple autopilot systems exist that take care of the waypoint navigation of the UAV. Such a system consists of a ground station, an autopilot board on each UAV, software running on both the ground station and the autopilot board and finally a communication link between the ground station and the UAVs [50]. The ground station is used to show and store the UAV positions obtained through the communication link. Section 4.10 elaborates on the ground station requirements and hardware. The current section describes the choice of an autopilot software and hardware. Several of the autopilot software options are listed in Table 4.9.

Table 4.9: Various options for autopilot systems.

System Option	Characteristics
Paparazzi	Open source. XML-based, optionally graphical waypoint flight planning with extensive options, hardware-in-the-loop (HITL) simulation capability, telemetry to ground station. Linux-based. [50]
OpenPilot	Open source. Ground control software compatible with major computer operating systems, HITL simulation capability, telemetry to ground station. Waypoint flight planner in development. [51]
ArduPilot	Open source. Graphical waypoint flight planning, HITL simulation capability, telemetry to ground station. [52]

The chosen autopilot system is Paparazzi. This is mainly because of the extensive options that it has regarding flight plans, which incorporate waypoint navigation[53]. This allows for the design of a complex autonomous flight plan, capable of performing the chosen mission elements for the IMAV 2014. Furthermore, it allows for a logical tree of autonomous decisions to be used in-flight [54], which allows for meeting requirements such as the avoidance of certain no-fly zones and performing return-to-home flights or emergency landings once it enters a no-fly zone or loses communication.

For use in real-life search and rescue (SAR) missions, a graphical user interface for the creation of a flight plan is preferred over one that needs to be written, as intuitive graphic planning is expected to cut down the flight plan preparation time of the UAV operator. Both ArduPilot and Paparazzi have a graphical user interace [55] [50], but ArduPilot looks more accessible than Paparazzi in this matter. As Paparazzi flight plans are written in extensible markup language (XML), a simple and flexible information format [56], it is expected that improvement of the operator-friendliness of the graphical user interface can be achieved.

HARDWARE SELECTION

Having chosen the software for autopilot navigation, the choice for hardware can be made. Table 4.10 shows several options regarding autopilot boards that are compatible with Paparazzi [57].

Table 4.10: Hardware options for autopilot boards compatible with the Paparazzi autopilot.

Feature	**Lisa/L v1.1 [58]**	**Lisa/M v2.0 [58]**	**Lisa/S [58]**	**NavGo v3 [58]**
Clock	72MHz	72MHz	72MHz	60MHz
IMU	no	Aspirin	yes	yes
Magnetometer	?	?	yes	yes
Barometer	yes	yes	yes	yes
GPS	no	no	yes	no
UART	3 & 1RX	2 & 2RX	1 & 1RX	2
GPIO	?	1	0	0
Weight	30 g	9.9 g / 10.8 g (with Aspirin)	2.8 g	?
Dimensions	100 x 50 mm	34 x 60 x 10 mm	20 x 20 5 mm	35 x 35 mm
Typical usage	Advanced payload and controls development using Gumstix; fixed-wing or rotorcraft	Small, general purpose with IMU; fixed-wing or rotorcraft	?	Small, general purpose with IMU; rotorcraft
Availability documentation	medium	high	low	medium
Cost	€ ?	€169 with Aspirin, €92 without [59]	€235 with GPS, €206 without [60]	€ ?

The board that is chosen for this design is the Lisa/M v2.0. It is light-weight and medium-sized (compared to other options), has multiple universal asynchronous receiver/transmitter (UART) ports and a general-purpose input/output (GPIO), which can be used to connect hardware like the Raspberry Pi onboard processor and a GNSS receiver. A significant advantage of the Lisa/M v2.0 is that documentation on this board and its pin-out is readily available, more so than the other options. According to staff of the Delft University of Technology (TU Delft) Micro Aerial Vehicle Laboratory (MAVLab) it is one of the cheapest in its class, which is beneficial as multiple UAVs are involved in the design and a limited budget is available. Lisa/M is also readily available, as opposed to the Lisa/S and NavGo. Limited availability before August 2014 is a significant disadvantage for the other options, as time is a sparse resource between the design synthesis exercise (DSE) and the IMAV competition day. Furthermore Lisa/M v2.0 has a recommended inertial measurement unit (IMU), namely one of the brand Aspirin, of which the newest unit is version 2.2. The Lisa/M v2.0 board can be bought with the Aspirin v2.2 IMU attached, thereby verifying their compatibility[59]. Deeming the Aspirin a viable design option, see Section 4.4, the choice for Lisa/M v2.0 is made in conjunction with the Aspirin v2.2.

In order to get telemetry of this autopilot board to the ground station, a data link is required. Paparazzi recommends a telemetry baud rate of 57 600, which can be approximated by 7.2 kilobytes per second[61]. This data rate is therefore used as an input for the choice of a data link in Section 4.7.

Verification & Validation

The applicability of Lisa/M v2.0 is verified by conversing with staff of the TU Delft MAVLab. The TU Delft has been using this board successfully on multicopters. A demonstration of a quadcopter with this board has been given during the project, which showed its rapid attitude control. Lisa/M v2.0 is therefore deemed an appropriate choice.

4.3.5. Manual Control

Requirement Analysis

For safety reasons and to save points, one would want to be able to manually control any UAV that may behave differently than expected. Manual control involves a transmitter and a receiver that are compatible with each other. This compatibility may involve a specific transmitter module inside the handheld transmitter. Furthermore the receiver should be compatible with the autopilot board. Options for these units are shown in Table

4.11.

Hardware Selection

Table 4.11: Hardware options for manual control transmitters and receivers

Part	Brand	Specification	Channels	Cost	Source
Transmitter	Turnigy	9XR (no module)	9	€37.08 [62]	[63]
Transmitter	Spektrum	DX7S, with AR8000 receiver	7	€220.60	[64]
Transmitter module	OrangeRX	DSMX/DSM2 2.4Ghz Transmitter Module (JR/Turnigy compatible)	(N/A)	€22.13	[65]
Receiver	Spektrum	AR8000 DSMX receiver	8	€95.59	[66]
Receiver	Spektrum	SPM9645 DSMX remote receiver	multiple through single JST-connection	€25.73	[67]

The Spektrum DX7S is sold together with the AR8000 receiver. This receiver however features 8 physical channels. Physical channels, which are to be connected to individual servo's, are not needed however. This is because only a single connection to the autopilot, able to transmit the various input signals received from the transmitter, is required for this design. This can be achieved by using a Spektrum SPM 9645 DSMX remote receiver [68]. To make the cheap Turnigy 9XR compatible, the compatible OrangeRX DSMX transmitter module is used. In the OrangeRX transmitter manual it is stated that the unit is able to bind to 5 unique receivers, which means that a single transmitter can be used on a maximum of 5 UAVs without having to make a new connection with one of them, given that a binding process has been performed once before.

Verification & Validation

Tthe TU Delft MAVLab uses the Turnigy 9XR for manual control of multicopters, thereby verifiying its usability. The Spektrum SPM9645 remote receiver is mentioned by Paparazzi as a unit that works well and is simple to connect [68].

Additional Requirements

During this section, new requirements have been generated flowing from the use of an autopilot system and the choice for manual control functionality. These requirements are summarised in Table 4.12.

Table 4.12: Additional requirements following from the choice for an autopilot system and manual control functionality

Requirement ID	Description
IMAV-AU-13	The ground station shall have paparazzi ground control station-software available for telemetry
IMAV-AU-13-1	The ground station shall have a ground station based on the Linux Operation System
IMAV-AU-15	The system shall have a communication link able to handle 7.2 kB/s between the ground station and the autopilots of all UAVs
IMAV-SR-20-1	The system shall have one manual transmitter available for every five UAVs

Next to these requirements, the choice for the Paparazzi autopilot results in the need for a GNSS receiver, an attitude sensor and an altitude sensor on board of the UAV [50]. These are discussed in Section 4.4 which covers the topic of location determination.

4.4. Location

The location of each UAV must be known for multiple reasons. The UAVs on-board autopilot requires input on the current location in order to know whether the UAV is at the location it has to be. Furthermore, the system and the operator must know where the UAVs are located in order to ensure that an UAV will not surpass the boundaries of the allowed flight zone set by the IMAV regulations [4]. This functionality is relevant to all mission elements.

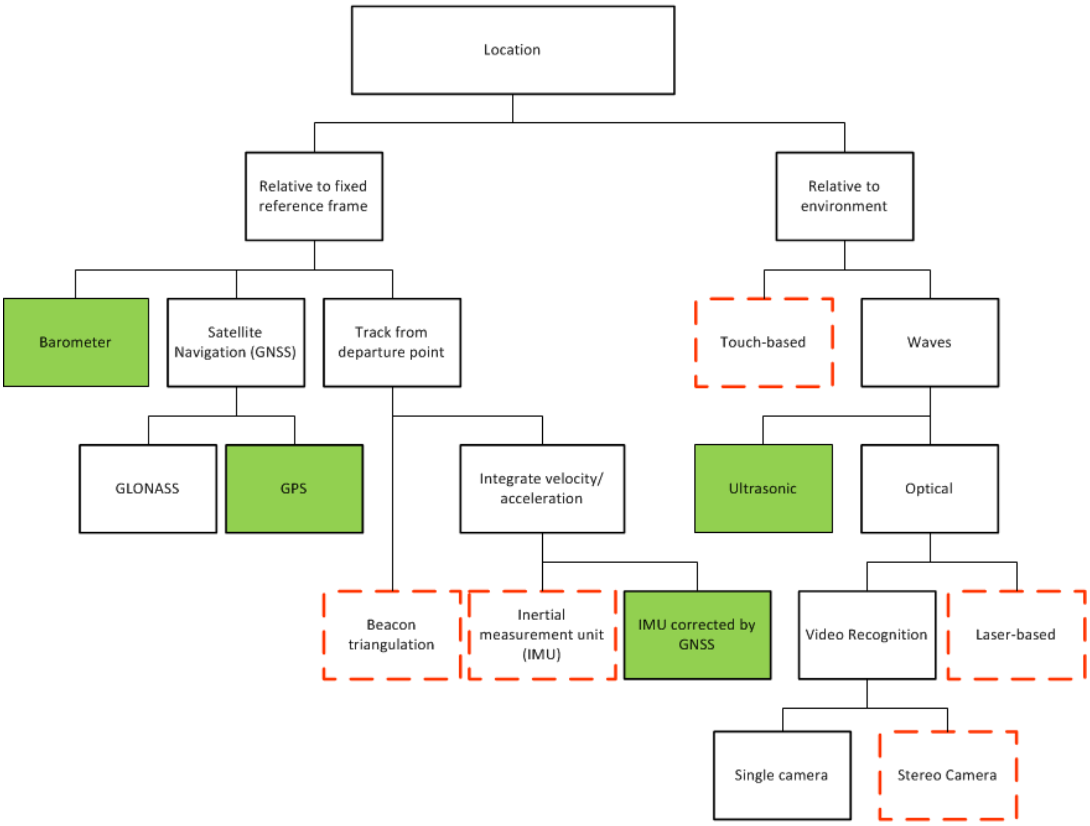

Figure 4.7: Design option tree for determination of UAV location. The (red) dashed line indicates infeasible concepts, the (green) filled blocks indicate selected concepts.

4.4.1. Requirement Analysis

There are multiple requirements relevant to location determination. As was stated in Section 4.3, the choice for the Paparazzi autopilot results in the need for a GNSS receiver, an attitude sensor and an altitude sensor on board of the UAV. Additionally, requirement *IMAV-CR-ME8-1* plays a part in this section, which states that: all UAVs shall land on the building with the flat roof in zone D. Furthermore, *IMAV-CR-ME4-1* is relevant for this section as all hardware used as payload shall be compatible with the Raspberry Pi Model B.

4.4.2. Design Option Selection

Multiple options exist that may fulfil the functionality of determining the location of a UAV. These are depicted in a DOT in Figure 4.7. This section describes which of the options are chosen and the corresponding hardware choices that were made.

Global Navigation Satellite System

Two GNSSs are currently operational, namely the American GPS and the Russian GLONASS. The one generally used in Paparazzi systems is GPS; GLONASS is not mentioned on the website [69]. GPS was therefore the initial candidate. For this design, the possibility of a multi-constellation system was also researched. Because this project is related to urban areas, which have buildings that could diminish the view of the sky, coverage is an aspect of interest. Addressing both the GPS and GLONASS constellation could increase coverage. A field test was performed for this hypothesis by using three smartphones that could receive both constellations, see Figure 4.8. This test showed that, on that particular time and day, the number of satellites in view increased between 28% and 45% with the use of GLONASS and GPS satellites as opposed to GPS satellites only. A multi-constellation receiver is therefore, if available, a preferred option.

Figure 4.8: Smartphones used in a field test on satellite coverage. Filled circles indicate GPS satellites, filled triangles indicate GLONASS satellites.

Attitude Sensor

A Paparazzi-supported type of attitude sensor is the IMU. This is a unit that senses attitude based on three-axes gyroscopes and three-axes accelerometers (six degrees of measurement), with possibly an additional three-axes magnetometer (nine degrees of measurement) [70]. All Paparazzi autopilot boards support this type of sensor [50], making it a feasible option to fulfil the functionality of attitude determination.

Altitude Sensor

At least two types of sensors are supported by Paparazzi that can be used to determine altitude [50]: one is a barometer, based on barometric pressure, the other is an ultrasonic rangefinder, based on sound propagation. A barometer can determine an absolute altitude, relative to a pressure that is set as ground level. An ultrasonic rangefinder can determine a distance relative to its direct environment.

Both methods are chosen to fulfil the functionality of altitude determination of this design. A barometer is chosen as main altitude sensor for the autopilot waypoint navigation. An ultrasonic range finder is chosen, which is to be attached to the UAV with a nadir orientation, to determine the altitude of the UAV relative to its direct environment. The latter can be used in order to determine the vertical distance between the UAV and the roof on which it is supposed to land (requirement IMAV-CR-ME8-1).

Landing Sensor

The UAV is required to perform the roof landing of mission 8 autonomously (requirement IMAV-CR-ME8-1). A sensor that can determine whether the UAV has landed is a valuable addition to the design: thrust can be cut at the instant the UAV touches down, in order to diminish the chance that the UAV drifts from its location during its landing attempt or even that a touchdown is falsely signalled, that is when the UAV is still in flight, which could have damaging consequences for the UAV.

Sensors that might be used for determining a touchdown are distance measurement sensors (like the already present ultrasonic rangefinder), an accelerometer (already present in the IMU) that detects a deceleration, or a pressure sensor. From these options, the first two are deemed less responsive than a direct pressure sensor, while one would want the thrust to be cut at the instant of touchdown, as stated before. Therefore the choice is made for a push button. This is a generally lightweight, small and cheap sensor that gives an output when enough pressure is applied such that the button is pressed. A choice for the exact hardware is made in Section 4.4.3.

4.4.3. Hardware Selection

Now that choices have been made for certain design options, the specific hardware corresponding to these choices has to be determined. This section describes the hardware that was chosen in agreement with the chosen design options.

Global Navigation Satellite System

For the selection of the GNSS receiver, multiple units were considered. Modules from the brand U-blox were researched, as this brand is renowned for its high performance [69]. Because of ease-of-integration reasons combined with a stringent time schedule within which the design is to be built, only modules readily available were considered. This included modules from the 6-series. An available multi-constellation receiver was found of the 8-series. The compared hardware is shown in Table 4.13. The circular error probable (CEP) for a GPS system, is the radius of a circle, centred about the mean, whose boundary is expected to include 50% of the location readings [71].

Table 4.13: Hardware options for GNSS receivers

Feature	**U-blox LEA-6H [72]**	**U-blox NEO-6M [73]**	**U-blox NEO-M8N [74]**
CEP	2.5 m	2.5 m	2.0 m
CEP with SBAS	2.0 m	2.0 m	
Antenna	25x25 mm patch	18x18 mm patch	dual band GPS and GLONASS
Connection	UART (with 6-pin JST)	UART (with 4-pin JST)	UART, USB
Acquisition cold/hot start	26/1 s	27/1 s	26 s
Sensitivity cold/hot start	-148/-157 dBm	-147/-156 dBm	-148/-156 dMb
Backup battery	yes	yes	yes
Cost	€40.36	€12.98	€58.78
Weight	28 g	18 g	24 g

The NEO-M8N is an interesting unit because it is capable of connecting with GLONASS space vehicles. However, it is marked an *evaluation* board, connecting with USB. The applicability to flying vehicles is therefore questioned because the design is meant to be buildable before August 2014, when the IMAV 2014 takes place, it is crossed out. Research into this module and others capable of connecting with GLONASS in addition to GPS is recommended for future development of the system.

The specifications of the U-blox LEA-6H and NEO-6M are very similar. The module with the NEO-6M engine however has a lower cost and weight, which are both advantageous. Therefore the NEO-6M module is chosen.

Concerning the accuracy of the GPS, only the CEP is given as a measure for accuracy, which involves a 50% certainty. A measure with a higher certainty is wanted for the accuracy of the location determination, in order to allow the design of the operations involved in performing the mission. According to ir. C. de Wagter of the TU Delft MAVLab, the radius of a location estimate of a GPS system is in practice approximately 5 metres, with a 95% certainty. From this, a new requirement is generated for the operations design, see Table 4.15 at the end of this section.

Inertial Measurement Unit

The choice for hardware of the IMU was made in conjunction with the Lisa/M v2.0 autopilot. An Aspirin IMU was recommended for the autopilot board. The autopilot can be ordered with an Aspirin v2.2 pre-soldered, which made this the prime candidate, as this verifies the possible integration of these two components. It is noted however that, in order to decrease interference effects, the IMU is chosen to be placed away from the autopilot board and Raspberry Pi. Furthermore, the Aspirin v2.2 was found to be a 10-degrees of measurement unit, involving a 3-axes gyroscope, 3-axes magnetometer, 3-axes accelerometer and a barometer. As this combines the wanted 9-degrees of measurement and barometer, the choice was made to use the Aspirin v2.2. Specifications identifying the hardware inside this IMU are given in Table 4.14.

Table 4.14: Hardware specifications for the Aspirin v2.2 IMU [59].

Part	**Brand**	**Model**	**Specification**
Barometer	Measurement Specialties	MS5611-01BA03	
Accelerometer	InvenSense	MPU-6000	3 axes
Gyroscope	InvenSense	MPU-6000	3 axes
Magnetometer	Honeywell	HMC5883	3 axes

Barometer

A barometer is present in the chosen Aspirin v2.2 IMU, which is a unit of the brand Measurement Specialties, model MS5611-01BA03. A separate barometer is not required.

Range Finder

The specific hardware selection concerning the range finder is done by using the same model as is chosen for object detection, see Section 4.2. This is the HC-SR04 ultrasonic range finder module. For object detection, the range finder is placed horizontally. The range finder that follows from the current section however, used for navigational purposes, is to be placed vertically downwards. It is therefore an additional unit.

Push Button

Push buttons are used as landing detection sensors. A lightweight, cheap and small unit of the brand SparkFun was chosen. This unit, which is designated as model COM-09190, costs €0.50 each, with a weight of 1.0 grams and dimensions of 12 by 12 millimetres[75]. In order to be sure to detect a landing as soon as a touchdown is performed, it is chosen to include a push button at every strut of the landing gear of the UAV design.

Verification & Validation

According to Paparazzi, Lisa autopilot boards are designed for use with a U-blox 4-, 5- and 6-series GPS receiver that can handle the UBX protocol [76]. The NEO-6M complies with both requirements and is therefore deemed verified for use with the Lisa/M v2.0 autopilot. The Aspirin v2.2 IMU is verified by it being order-able pre-soldered to the Lisa/M v2.0 autopilot board. Transition Robotics would not be able to do this for long if these pieces of hardware would not be able to communicate correctly. The HC-SR04 range finder verification has been given in Section 4.2.

Additional Requirements

In this section on location determination, multiple new requirements have been generated. To conclude this section, an overview of these requirements is given in Table 4.15.

Table 4.15: Requirements following from hardware used for location determination.

Requirement ID	**Description**
IMAV-AU-12	All UAVs shall have one nadir orientated ultrasonic rangefinder
IMAV-CR-ME8-13	All UAVs shall have a sensor that indicates a landing
IMAV-AU-11	Navigational waypoints shall be chosen with a 5 metres clear-of-obstacles radius in the horizontal plane

4.5. Number Recognition

In the following section, and investigation is made into the requirement of number recognition. The former obtained object recognition DOT, which includes all design options, may be seen in Figure 4.9. This DOT follows from the requirement *IMAV-CR-ME4*, which states that: all UAVs shall be able to identify the building numbers in zone B. Furthermore, the hardware used as payload shall be compatible with the Raspberry Pi Model B, as stated by requirement *IMAV-CR-ME4-1*.

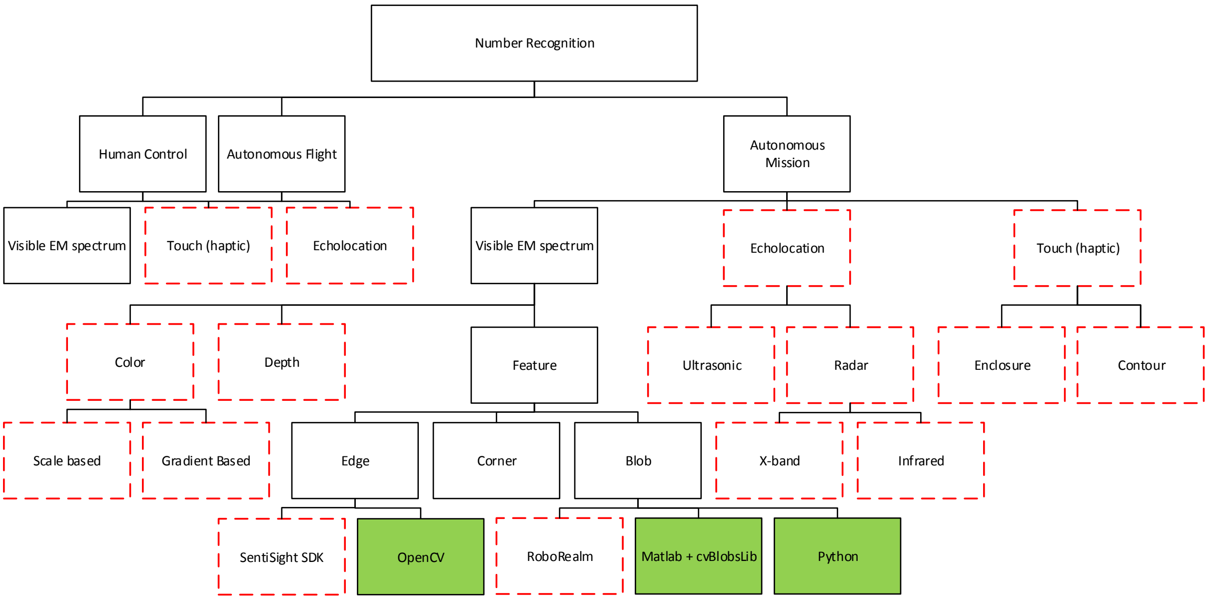

Figure 4.9: Design option tree for object recognition. The (red) dashed line indicates infeasible concepts, the (green) filled block indicates the selected concept.

As object recognition now only consists of the recognition of numbers, some infeasible concepts can be crossed out immediately. The use of touch or haptics is not possible, as is the use of echolocation due to the two-dimensional nature of numbers printed on a sheet. The only feasible design option is the use of the visible electro-magnetic (EM) spectrum. Three different methods can be distinguished within the use of the visible EM spectrum, namely depth, color and feature based object recognition [77] [78]. The use of depth can also be eliminated for the same reason as haptics and echolocation were found to be infeasible. Number recognition on a paper can be divided into two functions; the recognition of the white sheet and the recognition of the number. The software available to perform these two functions is divided into RoboRealm, Sentisight SDK, OpenCV and either Matlab or Python using libraries of the latter. As Roborealm and Sentisight are relatively expensive, the free-ware of OpenCV is preferred. In order to check whether the tasks can actually be performed and with which method of object recognition, some tests are performed.

4.5.1. Number Recognition Test

The first test is to check or verify whether recognising numbers on a sheet is possible. The next section describes this test from methodology to conclusion.

Methodology

When recognising the number on the sheet, the software uses a Hough transform which makes use of feature extraction [79]. The code is written in Python and can therefore be run on the on-board processor. The function that is used is the ’pytesser’ function which is based on OpenCv libraries [80]. The software was adjusted such that a ’z’ will be transformed into a ’2’, as it was noted that this was a common error in the output. The output of the software is given in a text file with all the numbers that were found. Afterwards, the correct numbers are manually filtered out.

Test Set-up

A sheet with a number was hung on a wall. The distance with respect to the webcam of the laptop was measured and increased by steps of 0.25 metre in a range from 0.5 to 2.5 metres. For each measurement, ten photos were taken and the recognition software was applied. The entire test was performed twice in order to test consistency. Furthermore, the lighting conditions were observed as well. A picture of the test set-up may be found in Figure 4.10.

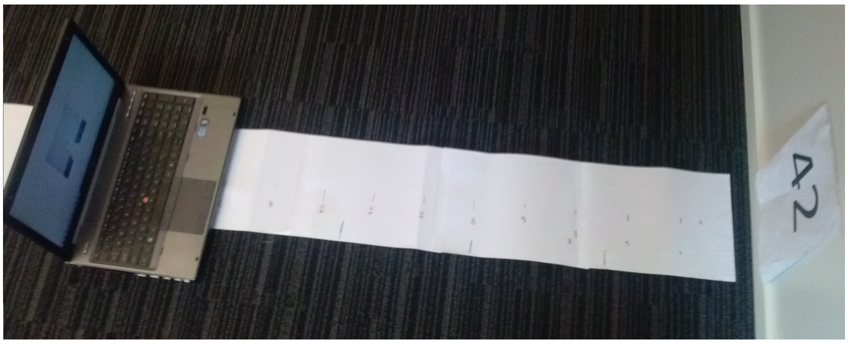

Figure 4.10: Test set-up for the number recognition test showing a laptop with recognition software and a distance indicator.

Experimental Results

Two tests were performed in which the amount of positive results was determined. These two tests were then put into a graph, as can be found in Figure 4.11. As can be seen in the figure, the optimal distance for this set-up is 1.5 metre with a margin of 0.5 metre. In order to obtain these numbers for the Raspberry Pi camera, experiments should be performed with this camera, otherwise the results will have to be scaled. Furthermore, it was found that lighting conditions affect the number of positives and that an optimal resolution can be found.

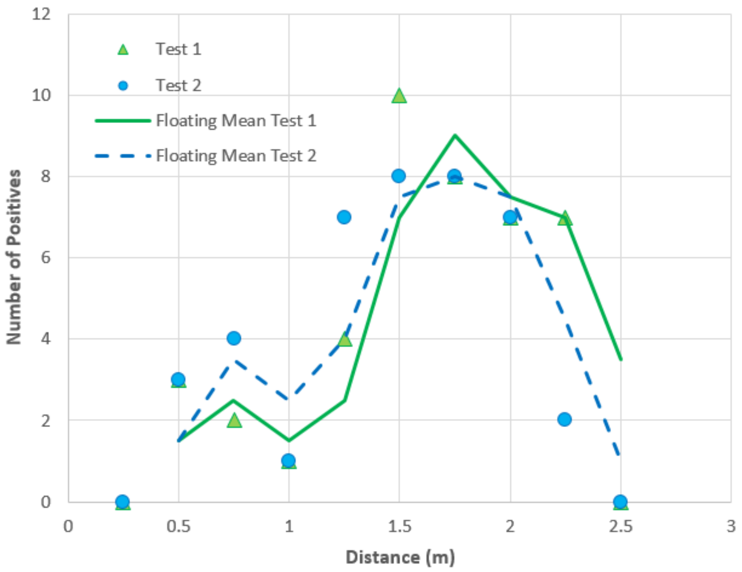

Figure 4.11: The results of the number recognition experiment, showing the number of positive results out of ten, versus the distance from the sheet

Verification and Validation

Not only the number of correct results was determined, the number of false positives or recognitions of other numbers was determined as well. It was found that a occasionally 2's and 4's were recognised if the current number was 42. This indicates that further calibration could enhance the performance of the software. Furthermore, false positives in shape of numbers other than 4's and 2's were recognised, though not as much and consistent as the previous false positives. As the test was performed twice, the outcome was verified.

Conclusion

Number recognition seems to be possible to do with pre-developed software, even though the impact of other camera specifications of the Raspberry Pi camera module still need to be taken into account. For this first experiment a distance of 1.5 metre followed as an optimal distance from the sheet. The reliability was high enough to have confidence in the script as being a design option.

4.5.2. Sheet Recognition Test

Next to recognising numbers, the sheet the numbers are printed upon should be located as well, in order to make the recognition of the number easier. The following section describes the test that was performed in this respective field. Again first the methodology is discussed, followed by a test set-up and the experimental results and ending with a verification,validation and conclusion.

Methodology

The software used is written in Matlab and the methodology was already available on the internet [81]. RGB color vectors are used, converted into binary images and then blob detection is applied [82]. Finally, a filter gives the result that was asked for. A constant tracking of the white paper is performed.

Test Set-up

The Matlab-written code is run on a personal laptop. A white sheet and other white objects are now held in front of the webcam at different distances. Furthermore, lighting conditions were varied, the object was moved with varying speeds and in different directions.

Experimental Results

The largest impact on the results was found to be the lighting conditions. Depending on the location in the room where the sheet was held, the object was either continuously tracked or not found at all. Poor lighting conditions turned out to be least efficient. Distances until 3 metres did not impact the ability to recognise the sheet when in proper lighting conditions. Also small objects like disks with a diameter of 5 centimetres and large objects such as tables could be detected in the same frame. A result of the test can be seen in Figure 4.12.

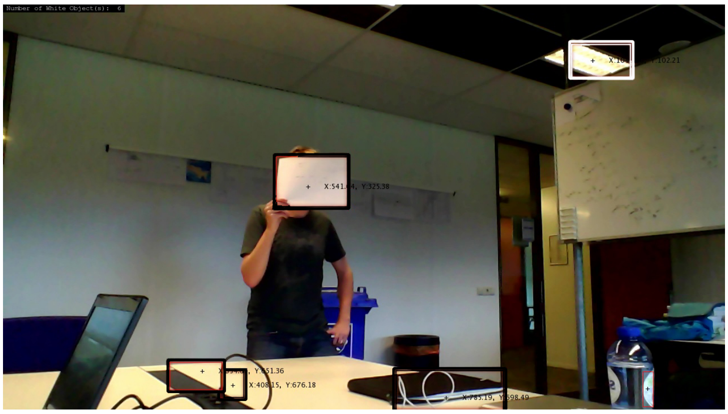

Figure 4.12: The result of the white sheet recognition test, showing multiple recognitions at indoor lighting conditions represented by the rectangles.

Verification and Validation

The tests were conducted on two separate days with two different computers, in order to check for consistency. As described in the previous section, different lighting conditions and set-ups were used. The code was adjusted to recognise different colors as well, which turned out to be not a problem. The number of false positives in terms of white objects, other than the sheet, depends on the environment and therefore software has to be developed in order to converge to the program only giving the sheet as an output.

Conclusion

From these first simple tests, it may be concluded that enough evidence is present to verify that sheet detection is possible at distances of at least 3 metres. However, as the camera used was only a fraction of the quality the Raspberry Pi camera module has and the software was not calibrated, this distance can most likely be increased by doing more elaborate research during the post-DSE phase of the project. Simple software seems to be adequate enough and therefore the choice can be made for the design option of using Matlab with blob detection in order to recognise white sheets. However, the software does need to be developed further in order to converge to only one outcome, as the blob detection now finds multiple blobs, or areas, of which the color white is the primary color.

In conclusion to both experiments, the Matlab and Python programming languages can be used in combination with blob detection and feature detection, in order to recognise numbers. Both can be run on the Raspberry Pi or can be converted to C which runs on this processor. Some requirements may be drawn from those two programs and are listen in Table 4.16.

Table 4.16: Additional requirements following from the design option for number recognition.

ID	Requirement
IMAV-CR-ME4-7	All UAVs shall be able to process a script written in python on the on-board processor
IMAV-CR-ME4-8	All UAVs shall be able to process a script written in Matlab on the on-board processor
IMAV-CR-ME4-9	All UAVs shall be within a TBD of the TBD metres from the sheet of paper when starting the sheet recognition
IMAV-CR-ME4-10	All UAVs shall be within a TBD of the TBD metres from the sheet of paper when starting the number recognition

4.6. Map Stitching

For the second mission element, a photomap must be created. This map comprises of multiple photos that have to be stitched together. The next section reviews the different design options possible for the generation of this map. Each of these options are represented in a DOT in Figure 4.13. In the figure, a distinction is made between panoramic and orthorectified photo stitches.

4.6.1. Requirements

Before going into more detail, first all relevant requirements are discussed within this section. From requirement *IMAV-CR-ME2* and Chapter 3.3 it follows that an additional 10 minutes on top of the total mission time could be used for stitching the photos and locating the blockades. In total approximately 10 minutes are reserved for creating the photomap.

Due to the time constraint, all self-developed software is considered to be infeasible. Furthermore no software or hardware could be found that could create an orthorectified map with use of a digital elevation model (DEM) within 10 minutes. Pre-developed panoramic stitching software available on the market was found and compared. A trade-off between the four software packages was performed and Microsoft ICE ranked first due

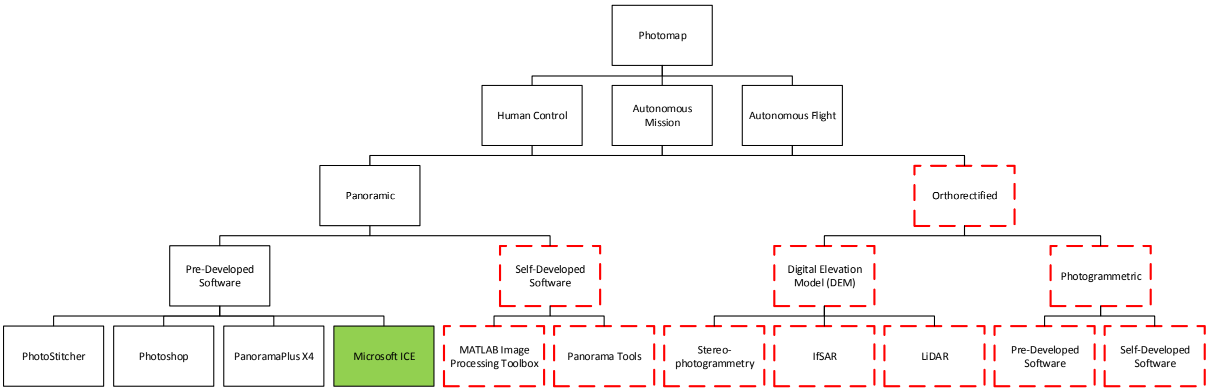

Figure 4.13: Design option tree for map stitching. The (red) dashed line indicates infeasible concepts, the (green) filled block indicates the selected concept.

to its free license, wide-spread use and the smaller overlap needed according to its specifications [22] [83]. Note that this software must be applied on a personal computer on the ground station due to its processing power demand. In order to check what the actual specifications and requirements are on this software and whether it performs as expected, an experiment was conducted.

4.6.2. Photo-stitching Experiment

The Microsoft ICE software was tested in order to verify its panoramic map stitching capabilities. The following sections describe the different aspects of the experiment performed. The main goal of this additional research is to find what the required overlap should be in order for the software to produce valid results.

Methodology

The software uses multiple pictures taken in either a zigzag (every lane in the same direction) or a centipede (every other lane in the same direction) order. An overlap percentage must be specified and the amount of pictures must be equally spaced and provided as well. Furthermore, different layouts of photos are tested, such as L-shapes or other 'Tetris' shapes. The photos are taken with a camera representative of a camera used on the actual UAV. After stitching, the photos are verified and validated and data on stitching-time, size and resolution of the picture is determined.

Test Set-up

First, a grid was made in order to do accurate measurements of overlap percentages (Figure 4.14). After this, the actual photomap, obtained from Google Earth, was printed in a 3 by 2 metre area. Objects were placed on the map in order to simulate three-dimensional effects such that orthorectification could be crossed out. Then, crosses were drawn on the map in order to ensure that overlap is correctly measured and photographed (Figure 4.15).

Figure 4.14: First set-up of the map, a grid used for overlap measurement, with objects for a three-dimensional simulation.

Figure 4.15: The second set-up of the map: a scaled version of the real map with objects for a three-dimensional simulation.

Experimental Results

The first map introduced difficulties with regards to stitching. The hypothesis is that the grid introduced to many similarities and therefore to much overlap between different photos was present. The stitched map may be found in Figure 4.16. From experiments with this new map it followed that 10% overlap was too little. A 20% overlap produced accurate results and is more time-efficient than a 30% overlap. The results are shown in Figures 4.17 through 4.19.

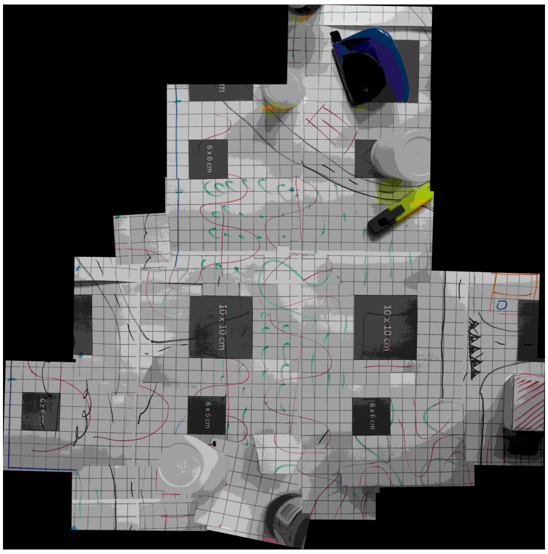

Figure 4.16: The stitched photomap consisting of photos of the first map, overlapping by 20 percent.

Figure 4.17: The stitched photomap consisting of photos of the second map, overlapping by 10 percent.

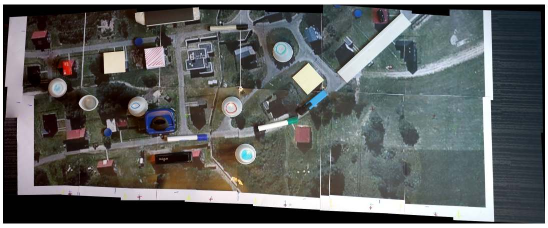

Figure 4.18: The stitched photomap consisting of photos of the second map, overlapping by 20 percent.

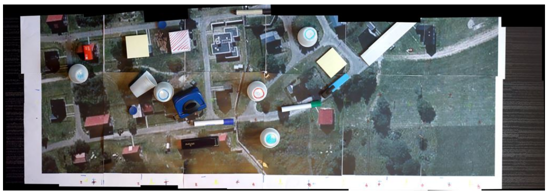

Figure 4.19: The stitched photomap consisting of photos of the second map, overlapping by 30 percent.

When a 20% overlap between pictures is used, an increased overlap should be present when taking pictures, due to attitude control issues. When both a pitch, roll and yaw angle error are present, as well as a translational mismatch, the real attitude is increased. This deviation over the height at which the photo is taken can be found in Figure 4.20. Moreover, to obtain an optimal ground resolution, the angle of width has to be varied over the height. This is shown in Figure 4.21. Both of the figures indicate the amount of photos that need to be taken in order to get a complete map. As only 99 photos can be taken due to the time constraint and the maximal height is 152 metres, only a few feasible options are available. These are presented by the square blocks. Furthermore, as trees can grow as tall as 43 metres, the options at the bottom of the graph may be crossed out as well [84]. Concluding, it can be seen that, when using a camera angle of view of 36 degrees width, a height of 51 metres must be achieved in order to have a need of 99 photos.

Camera Selection

The scoring for the photo map mission element is based on the resolution of a sheet of paper located on the ground. During the iteration of calculations based on the experiment, it was found that the highest scoring resolution of 10 mm in 5 pixels could not be met with a camera below 20MP that flies above the threes. Therefore the 6 times multiplier is chosen which demands a ground resolution of 50mm in 5 pixels. It was found that the least expensive camera was the Sony Cybershot DSC W800, which still has an adequate resolution and even an surplus in pixels. Cheaper cameras will need to fly too low, resulting in flight at ground level. More expensive cameras did not pay off in terms of the amount of photos that have to be taken and thus time consumption.

Verification and Validation

The photo-stitches are compared with the real map and discrepancies or deficiencies are located. Multiple stitching times are measured in order to obtain an accurate average that can be used to extrapolate stitch-time to a hundred photos. Also, the time needed for storing the pictures with the adequate resolution onto a local

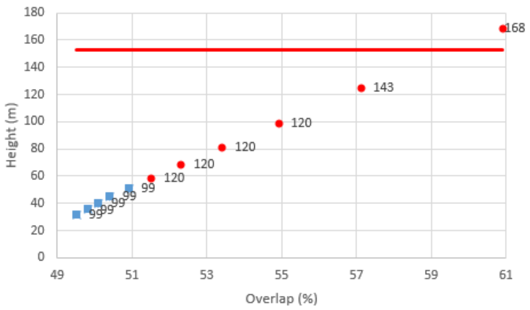

Figure 4.20: Number of photos needed with respect to height and minimum overlap between pictures. The horizontal line indicates the maximum height restricted by IMAV and the square blocks are the feasible options.

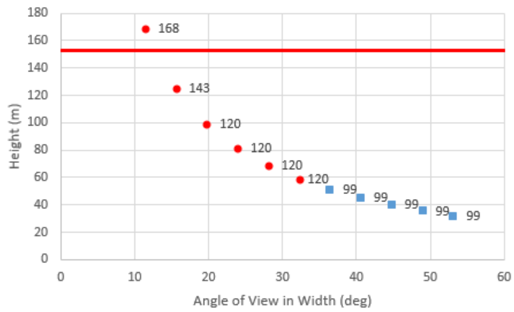

Figure 4.21: The number of photos needed with respect to height and angle of view in width. The horizontal line indicates the maximum height restricted by IMAV and the square blocks are the only feasible options.

drive is measured a number of times. Verification of the resolution is achieved by measuring the resolution of a reference area that lies on a division line of two photos (in this case a yellow sticky-note) on both the original photo and on the stitched map.

Results & Conclusion

From the test, it followed that only a 20% overlap of the pictures is needed in order to let the panoramic stitching be successful. Now, an iterative step was made. By performing an attitude and mission operation analysis, a flight speed of 5.6 m/s was obtained which leads to a total amount of 99 photos. With a size of 6.6 MB per photo, this gives a total of 654 MB of data to be stored, which means that the required data rate is 1.65 MB per second [85].

Now that Microsoft ICE has been verified to work, some requirements can be drawn and may be listed in Table 4.17. The requirements *IMAV-CR-ME2-1* through *IMAV-CR-ME2-4* follow from the specifications of Microsoft ICE and the last two requirements follow from the extrapolated results of the experiment [22].

Table 4.17: Additional requirements following from the design options that followed from the map stitching mission element.

ID	Requirement
IMAV-CR-ME2-1	The system shall make pictures with an overlap of at least 20%
IMAV-CR-ME2-2	The system shall have Microsoft ICE available on the ground station for photo stitching
IMAV-CR-ME2-3	The system shall have Microsoft Visual C++ available on the ground station for photo stitching
IMAV-CR-ME2-4	The system shall have .NET Framework version 4 available on the ground station for photo stitching
IMAV-CR-ME2-5	The system shall have a memory of at least 645 MB for creating the photomap
IMAV-CR-ME2-6	The system shall support a data rate of at least 1.65 MB/s for creating the photomap

4.7. Data Transmission

From requirements *IMAV-SR-20* it follows that every UAV should have some form of communication with the ground station. This chapter describes the various possibilities for the transmission or storage of data for every mission element. All relevant options for data transmission are listed in a DOT in Figure 4.22. In the figure, a distinction is made between real-time wireless communication and the storage of data.

4.7.1. Requirement Analysis

In order to decide on a data transmission system, the relevant requirements need to be analysed first. The requirement related to data transmission can be seen in Table 4.18.

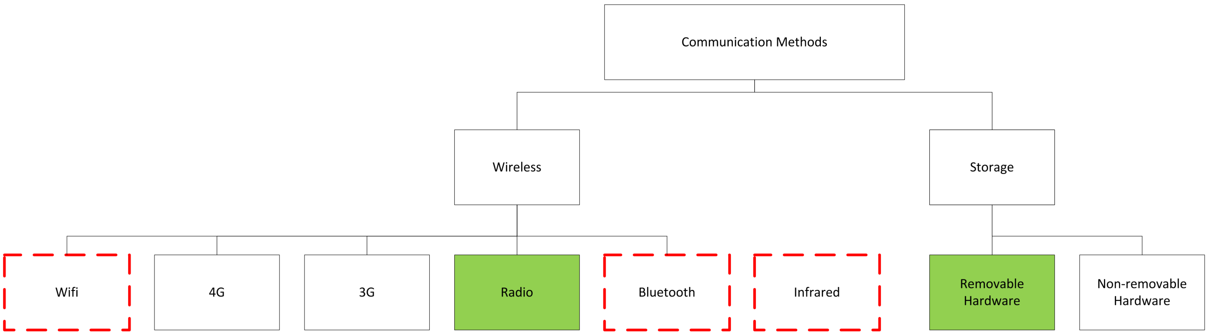

Figure 4.22: Design option tree for on-board computer hardware selection. The (red) dashed line indicates infeasible concepts, the (green) filled block indicates the selected concept.

Table 4.18: The relevant requirements for the data transmission subsystem.

ID	Requirement
IMAV-AU-14	The system shall have a communication link able to handle 7.2 kB/s between the ground station and the autopilots of all UAVs
IMAV-CR-ME2-6	The system shall support a data rate of at least 1.65 MB/s for creating the photomap
IMAV-SR-03	The transmission of electro magnetic radiation shall be on frequencies that are legally allowed in the Netherlands
IMAV-SR-04	The transmission of electro magnetic radiation shall be in modes that are legally allowed in the Netherlands
IMAV-SR-05	The transmission of electro magnetic radiation shall be within the power limit legally allowed in the Netherlands
IMAV-SR-14	A UAV shall perform an emergency landing after entering the red zone

Besides these requirements, the power consumption and the weight of the system should be as low as possible, as is described in Section 2.4. Finally, Pythagoras' theorem was used to analyse requirement *IMAV-SR-14*. This analysis concluded that with the dimensions of this red zone (lxwxh 277 x 170 x 290 meter) 3.3, a minimal range for the data transmission system can be determined to be 436 metres [4].

4.7.2. Design Option Selection

For every option in the DOT, a literature study is performed. The results can be found in Table 4.19. It can be seen that bluetooth and infra-red are not feasible for this design because of their limited range [86] [87]. Wi-Fi should theoretically be able to transmit data over the required distance, but no practical devices could be found [88]. The data rates of both a 3G connection as well as a USB1.1 connection are not able to process the required data within the given amount of time [89] [90]. Mission element 2 is performed by using a stand-alone camera with a remote trigger in order to create the photo stitch. As the camera does not support USB2.0, but is able to write data to an SD card, it is convenient to choose the latter and cheaper option for data processing.

Requirement *IMAV-SR-20* states that the team shall be able to manually take over control of all UAVs. From this requirement it follows that the UAV shall always have a direct communication link with the ground station. In combination with the autopilot, the data rate does not exceed 7.2kB/s. The only technically viable options left are radio controlled, 3G or a 4G connection. The main difference between these techniques are the costs, which are a factor 30 higher for 3G and 4G. Therefore, the most viable option for this is the radio controlled option.

4.7.3. Hardware Selection

Now that the design options are known (SD Card and radio frequency data transmission), it is possible to select specific hardware. The main goal is to find lightweight, low power and cost efficient hardware. The options that exist for the hardware, that allow the UAV to communicate with the ground station over a radio frequency band, can be found in table 4.20. Combining the requirements for range, data rate and minimal cost, the XBee

Table 4.19: The specifications of all design options. Listed are the range, bandwidth, size and price.

Device	Range (km)	Max Data Rate (MB/s)	Size (GB)	Price (€)
USB 1.1 [90]	-	1.5	4	5.49
USB 2.0	-	60	4	3.71
SD class 4 [91]	-	4	4	2.95
Bluetooth [86]	0.1	-	-	-
Infra-red [87]	0.005	-	-	-
3G [89]	Available in competition	2	-	450
4G [92]	Available in competition	3.6 (Vodafone)	7	450
Wi-Fi IEEE 802.11a [88]	0.3 in line of sight	6.75	-	
Wi-Fi IEEE 802.11n	0.3 in line of sight	37.5	-	50
Radio [93] [94]	1.6	0.25	-	14

Series 1 Pro was chosen for the UAV. This hardware selection complies with requirements *IMAV-SR-03* to *IMAV-SR-05*, concerning electro magnetic radiation in the Netherlands [95]. Both the transceiver for the UAV, as well as the one for the ground station can be found in Table 4.21.

Table 4.20: Several hardware options for radio frequency data transmission between the UAV and the ground station [94]

Device / Feature	Frequency (GHz)	Power (mW)	Mass (g)	RF Speed (kbps)	Price (€)	Range (km)
XBee Series 1	2.4	1	4	250	16	0.1
XBee Series 1 Pro	2.4	100	4	250	14	1.6
XBee Series 2 Pro	2.4	50	4	250	28	1.6
XBee 868LP	0.868	5	5	80	18	4
XBee Pro 900HP	2.4	250	8	20	32	4
Digi 9XTend	2.4	1000	18	115	150	5.6
Aerocom AC4790-200	0.928	200	20	76.8	52	6.4

As power consumption is not a property determined by the SD Card and weight does not change significantly for different SD cards, the selection can only be based upon cost. Combining this with the data rate and total amount of data to be stored, an SD card was selected and can be found in Table 4.21 [91].

Table 4.21: The final selected hardware and its specifications for the data transmission functionality of the payload.

Device	Description	Power (W)	Cost (€)	Mass (g)
Kingston SDHC 4GB - Class 4	SD Card [91]	-	2.95	2.3
XBee Series 1 Pro	UAV communication [94]	0.165	14	4
XBee Pro PKG-U - USB	Ground station comm. [93]	2.7	118	150

4.8. Blockade Mapping

The main requirement of mission element 3 requirement *IMAV-CR-ME3* states that: the system shall indicates all blockades in zone A on the photomap of mission element 2. Figure 4.23 shows all design options for this specific mission element. Within this figure the eliminated design options are marked striped (red), whereas the final chosen design option is filled (green).

4.8.1. Design Option Selection

As the photomap is created using panoramic stitching instead of orthorectified stitching, it is not possible to use a height-profile for blockade determination. Furthermore, it should be noted that very narrow blockades, for example fences standing on the road, are not clearly visible from above. Another viable option of determining the location of blockades is recognising them separately with a UAV and sending the location of the UAV at that instance to the ground station. However, due to inaccuracies in the IMU and GPS at low level flight

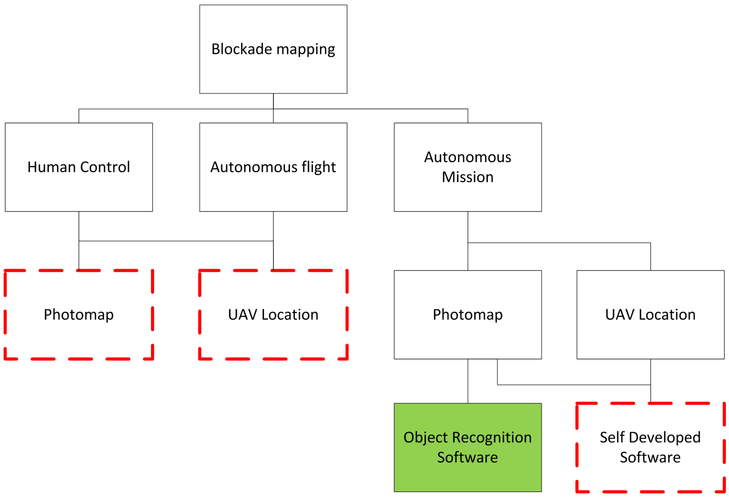

Figure 4.23: Design option tree for blockade detection. The (red) dashed line indicates infeasible concepts, the (green) filled block indicates the selected concept.

(as discussed in Section 4.3.3), in combination with unknown obstacles on the road, it is impossible for the UAV to use the roads as a guide towards the blockades. As blockades are always placed on the roads, it is also possible to use the photomap from mission element 2 to detect the blockades. First of all, color detection can be used to find the roads on the map, which is least expensive compared to other recognition options. Then, the same recognition method can be used to distinguish obstacles from the road. As it is only required to indicate and not to identify blockades, object recognition exceeds its purpose. Therefore color detection is chosen as the most viable design option for blockade detection. It is recommended to further verify the use of color detection, in combination with the roads and blockades present during the IMAV 2014 competition.

4.8.2. Additional Requirements

In order to apply color detection, some requirements can be drawn. First of all, Matlab or Python has to be available in which the code may be written. A requirement following from software is that the photomap should be in color. These requirements are listed in Table 4.22.

Table 4.22: The additional requirements obtained from the hardware choices that were made with respect to blockade detection.

ID	Requirement
IMAV-CR-ME3-1	A photomap of the area shall be available for blockade mapping
IMAV-CR-ME3-11	The photomap shall be in color
IMAV-CR-ME3-4	The system shall have Python or MATLAB available on the ground station for blockade mapping

4.9. Attitude Control

From all previous sections it follows that a certain amount of attitude control is required in order to perform all mission elements. The amount of attitude control needed for each of these mission elements will be discussed in this section. The requirements on which this section is based are presented in Table 4.23.

Take-off
During take-off, the propellers may fail and a gust may occur, pushing the UAV down on the ground. The estimated loads acting on the structure are determined in Section 7.2. The actual height and thus translational error that is induced by this load has to be researched more in depth. However, it is assumed that the landing mission elements are putting more restrictions on the system due to the velocity pointing nadir. The only attitude requirement that follows for the first mission element, is that the UAV may not land on its propellers. Therefore the attitude has to be controlled with an accuracy of 45 degrees when ascending.

Table 4.23: The requirements related to the topic of attitude control.

Requirement ID	Description
IMAV-CR-ME1	All UAVs shall take off from the designated take-off area in the LCC
IMAV-CR-ME2	The system shall create a photomap of zone A within 10 minutes after the end of the mission
IMAV-CR-ME3	The system shall indicates all blockades in zone A on the photomap of mission element 2
IMAV-CR-ME4	All UAVs shall identify the building numbers of buildings in zone B
IMAV-CR-ME8-1	All UAVs shall land on the building with the flat roof in zone D
IMAV-CR-ME10-1	All UAVs shall make a precision landing in the designated landing area in the LCC

Photomap
In order to obtain attitude control estimations for the second mission element, tests have been performed as described in Section 4.6. From these tests a maximum amount of photos followed that can be stitched in 10 minutes. When looking at the field of view of the camera at a certain height and implying a minimum of 20% overlap, the attitude of the camera has to be controlled to a certain degree as well as the position of the UAV. These attitude and location requirements are listed below.

- 2.5 metres in translation
- 1 degree in roll and pitch control
- 6 degrees in yaw control

Blockade Mapping
The software used for detecting blockades on the already stitched photomap has not yet been tested or developed. Therefore, it is assumed that this mission element has the same attitude control requirements as the mission element consisting of the photomap, as previously discussed. When the software performs inadequately, manual recognition will be performed.

Quick Visual Inspection
From tests performed in Section 4.5 it followed that a distance of 1.5 metres from the sheet must be guaranteed with a deviation of 0.5 metres in order to achieve a reliable recognition of the number. In order to achieve this distance, the range finder must have an accuracy of equal distance and should be aligned with the perpendicular distance to the wall. Furthermore, in order to face the right building, the pointing accuracy or yaw control accuracy must be at least 53 degrees, as this is the angle of view of the Raspberry Pi camera module.

Land on Roof
The landing zone consists of a 12 by 6 metre rectangular landing zone. In order to navigate onto this zone, the translational control accuracy should therefore be a sphere with radius of 5.5 metres when it is assumed that it is known by the UAV whether it is located above the building and perpendicular to the house. The landing itself is determined again with the use of the parameters discussed in the take-off mission element.

Precision Landing
As the precision landing area consists a circle of with a radius of 5 metres, the translation of the UAV must be controlled within 2.5 metres. The vertical translational accuracy must again be defined by the structural integrity of the UAV, while the attitude control in pitch and roll is determined by the maximum impact of a gust.

4.9.1. Requirements

Now that all mission elements have been analysed with regards to attitude control and location, the corresponding requirements can be listed in Table 4.24. Only the most stringent requirements are listed as they cover the less stringent requirements as well. Note that the most demanding requirements on attitude control for the complete UAV as well as the photomap camera, are those following from mission elements 1, 2 and 4.

Table 4.24: Additional requirements following from the design options that followed attitude control.

ID	Requirement
IMAV-CR-ME1-1	All UAVs shall have a roll and pitch control accuracy of at least 45 degrees
IMAV-CR-ME2-8	The photomap camera of all UAVs shall be controlled in roll and pitch with at least 1 degree of accuracy
IMAV-CR-ME2-9	The photomap camera shall be controlled in yaw angle with at least 6 degrees of accuracy
IMAV-CR-ME2-10	All UAVs shall have a translational control accuracy of at least 2.5 metres in all three axes
IMAV-CR-ME4-5	All UAVs shall have a translational control accuracy of at least 0.5 metres in the horizontal plane
IMAV-CR-ME10-11	All VTOL UAVs shall make a precision landing on the LCC within a circle of 5 metres
IMAV-CR-ME10-14	All CTOL UAVs shall make a precision landing on the LCC within a circle of 10 metres

4.9.2. Gimbal

Within this section a solution is found for the challenge of increasing the pointing accuracy of the camera in order to create a photomap. A gimbal was found to be the best design option. The next section discusses this attitude controlling device.

Requirements Analysis

From requirement *IMAV-CR-ME2-8* it follows that roll and pitch control of at least 1 degree is required from pointing nadir, which is quite difficult do to with respect to gusts and even the UAV's constant propelling inclination. Therefore, in order to obtain this accuracy, a passive or active 2- or 3-axis gimbal system is required. A passive gimbal uses gravity in order to damp the motions that the UAV applies to the camera system. An active gimbal uses a combination of motors and an acceleration sensor in order to balance the camera. As a passive gimbal system would easily start swaying and is not damped quick enough, it is therefore found to be infeasible. Specifications of readily available active 2- and 3-axis gimbal systems are shown in Table 4.25.

Table 4.25: Specifications of various gimbal systems

Device	No. of Axis	Acc. x (°)	Acc. y (°)	Acc. z (°)	Power (W)	Mass (g)	Price (€)
Zenmuse H3-3D [96]	3	0.02	0.02	0.03		168	280
SMART3 [97]	3					262	184
Libran 3-axis [98]	3				<32	170	67
Stella Brushless [99]	2	0.05	0.05	-		120	218
Mobius Gimbal [100]	2			-	<15.2	171	85.7

Gimbal Selection

It can be seen that the *Mobius* is a lightweight and cheap, but still accurate active gimbal system. One of the advantages of this system is that is can easily be assembled. Therefore, a supporting structure can be self-developed to fulfil the UAV's needs. The components that the gimbal consists of are two motors and a control board [101] [102]. These are all connected by 3D printed parts which are custom designed in Chapter 6.1.

4.10. Ground Station

An important part of the design is the ground station. It is required according to the IMAV competition rules[4] and it is used, for example, to show the current location of every UAV and to perform the stitching of the aerial photos. Any requirements relevant to the ground station are listed in Section 4.10.1. The design of the ground station is described in Section 4.10.2.

4.10.1. Requirement Analysis

Multiple requirements have been generated that are relevant for the ground station. These have been summarised in Table 4.26.

Table 4.26: Requirements for the ground station.

Requirement ID	**Description**
IMAV-CR-ME2-2	The system shall have Microsoft ICE available on the ground station for photo stitching
IMAV-CR-ME2-3	The system shall have Microsoft Visual C++ available on the ground station for photo stitching
IMAV-CR-ME2-4	The system shall have .NET Framework version 4 available on the ground station for photo stitching
IMAV-CR-ME2-5	The system shall have a memory of at least 645 MB for creating the photomap
IMAV-CR-ME3-4	The system shall have Python or MATLAB available on the ground station for blockade mapping
IMAV-SR-30	The main ground station screen shall be shared via VGA output
IMAV-AU-13	The ground station shall have paparazzi ground control station-software available for telemetry
IMAV-AU-13-1	The ground station shall have a ground station based on the Linux Operation System
IMAV-AU-14	The system shall have a communication link able to handle 7.2 kB/s between the ground station and the autopilots of all UAVs

4.10.2. Design Option Selection

It follows from the requirements that two operating systems are required, as .NET Framework (requirement IMAV-CR-ME2-4) only runs on Windows operating systems, while Paparazzi runs on Mac OS X and Linux-based systems [103] [50]. It is therefore chosen to use two portable computers or laptops, designated Ground Station A and B, that together form the ground station. Further specifications on these two computers are given in this section.

Ground Station A

Ground Station A is a computer with a Linux operating system. It has Paparazzi ground control station software installed such that it can show the current location of the UAVs. In order to get the telemetry of the UAVs, it has an Xbee modem connected to it. To enable the IMAV jury to observe the system using an additional screen, a VGA-output is present.

Ground Station B

Ground Station B is a computer with a Windows 7 or 8 operating system and at least 654 megabytes of memory available. It has .NET Framework 4, Microsoft Visual C++ and Microsoft ICE installed in order to stitch photos into a photomap. It also has Python or MatLab installed in order to perform blockade recognition on the generated photomap. It can read an SD-card in order to be able to import photos taken by the UAVs.

In order to save on costs, laptops that are available within the team will be used as ground stations A and B.

4.11. Payload Conclusion

In this chapter, all hardware choices for the payload of the UAV design have been presented. These choices were required for a system to successfully complete the mission it was designed for, as discussed in the previous chapter. An overview of the UAV payload selection is presented in Table 4.27. An overview of the ground station selection is presented in Table 4.28.

Table 4.27: Overview of the selected UAV payload

Category	**Type**	**Name**	**Power (W)**	**Cost (€)**	**Mass (g)**
Sensing	Camera	Raspberry Pi Camera Module	0.825	21.21	3
Sensing	Camera	50 cm Raspberry Pi CSI/DSI Camera Module Flat Ribbon Cable	0	6.23	10
Sensing	Camera	SONY DSC-W810	0	78	127
Sensing	Trigger Camera	TE Connectivity - IME03GR - Relay DPST 5V	0.14	1.81	3
Sensing	Trigger Camera	Multicomp - 2N2222A - Transistor NPN	0.4	0.84	0.35
Sensing	Trigger Camera	Resistor 1kOhm MultiComp MC-CFR0W8J0102A20	0.125	0.01	2
Sensing	Gimbal	2x 2206-140Kv Brushless Gimbal Motor	6.2	21.96	64
Sensing	Gimbal	2-Axis Brushless Camera Gimbal Stabilization Control Board	3.6	28.72	25
Sensing	SD-card	2x Kingston SDHC 4GB - Class 4	0	6	4
Navigation	Echolocation	2x Ultrasonic Rangefinder HC-SR04 Module	0.15	5.90	30
Navigation	Echolocation	2x Resistor 330 Ohm MultiComp MC-CFR0W8J0331A20	0.25	0.02	4
Navigation	Echolocation	Resistor 470 Ohm MultiComp MC-CFR0W8J0471A20	0.25	0.02	4
Navigation	Push button	3x Momentary Push Button Switch - 12mm Square	0	1.50	3
Navigation	Push button	Resistor 1kOhm MultiComp MC-CFR0W8J0102A20	0.125	0.01	2
Navigation	Push button	Resistor 10 kOhm	0.125	0.01	2
Navigation	Autopilot board	Lisa/M v2.0, including: Aspirin v2.2 IMU, barometer	1.25	169	11
Position	GPS	UBLOX NEO-6M GPS Module w/Built-in Antenna	0.1287	12.99	18
Communication	Radio receiver	Xbee Series 1 Pro	0.165	14	4
Manual control	Receiver	Spektrum SPM9645 Remote Receiver	0	28.82	3
Processing	On-board computer	Raspberry Pi Model B	5	30	39
Total			**19 (W)**	**426 (€)**	**360 (g)**

Table 4.28: Budget breakdown of the ground station used for the UAVs

Category	**Name**	**Type**	**Power (W)**	**Cost (€)**	**Mass (kg)**
Communication	Radio transmitter	XBee-PRO PKG-U - Connection via USB	2.7	118	0.15
Manual control	Transmitter	Turnigy 9XR (no module)		37.08	1.28
Manual control	Transmitter module	OrangeRX DSMX module, Turnigy-compatible	0	22.13	0.074
Battery	Battery adapter	iCharger 206B	300	97.77	0.35
Total			**303 (W)**	**275 (€)**	**1.9 (kg)**

5

Propulsion and Airframe Design

The propulsion and airframe can be designed in order to perform the missions selected in Chapter 3 and support the payload subsystems designed in Chapter 4. This whole section is therefore dedicated to the airworthiness of the unmanned aerial vehicle (UAV), as required by *IMAV-SR-26* of the international micro aerial vehicle (IMAV) safety regulations [4].

First, the requirements which need to be fulfilled by the propulsion and airframe are discussed in Section 5.1. With these requirements, a trade-off is performed in order to select which flying method is best suited for the mission in Section 5.2. With the flying method chosen, an iterative design approach is used for the propulsion and airframe subsystem. A description of the design is given in Section 5.3. Afterwards, the different parts which make up the propulsion are discussed in the next sections. First, the propeller selection is described in Section 5.5. Second, Section 5.6 discusses the selection of the motor to drive the propellers. Third, to control the motors an electronic speed controller (ESC) is selected in Section 5.7. Fourth, to power the whole system a power supply is considered in Section 5.8. With the power subsystem complete the airframe which supports the payload and propulsion subsystems is designed in Section 5.9. This chapter concludes with an overview of the propulsion and airframe subsystem in Section 5.10.

5.1. Requirement Analysis

All requirements related to the propulsion and airframe design can be found in Table 5.1. Note that the table only includes the most restricting requirements concerning rotational and translational control accuracy.

Table 5.1: All requirements related to the propulsion and airframe design.

ID	Requirement
IMAV-CR	The system shall win the IMAV 2014 competition
IMAV-CR-ME1	All UAVs shall take off from the designated take-off area in the LCC
IMAV-CR-ME8-1	All UAVs shall land on the building with the flat roof in zone D
IMAV-CR-ME8-3	All UAVs shall take off from the building with the flat roof in zone D
IMAV-CR-ME8-13	All UAVs shall have a sensor that indicates a landing
IMAV-CR-ME10-1	All UAVs shall make a precision landing in the designated landing area in the LCC
IMAV-CR-ME10-2	All UAVs shall demonstrate airworthiness in case of rough landing
IMAV-SR-01	The system shall only use electric propulsion
IMAV-SR-16	An emergency landing of a UAV with rotary, flapping or hybrid wings shall be performed at minimum power setting
IMAV-SR-17	An emergency landing of a UAV with fixed wings shall be performed without propulsion
IMAV-SR-23	All UAVs shall have a maximum dimension of 1.50 m
IMAV-SR-24	All UAVs shall have a maximum weight of 5 kg
IMAV-SR-25	All UAVs shall have a maximum momentum of 20 $\frac{kg \cdot m}{s}$
IMAV-SR-26	All UAVs shall be airworthy

5.2. Flying Method Selection

This section describes the design process of selecting the flying method to perform the mission selected in Chapter 3, which satisfies the requirements as stated in Section 5.1. First, possible design options are listed in Section 5.2.1. Second, non-feasible options will be eliminated in Section 5.2.2. Third, the criteria for which the remaining feasible concepts are evaluated, are introduced in Section 5.2.3. Fourth, the conceptual analysis is performed in Sections 5.2.4 through 5.2.7. Fifth, Section 5.2.8 uses the conceptual analysis to trade off all feasible concepts and determine the final method that used for the propulsion and airframe design. Finally, an overview of the requirements generated in this section is given in Section 5.2.9.

5.2.1. Design Options

This section discusses possible design options for the propulsion and control subsystem. An overview of all design options is given in the design option tree (DOT) presented in Figure 5.1.

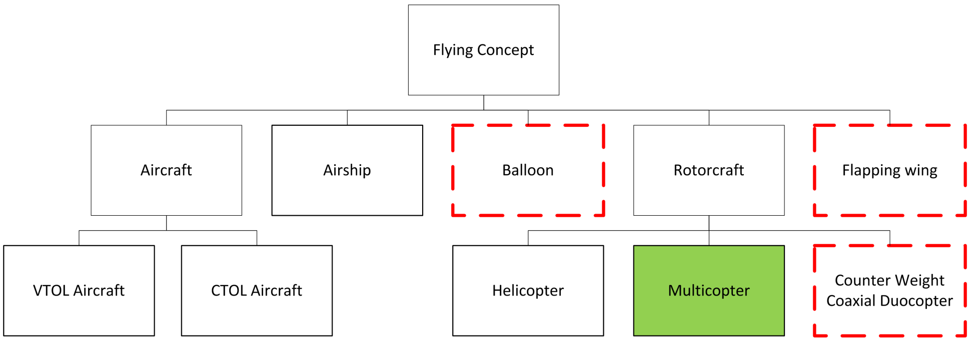

Figure 5.1: Design option tree for flying method selection. The (red) dashed line indicates infeasible concepts, the (green) filled block indicates the selected concept.

Vertical Take-off and Landing Aircraft

The aircraft in the vertical take-off and landing (VTOL) group have vertical take-off and landing capabilities and can transition into a forward flight with capabilities similar to conventional take-off and landing (CTOL) aircraft. Examples within this group are the ATMOS vehicle [104], LTV XC-142 [105] and a scale model Bell Boeing V-22 Osprey [106].

Conventional Take-off and Landing Aircraft

The aircraft in the CTOL aircraft group use a fixed wing to generate aerodynamic lift for take-off, cruise and landing. Therefore, aircraft in this group need a runway to take off and land. Examples within this group are the Sensefly eBee [107] and the Lockheed Martin Desert Hawk III [108].

Airship

The airship group only contains vehicles utilising lighter-than-air principles to lift the system, either using hot air or lighter-than-air gases. Furthermore, the group uses additional propulsion systems, besides the burner within a hot air airship, to control the vehicle's altitude and attitude. Examples within this group are the Silent Runner [109] and the do-it-yourself project Ollie [110].

Balloon

The balloon group contains vehicles that make use of lighter-than-air principles, like the airship group. However, balloons do not have an additional propulsion system, besides the burner within a hot air balloon, to control the vehicle's altitude and attitude. An examples within this group are a hot air or gas balloon.

Helicopter

The helicopter group contains vehicles utilising rotor blades, which are essentially rotating wings, to generate lift and thrust. The helicopters are controlled by varying the pitch of the rotor blades to adjust thrust generated by the propellers. Examples within this group are the Rotomotion SR-5 [111] and the AUAVT AT-10 [112].

Multicopter

The multicopter group contains vehicles that employ rotor blades, like the helicopter group. However unlike the helicopter group, the pitch of the propeller blade of a multicopter is fixed. The attitude of a multicopter is controlled by varying the thrust generated by the different propellers. Examples within this group are the Aibot X6 [113], the DJI Phantom series [114] and the HALO UAV [115].

Counter-Weight Coaxial Duocopter

The counter-weight coaxial duocopter is a vehicle that uses a coaxial rotary system. The counter-rotating pair of blades are mounted on top of each other, which results in zero net torque on the system. The vehicle uses a counter-weight to control the attitude of the system. There are no prove of concepts of any counter-weight coaxial duocopter on the market. Therefore, a sketch of this concept is presented in Figure 5.2.

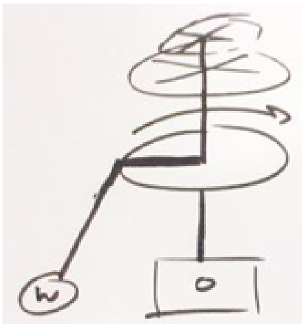

Figure 5.2: Sketch of the counter-weight coaxial duocopter flying method concept.

Flapping Wing

The flapping wing group contains vehicles utilising flapping wings to generate lift and thrust. These vehicles are inspired by either birds or insects and try to imitate their methods of flight. Examples are the DelFly series [116], DragonFly [117] and Pteryx Skybird [118].

5.2.2. Infeasible Design Options

This section discusses three infeasible design options, which are not further considered for this design project. The balloon, counter-weight coaxial duocopter and flapping wing groups are deemed infeasible.

Balloon

The balloon group is considered to be an infeasible design option, as it cannot be controlled, making it unable to complete the selected mission. The balloons are free to float in the direction that the wind takes the vehicles. The vehicles can therefore not comply with the IMAV safety rules [4] as specified by requirement *IMAV-SR*. Note, that adding any type of propulsion device to control this attitude would make the concept an airship rather than a balloon.

Counter-Weight Coaxial Duocopter

The counter-weight coaxial duocopter is considered to be a infeasible design option, as there is no proof of concept in either scientific publications or industry. Therefore, the development of the system cannot be completed with the available project resources and the risk for developing this system are considered too large.

Flapping Wing

The flapping wing vehicles are considered to be an infeasible design option, as there is no proven concept capable of performing a mission similar to the chosen mission concept. Therefore, the development of the system cannot be completed with the available project resources and the risk for developing this system are considered too large.

5.2.3. Design Option Analysis

A total of four trade-off criteria were selected to compare the remaining design options for the flying method selection. As discussed in Section 3.2.2, the number of trade-off criteria is limited [19]. The trade-off criteria selected for the flying method trade-off and the arguments to include those criteria are discussed in this section.

Dimensions

An estimation of the dimensions of the flying method is important, since the maximum dimension is used to compute the total amount of points scored in the IMAV competition [2]. Furthermore, all UAVs are restricted by a maximum dimension of 1.50 metres. This criterion is thus related to requirements *IMAV-CR* and *IMAV-SR-23*.

Feasibility

Evaluating the feasibility of all design options is important, as the current technology has to be mature to be able to compete in the IMAV 2014 competition. Furthermore, the design has to be produced within the 37 days in the period between the end of the design synthesis exercise (DSE) and the start of the IMAV competition. This criterion is thus based on the two top-level requirements *IMAV-CR* and *IMAV-TU*.

Performance

The mission performance criterion involves a short initial analysis of the applicability of each design option to the selected mission elements. Therefore, this criterion relates to all requirements considering a mission element as listed in the requirement analysis of Section 5.1.

Control System Complexity

The control system complexity discusses the availability of control systems for each design option as well as the difficulty of implementing such a system. Therefore, this criterion indirectly relates to all requirements considering translational and rotational accuracy as listed in the requirement analysis of Section 5.1.

5.2.4. Dimensions

In this Section, the performance of the five concepts is analysed on their dimensions. From the IMAV safety rules there is a direct restriction on the maximum dimensions of 1.5 metres [4]. Also, the smaller the UAV, the higher the amount of points that are given in the competition. The exact relation between these is given earlier in Section 3.1.1.

Airship

The dimensions of a airship can be calculated with the fact that the amount of gas inside the airship has to be high enough to generate all the needed lift. The most optimal gas for this is the gas with the lowest density. This is hydrogen, but this is very flammable and therefore not usable for a UAV. The second best gas is helium with a lifting capacity of 1.02 kilograms per cubic metre. With this value, the volume of helium can be calculated and from this, a general dimension estimation can be calculated for an airship using Equation 5.1 [119].

$$L^3_{airship} = \frac{4 * F^2_{airship} * V_{helium}}{C_v * \pi} \tag{5.1}$$

Here, $L_{airship}$ is the length of the airship, $F_{airship}$ the slenderness ratio, V_{helium} the volume of the helium and C_v is the prismatic coefficient. The total volume of the helium is determined by the lifting capacity. The prismatic coefficient and slenderness ratio are determined using literature and estimated at 0.65 and 2 respectively [119]. At the maximum dimension of 1.5 metre, the total lift of the UAV can only support 0.439 kilograms. Because the payload and structural mass combined is higher then that, the dimensions for an airship will exceed the maximum dimensions. Moreover, the dimensions would still exceed the limit if the slenderness ratio is changed.

Conventional and Vertical Take-off and Landing Aircraft

The dimensions for VTOL and CTOL aircraft are estimated to be equal, as both design options use a wing to generate lift aerodynamically. The maximum dimension of the aircraft is the wing span. The wing span of the VTOL and CTOL aircraft can be estimated by using Equation 5.2.

$$L = \frac{1}{2} \cdot \frac{C_L \rho V^2 b^2}{A} \tag{5.2}$$

Where L is the lift force, C_L the lift coefficient, ρ the air density, V the airspeed, b the wing span and A the aspect ratio of the wings.

All parameters within Equation 5.2 are estimated to enable an estimation for the dimensions of a CTOL and VTOL aircraft. For the lift coefficient, an approximation of 1.5 is used. The air density is 1.225 kilogram per cubic metre at sea level and the lift is the mass of the aircraft multiplied with the gravitational acceleration of 9.81 m/s^2. Using the initial total mass estimation of 1 kilograms, the total lift force becomes 9.81 Newton. Also, estimating the aspect ratio at 2.5 and the velocity at 5 metre per second, the wing span becomes 1.03 metre.

Helicopter

In order to get a good estimation for the size of the helicopter, existing helicopters are investigated and compared. For this helicopter UAVs with the same weight range are taken. A maximum dimension range between 60 and 100 centimetre is found [120].

Multicopter

The size of a multicopter is about three times the propeller size [121]. The size of a propeller varies between 10 and 15 inches (between 25 and 38 centimetre), so this means that typical multicopter will have a maximum dimension between 75 and 114 centimetre.

5.2.5. Feasibility

This section evaluates the feasibility of each of the proposed mission concept. This evaluation consists of the technical maturity, complexity and its applicability to the project. The technical maturity has two separate elements, namely the technical maturity of the flying concepts applied to micro UAV and the technical maturity of the flying concepts applied to autonomous vehicles.

Vertical Takeoff and Landing Aircraft

The VTOL aircraft group has been miniaturised successfully as an radio controlled model, demonstrated by a 2.5 kilograms scale model of the V-22 Osprey [106]. Besides, the ATMOS and Extractor X were found as VTOL vehicles with autonomous capabilities. Both vehicles competed in the UAVForge competition aimed at simulating a military perch-and-stare reconnaissance mission [122]. The ATMOS team claims to have flown the first fully automated flight of a multi-modal UAV in May 2012 [123], which shows that the fully autonomous VTOL vehicle is not yet a mature technology.

The VTOL vehicles adds two flight modes to the system next to the hover mode, namely a forward flight mode and a transition mode. A reference vehicle makes this transition between the different modes for velocities above 8 metre per second [124], which is larger than the estimated 6 metre per second flight velocity [1].

Therefore, these flight modes add complexity to the system, while the forward transition is not applicable to the mission.

Conventional Takeoff and Landing Aircraft

Three examples of miniaturised aircraft utilizing conventional take-off and landing are were found to demonstrates the concepts feasibility. All of these aircraft have a take-off weight between 2 to 3 kilograms and a payload capacity of 1 kilogram [108] [125] [126]. These figures correspond to the concept estimates presented in the mid-term report [1]. Furthermore, three examples were found of autonomous CTOL aircraft performing similar missions as the missions to be performed by the designed system [107] [126] [125]. These examples clearly show the concepts technical maturity.

A minor issue was found for the concepts applicability to the mission concept. The Sensefly ebee proves the concept of autonomous landing [107], however most CTOL aircraft are hand launched [127]. Masuko et al. have shown that micro UAV are able to autonomously take-off using a runway instead of a hand launch [128]. But, this technology might be difficult to implement in the concept as no industrial application was found for this specific technology.

Airship

The miniaturisation of airships is still in a development stage, as almost no airships were found within the dimension constraints given by the IMAV competition [4]. Although some larger airships, like the Silent Runner [109] and a research performed by Saiki et al. [129], prove to have specification capable of performing the competition's mission elements.

Also the autonomous capabilities of airships are not yet mature. Two examples were found, which are capable of autonomous flight, but their system specifications are not at all capable of performing the IMAV competition's mission elements [130] [110].

Helicopter

The miniaturisation of helicopters as well as the autonomous capabilities are demonstrated by the Rotomotion SR-5 [111], AUAVT AT-10 [112] and Helipse HE-190 helicopters [131]. These helicopters all present specifications that could potentially support the selected mission.

A drawback of the helicopter concept is the inefficiency of the lift producing mechanism. As discussed by Leishman, the aerodynamical lift generation of the VTOL or CTOL aircraft is more efficient than the mechanical lift generation of the helicopter [132].

Multicopter

As for the helicopter concept, the multicopter concept is well proven as micro UAV with mapping or observation capabilities. This is shown by multiple UAVs produced by companies like Aibotix [113], DJI [114] and Microdrones [133].

The HALO and Aeroquad UAVs as well as vehicles from the Delft University of Technology (TU Delft) Micro Aerial Vehicle Laboratory (MAVLab) are examples of autonomous vehicles with specifications capable of completing the IMAV competition's mission elements [115] [134] [135]. Furthermore, both drones outperformed the VTOL aircraft, ATMOS and Extractor X, at the UAVForge competition [122]. Furthermore, the Microdrones company has proven the industrial applicability of this concept [133].

As for the helicopter, the multicopter concept has the drawback that the lift is mechanically generated. Again, this method of lift generation is less efficient than the aerodynamical lift generation of the VTOL or CTOL aircraft [132].

5.2.6. Mission Performance

This section will analyse the mission performance of the various designs options for the flying method. Mission performance is here defined as how well mission elements can be performed by the various concepts.

Mission element 1 can be done by all concepts, as none of the concepts is expected to have difficulties taking off. Furthermore, mission element 3 is performed based on the photomap of mission element 2, as specified by the mission strategy discussed in Section 3.3. Therefore, all design options have a similar performance for this mission element.

For mission element 2, the concepts need to fly quickly during the making of the photomap. The VTOL aircraft and CTOL aircraft can fly faster than the multicopter, helicopter and the airship. However, a restriction on the maximum flight speed is given by the IMAV. This maximum flight speed is lower than the maximum speeds that the flying concept can achieve so no additional benefits or restrictions are given by mission element 2 for the various concepts.

Mission element 4 is the recognition of numbers on houses. But before the numbers can be recognised, they have to be found. This is easier while the UAV is hovering. While hovering, the UAV can also go in any direction, which is beneficial for pointing the payload towards the house numbers and for stabilisation. Because of this, the CTOL plane has a disadvantage. The other design options have no particular disadvantages for mission element 4.

Mission element 8 is the landing on the roof. The area on which the UAV has to land was using Google Earth as 6 by 12 metres [25]. Thus, the roof provides enough room to land and take-off for vertical take-off and landing design options. There is, however, not enough room for a CTOL plane to land, turn and take-off, especially when this is done autonomously. The extra challenge posed for the autonomous vehicle is the location inaccuracy of 5 metres as discussed in Section 4.4. This would become a large disadvantage for a CTOL. The other design options all have VTOL capabilities, therefore these options do not have disadvantages for this mission element.

Usually, a landing is done more precisely with a VTOL UAV because no runway is needed for a VTOL UAV. For mission element 10, however, different rules apply for VTOL UAV as for CTOL planes. For CTOL, the plane has to land within a circle with diameter of 20 metres in order to get points and within a circle with a diameter of 10 metres in order to get maximum points. For VTOL, the plane has to land within a circle with diameter of 10 metres in order to get points and within a circle with a diameter of 5 metres in order to get maximum points [2]. This means that a VTOL plane has no advantage above a fixed wing aircraft for mission element 10.

Overall, the mission can be performed using all the design options but the fixed wing aircraft has real difficulty during mission element 8.

5.2.7. Control System Complexity

This section discusses the control of different flying concepts. It lists the challenges involved in stabilizing the different concepts which will be used as input for the trade-off in section 5.2.8.

Vertical Take-off or Landing Aircraft

The control of a VTOL aircraft poses several difficulties. First there are three different flight modes that have to be controlled: helicopter mode, transition mode and aircraft mode. Either different controllers are designed for the different modes or a more elaborate controller which is used for all modes is used [136]. Another difficulty is found within with transition mode. This is the mode were the rotors transition from a vertical to a horizontal position [136].

Conventional Take-off and Landing Aircraft

The control of a CTOL aircraft is the most straight forward of the UAVs. This is due to the possibility to decouple the lateral and longitudinal dynamics [137]. This simplifies the calculations by assuming there is no coupling between the longitudinal and lateral motion of the UAV. When the aircraft is in steady-state flight or a coordinated turn even more simplifications can be made [137].

The most difficult part is the take-off and landing of the aircraft. It was shown in [128] that if the nose it pulled up too hard during the landing flare the aircraft will land too hard and might tumble over. But when the right balance is found (possibly through testing) this can be compensated.

Another issue found was the detection of the landing zone by using a camera. But this would be no problem with the UAV since the location of the landing site at the LCC and flat roof are given [2]. The size of the landing sites is a circle with 10m radius [2] and a roof which was found to be 11 by 6 metre respectively. According to Ir. C. de Wagter, employed at the TU Delft MAVLab, the practical 95% confidence interval of a global positioning system (GPS) receiver is 5 metre.

Airship

For the control of an airship the most important part is the wind [129]. A controller for an airship must take into account the drift caused by the wind [129]. In [129] the controller does this by detecting were the airship left the intended path and to steer it back to that position. For the controller the longitudinal and lateral forces acting on the airship can be decoupled[129]. For this controller a GPS, inertial measurement unit (IMU) and wind sensor are used. The method shows promise but it needs to be further developed in order to use it for mapping within windy conditions [129].

Another system that was found was Blimpduino [138]. This system is used for the control of a small airship. It is small, light and simple but it can only be used indoors. Because of this it cannot be used for the UAV.

Helicopter

For a helicopter there are two control systems, flybar and flybar-less. A flybar is a rod with small paddles on either side and is used to stabilize the helicopter [139]. This is achieved by mechanically linking the flybar to the main rotors. This results in a complex rotor system with many links [139].

A helicopter can also be designed without the flybar. The control of such a helicopter would be achieved via an electronic control system [139]. The main advantages of a flybar-less system are less weight and a simpler rotor head. The main downside is the susceptibility of the system to vibrations [139]. Several flybar-less systems are available on the market which could be adapted to be used in the UAV [140].

Despite the flybar-less system having a simpler rotor head than a flybar system it still requires a rotor head which can change the pitch angle of the rotor blades. This is achieved by the use of a swashplate. This swashplate is a system which connects the non-rotating control systems to the rotating rotors. This makes the rotor head of the helicopter quite complex relative to other UAV control systems.

Multicopter

The control of a multicopter has proven to be difficult. This is due to the natural instability of a multicopter [141]. Despite this the control of a multicopter is quite mature. Many articles were written about the control of a multicopter with successful results [141] [142] [136]. It is even possible to buy of-the-shelf control boards to stabilise the multicopter at a low price [143]. It is also possible to use more elaborate boards which also have a build in autopilot [58].

Additionally the control of a multicopter is performed by changing the thrust from the motors. So there is no need for additional servo motors or control surfaces. This greatly simplifies the design of a multicopter.

5.2.8. Flying Method Trade-Off

The flying method trade-off is performed using the input generated in the previous sections. The trade-off utilizes the analytical hierarchy process (AHP) to generate the criteria weight factors [23]. The graphical trade-off is used for the trade-off itself. The methods, tools and rationale for using these methods are similar to those used in Section 3.2.1 for the mission design trade-off.

The AHP resulted in the criteria weight factors as listed in Table 5.2. This table also presents the most common reasons of the three participants to determine the importance of each criterion. Note that the AHP input to generate the criteria weight factors has a 97 percent consistency for the different criteria and a 93 percent consensus between the three participants.

The trade summary table was generated using the graphical trade-off method and utilising the aforementioned criteria weight factors. The graphical trade-off table uses a total of four different categories defined as excellent,

Table 5.2: The criteria weight factors including rationale for flying concept trade-off

Criterion	Weight factor	Rationale
Dimensions	0.12	Section 3.2.3 proved that the dimension of the UAV has a large influence on the amount of points scored for all mission elements.
Feasibility	0.61	The design option can only score points and win IMAV, if the concept is feasible and can be produced before the competition day.
Performance	0.06	The design option's specifications can have large effect on one or more mission elements.
Control System Complexity	0.21	The control system complexity influences the ability to perform the mission as well as the accuracy with which the mission elements can be performed.

good, fair and poor, identical to the trade-off of Section 3.2.1. The trade summary table combining the design option analysis of this chapter as well as the trade-off methods of this section is shown in Table 5.3.

Table 5.3: Trade Summary; Converging from 5 to 1 design options by selecting the multicopter

Options\Criteria	Dimensions	Feasibility	Performance	Control System Complexity
VTOL Aircraft	Good 80 - 150 cm	Fair Successful miniaturisation, however autonomous capabilities are not yet mature; The additional light modes add complexity, while not necessarily applicable to the mission	Excellent Possible	Poor Three control modes need to be designed; Transition mode difficult to control
CTOL Aircraft	Good 80 - 150 cm	Excellent Succesful miniaturisation and autonomous capabilities are technically mature; Minor issue with respect to autonomous takeoff and landing	Poor Not Possible	Excellent Straight forward control, a landing scheme can be created with some tuning
Airship	Poor 150 - 200 cm	Poor Unsuccesful miniaturisation and few examples of autonomous capabilities not able to perform the IMAV competition's mission elements	Excellent Possible	Fair Straight forward control; High susceptibility for gusts
Helicopter	Excellent 60 - 100 cm	Excellent Succesful miniaturisation and autonomous capabilities are technically mature; Less efficient than fixed wing aircraft due to mechanical lift production.	Excellent Possible	Fair Flybar-less systems used for stabilization; Swashplate still complex
Multicopter	Excellent 75 - 114 cm	Excellent Succesful miniaturisation and autonomous capabilities are technically mature; Less efficient than fixed wing aircraft due to mechanical lift production.	Excellent Possible	Good Off-the-shelf control boards; Small amount of moving parts.

The final design option selected based on the trade-off shown in table 5.3 is the multicopter. This design option has an excellent overall score as it only has a minor deficiency with respect to the control system complexity of the option. However, it was concluded that this issue can be overcome by the team within the available project resources.

5.2.9. Renewed Requirement Analysis

Two requirements are discarded based on the multicopter concept selected, these are listed in Table 5.4.

Table 5.4: Discarded requirements due to the selection of the multicopter concept

ID	Requirement
IMAV-SR-17	An emergency landing of a UAV with fixed wings shall be performed without propulsion
IMAV-CR-ME10-14	All CTOL UAVs shall make a precision landing in the LCC within a circle of 10 metre

5.3. Design Process Description

This section describes the design process of the propulsion and airframe subsystems based on the multicopter design option selected in the previous section. An initial analysis of this design process found a total of four inputs: payload weight, dimensions and power and the total weight. However, the total weight of the system is also an output variable of the design process. Therefore, a design iteration loop was required to be able to finish the design process. A flowchart of this design iteration can be seen in Figure 5.3. The total weight estimation of Chapter 3 was taken as input for the first design iteration. The final concept can be designed once the input total weight equals the output total weight of the design loop. The upcoming sections will elaborate on each block of the flowchart. All sections present the design process as well as the results of the final iteration.

The design iteration flow has a strong snowball effect with respect to the mass and power of the system. For

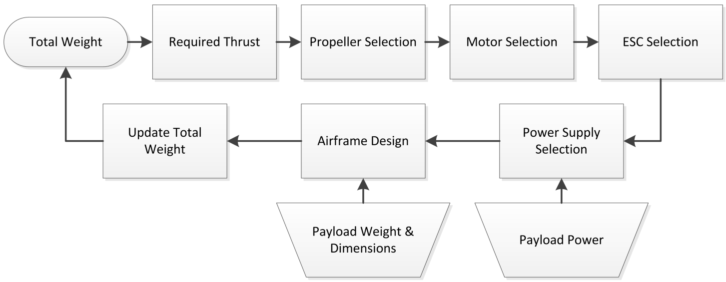

Figure 5.3: The design iteration flowchart used to select the propulsion and airframe system.

example, the required thrust increases if the payload mass to be carried by the UAV increases. Therefore, the power delivered by the motor increases, which results in more energy to be stored in the battery for a similar mission time. Due to this effect, the mass of the battery has to increase to be able to store the extra energy. Thus, an increase in the mass of an external parameter results in a larger increase in mass due to this snowball effect. Of course, this snowball effect also results in a additional mass decrease, if the mass of an external parameter decreases.

An overview of a single UAV with the finished propulsion and airframe design is presented in Table 5.5. This overview contains the specifications for a single UAV for the first iteration loop, based on the results of Chapter 3, and the final design iteration. The later specifications can be used as a reference for all calculations performed during the final design iteration in this section.

Table 5.5: Propulsion and airframe characteristics of a single UAV.

Specification	**First Iteration**	**Final Iteration**
UAV Mass	3.5 kg	2.3 kg
UAV Cost	€1120	€1150
Total number of propellers/engines	-	6
Maximum thrust-to-weight ratio	1.7	2.2
Continuous thrust-to-weight ratio	1.7	1.65

5.4. Required Thrust-to-Weight Ratio

The first step in the propulsion and airframe design process is the determination of the required thrust, as seen in Figure 5.3. The required thrust is expressed indirectly as a thrust-to-weight ratio. The required thrust-to-weight ratio is based on a literature study as well as the evaluation of three scenarios. These three scenarios are: the effect of a gust on the UAV, the effect of translation motion on the UAV and the effect of rotor aerodynamics on the UAV.

Gust Stabilisation

The change in thrust generated by the engines of the UAV to compensate for a gust of wind, is estimated assuming that a UAV starts out from a stable hovering flight with no wind. After analysis, a wind velocity is added at an angle to the UAV and the thrust forces needed to continue stable hovering flight are calculated. It should be noted that for the first approximation, the UAV is considered a flat plate and only two-dimensional forces and moments are considered.

The choice for a flat plate idealisation is made because no detailed data could be found on the lift or drag generated by the UAV, neither was it possible at this stage to perform wind-tunnel tests on a model version to determine the lift and drag. A flat plate has well-documented lift and drag data, furthermore this is considered to be a conservative estimation as many scientific papers model the micro UAVs or multicopters without body drag [144] [145].

At this point in the design, it is only decided that the UAV shall be a multi-copter. Therefore, the systems is assumed to be a quadcopter for this analysis. This is done to simplify the effects of gust due to the symmetric properties of the aircraft. The strength of a gust in August, the month of the IMAV competition, is estimated as 9 metre per second by taking the average of the maximum gust strengths over the month of August 2013 as provided by the Royal Netherlands Meteorological Institute (RNMI) [146].

Using the above assumptions, a tool was developed in Excel to estimate the response of the system under a gust. However, since the angle of attack of a gust cannot be known, this tool is used to determine some limits. With a gust speed of 9 metre per second, and thruster input set to counter the resulting aerodynamic moment, it can be seen that a control system would have to respond and correct the attitude of the system within half a second before a UAV could potentially rotate beyond 45 degrees, lose over 2 metres of altitude and drift over 1.5 metres in horizontal direction. without enough altitude to recover (for example during landing), this could lead to loss of the system.

It should be noted that the thruster levels are set to counter the resulting aerodynamic moment, and with an overall thrust-to-weight ratio of 1.0. It can be seen that it is possible to counter the 9 metre per second gust up to an angle of attack of 23 degrees.

Translation Motion

The thrust-to-weight ratio needed to fly at constant forward speed was estimated using a mathematical discretisation. As mentioned for the wind stability, a 2D flat plate model was used to model the drag coefficient of the UAV. Equation (5.3) presents the drag coefficient, C_D, for a flat plate model as found in literature [147]:

$$C_D = 2\sin^2\alpha \tag{5.3}$$

In which α represents the angle of attack in radians. This angle of attack is assumed equal to the pitch angle of the UAV. The drag coefficient is afterwards converted to a drag force using Equation (5.4):

$$D = 0.5\rho V^2 S C_D \tag{5.4}$$

In which, ρ represents the standard sea-level density of 1.225 kilograms per cubic metre, V represents the free stream velocity in metre per second and S represents the chord length of the flat plate in metre. An equivalent chord length for the UAV was not known, therefore a length of 1 metre was chosen based on the L_{max} parameter found in the IMAV competition rules [2]. The maximum free stream velocity is estimated to be 8.1 metre per second, based on the velocity estimation of Chapter 3, 5.7 metre per second, and the average wind velocity at the competition site in August, 2.4 metre per second [1] [146].

The horizontal and vertical thrust forces acting on the system were modelled using the pitch angle and a total thrust force generated by the propellers. Furthermore, it was assumed that the system travels in a straight horizontal path, resulting in the assumption that the sum of forces in horizontal direction are zero. Finally, the angle of attack was kept constant throughout the full simulation.

A backward discretisation resulted in the relation between V, the velocity in metre per second, a, the acceleration in m/s^2 and t, the time in seconds as presented in Equation (5.5).

$$V_i = V_{i-1} + a_i(t_i - t_{i-1}) \tag{5.5}$$

The results of the discretisation gives an estimate of the time needed to accelerate to the maximum velocity. This estimate depends on the constant pitch angle given to the system. The results are presented in Figure 5.4. An optimum angle of attack was found at 15 degrees, which corresponds to a required thrust-to-weight ratio of 1.04.

Rotor Aerodynamics

Finally, a literature study concerning rotor aerodynamics showed that the thrust produced by propellers is reduced, when the free stream velocity increases [148] [149]. As shown by Powers et al, this thrust reduction only has a large effect if the free stream velocity comes straight from above [149]. This phenomenon was therefore evaluated at a climb velocity of 5.7 m/s, based on the maximum velocity estimation of Chapter 3. Test performed on Stanford's STARMAC were used as a reference to evaluated the magnitude of the described effect, as this UAV is about the same size as the designed system. It was therefore estimated that the UAV requires a thrust-to-weight ratio of at least 1.45 to over come these aerodynamic effects [148].

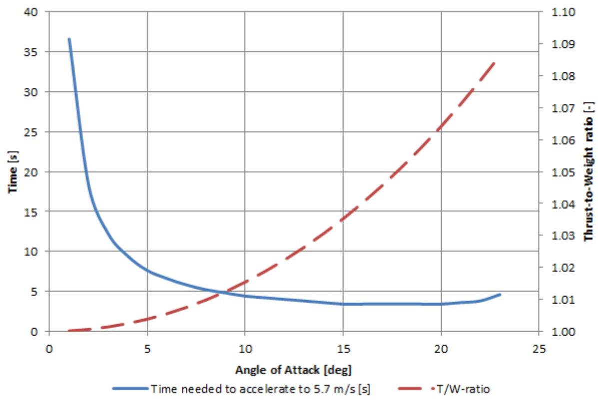

Figure 5.4: Time needed to accelerate to a maximum velocity of 5.7 m/s for constant angles of attack

Thrust-to-Weight Ratio Required

The continuous thrust-to-weight ratio needed throughout the mission was estimated as a thrust-to-weight ratio of 1.5, based on the three scenarios simulated in this section. This continuous thrust estimation is important for the total energy that needs to be stored in the power supply subsystem. Therefore, the system efficiency was optimised for this specific thrust-to-weight ratio. However, it was found in literature that the propeller system must be capable of delivering a thrust-to-weight ratio of 2, since the control is performed using thrust of the propellers while it should still remain airborne [150]. Therefore, this thrust-to-weight ratio serves as a peak thrust estimation, which the propellers must be able to achieve.

5.5. Propeller Selection

The propeller of a multicopter is used for multiple purposes. Firstly, the propellers provide the main lifting force to keep the multicopter in the air. Secondly, the attitude of the multicopter is controlled by varying the thrust levels of the different propellers.

The thrust generated by a propeller can be computed with equation (5.6) and the power used by a propeller can be computed with equation (5.7) [151].

$$T = C_T \cdot \rho \cdot n^2 \cdot D_p^4 \tag{5.6}$$

$$P = C_P \cdot \rho \cdot n^3 \cdot D_p^5 \tag{5.7}$$

In these equations, T is the thrust in Newtons, C_T is the dimensionless thrust coefficient, ρ is the air density in kilograms per cubic metre, n is the rotational speed in revolutions per second (RPS), D_p is the propeller diameter in metres, P is the power in Watts and C_P is the dimensionless power coefficient of the propeller. The thrust and power coefficients of the different propellers were found in an extensive propeller database made by the Department of Aerospace Engineering of the University of Illinois [152].

For efficient thrust generation, a high thrust-to-power ratio is preferred. This usually means having larger propellers which turn at low revolutions per minute (RPM), which can be seen in equations (5.6) and (5.7). For stability and control however, smaller propellers are preferred, since they have a smaller moment of inertia and therefore react faster to changes in RPM as demanded by the control system [150]. Also due to the score system of the IMAV a smaller UAV will score more points.

In Section 5.4 it was found that the system must have a maximum thrust-to-weight ratio of 2:1. This means that all the propellers together must be capable of providing twice as much thrust as the UAV weighs. This is the maximum it should be able to achieve. Besides the maximum thrust-to-weight ratio, the efficiency at a thrust-to-weight ratio of 1.5:1 is examined. It was calculated in Section 5.4 that this will be the nominal thrust-to-weight ratio. So, optimising the propellers with respect to the power for this thrust level will result in a system with the lowest power consumption. This will lead to a smaller battery for the given flight time and will result in a lighter system overall.

For the final propeller selection it was found that the smallest diameter which can still provide the lift required for the thrust-to-weight ratio of 2:1 is eleven inches. This diameter was selected due to smaller propellers being better for control and points as stated before.

With a total mass of 2.3 kilograms and six propellers, the final system will require a thrust of 840 grams per propeller. So all propellers of eleven inch which can generate 840 grams thrust were examined for their efficiency. It is clear from Figure 5.5 that the APC Slow Flyer 11x4,7 uses the least amount of power to provide the nominal thrust of 630 grams compared to all other propellers available within the database. The specifications of the APC Slow Flyer 11x4,7 propellers can be found in Table 5.6.

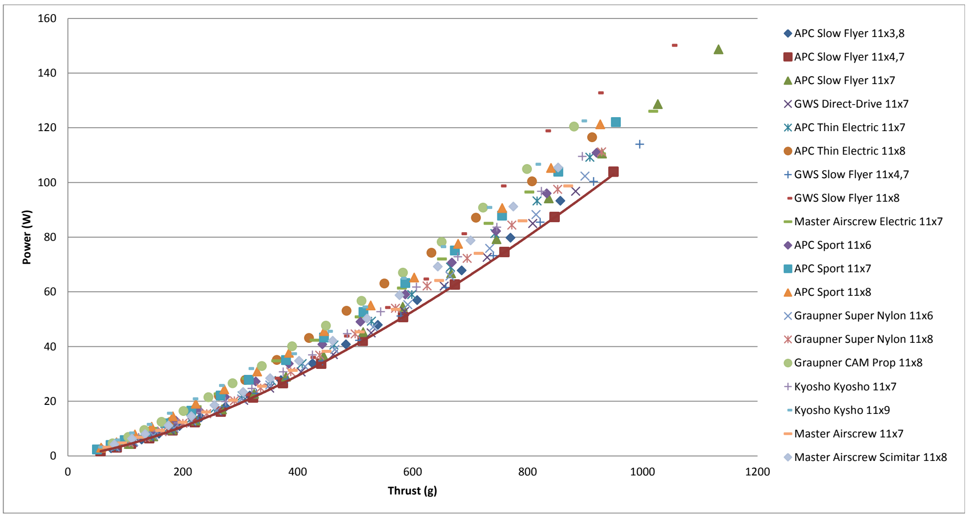

Figure 5.5: Thrust to power for 11" propellers with over 850 grams of thrust. Each set of points corresponds to a different propeller and the line with square dots represents the APC Slow Flyer 11x4.7 propeller

Table 5.6: Specifications of the APC Slow Flyer 11x4,7 propellers [153]

Parameter	**Single propeller**	**Six propellers**
Diameter	27.9 cm (11")	27.9 cm (11")
Pitch	11.9 cm (11")	11.9 cm (11")
Power consumption at nominal thrust (630 g)	58 W	348 W
Revolutions per minute at nominal thrust (630 g)	5066 RPM	5066 RPM
Power consumption at maximum required thrust (840 g)	88 W	528 W
Revolutions per minute at maximum required thrust (840 g)	5762 RPM	5762 RPM
Mass	13.9 g [153]	83.4 g
Cost	€2.90 [153]	€17.40

5.6. Motor Selection and Gearbox Design

The motor subsystem is used to convert the energy stored in the power supply subsystem into mechanical energy used by the propeller to generate thrust. An electric motor should be selected for this purpose as indicated by requirement *IMAV-SR-01*; the system shall only use electric propulsion.

The motor selection process was supported by an online program, eCalc Multicopter, developed by Markus Mueller [154]. This program includes a database of 3748 motors, based on 65 manufacturers. However, the program had to be validated, such that the motors could be selected with certain accuracy. The results of this validation are therefore essential for the feasibility of the motor selection.

ECALC MULTICOPTER MOTOR PROGRAM VALIDATION

The online program has to be validated for the RPM and motor efficiency, as these two parameters are used within the design iteration loop. However, no test data could be found for the motor efficiency of motors included in the eCalc program. Therefore, the motor efficiency is validated by validating the output shaft power. This is possible as the motor efficiency is equal to the ratio of input power and shaft power.

The validation was performed using test data found from two different sources. The first source includes approximately 10,000 data points of different motor and propeller combinations for input power, RPM and thrust [155]. An elaborate description of the test stand and test procedures is included. The second source used for the validation process was the propeller test data found as discussed in the previous section [152]. The latter source is used to convert the output shaft power, computed by the program, to the thrust generated by the propeller. This way, both the RPM as well as the motor efficiency could be validated.

The validation was done for a nominal input voltage of 11.1V, which corresponds to three Lithium Polymer cells in series. Furthermore, the validation was performed by matching the input current of the test data to current presented by the eCalc program. This resulted in 16 unique motor propeller combinations available in the program, as well as the corresponding test data. The results of the validation can be seen in Table 5.7.

Table 5.7: Validation of eCalc Multicopter motor program, using motor and propeller test data ordered alphabetically [155] [152]

				eCalc Results			Test Data		
Motor	**Prop**	**RPM Error [%]**	**Efficiency Error [%]**	**Revolutions [RPM]**	**Input Power [W]**	**Thrust [g]**	**Revolutions [RPM]**	**Input Power [W]**	**Prop Thrust [g]**
Ammo 20-40-3500 4.0:1	8x6 APC E	-7.3	-8.4	8151	144.7	565	8790	146	617
AXI 2212/26	8x6 APC E	**-9.8**	-4.7	7548	119.7	484	8370	121	508
AXI 2212/26	9x3.8 APC SF	-9.6	2.7	7568	118.8	732	8370	120	713
Axi 2212/34	11x4.7 APC SF	-1.3	4.6	5332	97.6	706	5400	96	675
Axi 2212/34	9x7.5 APC E	-3.7	8.9	5692	82.8	403	5910	82	370
Dualsky XM 3536-8	9x4.5 APC E	5.6	4.8	9757	136.4	870	9240	137	830
E-max BL 2215/25	10x5 APC E	5.1	4.7	7880	130.5	829	7500	131	792
Hacker A20-22L	8x6 APC E	-1.6	4.4	8527	145.3	592	8670	148	567
Hacker A20-26M	8x4 APC E	-0.3	8.0	10196	133.3	715	10230	135	662
Himax 2825-2300 2.5:1	9x9 APC E	5.3	**9.9**	7995	212.8	810	7590	217	737
Hyperion Z2213-24	10x5 APC E	-0.1	2.8	7553	128.1	846	7560	129	823
Hyperion Z2213-24	9x4.7 APC SF	-2.4	1.0	7875	103	702	8070	104	695
Hyperion Z2213-24	9x5 Graupner SLIM	-3.8	4.6	7876	96.9	640	8190	98	612
Mini AC 1215-20 3:1	8x6 APC E	-2.4	2.7	7880	128.9	524	8070	131	510
Turnigy 2217-20T	10x7 APC E	1.9	-0.3	7187	142.1	798	7050	145	800
Turnigy 2217-20T	11x4.7 APC SF	1.8	3.9	6537	172.1	1081	6420	174	1040
	Average Error	**3.9**	**4.8**						

The results in Table 5.7 clearly show that the results computed by the eCalc multicopter program have a maximum error of 10% for the RPM and the motor efficiency. There are several occasions at which the maximum error is almost reached, indicating that this value is not based on a single outlier. Besides the maximum error, the average error is 3.9% and 4.8% for the RPM and efficiency respectively. Finally, it is concluded that there is no apparent relation between the magnitude of the errors and the input provided to the program based on the results of Table 5.7.

Therefore, the design thrust of the UAV was increased with a safety factor of 1.1 to account for the maximum error of 10%. Thus, the UAV is designed for a maximum thrust-to-weight ratio of 2.2 and a continuous thrust-to-weight ratio of 1.65 to fulfil the required thrust-to-weight ratios as specified in Section 5.4.

MOTOR SELECTION PROCESS

The motor selection process included the evaluation of all motors available in the program. The total database of available motors was reduced using the mass, power and cost budget within the final iteration loop. The maximum mass available per motor was estimated within the first iteration as 51 grams. Furthermore, the minimum power limit required to power the propellers was 110 Watts for a motor running at almost 100% efficiency. This reduced the total set of 3748 available motors to 312. Afterwards, the database was cleared from any discontinued or not readily available motors, such that 109 motors remained feasible.

The remaining motors were run through the eCalc multicopter program and the RPM at maximum thrust and efficiency at nominal thrust were found for each motor. This process showed that many motors are running at an RPM a factor 1.5 to 4 higher than the RPM specified for the propeller. Therefore, a gearbox subsystem was added to the assembly, which matches the RPM of the motor to the RPM specified for the propeller.

The gearbox was designed based on two existing gearbox concepts, which are used to estimate the mass as well as the cost of a gearbox. The two existing gearbox concepts slightly vary in mass and cost, with one being lighter and the other cheaper [156] [157]. The gearbox efficiency was estimated, based on several sources, to be 85%, since the gearbox efficiency is not provided by the manufacturer [158] [159] [160].

Two main principles were used to select the gears used for the gearbox. First, the ratio between the number of teeth of both gears, i.e. the gear ratio, is selected based on the difference in RPM between the propeller and the engine. Second, gears must have the same module (pitch) and pressure angle for both gears to mesh [160]. Based on these two principles, the appropriate gears were selected for the gearbox design [161].

All 109 remaining motors, including a gearbox if required, were evaluated for the motor efficiency and motor mass. These two outputs were used to complete a full design iteration, as described in Section 5.3, including the battery selection and airframe design. This process showed that only three motors can be used for the UAV. These motors are listed in Table 5.8. The mass and cost given for each motor is based on the mass and cost of the motor, gearbox and battery. The latter two subsystems are included, since the mass and cost of these systems are different for each motor listed in Table 5.8.

Table 5.8: Feasible motor selections; mass and cost refer to the total mass and cost of the motor, gearbox and battery subsystems

Motor Name	**Mass [kg]**	**Costs [€]**	**Motor Efficiency [%]**	**Gear Ratio** [-]	**Energy Needed [Wh]**
Tiger MN1806-2300 [162]	1.24	438	84.4	3.61:1	159
Cobra C-2204/32 [163]	1.29	511	83.8	3.00:1	167
Tiger MN2206-2000 [164]	1.34	608	85.5	3.11:1	168

Based on the finding as listed in Table 5.8, the Tiger MN1806-2300 was selected for the design as this is the cheapest and lightest of all feasible options. The gearbox chosen along with the concept has a gear ratio of 3.61:1. It has a 65T acetal spur gear together with 18T acetal pinion gear, both with a module of 0.5 and a pressure angle of 20° [161]. The final motor subsystem specification are presented in Table 5.9.

Table 5.9: Specifications of the Tiger MN1806-2300 Motor with 3.61:1 Gearbox [162].

Specification	**Single Motor + Gearbox**	**Six Motors + Gearbox**
Power consumption at nominal thrust (640 g)	79.4 W	476 W
RPM at nominal thrust (640 g)	21,900 RPM	21,900 RPM
Power consumption at maximum required thrust (840 g)	121 W	723 W
RPM at maximum required thrust (840 g)	20,829 RPM	20,829 RPM
Mission power consumption	26.5 Wh	159 Wh
Mass	31 g	186 g
Cost	€42.85	€257.07

5.7. Electronic Speed Controller

With the motor selected, the next step of the iteration is to select the motor controller or electronic speed controller (ESC). This ESC converts the direct current (DC) from the battery to the alternating current (AC) for the motors. Furthermore the ESC uses the signal from the autopilot to control the engine RPM and power [165]. The most important parameter for the ESC is the motor current. The maximum current the motor can draw from the ESC should be lower than the rating of the ESC. Last the ESC must be compatible with the autopilot. The autopilot outputs a pulse width modulation (PWM) signal [166].

The current rating of the motor is $14A$ [162] so the ESC should have a continuous rating of at least $14A$. Furthermore the ESC will be optimized with respect to its mass. This will positively impact the mass related snowball effect as described in Section 5.3.

The lightest ESC which can handle the 14A of the motor was found to be the Afro Slim 20Amp Multi-rotor Motor Speed Controller. This ESC has a rated current of 20A and accepts a PWM signal as control input [167]. It costs €10.21 and weighs only 13.7 grams [167].

5.8. Power Supply

For the propulsion and payload subsystems, a power supply is needed. This subsystem will be discussed in this section. The ground station will be powered by plugging it into the power grid. However, connecting a long cable to each UAV is not a viable option. Therefore, an alternative method is required to power the UAVs. In Section 4.11 the total power needed by the payload was found to be 10.3 Wh, while the propulsion subsystem needs 158.6 Wh, as explained in Section 5.6. Including an additional 5% for unforeseen factors yields a total power requirement of 178 Wh. The possibilities for a power source are limited by the safety requirements given in Table 5.1. Requirement *IMAV-SR-01* is the most defining for the system: since only electric propulsion is allowed, many conventional propulsion systems cannot be used. De facto only two options remain: in-flight energy harvesting and using battery packs.

Energy Harvesting

Energy harvesting is an increasingly promising source of energy and is used in the broadest sense here: generating any type of energy from the environment to power the systems on the UAV. This energy can come from vibrations or strain, using piezoelectric devices, or through the use of so-called "green sources" or renewable energy; solar and wind energy harvesting are some of the most well-known applications. However, as described in Section 5, the energy requirements of the system are significant, while the maximum allowed UAV dimensions are limited to 1.5 metre by *IMAV-SR-23*. Currently available solar panels cannot generate the required power while complying with size, weight and cost restrictions [168], while wind energy would interfere with the airflow around the propellers. Most importantly though, the system is designed specifically for extreme situations. Both during the IMAV competition day and in a search and rescue (SAR) mission, weather conditions will not be known in advance. Solar panels require an increased surface area on a clouded day, and wind turbines are insufficient if there is no wind. However, powering the ground station using renewable energy is not only feasible, but might be desirable during SAR missions. A detailed evaluation of this can be found in Section 7.4.

Battery Power

Clearly, it is not possible to generate the energy required by all subsystems during the mission. Therefore, the only viable option is the use of batteries. However, since both the current and voltage need to be high throughout the flight, this limits the list of possible batteries to specialised battery packs for UAVs. It is possible to use a DC-DC converter to adjust the voltage of other batteries, but this will cause a decrease in efficiency to 85% [169]. Considering that there are no commercially available single-cell batteries with Wh/kg ratings higher than 200 [170], and that the best battery pack found has an energy density of 189 Wh/kg, manually building battery packs and then using a converter is not the best option. A large selection of ready-to-use battery packs is available online [171] [172]. A spreadsheet was created that lists many 11.1 and 14.8 Volt batteries, since the propulsive systems require one of those two values. An overview of the spreadsheet is shown in Table 5.10 for the 11.1V options, since the selected propulsion systems requires an input voltage of 11.1.

The leftmost column in the spreadsheet contains a hyperlink to a web page with detailed information for each battery pack. As stated earlier, the system needs a total of 178 Wh to power the payload and propulsion, with 5 % contingency included. By dividing the required Wh by the amount that each battery pack can deliver, a required number of parallel cells is found. Combining this with the mass and price per battery pack, the total mass and cost for each type were found.

These values were used to determine the optimum pack during the first iteration of the loop shown in Figure 5.3, since this can be done automatically. However, this only optimises for a set of identical battery packs. Instead, it might be better to determine the specific energy in Wh/kg and cost efficiency in Wh/€ of each cell. This is shown in the last two columns. Using this information in the iterations that followed, the battery system was optimised for mass by picking the pack with the highest specific energy, checking how many watt-hours

Table 5.10: Spreadsheet listing the energy content, discharge rate, mass, price, specific price and energy density of ten possible battery packs.

Battery Pack	*Wh Provided*	*Ah*	*Discharge Rate [C]*	*Mass [g]*	*Price*	*Wh/€*	*Energy Density [Wh/kg]*
Required:	175						
Battery 1	244	22	40	1290	€315	0.78	189
Battery 2	133	12	100	840	€200	0.67	159
Battery 3	122	11	40	645	€185	0.66	189
Battery 4	121	10.9	120	693	€185	0.66	175
Battery 5	100	9	100	654	€150	0.67	153
Battery 6	89	8	150	600	€135	0.66	148
Battery 7	72	6.5	150	483	€120	0.60	149
Battery 8	67	6	100	435	€120	0.56	153
Battery 9	58	5.2	30	380	€41	1.41	152
Battery 10	56	5	40	414	€38	1.46	134

were still needed and then selecting the battery with the highest specific energy from those that just provide the required value, or by combining several smaller batteries with optimal characteristics. In case of multiple batteries with similar specific energy values, the cost efficiency was used to determine which pack would be used for the optimisation. Since this process required manual computations, the required time was much greater, hence it was not used for the initial estimation. An improvement of 225 grams was obtained relative to the case where identical battery packs were selected. This process resulted in Table 5.11, which was then used as input for the next iteration cycle; the final values are shown here for a relevant range of required Wh.

Table 5.11: Overview of the battery pack combinations with lowest weight for a total power requirement in the range of 170-182 Wh. The costs are also displayed

	Wh required	*Minimum mass [g]*	*Corresponding price*
Batteries: 3, 15	170	976	€219
Batteries: 3, 15	171	976	€219
Batteries: 3, 9	172	1025	€226
Batteries: 3, 9	173	1025	€226
Batteries: 3, 9	174	1025	€226
Batteries: 3, 9	175	1025	€226
Batteries: 3, 9	176	1025	€226
Batteries: 3, 9	177	1025	€226
Batteries: 3, 9	178	1025	€226
Batteries: 3, 9	179	1025	€226
Batteries: 3, 9	180	1025	€226
Batteries: 3, 8	181	1080	€305
Batteries: 3, 8	182	1080	€305

Selected Hardware

When the optimisation for mass was completed, the battery system was fixed. Its characteristics are shown in Table 5.12. Both are lithium-polymer battery packs with three cells connected in series. To charge these batteries, an iCharger 206B is selected, which is rated at 300 W for 20 A charging of batteries up to 22.2 V, with a maximum charge rate of 1C [173]. This is a normal rate for lithium-polymer batteries [174].

Table 5.12: Specifications of the battery system

Battery Pack	*[Wh]*	*[Ah]*	*Discharge Rate [C]*	*Mass [g]*	*Price [€]*
Primary battery pack	122	11	40	645	185
Secondary battery pack	58	5.2	30	380	41
Total	180	16.2	35	1025	226

5.9. AIRFRAME

The airframe is needed to support all subsystems and transfer generated loads between subsystems. This section will discuss the shape of the airframe, the material used in, the landing gear design and the engine mountings. The dimensions of the cross section are based on a detailed structural analysis, which is discussed in Section 7.2. The inputs for the airframe are the propeller size and the number of motors that are used.

5.9.1. CONFIGURATION

The UAV consist of a central platform that supports the payload and three arms that each have two engines attached, called a Y6 configuration. Placing the engines in a push-pull configuration causes an additional thrust of 5 % [175]. The Y6 configuration is chosen because it results in the lightest airframe, as this configuration only has three arms instead of four, six or eight for traditional quad-, hexa- or octocopters.

The middle section is a plate on the upper side, on which most of the payload is placed. Between the plates and the frame, rubbers are placed. In this way, the vibrations caused by the motors are damped and the payload is less affected by the vibrations. In order to let the propellers function properly, a minimum distance of one full propeller length is needed [121]. Based on this principle, the arms are placed with equal angles of 120° between each two arms to minimize maximum dimension of the UAV. The maximum dimension is preferably as small as possible because this gives the most points in the competition [2].

The length of a single arm can be computed using Pythagoras theorem and the discussed angle between the arms. The arm length was determined to be 32.3$[cm]$, because propellers were chosen with a length of 27.9$[cm]$ (11 inches). Where the arms come together, in the middle, a casing is used to keep the arms together. An overview of final configuration of the design is presented in Figure 5.6.

Figure 5.6: Configuration overview of the three-armed hexacopter airframe with a generic propulsion system.

5.9.2. MATERIALS

The airframe needs to be light, because then the propulsion subsystem needs to generate less thrust. This results in a further weight decrease due to the snowball effect, discussed in Section 5.3. This results in a lighter propulsion system and also a overall design. Materials with a high specific strength, i.e. a high strength-to-density (σ/ρ) ratio, are needed in order to achieve a light airframe. Commonly used light materials for structural components are aluminium, carbon fibre, glass fibre, plastics, bamboo and balsa wood. When looking at the strength-to-density ratio, it can be found that the best option for the material carbon fibre is for the airframe [176]. At first sight, however, carbon fibre is not the most sustainable material. But when the frame is made from carbon fibre, the mass of a UAV becomes so much smaller that less powerful propulsion and smaller batteries can be used. And because the propulsion and batteries become smaller, the total UAV becomes more sustainable. The structural characteristics of the materials can be found in Table 5.13. Also, characteristics of other materials that are used in the UAV are given.

5.9.3. LANDING GEAR DESIGN

As multiple landings occur within the IMAV competition, it is wise to design a landing system in order to protect the UAV. When designing the landing gear, three main design choices have to be made: material, location and shape.

Table 5.13: Structural characteristics of the materials used for the UAV [176].

Material	**Compression Yield Stress**	**Tension Yield Stress**	**Shear Yield Stress**
Carbon Fibre	570 MPa	600 MPa	66 MPa
3D printed (PLA)	48 MPa	48 MPA	10 MPa
Safety Glass (PMMA)	80 MPa	80 MPA	10 MPa

Material choice

In case of an impact (which could be the case in landing) carbon fibre behaves poorly. Because of the relatively high stiffness of the material, hardly any energy is stored in the part that transfers the load [176]. In combination with the complicated shape of the products, it is decided to go for a 3D printed material. As the landing is commenced, the landing struts are allowed to bend to a certain limit, thereby absorbing energy in the landing struts.

Location of Landing Gear

Next the optimal location of the landing gear needs to be selected. This is done by considering the effects of a rough landing, as requirement *IMAV-CR-ME10-2* states that a UAV shall be able to demonstrate airworthiness after a rough landing. The maximum load in this scenario is estimated by defining a rough landing as hitting the ground with a vertical velocity of 1 m/s at an angle of 45 degrees. The landing strut should be able to withstand these loads. The landing gear can be mounted either between the central payload dome or at the tip of the arm. The prior option results in a significantly longer arm than the latter case. Therefore the landing gear is placed at the tip of each arm. This has the additional advantage of protecting the propellers when landing under an angle.

Impact Resistance

Several designs, driven by the requirements from Table 5.1, can be found in Figures 5.7a,5.7b, 5.7c and 5.7d.

(a) Shock absorbing ring (b) Spring-like design (c) Moving landing strut (d) Landing switch

Figure 5.7: Four design options for the landing gear are shown.

The shock absorbing ring and the spring-like design are infeasible concepts, because they do not allow measurement of landing, thus violating requirement *IMAV-CR-ME8-13*. The moving landing strut works by a moving lever, which is held back by a rubber band. When the lever moves due to landing, a switch is triggered, which indicates contact with the landing site. The levered design is more complicated and heavier than the landing strut. Since the design could not be tested during this project, the safer and less complicated option is selected. A strut with a pressure switch attached to the tip is designed.

5.9.4. Engine Mounting

The engines need to be mounted onto the airframe using bolts [162]. However, a drawback of the carbon fibre is that the strength of the beam decreases when holes are drilled into the beams for the motors [177]. Therefore, no holes will be drilled into the beams. Instead, plates are glued on the upper and lower side on the beams, which the motors can be mounted. These plates are made from 3D printed polylactic acid (PLA). An overview of this can be found in Figure 5.8.

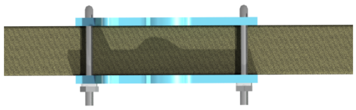

Figure 5.8: Engine mounting using plates to avoid drilling holes into the airframe.

5.10. Propulsion and Airframe Conclusion

The propulsion and airframe design was based on an initial flying method trade-off. This trade-off concluded that the multicopter design option is most suitable for this project. Afterwards, the propulsion and airframe subsystems were designed in more detail. An overview of the design is presented by means of two tables. Table 5.14 presents the requirements following from the propulsion and airframe design. Table 5.15 presents the selected solutions to fulfil the requirements presented in Table 5.14.

Table 5.14: Requirements following from the propulsion and airframe selection

ID	Requirement
IMAV-CR-ME10-21	All UAVs shall be able to land with a descent rate of 1 m/s and hitting the ground under an angle of 45 degree
IMAV-SR-26-1	The power supply system shall store energy needed to fly at a thrust-to-weight ration of 1.5 throughout the entire mission.
IMAV-SR-26-2	The propellers shall be able to generate a maximum total thrust equal to twice the weight of the system.
IMAV-SR-26-3	The motor shall provide a maximum required thrust of 88 W at 5,762 revolutions per minute.
IMAV-SR-26-4	The electronic speed controller shall be able to handle a maximum current of 14 Ampere.
IMAV-SR-26-5	The propellers shall be separated by at least one propeller diameter.
IMAV-SR-26-6	The airframe shall support all subsystems and transfer all loads generated by other subsystems.

Table 5.15: Budget breakdown of the propulsion and airframe subsystems of the Soteria UAV

Category	**Type**	**Name**	**Power** $[W]$	**Cost [€]**	**Mass** $[kg]$
Battery	Cells	LiPo 22,000 mAh 3s Battery Pack		185	0.645
Battery	Cells	LiPo 5,200 mAh 3s Battery Pack		41	0.38
Propulsion	Motor	6x Tiger Motor MN1806-2300kv	476	172	0.108
Propulsion	Motor Controller	6x Afro Slim 20 Amp Multi-rotor Motor Speed Controller		61	0.082
Propulsion	Gearbox	6x 3.61:1 gearbox frame		70	0.078
Propulsion	Gearbox	6x 3.61:1 65T, Mod 0.5, Acetal Gear		12	0.018
Propulsion	Gearbox	6x 3.61:1 18T, Mod 0.5, Acetal Gear		2.90	0.006
Propulsion	Propeller	6x APC Slow Flyer 11x4.7		17	0.083
Airframe	-	Hexacopter carbon fibre Y6-Frame		45	0.241
Total			**476**	**606**	**1.64**

The airframe was designed in more detail, besides the selection of carbon fibre Y6 configuration, resulting in the lightest structure. First, it was concluded that the landing gear should be placed outboard of the propellers, to save weight and offer better protection during a rough landing. Second, a push button was placed on each strut of the landing gear to fulfil requirement *IMAV-CR-ME8-13*. Finally, a special 3D printed engine mounting plate was the best option to mount the engines to the airframe, as it avoids drilling of holes in the carbon fibre frame.

6

System Integration

In Chapter 4, the payload carried by the designed unmanned aerial vehicle (UAV) was presented. Now that Chapter 5 has discussed the propulsion method and airframe of the design, it is possible to design the topology of the UAV. Within this chapter all elements are integrated into a single optimised design, which may be seen in Figure 6.1.

The designs of the subsystems will be discussed with the use several of methods. Firstly, the configuration and layout of the UAV itself shall be discussed in Section 6.1. Next, an overview the functions corresponding to the various mission elements can be found in Section 6.2. From there on, the communication between each of the subsystems will be elaborated upon in order to create an overview of the data flows within the system. A hardware and software block diagram will then be discussed in Section 6.3. These diagrams illustrate the individual components of the system, and create a better understanding of the interactions between the individual components. To get an overview of how each of the electrical power consuming systems are connected, two electric diagrams are shown. These may be seen in Section 6.4. As each of the subsystems has a certain chance of failure, each subsystem and the consequences of its failure are analysed in order to reduce the risks. From this, mitigation possibilities for the analysed risks will be investigated. These consequences and mitigation possibilities are considered in Section 6.5. The budget breakdown will be discussed in Section 6.6 with the use of the hardware that has been chosen. Lastly, the compliance matrix of Section 6.7 will list all requirements for the design and verify that they are met, after which a short conclusion to the chapter will be given (Section 6.8).

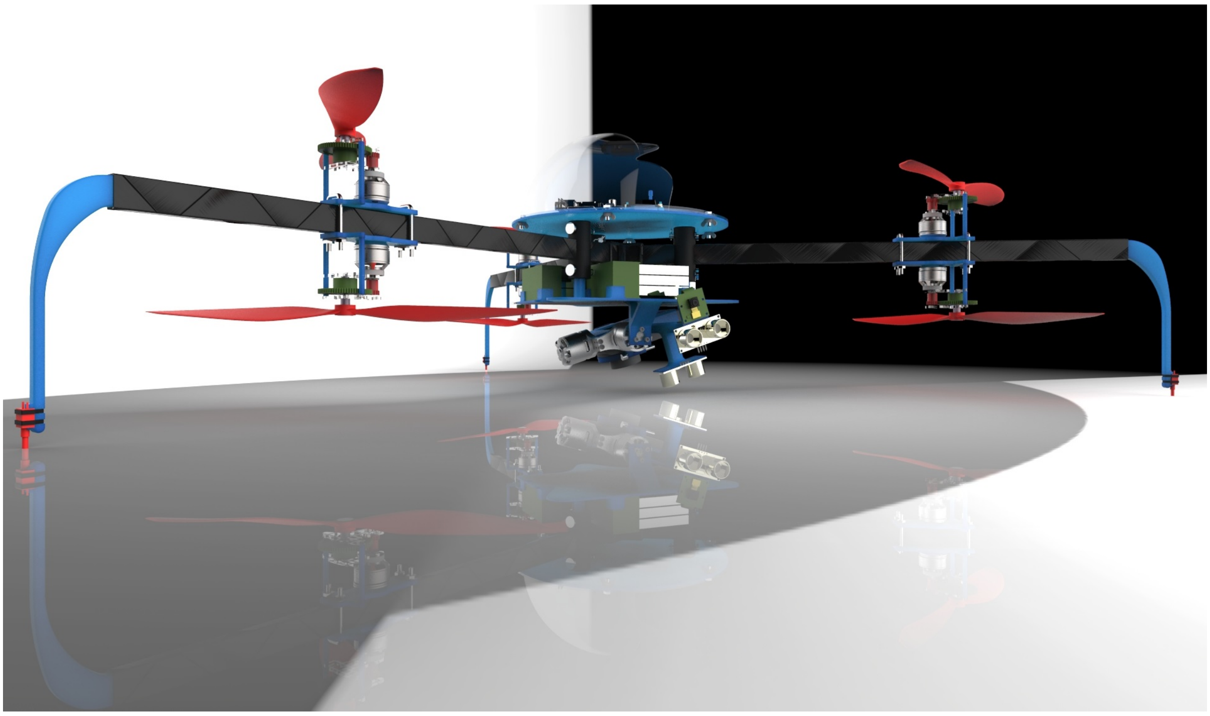

Figure 6.1: Computer drawing of one of the UAVs designed by Soteria.

6.1. Configuration and Lay-out of Aerial Vehicles

As described in Chapter 4, a total of four UAVs will complete the mission elements. In order to identify these UAVs, they were given colour-coded names, *Cyan, Magenta, Red* and *Yellow*. Painting the UAVs in these colours will enable distinguishing between them. As all materials and dimensions are known, the weight, center of gravity (COG) and mass moment of inertia (MMOI) can be calculated. A summary of the technical specifications of the UAVs can be found in Table 6.1. When integrating the individual payload and propulsion parts, several sub-parts need to be designed, this process is explained in the following sections. The technical drawing of the UAV can be found in Appendix A.

Table 6.1: Technical specifications of the Soteria UAVs. The colours and numbers indicate different materials used, corresponding to those used in Figure 6.1.

Parameter	**Value**	**Unit**
Dimensions (L x W x H)	830 x 777 x 208	[mm]
Total weight	2,3	[kg]
Mass moment of inertia	0.08 x 0.15 x 0.08	[kg m²]
Centre of gravity	0.12 x -0.13 x -22	[mm]
Materials	**Color**	**% Mass**
3D printed (PLA)	1	3
CFRP (Carbon fibre)	2	10
Batteries (LiPo)	3	44
Injection moulding	4	4
Other components	Various	39

6.1.1. Payload Section Design Integration

This section discusses the integration and topology of the payload, propulsion and airframe subsystems to form the complete UAV.

Payload Platform Design

In order to meet the requirement of keeping the global positioning system (GPS) sensor and the magnetometer separated from the propulsion and battery system, a double payload platform is designed. Both are connected via a rubber fastener to the carbon fibre frame to dampen possible vibrations. The upper platform contains all low-power payload, while the lower platform contains the gimbal, the ultrasonic range finders, the cameras and the battery system. The entire payload section is displayed in Figure 6.2. Here the payload protection dome is cut away for better visualisation.

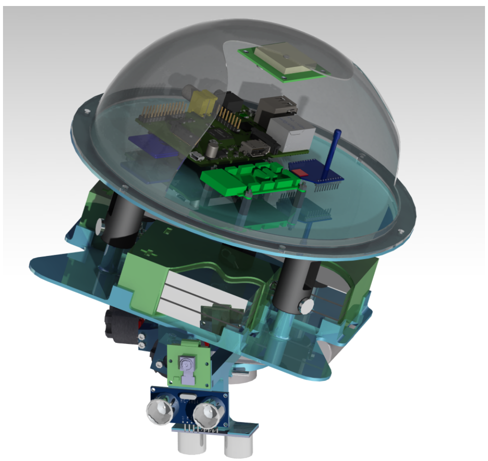

Figure 6.2: Computer drawing of the payload section, with the payload protection dome cut open.

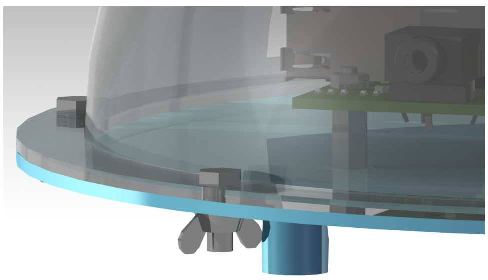

Figure 6.3: Close-up of the payload dome connection method, including the butterfly nuts.

Payload Protection Dome

In case of a crash or in the event of moisture or rain, the payload is protected from the environment by a dome made of safety glass. A convenient feature of this dome is that it creates the possibility of placing sensitive payload even further away from the high-power section by attaching it to the ceiling of the dome. The dome is attached to the upper payload platform by means of screws and butterfly nuts. This allows fast removal of the dome, which is convenient during the testing phase. Figure 6.3 shows a close up of this connection method. It should however be noted that this dome will act as a greenhouse during clear weather. Ventilation holes may thus be drilled into upper payload platform in order to prevent the electronics from becoming too warm.

Payload Platform Topology

In order to fit all components in an optimal fashion, several designs were made of the upper payload platform. The hardware list with all required payload components can be found in Section 4.11. The criteria concerning the topology are:

- The payload should be placed such that the total cable length is minimised
- The GPS and magnetometer should be placed as far away from other payload as possible
- The circular payload platform shall have a diameter smaller than or equal to that of one propeller
- The payload should always be protected from impact, vibrations and moisture
- The individual parts should be easily replaceable

Figure 6.4 shows the final design of the upper payload platform including the placement of the payload parts.

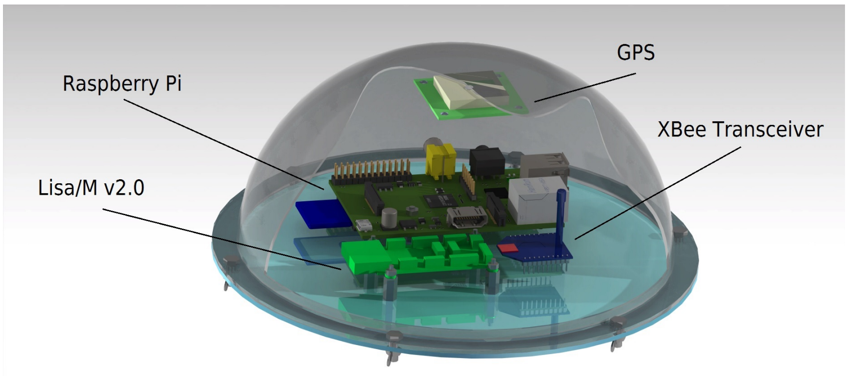

Figure 6.4: Topology of the upper payload platform showing the placement of all payload parts.

Camera Holder Design

In order to connect the camera that is used for the photomap to the UAV, a camera mount is needed. Because the camera has a complicated shape, for which no camera mount exists yet, a custom design is required. Three dimensional printing creates the possibility of producing custom parts. As was already explained in Section 4.9, the camera is attached to a gimbal, therefore an integrated design has to be made. A computer drawing of the camera mount, including its connection to other payload attached to the gimbal, can be found in Figure 6.5a.

Gimbal Design

As is described in Section 4.9, a gimbal is required. In order to minimise weight and make the selected gimbal compatible with the Sony Cybershot camera, a custom design is created. Using 3D printed parts, the camera mount is connected to a horizontally oriented motor, which makes sure the camera module is stabilised for pitch motion. A second motor is used as a roll stabiliser and is connected to both the first motor and the UAV.

As the ultra-sonic range finders and the Raspberry Pi camera module also need to be stabilised, as is explained in Section 4.2, it is convenient to place them on the same gimbal system. This is done by including additional 3D printed brackets on the front side of the gimbal. An exploded view with part names can be found in Figure 6.5b.

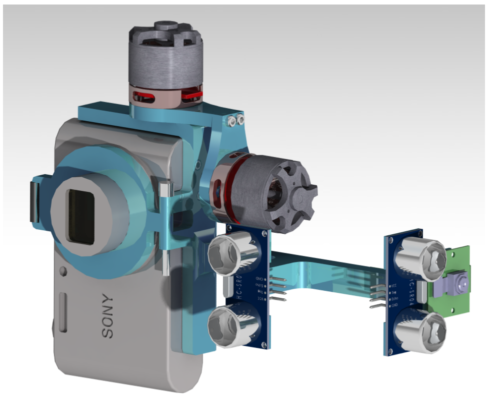

(a) Integrated camera mount design overview.

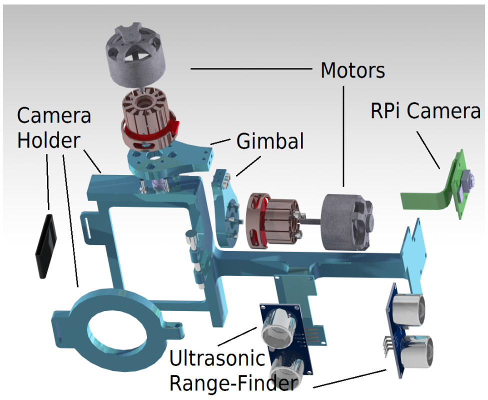

(b) Exploded view of the gimbal design.

Figure 6.5: Both an overview and an exploded view of the gimbal and camera system

Battery and Gimbal Platform

Finally the gimbal has to be connected to the bottom side of the UAV. Furthermore, the batteries which were found in Section 5.8 need to be integrated in the design. For stability reasons, which are explained in Chapter 7, it is preferred to design the COG as much in-plane with the propulsion as possible. In order to integrate these two parts a second payload platform is designed which will be 3D printed. The final design can be found in Figure 6.6. It can be seen that the batteries are held in place by straps. These straps allow quick replacement of the battery between missions.

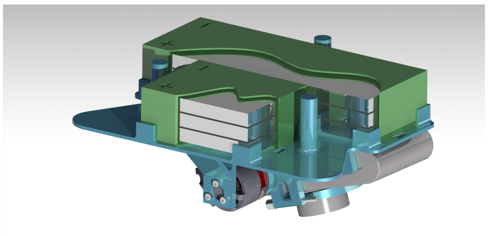

Figure 6.6: Computer drawing of the battery and gimbal payload platform.

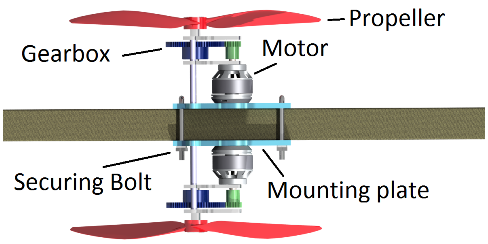

Figure 6.7: Computer drawing of mounting of the propeller, gearbox and motor mounting to the airframe.

Propulsion Mounting

The propulsion system is mounted to the airframe by a plate which will be glued and bolted to the airframe. The bolts are on the outside of the airframe so no holes have to be drilled through the carbon fibre so it does not lose its strength as discussed in Section 5.9. The motor will then be secured on the plate. The gearbox will be secured to the output shaft of the motor which in turn will hold the propeller. An overview of this mounting is given in Figure 6.7.

6.2. Mission Functions

This section presents the integration of the system with the mission. This is accomplished by presenting the functional breakdown structure (FBS) and functional flow diagram (FFD) of the various mission tasks.

The FBS is shown as a tree of functions that must be done by the system to perform its mission. This is followed by the FFD where the steps are shown in the order that the system has to execute them during its mission cycle. It does not necessarily describe how the system performs its functions.

6.2.1. Take-off

Every UAV will have to take off in order to participate in another mission element. All functions should therefore be listed. They are shown in Figure 6.8 in an FBS, followed by an FFD in Figure 6.14.

6.2.2. Create Photomap

In order to create a photomap of the competition area, the UAV will need to be able to perform some additional functions. These are displayed in Figure 6.10 as an FBS and in Figure 6.16 as an FFD. In the flow diagram it is visible that the UAV will return to the local command centre (LCC) to perform a landing to deliver the SD card; this strategy is further described in Section 3.3.

6.2.3. Create Blockade Map

The system will also be able to find blockades on roads. The determination of the blockades will be done by analysing the photomap. Because of this it has to fly back to the LCC, as stated in Section 6.2.2. These functions are shown in Figure 6.11 as an FBS and in Figure 6.17 as an FFD .

6.2.4. Quick Visual Inspection

The quick visual inspection requires the UAVs to fly towards certain houses and find their house numbers. The functions required to do this are also listed in an FBS in Figure 6.12. This is followed by the FFD in Figure 6.18. Because of the difficulty with navigating at lower altitudes the UAV has more functions that will be used for navigation.

6.2.5. Land on Roof

For the next mission element, the UAVs should fly to a specified house in the competition area and land on the flat roof. After landing, they should remain there for at least 10 seconds before taking off. In Figure 6.13, the FBS for this is shown, and in Figure 6.19 the FFD is shown.

6.2.6. Precision Landing

After the previous mission elements are successfully performed, the UAVs should land again in the landing zone. In Figure 6.9 the FBS for the precision landing is presented with all of the needed functions. Finally, the FFD for this function is shown in Figure 6.15. After the precision landing, the UAVs might need to take off again, in case it will continue with mission element 4. Otherwise, they will need to switch off and end their mission.

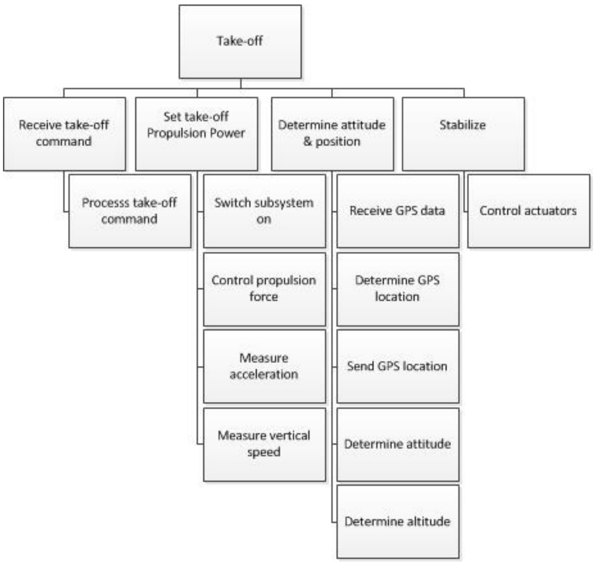

Figure 6.8: Functional breakdown structure showing all functions which the system must perform in order to take off.

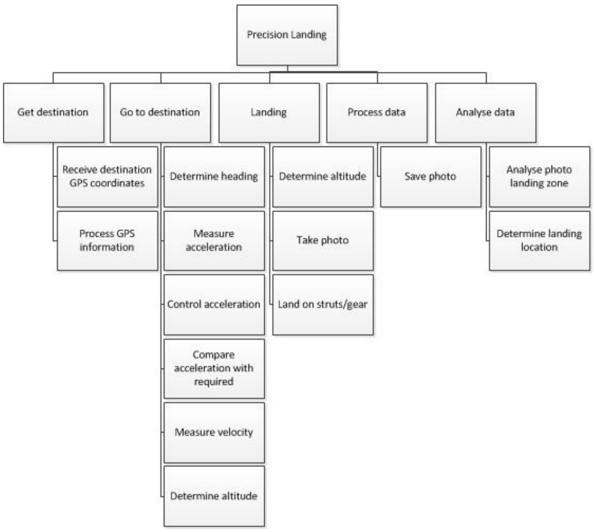

Figure 6.9: Functional breakdown structure showing all functions which the system must perform in order to perform a precision landing.

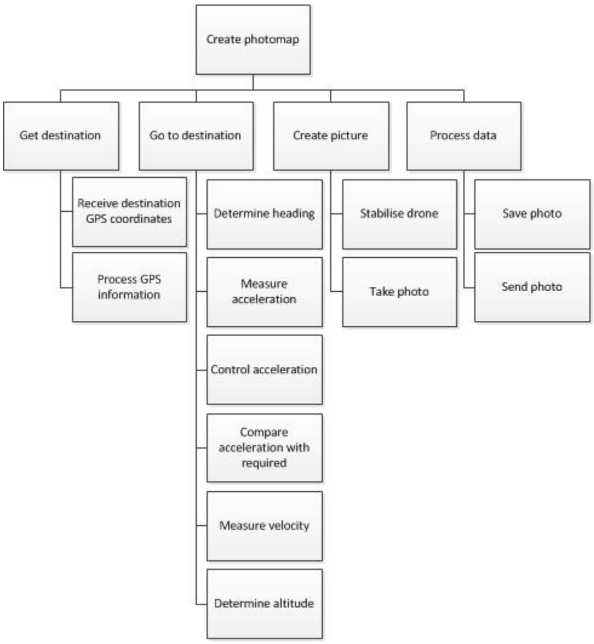

Figure 6.10: Functional breakdown structure showing all functions which the system must perform in order to make the photomap.

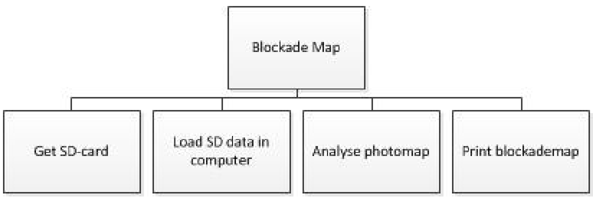

Figure 6.11: Functional breakdown structure showing all functions which the system must perform in order to make the blockade map.

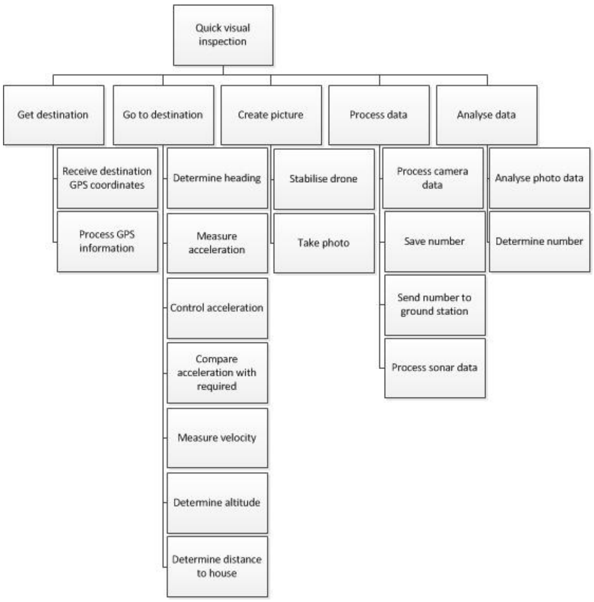

Figure 6.12: Functional breakdown structure showing all functions which the system must perform in order to perform the quick visual inspection.

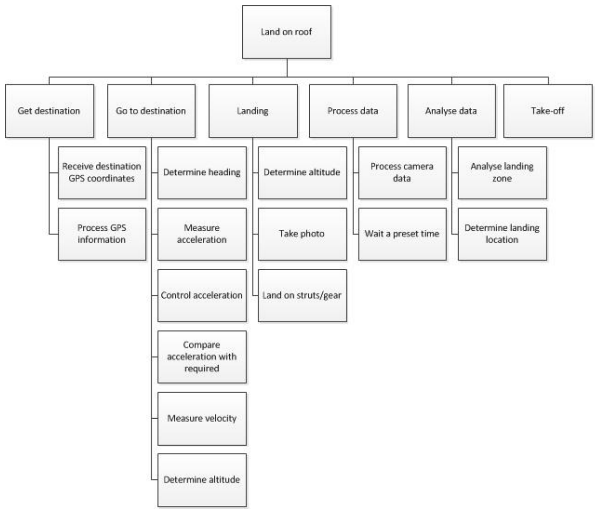

Figure 6.13: Functional breakdown structure showing all functions which the system must perform in order to land on a roof.

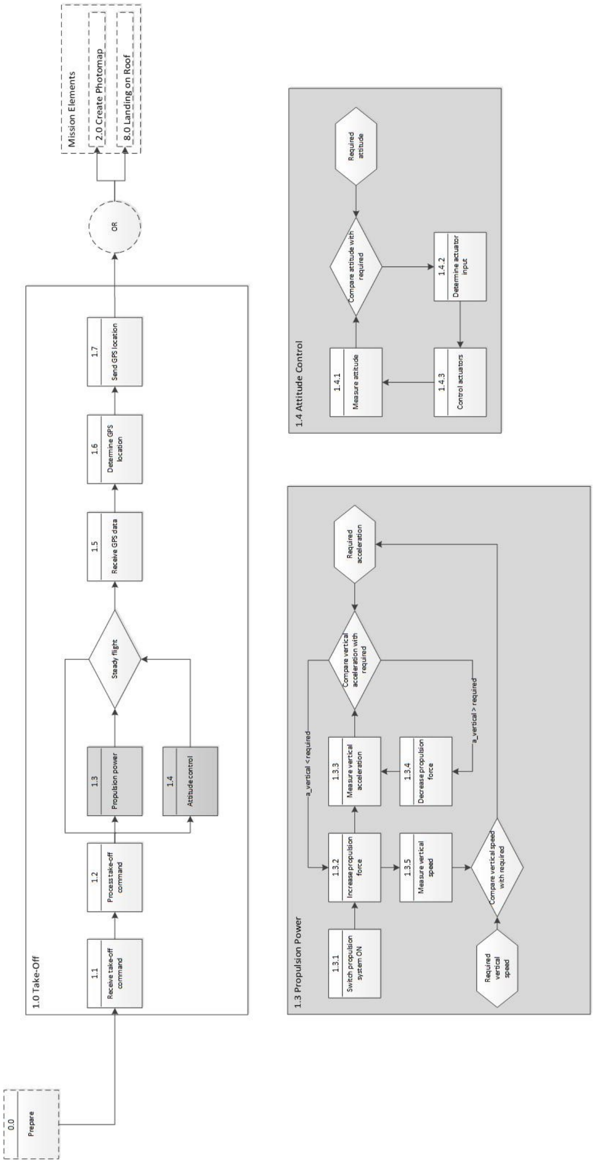

Figure 6.14: Functional flow diagram showing all functions which the system must perform in order to take off.

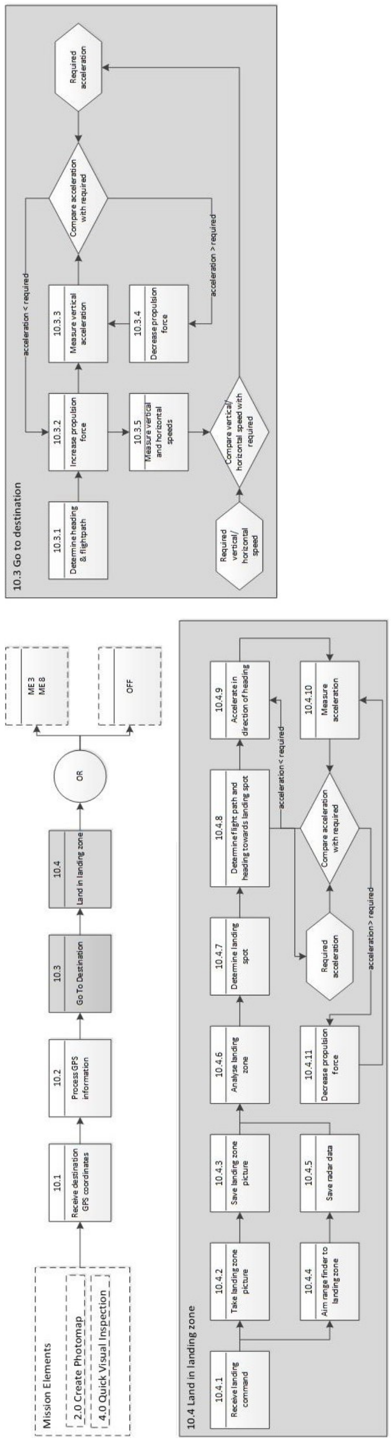

Figure 6.15: Functional flow diagram showing all functions which the system must perform in order to perform a precision landing.

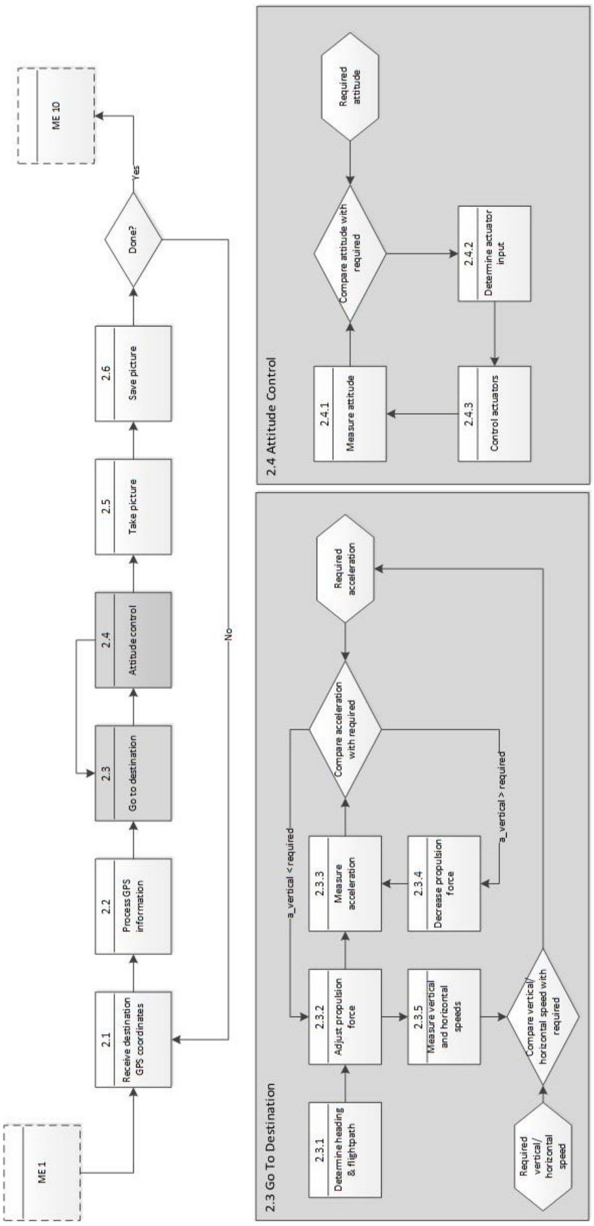

Figure 6.16: Functional flow diagram showing all functions which the system must perform in order to make the photomap.

Figure 6.17: Functional flow diagram showing all functions which the system must perform in order to make the blockade map.

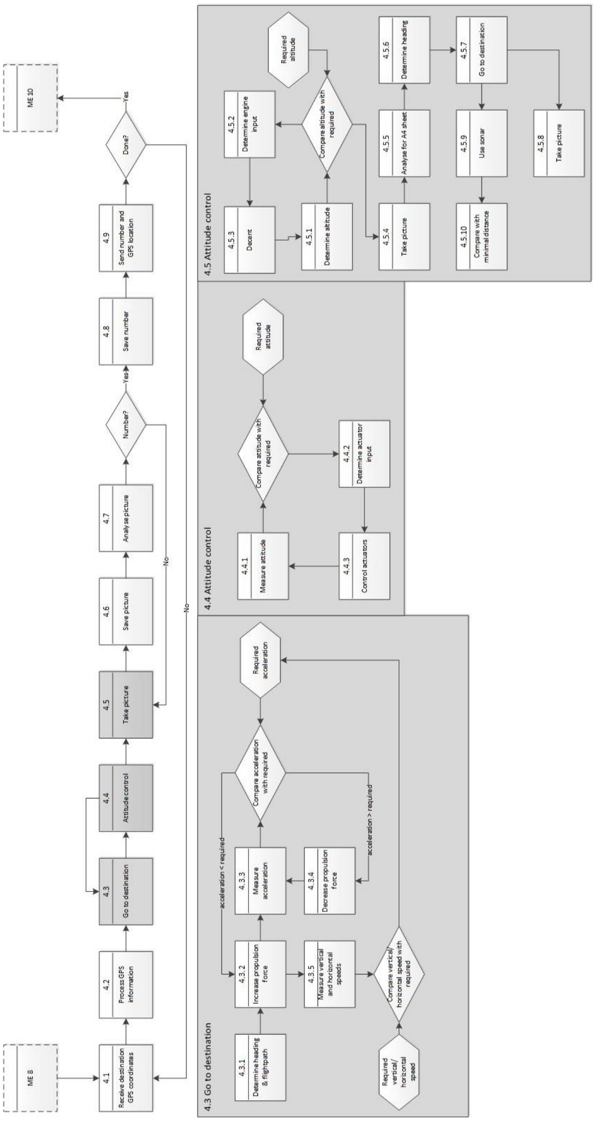

Figure 6.18: Functional flow diagram showing all functions which the system must perform in order to the quick visual inspection.

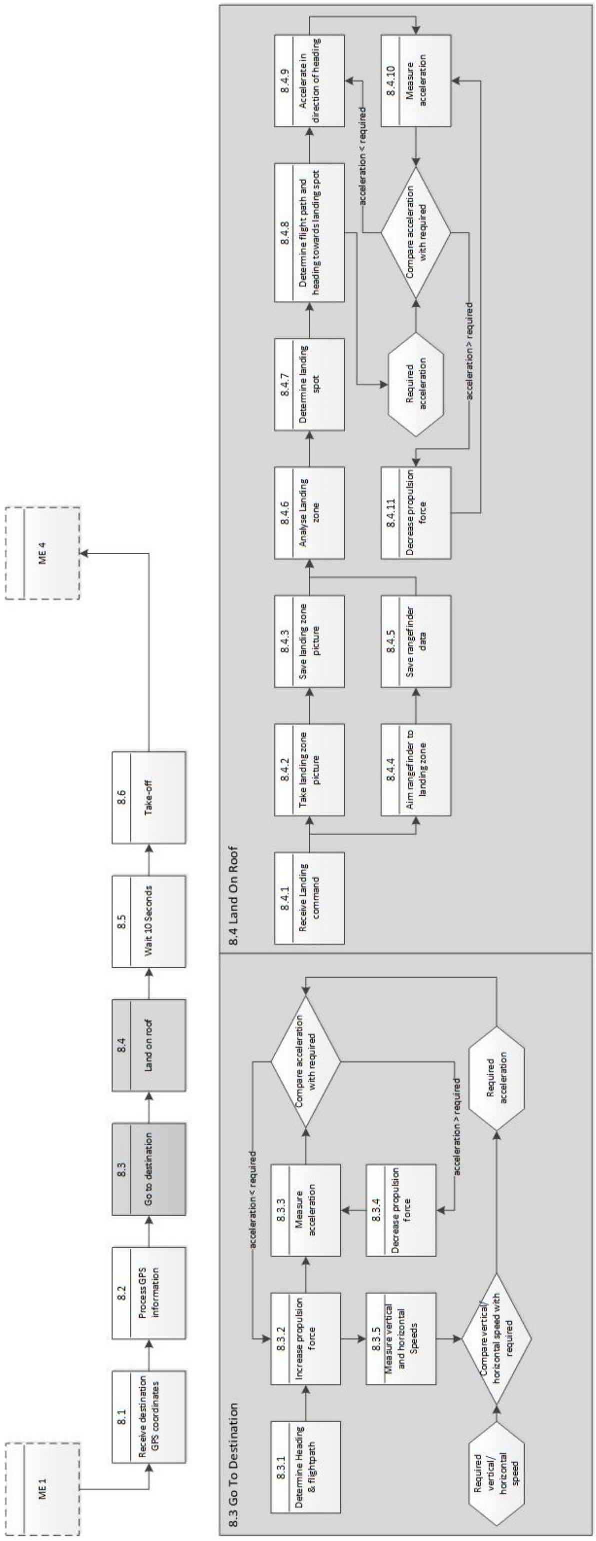

Figure 6.19: Functional flow diagram showing all functions which the system must perform in order to land on a roof.

6.3. Communication & Data Handling

This section covers both the hardware block diagram (HWBD) and the software block diagram (SWBD). Their purpose is to illustrate the individual components and to create a better understanding of the interactions within the system. Within the block diagrams presented here, the lines represent a description of the interaction and the blocks contain the name of the different sub-components of the UAV and the ground station.

6.3.1. Hardware Interfaces

The HWBD is discussed here. The UAVs and the ground station are constantly connected, therefore a transceiver is required which is installed both on the UAV and on the ground station, as can be seen in Figure 6.20.

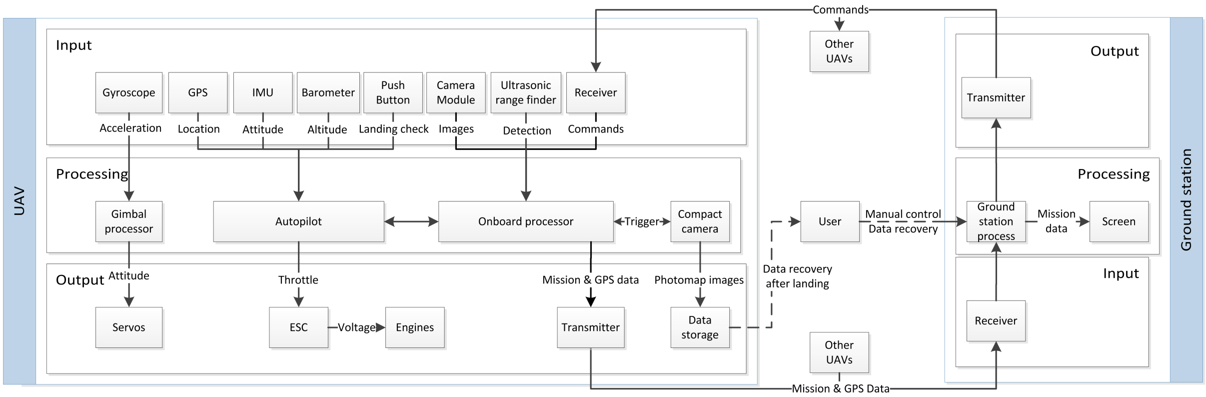

Figure 6.20: Hardware block diagram showing the different components of the system

6.3.2. Software Interactions

The software block diagram is shown in Figures 6.21a and 6.21b. First, the software on the UAV is discussed and then the ground station is described. The UAV requires a large group of drivers for all subsystems in order to process their inputs. These inputs are then sent to either the autopilot or the board computer where the input gets processed. Depending on the inputs, a certain signal is sent to the propulsion system. Furthermore the UAV has a constant connection with the ground station. The ground station will consist of a high-end desktop computer with all required software installed. It has to be able to communicate with both the UAV via a transceiver and all input devices, such as keyboards and SD-slots.

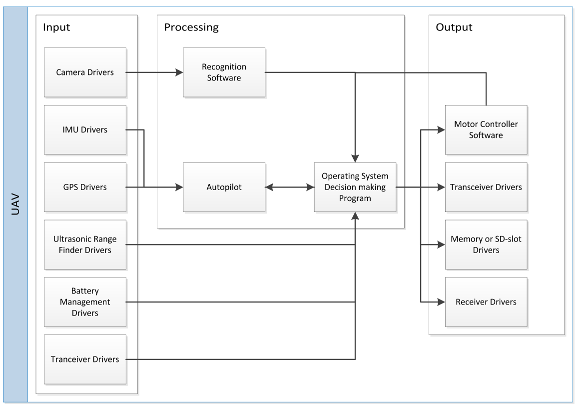

(a) Software block diagram showing the interaction between the subsystems on the UAV

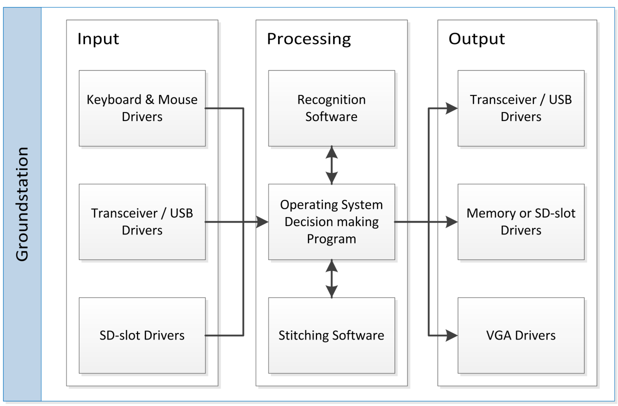

(b) Software block diagram showing the interaction between the subsystems on the ground station

6.3.3. Combined Data Flows

Next, the communication flow diagram and the data handling block diagram are combined into a single figure. Together they create an overview of all data flows through, to and from the system. Within Figure 6.22, the hardware is displayed as blocks and the data flows are represented by arrows.

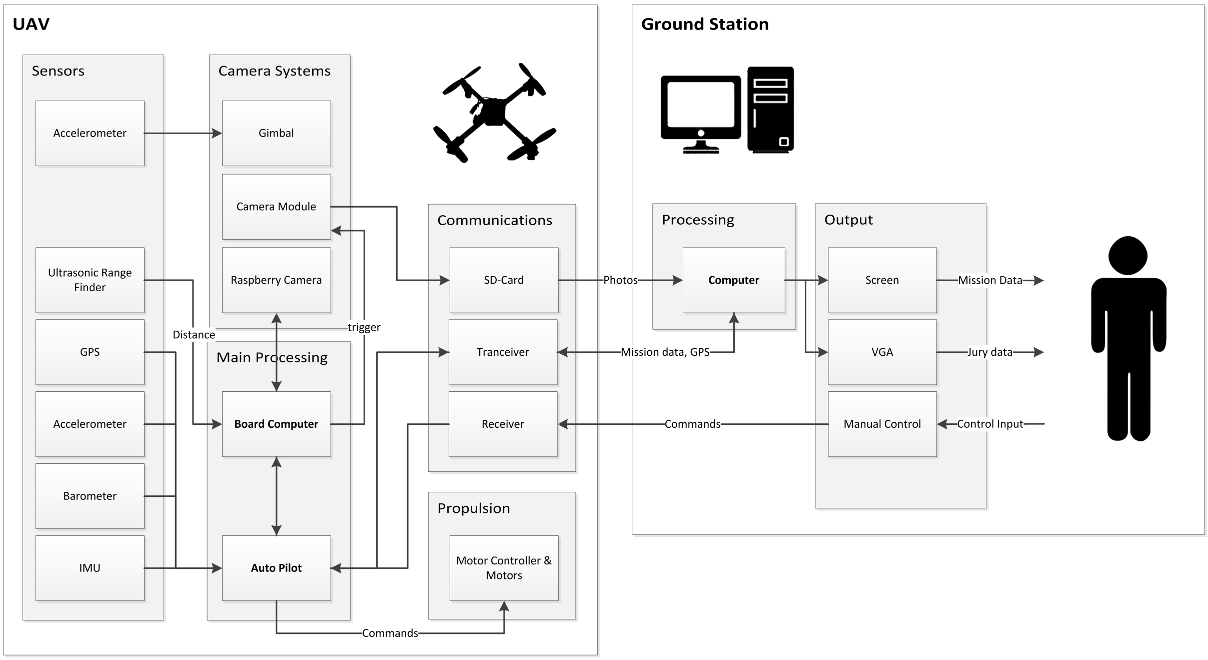

Figure 6.22: Data flow diagram showing the communication between the sub-systems

As can be seen in the UAV section of the figure, the board computer and the autopilot require a constant flow of data input from the sensors in order to allow the UAV to perform its mission. The Raspberry Pi computer is capable of operating the camera that is used in mission element 2. The autopilot sends commands to the motor controllers in order to control the attitude of the UAV. By means of an exchangeable SD-card, data is transferred from the UAV to the groundstation. Furthermore a constant down- and uplink is used to communicate in real time.

The ground station consists of a computer and a controller for manual inputs. The computer is capable of stitching all photos into a single map and analysing this map for blockades. Furthermore, as requirement *IMAV-SR-30* states, the main ground station screen shall be shared via VGA output.

6.4. Electrical Diagrams

In order to further design the topology of the system, the connections between each of the electrical power consuming systems in the UAV may be drawn. This was done with the use of an electic block diagram and a circuit diagram.

6.4.1. Electric Block Diagram

An electic block diagram may be used to get a schematic representation of the electrical flow between the systems. This diagram may be found in Figures 6.23 and 6.24. Note that all smaller electronic devices such as fuses, capacitors and resistors have not been drawn in this figure. These may be found in the circuit diagram shown in Figure 6.25.

As can be seen in Figure 6.23, the accumulator is the centre of the power distribution. Almost all systems are powered either trough a direct connection, or by means of a voltage converter. Certain systems such as the ultrasonic range finder are powered through another device such as the Raspberry Pi and are thus indirectly powered by the accumulator. When no voltage or power is presented, these values are either unknown or negligibly small.

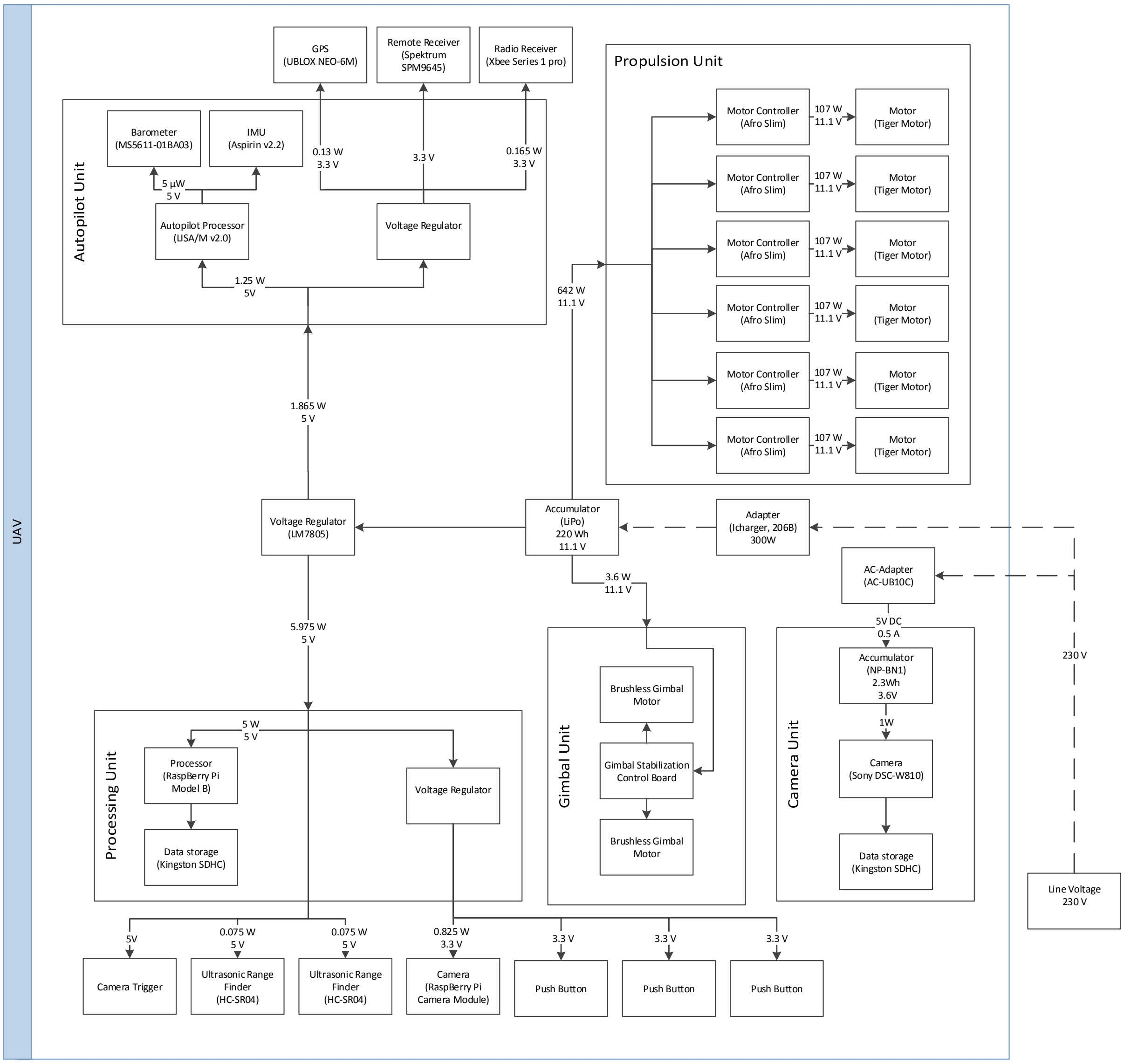

Figure 6.23: UAV part of the Electrical Block Diagram containing the power consuming systems

6.4.2. Circuit Diagram

In addition to an electic block diagram, a circuit diagram was made. This diagram may be used to get a more detailed overview of how each of the electrical systems are connected. The circuit diagram therefore shows the different ports to which each of the electrical subsystems is connected. The circuit diagram may be found in Figure 6.25. The system which are displayed in the circuit diagram will be discussed below.

Raspberry Pi Model B
As mentioned earlier, the Raspberry Pi Model B will be used as the on-board processor for the payload subsystem. The Raspberry Pi will obtain its needed power from the two battery packs present in the system, over a 5 Volt wire. A multitude of other payload subsystems is connected to the Raspberry Pi. These subsystems will next be elaborated upon.

Raspberry Pi Camera Module
The Raspberry Pi Camera Module is connected to the Raspberry Pi by means of a CSI Bus, which has a dedicated connector on the Raspberry Pi board. The camera therefore sends it data to and obtains its required power from the on-board computer.

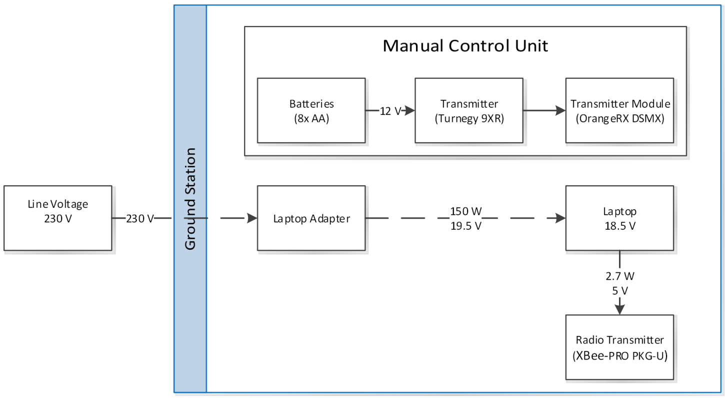

Figure 6.24: Ground station part of the Electrical Block Diagram containing the power consuming systems

single-pole single-throw switches
The single-pole single-throw switches in the form of push buttons will be used to detect that the UAV has landed. It may be noted from the circuit diagram that the system will normally read 'high' and when the button is pressed, the GPIO pin will read a 'low' value.

A 1 kΩ resistor has been put in place in order to prevent a short circuit between 3.3V and the ground when the pin is accidentally set to an output, and the button is pressed. The large (10kΩ) resistor ensures that little current is drawn whenever the button is pressed [178].

Sony Cybershot DSC-W810
The system should be able to autonomously take pictures in order to create the photomap. The Sony Cybershot will therefore need to be trigged by the Raspberry Pi. This trigger will be done with the use of a bipolar junction transistor (BJT) and a relay. When the command is given by the Raspberry Pi, the BJT will be triggered, in turn triggering the relay. The relay will be connected to the location where push button is normally. The Sony Cybershot will thus take a photo whenever the correct port, GPIO Port P25, is triggered.

HC-SR04 Ultrasonic Range Finder Modules
The two ultrasonic range finders used for navigation and detection are also connected to the Raspberry Pi. As mentioned in Section 4.2.4, the ultrasonic range finder requires and input voltage of 5 Volt, and has an output voltage of 5 Volt. As the maximum input voltage of the GPIO ports of the Raspberry Pi is 3.3 Volts, a voltage divider with a ratio of 1:2 should be used in order to prevent any damage to the Raspberry Pi. A 330Ω and 470Ω resistor between the echo output and GPIO port, and ground respectively [46] were therefore chosen.

Battery packs
The system will be powered by two battery packs in a parallel connection. These battery packs provide the required power to each of the subsystems of the UAV. Due to some subsystems requiring 5 Volt, and others 11.1 Volt, two separate circuits are used. This also means that two separate fuses and Zener diodes have been used to prevent any damage in case the battery packs fail.

Gimbal
The Gimbal is a nearly complete separate subsystem; it only requires power from the battery packs in order to be fully functional. The inertial measurement unit (IMU), Roll- and Pitch motors obtain their power from the Mobius Gimbal control board.

Lisa/M v2.0 Autopilot Board
The Lisa/M v2.0 also communicates with a multitude of other subsystems, each of which is therefore attached to the autopilot board. These subsystems include the manual control receiver, the GPS, the transceiver and the electronic speed controllers (ESCs). In order for the payload subsystem to be able to send its obtained data to the ground station, a link is needed between the Lisa/M v2.0 and the Raspberry Pi. This is done with the use of a Future Technology Devices International (FTDI) adapter which is connected to the Raspberry Pi over the USB port [179]. The FTDI adapter is connected to Lisa/M v2.0 over the ground, voltage and PC12 ports of the GPIO section of the autopilot board and the RX5 port of the universal asynchronous receiver/transmitter

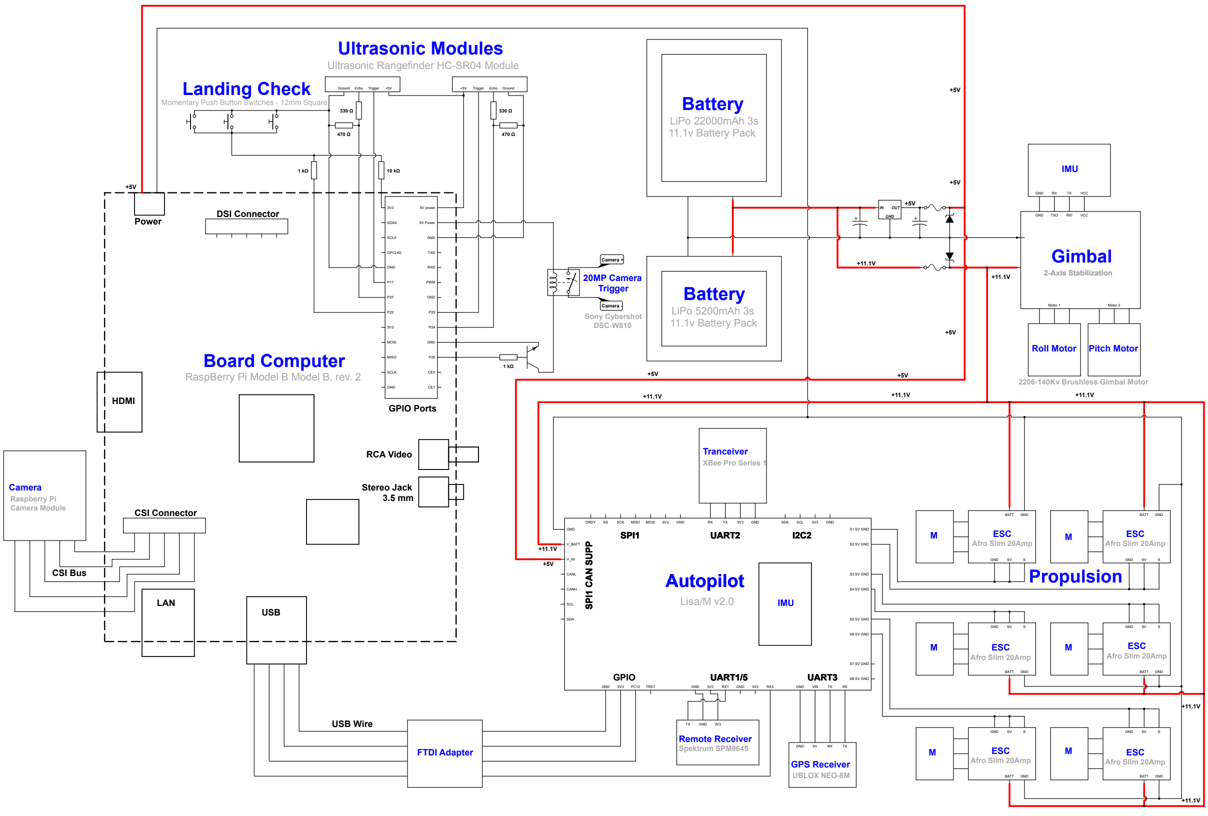

Figure 6.25: The Circuit diagram of the UAV.

(UART)1/5 section. The PC12 and RX5 ports will thus act as TX (transmit) and RX (receive) ports respectively. These ports together are equivalent to an UART connection, thus allowing an FTDI adapter to be used.

The Lisa/M v2.0 autopilot board also has two voltage inputs. The 5V input powers the autopilot board, while the 11.1V input may be checked by the autopilot board. The Lisa/M is thus capable of detecting whether a battery is running out of power. The autopilot is therefore capable of performing pre-defined action in such a case. This greatly improves the safety of the system.

Xbee Pro Series 1 Transceiver
The Xbee transceiver will be used to receive waypoints and send payload data back to the ground station. It is powered by the autopilot board and connected to it over a UART port.

UBLOX NEO-6M GPS Receiver
As the autopilot requires a location in order to navigate properly, the UBLOX NEO-6M GPS receiver will also be connected to the Lisa/M v2.0 autopilot board. It may be connected by one of the three UART ports that the autopilot board has.

Spektrum SPM9645 Remote Receiver
The Spektrum SPM9645 remote receiver will be used in order to receive the manual control input given by a user. This receiver has been implemented into the system such that the UAV may still be used in case the autonomy of the Lisa/M autopilot board, or the Xbee Pro Series 1 Transceiver fails. This will increase the overall safety and reliability of the system. Furthermore, it may be used to test the UAV without the need of a fully operational control subsystem. This in turn offers the possibility of testing the UAV while the autonomous control software is in development.

Propulsion
Lastly, the ESCs will be connected to the Lisa/M v2.0 autopilot board over a pulse width modulation (PWM) signal. This signal will control the ESC. These are connected over the dedicated servo ports. The ESCs will obtain their required power from the two battery packs over the 11.1 V wire. The engines themselves may then

obtain power from the ESCs.

6.5. Subsystem Failure Analysis

This section will elaborate on the consequences of specific subsystems failing and use this insight to develop several mitigation strategies. With these strategies the risk of failure of the system is decreased. This is achieved by first analysing the consequences of failure of several subsystems in Section 6.5.1 and second, in Section 6.5.2 possible mitigation strategies are developed.

6.5.1. Subsystem Failure Analysis

Raspberry Pi Model B
The Raspberry Pi is one of the most important subsystems of the UAV. If the Raspberry Pi fails, be it due to a driver failure or a software crash, the entire payload subsystem will no longer be operational. However, all the subsystems required to fly autonomously, except for the range finders, are independent of the Raspberry Pi. The UAV is able return to the LCC in such a case. This increases the safety of the UAV.

Raspberry Pi Camera Module
The Raspberry Pi camera module is used in mission element 4, the quick visual inspection. When the Raspberry Pi camera module fails, this mission element will no longer be possible. It should be noted that mission element 4 will be the final mission the system has to complete and that no autonomous flying capabilities are lost when the Raspberry Pi camera module fails.

SPST Switches
When the SPST switches (push buttons) on the bottom of the landing gear are no longer functional, mission element 8 and 10 will become a lot more difficult. As these SPST switches are used to determine whether the UAV has landed, the UAV will no longer be able to detect that it has landed when these switches fail. This may result in the UAV turning off its engines pre-emptively, and thus crashing into the ground. This should be kept in mind when programming the landing algorithm.

When one or two of the three SPST switches fail, the UAV will still detect its landing, as the SPST switches are connected in parallel. This may also be seen in Figure 6.25. No further consequences will therefore be present.

Sony Cybershot DSC-W810
The photomap of mission element 2 will be made with the use of a Sony Cybershot DSC-W810. When this camera fails, the photomap can therefore no longer be created. Mission element 3 in turn requires this photomap in order to detect the location of the blockades. The system can therefore also not complete mission element 3 when the Sony Cybershot DSC-W810 fails. However, the other mission elements and autonomous flying capabilities are not impacted.

HC-SR04 Ultrasonic Range Finder Modules
Two ultrasonic range finders will be used on the UAV. One of these will be used to give an altitude. When this ultrasonic range finder fails, the system will not have a relative altitude measurement. As discussed earlier, the barometer will be calibrated on the altitude of the ground station; therefore returning an altitude relative to the altitude of the ground station. It will thus not be able to measure the distance relative the landscape below the UAV. An ultrasonic range finder on the other hand is able to measure this relative distance. When the range finder is no longer operational, the distance relative to the landscape below the UAV cannot be obtained.

A second ultrasonic range finder is used to determine the distance to an obstacle. When this ultrasonic range finder fails, the risk of the UAV hitting an obstacle greatly increases.

Battery Packs
The battery is another crucial subsystem for the UAV to be able to function. The UAV will not be operational if the battery packs are not functioning. Another risk is one batteries suddenly outputting a higher voltage or current. In order to prevent the other components to be damaged by this, Zener diodes and fuses have been introduced into the circuit. The Zener diodes will prevent the system being damaged by a high voltage, while the fuses prevent the components from being damaged by a high current.

Gimbal
As mentioned earlier, both of the ultrasonic range finders and the Raspberry Pi camera module are attached to the gimbal. Meaning that the gimbal is used for the photomap, quick visual inspection and the altitude measurement.

The gimbal may fail in a multitude of ways; the IMU, motors and processing board may all fail separately. Each of these failures result in the gimbal not functioning properly, which in turn results in the three devices attached to the gimbal not properly being stabilised. The photomap may therefore be more blurry, thus potentially giving less points. Furthermore, as the ultrasonic range finders use the stabilisation of the gimbal, they will also no longer be able to accurately obtain a relative altitude. The camera used for quick visual inspection also uses the gimbal to obtain a blur-free image. A failure of the gimbal will thus result in a blurred image. This decreases the chance of the detection of the house number.

Spektrum SPM9645 Remote Receiver
The primary receiver is used for the manual control of the UAV. The ability to manually control the UAV may be used during early testing, or when the transceiver, autopilot algorithm or GPS fails. As the system is designed to perform the safety landing autonomously, the manual control is not needed for this landing. The UAV is therefore still able to completely perform all of the missions and score the calculated number of points.

Lisa/M v2.0 Autopilot Board
The Lisa/M autopilot board is the third crucial subsystem. A complete failure of the autopilot will result in the UAV no longer being able to operate. However, when only the autopilot software fails, manual control using the Spektrum SPM9645 Remote Receiver is still possible.

Xbee Pro Series 1 Transceiver
When the Xbee pro series 1 fails, the system is no longer capable of receiving new waypoints and sending its payload data. However, the UAV may be controlled manually when this failure occurs. The payload data may then be stored locally on the SD card.

UBLOX NEO-6M GPS Receiver
A failure of the GPS subsystem results in the UAV not knowing its position. The only viable option in order to continue the mission elements, is the use of manual control. From a technical consultation with C. de Wagter it was obtained that the Lisa/M v2.0 autopilot is capable of detecting when a GPS becomes inaccurate or fails. This option may be used to warn the pilot, who could then assume manual control.

Propulsion
The propulsion subsystem consists of the propellers, motors, gearboxes and the ESCs. If one of the engines or ESCs fail, the other five will continue to work. As the UAV has a maximum thrust-to-weight ratio of 2:1, the UAV will continue to have a thrust-to-weight ratio of 1.67:1 in the case that one engine fails. As discussed in Section 5.4, the UAV will still be able to perform a safe landing with such a thrust-to-weight ratio.

By adjusting the other five propeller speeds, the system may still be kept relatively stable.

Raspberry Pi - Lisa/M v2.0 Interface
The interface between the Raspberry Pi and the Lisa/M v2.0 autopilot is used to send the distance to an obstacle to the autopilot and the payload data to the transceiver. When this interface is no longer functional, the payload data has to be saved locally. The autopilot will also no longer know the distance to an object obtained from the ultrasonic range finder. This may result in mission element 4 becoming more difficult.

6.5.2. Risk Mitigation

As discussed in the previous section, two critical subsystems are present in the design: the battery packs and the Lisa/M v2.0 autopilot.

Possible mitigation strategies are the introduction of redundancies or by further identification the current risks. Several redundancies are currently present in the design. These redundancies are the use of three push buttons, six propeller, motor, gearbox and ESC combinations and the use of two battery packs. In case one of these subsystems partially fails, the rest of the subsystem may take over to prevent considerate damage to the system.

Further redundancies are not possible, as this increases the weight of the system. Which will result in the snowball effect as described in Section 5.3.

6.6. Budget Breakdown

With the hardware selected in Chapter 4 and integrated in this chapter, the budgets introduced in Section 2.4 can be evaluated. This is done separately for the UAV and the ground station since the UAV costs scale with the number of UAVs used, while the ground station costs remain constant. This will be discussed in Sections 6.6.1 and 6.6.2 respectively.

6.6.1. Unmanned Aerial Vehicle Budget Breakdown

Within the UAV there are four subsystems for which breakdowns of the power, cost and mass have been performed. The subsystems are propulsion and airframe, payload, structural and general. The propulsion and airframe budget can be found in Table 5.15 in Section 5.10. The payload budget can be found in Table 4.27 in Section 4.11. The general budget is presented in this Section in Table 6.2.

These subsystems are then grouped and 5% unforeseen is added for any unforeseen additions in power, cost and mass which might occur during production. Last the contingency factors of 4% and 5%, for the cost and mass respectively, are added as stated in Section 2.4 to account for any cost or mass grow. The budget breakdown of the UAV subsystems can be found in Table 6.6.3. From this table it can be seen that a single UAV will use 632 Watts of power, cost €1150 and weigh 2.3 kilograms, which is the cheapest option that meets the requirements.

Table 6.2: Budget breakdown of the general subsystem of the UAV

Category	**Type**	**Name**	**Power** $[W]$	**Cost [€]**	**Mass** $[g]$
Low power	Wires	0.18mm^2 1.3 m	0.949	2.50	52
High power	Wires	0.6mm^2 1.3 m	0.949	2.50	21
Power	Voltage regulator	Standard Regulator 5 Volt 1 Amp 3 Pin 3+ Tab TO-220	0	0.29	3
Power	Capacitors	2x Panasonic RS 1microFarad 25VDC	0	0.34	2
Power	Diodes	2x 5v zener diode	0	0.08	2
Power	Fuses	2x fuses	0.5	1	2
Power	Connection	FTDI Adapter USB Controller - 5v	0	10.39	5
Total			**12**	**17.10**	**86**

Table 6.3: Budget breakdown of the UAV subsystems with unforeseen and contingency factors

Subsystem	**Power** $[W]$	**Cost [€]**	**Mass** $[kg]$
Propulsion and airframe	476	606	1.64
Payload	19	426.02	0.360
General	12	17.10	0.086
Unforeseen (5%)	25	55.24	0.104
Contingency (costs 4%, mass 5%)	0	45.89	115
Total	**532**	**1150**	**2.3**kg

The requirements for the cost and mass *IMAV-CO* and *IMAV-SR-24* state that the total cost for production of the system shall not exceed €5,000.- and all UAVs shall have a maximum weight of 5 kilograms respectively. It can be seen that the UAV complies with these requirements. Safety requirement *IMAV-SR-25* states that all UAVs shall have a maximum momentum of 20$\frac{kg \cdot m}{s}$ which would result in a maximum allowed velocity of 8.7$\frac{m}{s}$.

6.6.2. Ground Station Budget Breakdown

The budget breakdown of the ground station can be found in Table 6.4. This budget includes the parts used and the same 5% unforeseen and the 4% cost and 5% mass contingency factors as for the UAV budget.

For the ground station there are no requirements regarding mass and power. Furthermore power can be utilised from the power grid available at the competition area. This means there are no restrictions for the ground station regarding the power usage and mass. The only requirement that applies to it is that it should remain within the budget of €5000 allowed for the entire system. With a total cost of €300 this requirement is satisfied.

Table 6.4: Budget breakdown of the ground station used for the UAVs

Category	**Name**	**Type**	**Power** $[W]$	**Cost [€]**	**Mass** $[kg]$
Communication	Radio transmitter	XBee-PRO PKG-U - Connection via USB	2.7	118	0.15
Manual control	Transmitter	Turnigy 9XR (no module)		37.08	1.28
Manual control	Transmitter module	OrangeRX DSMX module, Turnigy-compatible	0	22.13	0.074
Battery	Battery adapter	iCharger 206B	300	97.77	0.35
Unforeseen (5%)			15	13	0.093
Contingency (cost 4%, mass 5%)			0	12.03	0.102
Total			**318** $[W]$	**300 [€]**	**2.0** $[kg]$

6.6.3. Total Budget Breakdown

With all components known a total budget for the entire system can be made. This budget includes a number of UAVs and the ground station and must not cost more than €5000 as stated by requirement *IMAV-CO*.

When the costs of the ground station are subtracted from the total budget, a budget of €4700 is left for the UAVs. With this budget a total of 4 UAVs can be built with €100 to spare. The €100 will be used for possible repairs such as new propellers which are prone to breaking when the UAV crashes during testing.

6.7. Requirements Compliance Matrix and Feasibility Analysis

This section presents the requirements compliance matrix as well as the feasibility analysis. First, this section presents the requirements which the Soteria system complies to. Second, this section performs a feasibility analysis on the requirements, which the Soteria does not yet comply to. The feasibility analysis presents the rationale why the design does not meet these requirements. The Soteria design complies with 62 out of 90 requirements, therefore there are still 28 requirements with which the Soteria system has to comply before a successful participation in the international micro aerial vehicle (IMAV) 2014 competition.

The requirements which the Soteria system complies to are presented in Tables 6.5, 6.6 and 6.7. These tables include a reference to the chapter or section in which the particular requirements are fulfilled.

The feasibility analysis performed on the unfulfilled requirements were split in two different parts, namely: requirements that need additional verification and validation and requirements that need to be executed on the IMAV 2014 competition day. The requirements that need additional verification and validation are presented in Table 6.8. The tests proposed to verify and validate these requirements are presented in Section 8.3. The feasibility analysis concluded that all requirements are technically feasible. For example, Section 4.3 concluded that the Lisa/M autopilot is a feasibility design option based on the requirements listed in Table 6.8. However, this claim could not be tested within the design synthesis exercise (DSE) due to lack of resources.

The unfulfilled requirements that need to be executed on the IMAV 2014 competition day are presented in Table 6.9. These requirements cannot be properly validated within the DSE without competing within the IMAV 2014 competition on the 13th of August.

Table 6.5: Requirement compliance matrix for the fulfilled competition requirements.

ID	Requirement	Reference
IMAV-CR-ME1	All UAVs shall take off from the designated take-off area in the local command center (LCC)	4+5
IMAV-CR-ME2	The system shall create a photomap of zone A within 10 minutes after the end of the mission	4
IMAV-CR-ME2-1	The system shall make pictures with an overlap of at least 20%	4.6
IMAV-CR-ME2-2	The system shall have Microsoft ICE available on the ground station for photo stitching	4.10
IMAV-CR-ME2-3	The system shall have Microsoft Visual C++ available on the ground station for photo stitching	4.10
IMAV-CR-ME2-4	The system shall have .NET Framework version 4 available on the ground station for photo stitching	4.10
IMAV-CR-ME2-5	The system shall have a memory of at least 645 MB for creating the photomap	4.7+4.10
IMAV-CR-ME2-6	The system shall support a data rate of at least 1.65 MB/s for creating the photomap	4.7
IMAV-CR-ME2-8	The photomap camera of all UAVs shall be controlled in roll and pitch with at least 1 degree of accuracy	4.9
IMAV-CR-ME2-9	The photomap camera shall be controlled in yaw angle with at least 6 degrees of accuracy	4.9
IMAV-CR-ME3-11	The photomap shall be in color	4.6
IMAV-CR-ME3-4	The system shall have Python or MATLAB available on the ground station for blockade mapping	4.10
IMAV-CR-ME4	All UAVs shall identify the building numbers of buildings in zone B	4.2+4.5
IMAV-CR-ME4-1	The hardware used as payload shall be compatible with the Raspberry Pi Model B	4
IMAV-CR-ME4-3	The ultrasonic range finder shall only be used within a range of 4 meters from an object	4.2
IMAV-CR-ME4-4	The on-board computer shall be able to recognise objects using images with a resolution of 2592 by 1944 pixels	4.2
IMAV-CR-ME4-7	All UAVs shall be able to process a script written in python on the on-board processor	4.5
IMAV-CR-ME4-8	All UAVs shall be able to process a script written in Matlab on the on-board processor	4.5
IMAV-CR-ME8-1	All UAVs shall land on the building with the flat roof in zone D	4+5
IMAV-CR-ME8-13	All UAVs shall have a sensor that indicates a landing	5.9
IMAV-CR-ME8-2	All UAVs shall remain at their position on the flat roof in zone D for at least 10 seconds	4+5
IMAV-CR-ME8-3	All UAVs shall take off from the building with the flat roof in zone D	4+5
IMAV-CR-ME10-1	All UAVs shall make a precision landing in the designated landing area in the local command centre (LCC)	4+5
IMAV-CR-ME10-11	All VTOL UAVs shall make a precision landing in the LCC within a circle of 5 metres	4+5
IMAV-CR-ME10-14	All CTOL UAVs shall make a precision landing in the LCC within a circle of 10 metre	5.2
IMAV-CR-ME10-2	All UAVs shall demonstrate airworthiness in case of rough landing	5.9
IMAV-CR-ME10-21	All UAVs shall be able to land with a descent rate of 1m/s and hitting the ground under an angle of 45 degree	5.9

Table 6.6: Requirement compliance matrix for the fulfilled safety requirements.

ID	Requirement	Reference
IMAV-SR-01	The system shall only use electric propulsion	5.6
IMAV-SR-03	The transmission of electro magnetic radiation shall be on frequencies that are legally allowed in the Netherlands	4.7
IMAV-SR-04	The transmission of electro magnetic radiation shall be in modes that are legally allowed in the Netherlands	4.7
IMAV-SR-05	The transmission of electro magnetic radiation shall be within the power limit legally allowed in the Netherlands	4.7
IMAV-SR-07	The system shall store the last reliable position of all UAV's	4.3
IMAV-SR-08	All UAVs shall not have potentially dangerous protrusions, except for normal propellers and helicopterblades.	6
IMAV-SR-12	A UAV shall return to the center waypoint after entering the orange zone	4.3
IMAV-SR-13	All UAVs shall never enter the red zone	4.3
IMAV-SR-14	A UAV shall perform an emergency landing after entering the red zone	4.3+4.7
IMAV-SR-15	A UAV shall perform an emergency landing in case of a navigational loss	4.3
IMAV-SR-17	An emergency landing of a UAV with fixed wings shall be performed without propulsion	5.2
IMAV-SR-20	The team shall be able to manually take over control of all UAV's	4.3+4.10
IMAV-SR-20-1	The system shall have one manual transmitter available for every five UAVs	4.3
IMAV-SR-23	All UAVs shall have a maximum dimension of 1.50 m	5.9
IMAV-SR-24	All UAVs shall have a maximum weight of 5 kg	6.6
IMAV-SR-25	All UAVs shall have a maximum momentum of 20 kg*m/s	6.6
IMAV-SR-26	All UAVs shall be airworthy	5
IMAV-SR-26-1	The power supply system shall store energy needed to fly at a thrust-to-weight ration of 1.5 throughout the entire mission	5.5
IMAV-SR-26-2	The propellers shall be able to generate a maximum total thrust equal to twice the weight of the system.	5.5
IMAV-SR-26-3	The motor shall provide a maximum required thrust of 88W at 5,762 revolutions per minute	5.6
IMAV-SR-26-4	The electronic speed controller shall be able to handle a maximum current of 14 Ampere	5.7
IMAV-SR-26-5	The propellers shall be separated by at least one propeller diameter.	5.9
IMAV-SR-26-6	The airframe shall support all subsystems and transfer all loads generated by other subsystems.	5.9
IMAV-SR-29	The GPS coordinates of all UAV's shall be shown on the ground station during the mission, when GPS is used	4.3
IMAV-SR-30	The main ground station screen shall be shared via VGA output	4.10

Table 6.7: Requirement compliance matrix for the fulfilled remaining top-level requirements.

ID	Requirement	Reference
IMAV-CO	The total cost for production of the system shall not exceed €5,000.-	6.6
IMAV-MU	The system shall comprise at least two UAVs	6.6
IMAV-TU	The design of the system shall be completed within 10 weeks with 10 students	2
IMAV-AU-1	All UAVs shall fly towards mission elements autonomously	3+4
IMAV-AU-11	Navigational waypoints shall be chosen with a 5 metres clear-of-obstacles radius in the horizontal plane	3.4
IMAV-AU-12	All UAVs shall have one nadir orientated ultrasonic rangefinder	4.4
IMAV-AU-13	The ground station shall have paparazzi ground control station-software available for telemetry	4.10
IMAV-AU-13-1	The ground station shall have a ground station based on the Linux Operation System	4.10
IMAV-AU-14	The system shall have a communication link able to handle 7.2 kB/s between the ground station and the autopilots of all UAVs	4.7+4.10
IMAV-SAR	The system shall be functional in disaster scenarios in urban areas	3.4

Table 6.8: Requirement compliance matrix for the requirements, which need additional verification and validation

ID	Requirement
IMAV-CR-ME1-1	All UAVs shall have a roll and pitch control accuracy of at least 45 degrees
IMAV-CR-ME2-7	The system shall stitch the photomap and analyse the blockades within 30 minutes
IMAV-CR-ME2-10	All UAVs shall have a translational control accuracy of at least 2.5 meters in all three axes
IMAV-CR-ME3	The system shall indicates all blockades in zone A on the photomap of mission element 2
IMAV-CR-ME3-1	A photomap of the area shall be available for blockade mapping
IMAV-CR-ME4-5	All UAVs shall have a translational control accuracy of at least 0.5m in horizontal plane
IMAV-CR-ME4-9	All UAVs shall be within a TBD of the TBD metres from the sheet of paper when starting the sheet recognition
IMAV-CR-ME4-10	All UAVs shall be within a TBD of the TBD metres from the sheet of paper when starting the number recognition
IMAV-SR	The system shall comply with the safety rules and the requirements of the IMAV 2014 competition set by its organisation
IMAV-SR-02	Equipment shall comply with the Dutch law
IMAV-SR-06	The system shall be able to execute the mission using a set of alternative frequencies
IMAV-SR-11	Operations shall comply with Dutch law
IMAV-SR-16	An emergency landing of a UAV with rotary, flapping or hybrid wings shall be performed at minimum power setting
IMAV-AU	The system shall demonstrate autonomy
IMAV-AU-2	All UAVs shall perform each mission element autonomously

Table 6.9: Requirement compliance matrix for the requirements, which need additional verification and validation

ID	Requirement
IMAV-CR	The system shall win the IMAV 2014 competition
IMAV-SR-09	The team shall always be responsible for the safety of their UAV's
IMAV-SR-10	The team shall always be liable for any accidents caused by the team and their UAV's
IMAV-SR-18	The team shall retrieve a UAV in case of a loss, assisted by the day's safety officer
IMAV-SR-19	The team shall retrieve a UAV in case of a field landing, assisted by the day's safety officer
IMAV-SR-21	All UAVs shall have an observer constantly following the UAV
IMAV-SR-22	Data transmission shall only be done with consent of the IMAV safety officer
IMAV-SR-27	All UAVs shall be clearly identified with name and address information of a team member
IMAV-SR-28	All UAVs shall be clearly distinguishable
IMAV-SR-31	The team shall convince the IMAV safety officer that all UAV's can be retrived after a emergency landing
IMAV-SR-32	The team shall provide a list of all radio equipment to the jury of the 2014 IMAV competition before July 1, 2014
IMAV-SR-33	The team shall provide a list of all frequencies to the jury of the 2014 IMAV competition before July 1, 2014
IMAV-SR-34	The team shall provide a list of alternative frequencies to the jury of the 2014 IMAV competition before July 1, 2014

6.8. System Integration Conclusion

This chapter started with a known list of payload, propulsion and structural components. Using computer-aided design (CAD), these were integrated into a single UAV design. Each of the UAVs features an airframe with payload section in the centre.

The payload section of the UAV is divided into two platforms, namely the upper and lower platform. The gimbal is attached to the lower platform, which also holds the battery system. The cameras and rangefinders are attached to the gimbal to stabilise these sensors. The upper platform houses the remaining sensors and electronics. These include the autopilot, GPS receiver, radio transmitter and on-board computer. The systems will be shielded from the electromagnetic interference by placing these away from the battery system. A dome is placed over the top payload deck to protect the electronics from weather influences and impact damage.

The propulsion system is mounted to the airframe through a plate which will be glued and bolted to the airframe. The bolts are on the outside of the airframe so no holes have to be drilled through the airframe and therefore loses no strength. The motor will be fixed on the plate and on top of it the gearbox is fixed. Lastly, the propeller is fixed to the gearbox.

With the physical layout fixed, the data and communication flows were indexed. Potential failures were considered and mitigation strategies were developed wherever possible in order to decrease the risk of a system failure.

The final budgets of the system were made and it was found that a single UAV will weigh 2.3 kilograms, which is within the requirements, and cost €1150. The ground station will cost €300. With the maximum budget of €5000 a total of four UAVs can be built.

The system complies with 62 out of the 90 requirements. The remaining 28 requirements are divided in two groups. The first groups need further verification and validation which will be done in the future testing. The second group are requirements which can only be satisfied at the IMAV competition.

7

System Characteristics and Design Analysis

With the design of the unmanned aerial vehicle (UAV) finalised, it is now possible to determine some characteristics of the system and analyse the overall design. It is important to know the limitations of the system and in what conditions it is best suited for. Knowing all characteristics is also important to grab the interest of potential customers. In order to examine the flight performance, aerodynamic characteristics, control and stability of the system, a simulation program is made. Section 7.1 will begin by explaining the program developed for this purpose, afterwards presenting the discoveries made by this program for the above mentioned characteristics of the system. Next in Section 7.2, the strengths of the material and structure is analysed and presented. With the help of the finite element method (FEM) method in Catia, the stresses within the structure can be evaluated to ensure that the system will not fail under the applied loads it is expected to endure. The chapter continues with Section 7.3, outlining the reliability, availability, maintenance and safety. These characteristics are especially interesting to know if the system is being brought on the market. A reliable, safe, easy to maintain and available system is more interesting to potential buyers. Each of these characteristics were evaluated and the outcome is discussed here. Next are the sustainability considerations in Section 7.4. In this section all the sustainable aspects of the system are outlined. Section 7.5 presents the sensitivity analysis where the systems' sensitivity to changes are explored. Finally the market analysis in Section 7.6 compares the complete system with its characteristics to other UAVs available on the market.

7.1. Performance, Aerodynamic and Stability Characteristics

The characteristics explained in this section are determined using a self-developed simulation tool. Before using this tool to generate results and quantify the characteristics of the UAV design, the tool is explained in Section 7.1.1. Section 7.1.2 will then discuss the verification and validation of the program which needs to be performed before the results of the program can be used.

Section 7.1.3 presents the UAVs aerodynamics and the response of the system to continuous wind and gusts. Also shown in Section 7.1.4 are the performance characteristics of the system, outlining for example the maximum velocities, accelerations and payload. Lastly, the stability & control characteristics are explained in Section 7.1.5.

These characteristics are especially interesting in combination with the requirements outlined in Section 4.9. These are repeated again in Table 7.1

Table 7.1: Requirements following attitude control

ID	Requirement
IMAV-CR-ME1-1	All UAVs shall have a roll and pitch control accuracy of at least 45 degrees
IMAV-CR-ME2-8	The photomap camera of all UAVs shall be controlled in roll and pitch with at least 1 degree of accuracy
IMAV-CR-ME2-10	All UAVs shall have a translational control accuracy of at least 2.5 meters in all three axes

7.1.1. Simulation Model

Because of the many possible inputs to the system in flight, it was decided to develop a program that can calculate the state of the system under these inputs and ouput the response. The choice was made to create the program in JAVA. This allowed for easier organisation of the calculations.

Assumptions

Before programming, some assumptions were made to idealise the UAV design, to simplify the model and to provide a first-order estimate of the system. These assumptions are listed below:

- The UAV does not produce lift
- The UAV is idealised as a flat square plate with the same weight, surface area and inertia as the full model
- A flat plate aerodynamic drag model offers an acceptable first-order approximation for the drag experienced by the UAV
- The drag experienced by the UAV will attach itself in the centre of pressure of the flat plate model
- Inviscid flow (no skin friction drag)

Force and Moment Equation Functions

The program contains functions that can individually calculate the total horizontal or vertical thrust generated by the UAV. This is done using Equations (7.1) and (7.2), where T_i is the thrust delivered by the i^{th} thruster and θ is the pitch angle of the UAV.

$$F_{vertical} = \sum_{i=1}^{6} T_i \cos\theta \tag{7.1}$$

$$F_{horizontal} = \sum_{i=1}^{6} T_i \sin\theta \tag{7.2}$$

Pure Horizontal Movement Functions

Another function exists to calculate the thrust levels required to provide pure horizontal movement. The inputs for this function are the external forces applied to the system. The program will then calculate the required thrust levels using Equations (7.3), (7.4) and (7.5), where Δ_i is the length from thruster T_i to the centre of gravity and m is the mass of the UAV.

$$\sum_{i=1}^{6} T_i \sin\theta - F_{horizontal,external} = m \cdot a \tag{7.3}$$

$$\sum_{i=1}^{6} T_i \cos\theta - F_{vertical,external} = 0 \tag{7.4}$$

$$\sum_{i=1}^{6} T_i \Delta_i = 0 \tag{7.5}$$

For any response-to-input calculations, the program will use $\sum F = m \cdot a$ and $\sum M = I \cdot \dot{\alpha}$, with I the area moment of inertia. For calculating the velocity and displacement, Equations (7.6) and (7.7) are used. At every interval of Δt seconds, the simulation program will recalculate all the forces and moments acting on the system, as well as the angles and displacements. This time step is taken to be Δt= 0.001 seconds to have an accurate reading.

$$v_{new} = v_{old} + \frac{\Delta v}{\Delta t} \cdot \Delta t = v_{old} + a \cdot \Delta t \tag{7.6}$$

$$s_{new} = s_{old} + \frac{\Delta s}{\Delta t} \cdot \Delta t = s_{old} + v \cdot \Delta t \tag{7.7}$$

Aerodynamic Drag

The equation used for the drag force is given by Equation (7.8), where D is the total drag, ρ is the density, V is the airspeed, θ is the pitch angle of the UAV and S is the surface area.

$$D = \frac{1}{2} \cdot \rho \cdot V^2 \cdot 2 \cdot \sin^2(\theta) \cdot S \tag{7.8}$$

Calculation of Maximum Velocities

To calculate maximum forward velocities, the simulation starts out by assuming a pitch angle of $\theta = 1°$, finding a solution for the thruster level to satisfy the condition of no vertical acceleration or angular acceleration. Using this solution, it proceeds by calculating the horizontal components of the thrust. It then calculates the difference with the aerodynamic drag to determine the forward acceleration. A loop runs to keep increasing the forward velocity, which increases the aerodynamic drag, until the aerodynamic drag matches the forward thrust. This means the acceleration becomes zero and a maximum velocity has been reached for this angle of attack.

Afterwards, the simulation increases the pitch angle by 1 degree and runs the loop once more. It will stop increasing the pitch angle once the condition of vertical equilibrium demands a thrust-to-weight setting higher than 1.65, which is the continuous thrust-to-weight ratio given in Section 5.

7.1.2. Verification & Validation

The simulation program and each of its functions discussed in Section 7.1.1 have to be checked for validity, before it can be used to generate useful results.

Each of the functions of the simulation program has been individually tested and verified to check if the program produces expected results from given input. The equations have also been worked out by hand and using random numbers as input to these equations, it could be seen that the program produces the same results as the hand-written calculations.

Validation of the system has been achieved in a limited manner as windtunnel data of the UAV is not available. Neither does a working prototype exist to test and validate the system. However, from literature research on other, similar UAVs, it was possible to determine that the calculated velocities of the system were in the same range as these UAVs [180][181].

7.1.3. Aerodynamic Characteristics

This section presents the aerodynamic characteristics relevant to the UAV design. Influences such as continuous wind and sudden gusts were researched, simulated and quantified to determine if the design could be feasible in real-world outdoor applications.

Gusts

While flying outdoors, a UAV will experience gusts of wind blowing it off of its path. Due to limited time resources, it was not possible to create a real-world model of the design and test it in a wind tunnel in order to determine its aerodynamic properties. Instead, the simulation program described in Section 7.1.1 was used to quantify the response of the system. Using data gathered from the Royal Netherlands Meteorological Institute (RNMI), the average gust strength for the month of August, when the UAV is planned to fly, was determined to be 9.0 m/s [146]. In the simulation, the UAV was subject to a 1.0 second lasting gust, and the response of the UAV was determined. This gave an indication of how fast a UAV can be blown away by a gust of wind and what kind of response would be required by the autopilot to correct for this.

For example, with a gust lasting for 1.0 second, which has a speed of 9.0 m/s and an angle of attack of 5.0°, it was determined that after 0.6 seconds, the UAV would have been blown away a distance of 0.17 metres and tilted over an angle of 45°. This gives an indication on how fast a control system would have to correct the movement due to gust, in order to remain within the limits of the requirements for pitch and roll accuracy as well as translational movement.

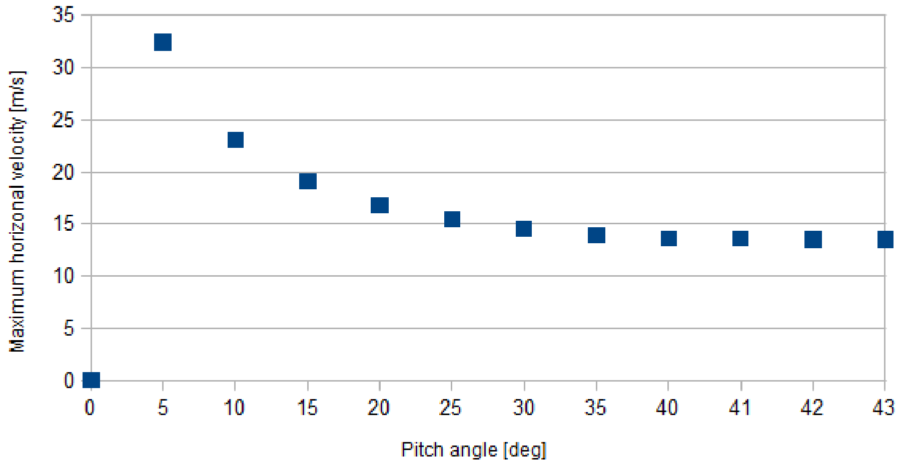

Figure 7.1: Maximum horizontal velocities in relation to the angle of the UAV w.r.t. the ground.

Continuous Wind

Using the simulation program mentioned in Section 7.1.1, a continuous wind disturbance was applied and the response of the system was determined. In the simulation, the UAV was stable, hovering in no-wind conditions from start to 2.0 seconds in, after which it underwent constant wind disturbance. For example: the simulation is run with a continuous wind disturbance with a velocity of 2.0 m/s, which is an average wind speed velocity for the month of August according to the RNMI[146]. Again, the wind affected the UAV with an angle of attack of 5°, to be able to compare this simulation with the gust example of the previous section.

From the resulting information out of the simulation, it was seen that after 3.0 seconds, the UAV would have tilted over an angle of 45°. This is the limit for which the UAV was designed to land and therefore, control systems would have to intervene before this happens should the system be trying to land during this wind condition. It was also seen that the UAV would have drifted almost 3 metres in a horizontal direction by this time if no change in thrust was applied. Finally, the system lost roughly 20 cm in altitude within these 3.0 seconds due to the wind disturbance.

7.1.4. Performance Characteristics

In this section, the estimated performance of the system is presented. During the performance analysis, the full potential of the UAV was quantified. The simulation model described in Section 7.1.1 was used to determine certain characteristics for this system, with its designed propulsion system and body framework. First, the maximum velocity is determined, followed by the maximum payload and range.

Maximum Velocity

The propulsion system has hard limits for the available thrust, as shown in Section 5. Furthermore, the UAV uses its propulsion system for both forward and upward movement. To move forward, the UAV would have to tilt its whole body forward. To find the maximum velocity of the system, the simulation model was used. When the maximum forward velocity is obtained, the forward component of the thrust will be equal to the drag, and the vertical component of the thrust equal to the weight of the system.

The results of the simulation simulation are shown in Figure 7.1. What can also be seen in this figure is that the maximum pitch angle is 43°. Beyond this angle, the vertical component of the thrusters cannot maintain vertical equilibrium, as the thruster power limit has been reached.

It should be noted that at low angles of attack, the drag is very low and therefore the maximum velocities are higher. As the pitch angle increases, so does the drag, which causes the maximum velocities to become lower.

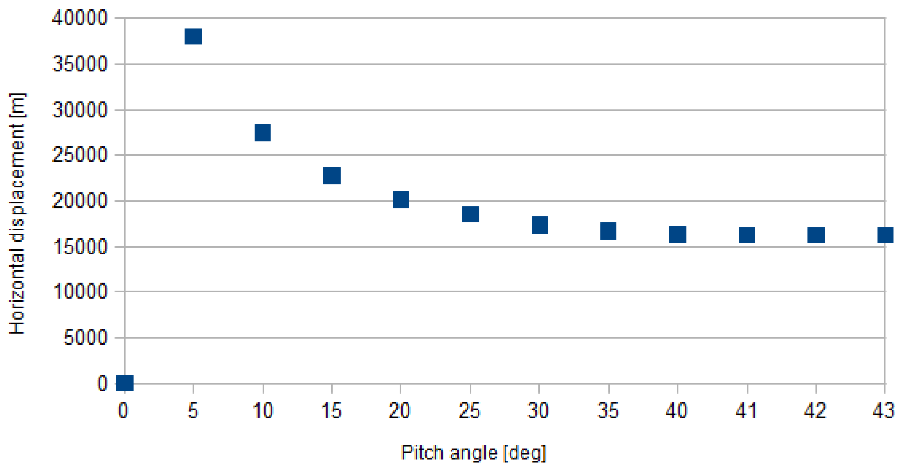

Figure 7.2: The maximum flight distance w.r.t. the pitch angle

However, due to the momentum limitation from the competition safety regulations, there is a maximum velocity that the UAVs are allowed to fly [4]. The simulation model calculated the time required for the system to reach this speed. With the maximum allowable speed being 8.62 m/s, the system was able to reach this speed after approximately 3 seconds.

Maximum Payload

Furthermore, it is possible to calculate the maximum payload that can be carried by the UAV, while still being able to move in all directions. As the maximum thrust-to-weight ratio that the UAV can carry is 2, the system could potentially lift up to 2.3kg of extra payload. However, applying maximum thrust on all thrusters would eliminate the ability of using these thrusters for control, as this requires a difference in thruster levels to alter the attitude of the system. Since the designed continuous thrust-to-weight ratio is 1.65, the UAV could carry roughly 1.5kg in additional payload and still be able to move horizontally without losing altitude.

Maximum Range

To find the maximum range of the UAV, the aforementioned simulation program is used again. For this calculation, the simulation loop will track the total horizontal displacement by simply integrating the velocity. The simulation program assumes that the UAV is only given a drag force by the aerodynamic drag, which increases as the system flies faster and when the pitch angle is increased.

Using the simulation program, the ranges were estimated and the results are displayed in Figure 7.2. This was done by calculating the distance travelled by the system over a time period of 20 minutes, which is the estimated battery life. It should be noted however that the range can also be limited by the communication link between the ground station and the UAV, which in this case is 1.6 kilometres, as discussed in Section 4.7. The distance shown in Figure 7.2 is solely the distance the system can fly until battery life runs out.

7.1.5. Stability & Control

In this section, the stability & control characteristics are explored. It begins by presenting the centre of gravity placement limit. This is useful information as it may be used to validate that the system can fly stable with the centre of gravity not exactly in the geometric centre. It is also useful to know limits, in case it is desired to mount additional payload on the system that is off-centre, such as extra cameras to film the UAV's flight. These characteristics are also useful for potential buyers of the system, in case a change of payload is desired. This is followed by an analysis of the vertical ascent rate in order to determine the kind of control available manoeuvres.

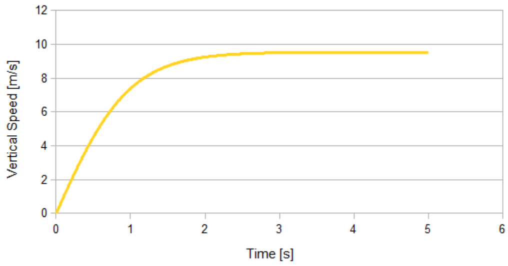

Figure 7.3: Vertical speed w.r.t. time

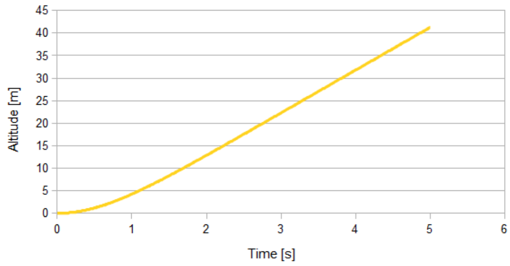

Figure 7.4: Vertical displacement w.r.t. time

Centre of Gravity Limits

With regards to stability, the simulation program was used to determine the range where the centre of gravity of the UAV may be, while still guaranteeing stable hovering. In order to do this, the program applied force and moment equilibrium (Equations (7.9), (7.10) and (7.11)). The boundary condition stating that $T_{max} = 2 \cdot m_{UAV} \cdot g_0$ was also used. From the program it follows that the centre of gravity may shift up to 16 cm in any direction in the horizontal plane and the system will maintain its equilibrium. With the distance from the centre of the UAV to the thrusters being 32 cm, the range for the center of gravity is about halfway towards the thrusters from the centre.

$$\sum F^{\uparrow} = 0 \tag{7.9}$$

$$\sum F^{\rightarrow} = 0 \tag{7.10}$$

$$\sum M = 0 \tag{7.11}$$

Vertical Ascent

To determine the maximum vertical ascent of the UAV, the simulated model applied full thrust in vertical direction, and prevented rotation. The simulation started with a vertical velocity and altitude of zero. Full thrust is applied using $T_i = T_{max} = \frac{2 \cdot m_{UAV} \cdot g_0}{6}$ for each of the 6 thrusters. The movement is purely in vertical direction; there is no horizontal velocity and therefore no horizontal component of the thrust or any drag. The program then calculated the force in vertical direction and the acceleration every 0.01 seconds, integrating the latter to find the velocity and again integrating this to find the altitude. The results of this simulation can be seen in Figures 7.3 and 7.4. These figures show the required time for the UAV to reach a certain altitude and the speed with which it can ascend.

7.2. Material and Structural Characteristics

During the flight and when the UAV is on the ground, the structure is constantly subjected to different kinds of loads. These loads need to be identified, and the structure should be designed in such a way that it will be able to carry these loads. The ability to carry these loads depends on the cross section design and the chosen material. In Section 5.9, carbon fibre was chosen as the primary material for all the load carrying parts. In Section 7.2.1, the stresses in the airframe are analysed. In Section 7.2.2, the vibrations of the UAV are discussed and the connection between the payload platform and the airframe is discussed in Section 7.2.3 .

7.2.1. Airframe Loads

The highest loads on the structural arms will be bending loads. To cope with these loads, a high moment of inertia is needed around the bending axis. The rectangle can be shaped is such a way that it has a high area moment of inertia around the bending axis. The loads during flight and mission tasks where not identified as the highest loads. From practice it is known that the handling loads are the most prominent loads for a small UAV. As one may pick up the drone at the end of one of the arms and may do this with quite an acceleration, this acceleration can be as high as $2.5G$ according to tests that were performed. The test was performed by picking up a bag with comparable weight to that of the UAV, in the bag a mobile telephone with accelerometer was present. The highest acceleration was recorded. The test was repeated multiple times and $2.5G$ was the upper limit. With the maximum weight and dimensions known and given in Section 5.9, the highest moment load the arms of the airframe will be able to carry is $58[Nm]$. Also a shear force of $122[N]$ will be present due to the handling of the UAV which the structure should also be able to cope with.

With the primary loads and the material characteristics known from Section 5.9 the cross sectional dimensions of the structural arms can be determined. A model was made where the applied loads and the material properties where imported. The maximum stresses that the material can handle were provided in Section 5.9 as well. Now an iterative process was started to find the optimal cross sectional area for the design with the use of an extra safety factor of 2, this safety factor was chosen because it is a common safety factor in the aerospace industry. At the end of the iterative process the following dimensions were found. The height should be $18[mm]$, the width $5[mm]$ and with a thickness of $1[mm]$. The cross-sectional details are also provided in Figure 7.5.

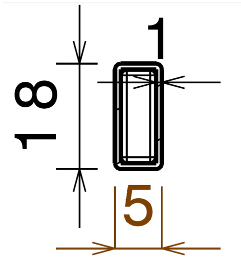

Figure 7.5: The cross-sectional layout of the structural arms of the UAV

With the cross-sectional layout dimensions and the loads applied, plots about the moment distribution through the arm, shown in Figure 7.6, and for the point with the highest moment a stress distribution through the cross section shown in Figure 7.7, can be made.

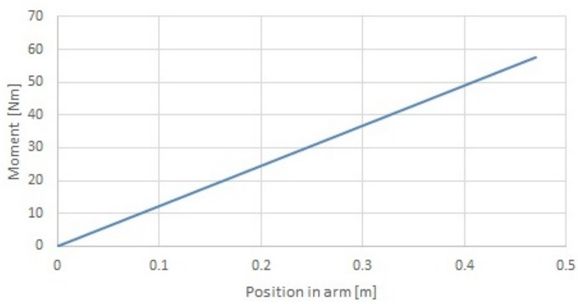

Figure 7.6: Moment distribution over the length of the structural arm of the UAV

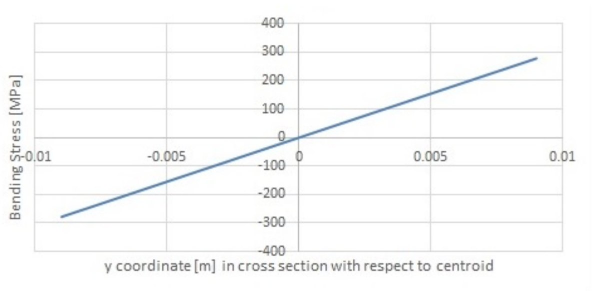

Figure 7.7: Bending stress distribution through the cross section at the highest moment location in the structural arm, this is where the beam is clamped or hold

As can be seen from Figure 7.7, the highest stress present is $278[MPa]$. With a safety factor of 2 this would become $756[MPa]$. Comparing this with the maximum compressive and tensional strength provided in Section 5.9 of respectively $570[MPa]$ and $600[MPa]$, one can conclude that the requirements are met.

Connection point

The triangular connection point (shown in Figure 7.8) connects the three different arms. Loads will be transferred through this part and, due to its unusual shape, it will be difficult to predict stress distributions. To ensure the connection point is able to carry the loads, and over-design it on purpose, the thickness was increased to $2[mm]$. The connection point will surround the structural arm. Its dimensions will be larger, thus having also a larger moment of inertia.

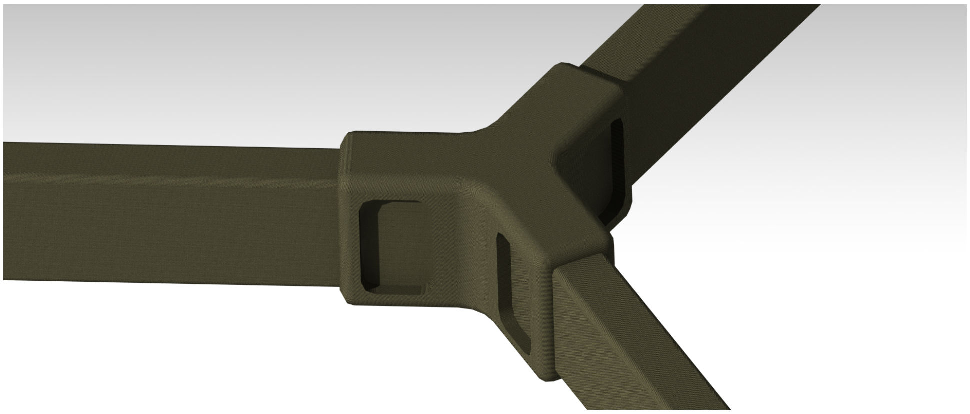

Figure 7.8: Visualisation of the three legged connection point for the structural arms

Using the FEM tool for Catia, an analysis was made of this connection point. This was done to evaluate the stresses and ensure the material will not fail under the applied loads. Again a safety factor of 2 was applied in the analysis. Two of the three legs were considered clamped and the load transferred from the structural arm would be applied at the third leg. This FEM analysis was verified by simulating the connection point in 2D. The results were that the highest loads are indeed halfway the connection but, but that it does not fail under the applied loads.

Landing Struts

The landing struts will evaluated in a similar fashion as was done the with connection point in Section 7.2.1. Because of the design of the struts, 3D-printing would be a more favourable option, as was discussed in Section 5.9. To ensure this part will be able to carry the loads, another FEM analysis was performed.

The outcome of this analysis was that the maximum deflection of the strut was 6[mm] and the material is able to deal with all the applied loads without yielding.

7.2.2. Vibrations

The propulsion system of the UAV will induce vibrations on the structure it is attached to. The sensing instruments and the remainder of the payload are very sensitive to vibrations and this might result in corrupted sensing data. To avoid this problem rubbers will be added to connect the payload platform to. These rubbers will cancel out the vibrations induced to the engines and propellers. Because specific sized rubbers are needed, they will be 3D printed [182].

7.2.3. Payload Connection

The different types of payload will be connected by means of an adhesive named Araldite [183]. This adhesive has the property that the connection is as least as strong as the carbon fibre structure itself. This ensures that the payload is attached properly to the main frame of the drone and will not fall off during operations. A weight and cost budget was accounted for in the budget breakdowns for the use of this adhesive. The weight of the adhesive budget is 40 grams which is incorporated in the total airframe weight and the cost is €4.59 per UAV.

7.3. Reliability, Availability, Maintainability & Safety

This section will evaluate four important characteristics of the system. Its reliability needs to be assessed in order to determine the probability that the system will perform as anticipated during the expected mission conditions. Availability refers to the probability that the system will be ready for use when it is required to be. Maintainability considers the ease and economy associated with maintenance of the system. Lastly, safety deals with the amount of potential hazards to humans and the environment. These aspects of the system are important pieces of information in order to have a complete overview of every characteristic of the system.

Knowing these aspects of the system will make it more interesting for potential buyers who will want to make sure their purchased equipment is for example easy to maintain and safe to use.

7.3.1. Reliability

In order to assess the overall reliability of the system, four key points must be evaluated: the definition of normal performance as well as the corresponding operating conditions, the percentage of times that the system can be expected to function normally and the duration over which the system must perform its mission.

Expected Performance & Operating Conditions

Starting with the two definitions, the system is designed to perform six mission elements. Therefore, expected performance is specified as being a successful execution of each mission element by each UAV. However, even if this criterion is not met, the system can still be said to have performed to a satisfactory degree if it wins the international micro aerial vehicle (IMAV) competition, since this is a top level requirement.

Soteria is designed to operate in sunny weather that is common in the Netherlands in August. However it can also withstand some windy conditions as well as rain. Naturally, optimal performance is expected on a clear day with little to no wind. However, the probability of a windless day is too low to rely on, so the effect of wind speeds of up to 9 m/s has been investigated and found satisfactory.

Also, reflections of sunlight on plastic can cause problems when the system attempts to identify house numbers, which are printed plastic-covered A4 sheets to enable them to withstand rain. This can be solved by maintaining an altitude higher than that of the sheet, since the sun will also be above the sheet during the competition timeslot. Therefore, reflections can only become a problem at an altitude lower than that at which the sheet is hung.

Reliability Issues

The main issue concerning reliability is that of the accuracy of the navigation. This is chiefly governed by two aspects: inaccuracies in the location module and external forces acting on the UAV. The GPS system has a specified accuracy of 5m. This means that the UAV will be within a radius of 2.5 m from the point where the GPS module says it is for 50 % of the time [184] [71]. This is sufficiently accurate for flying over the competition area, but not below roof height, since the risk of crashing into a building is very large using only GPS, as described in Section 4.3. To accommodate this, the system will navigate using a range finder and camera vision when it descends for the house number identification. External forces are also taken into account. The navigation module needs to be able to cope with gusts of up to 5 m/s. If the wind speed is below that, the UAV should not suffer any damage. The probability of higher wind speeds is too low to be worth accounting for.

Mission Duration

Naturally, the expected duration is simply the projected mission flight time of 20 minutes for the UAVs. For the entire system, this rises to 40 minutes, which includes the half hour in which the mission must be executed as well as the additional 10 minutes which are allowed for creating the photomap and indicating the blockades on it [2].

7.3.2. Maintainability

An important feature of any system is the ease with which it can be maintained. For Soteria, this problem can be split into two categories: pre-IMAV and post-IMAV. The latter refers to possible production for actual search and rescue (SAR) use. Leading up to the competition, there will be little maintenance required unless the UAVs crash during testing and will need to be repaired. The system will need to be constructed and is then tested once in a full mission scenario on the test day before the competition. If any problems arise or modules fail, these can be easily replaced due to the plug-and-play nature of the design. This also applies to the battery system, which will need to be removed after each mission for recharging.

If the system is taken into production, the same concept applies; the system was designed with ease of maintenance in mind. All parts can be acquired online or produced in fairly common and straightforward methods.

They can then be replaced quickly and efficiently. Naturally, considering the unpredictability of natural disasters, it is important to test the system frequently to detect any malfunctions before the system is needed for a real mission. Also, it is important to note that in most cases, only a like-for-like replacement of a broken part is needed to restore a malfunctioning part of the system to full functionality, greatly decreasing maintenance costs. Moreover, the system may see long shelf life in between uses, since natural disasters do not occur on a daily or even monthly basis. Sometimes the system could go unused for several years, especially if it is not tested regularly to ensure its continued functioning. Some of the most important parts, the airframe and propellers, will not corrode when left exposed for long periods of time, since they are made of carbon and plastics respectively. The only critical part that could corrode is the engine module, which is why the system should be checked regularly.

7.3.3. Availability

The system's availability can also be divided in two categories: the combination of reliability and maintainability, and the required time for production. The former is the typical definition of availability of a system, while the latter is specific to this project. Soteria will need to be produced in roughly five weeks if it is to be ready in time for the competition day, which places additional constraints on the design. Starting with the availability due to maintenance and reliability, this only applies to post-IMAV production. As mentioned in the section on maintainability, it is unlikely that real maintenance will be required between the test day, which is on Monday, August 11, and the actual competition on the following Wednesday. However, spare parts should be kept on hand in case a UAV crashes or malfunctions. In case any part malfunctions, this can be obtained in online stores quickly and easily. However, users should keep in mind that shipping the item can take some time. This is also the key factor in production of the design for the IMAV competition: of the five weeks available for production, some parts will take two just for delivery. However, this still allows three weeks to build and test the UAV, which is a manageable timeslot if the team is large enough.

7.3.4. Safety

The safety of the product is naturally very important. Hence, the organising committee of IMAV has created a specific set of safety requirements. Failure to comply will result in instant disqualification of the team [4]. All requirements have been taken into account in the design stage. All safety requirements, along with the report section that covers them, can be found in the compliance matrix in Section 6.7. Furthermore, all electronic systems are gathered within a casing to protect them against environmental influences such as rain.

7.4. Sustainability Considerations

This section will outline the sustainable aspects of the system. Taking sustainability into account for the design can for example limit the impact on the environment. These can be divided in two categories: sustainability considerations during the design process and the sustainable applications of the system during its lifetime.

7.4.1. Sustainability Considerations in Design Phase

During the design phase, due consideration was given to keeping the environmental footprint of the system as small as possible. The outcome of this is a modular design for the system, which greatly facilitates the replacement of malfunctioning or ageing parts and subsystems. Ranging from the chips used for navigation to the propellers and the airframe, every aspect of the aerial segment can be quickly accessed and removed. This means that the overall design will have a very long lifetime, rather than needing replacement each time a subsystem malfunctions. For example, in case of a crash the propellers are likely to be irreparably damaged, possibly along with the airframe. This is a catastrophic failure from a mission perspective. However, if the broken airframe and propellers are replaced, the system will once again be fully functional. This leads to less waste that needs to be disposed of, and means that it is not necessary to produce a completely new UAV, meaning that the system also has lower production rates and associated waste output.

Furthermore, the design includes a fully electric power supply. This means that it does not release any harmful substances, such as CO_2, which is a common by-product of combustion engines. To be more specific, the system will not have any lingering effects on its operational area once it is switched off and stored. The only energy consumption occurs during charging of the battery system, which will be done using a connection to the power grid.

However, in many locations the mains current is generated chiefly using fossil fuel such as coal or natural gas. To decrease the environmental footprint of the system even further during future design processes, energy harvesting systems can be created for the ground station. This way, the batteries can be charged by locally generated green energy. This has the additional benefit of making the system completely self-reliable. During the IMAV competition, mains current will be available to the teams. However, in the aftermath of a natural disaster, it is possible that the power grid is destroyed. It is then desirable to generate the energy for the system on site to ensure that it can perform regardless of the circumstances. Sticking to the modular design concept used so far, these harvesting systems can be made for so-called 'plug-and-play' functionality: by making them easy to attach and remove, it is possible to bring only a specific system. For example, if the weather is known to be sunny over the course of the mission, the user could bring only solar panels.

7.4.2. Sustainable Contributions of the System

During its lifetime, the system will contribute to a sustainable environment in several ways. The most prominent is the wide range of potential uses. While initially designed for SAR missions, it can also be used in other scenarios. Soteria could be used to map the affected area of environmental disasters such as an oil spill or nuclear reactor meltdown. The blockade detection software can be adapted, for example to detect flocks of birds caught in an oil spill, or to identify areas with an accumulation of toxic material.

It is also important to note that the majority of the parts and materials used for the system can be recycled when they are replaced. For electronics (such as the autopilot and Raspberry Pi modules) and plastics (like the propellers) this is already common practise [185] [186]. However, research shows that it is also possible to recycle carbon fibre by turning it into concrete [187]. This means that even the airframe will not simply end up on a scrapheap.

Naturally, the working environment is unpredictable and dangerous, so loss of a UAV during a mission is a likely scenario. If this were to happen, the UAV would have to be retrieved in order to minimise its impact on the environment since it is not constructed of biodegradable equipment. However, the system automatically stores its last known position, so this would facilitate retrieving lost UAVs. With this information, finding a lost UAV afterwards should not pose any great problems. If the mission area includes large bodies of water, such as a river with a strong current or a lake, the UAVs can be equipped with floatation devices. Water has a density of 1 $\frac{kg}{L}$, so roughly 2.3 L of air-filled balloons can keep it afloat. This means that a lost vehicle can be retrieved later, which is a desirable feature. After all, SAR teams will not spend precious time searching for crashed UAVs if there are still lives in danger. Using Soteria, they can prioritise rescuing without any compromise.

Overall, Soteria is developed in such a way as to minimise its ecological footprint, while also being capable of aiding in environmental disasters. Therefore, the design can be considered to be very environmentally friendly during every stage of its life.

7.5. System Sensitivity Analysis

In this section, a sensitivity analysis will be performed on the entire system. This will describe the relations between certain aspects to the total score that can be achieved during the competition. Considering these relations will create an overview of the impact that for example, changing the size of the UAV may have on the competition scoring. Four main topics will be covered:

- An increase in the size of the system.
- An increase in the mass of the system.
- A decrease in the time available for mission execution.
- An increase in the cost of the system.

Increase of Maximum Dimension

Since the competition scoring formula includes a factor based on the maximum dimension of a UAV, it is important to consider the effect on the total score if the size of each UAV is increased by a certain percentage. The formula used to compute the total score per UAV is repeated from Section 3.1.1 in Equation (7.12).

$$P_{UAV} = \sum_{n=1}^{N} \left(A_n \cdot M_n \cdot \left[2 - \frac{L_n}{L_{max}} \right]^2 \right) \tag{7.12}$$

The total score is the sum of the score for each mission element. For each mission element, the values in the equation are computed separately. Here, A_n is the autonomy level, M_n is the amount of mission points available, L_n is the maximum dimension of the UAV and L_{max} is a reference length, set to 100 cm for the competition.

Assuming that all other factors remain constant, the effect of a change in L_n can be computed. Figure 7.9 shows the effect of a change in L_n. It can be seen that even a small variation in size has a noticeable effect on the total score. This is due to the fact that the term which includes L_n is squared.

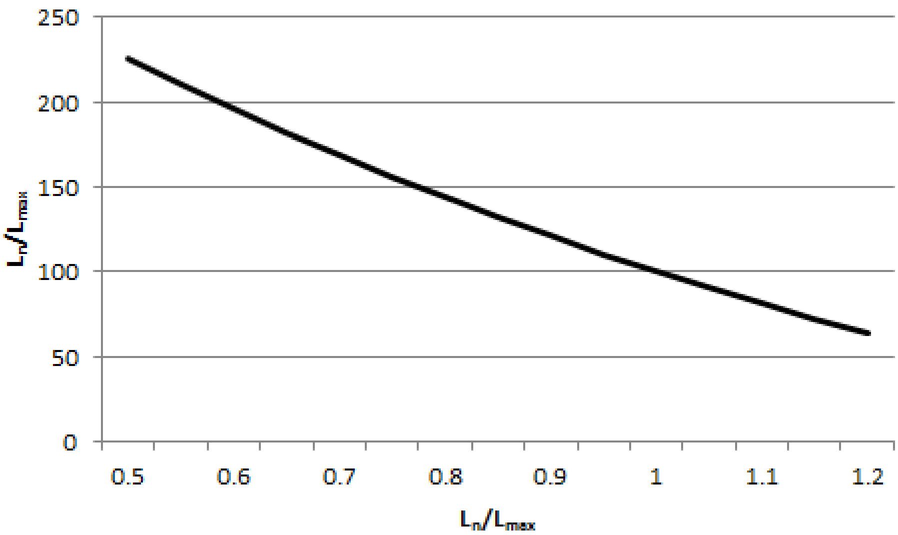

Figure 7.9: Variation in score for maximum UAV dimension ranging from 50 cm to 130 cm.

System Mass Increase

It is possible that the overall mass of the system increases, due to unforeseen additions or changes in the hardware due to incompatibilities that are not discovered until the production stage. The design take-off weight is 2.3 kg. This already includes a small measure of contingency. For the purposes of this section, this will be considered the total mass of the structure, and a 10 % increase is assumed. An example reason could be that the selected camera system is out of stock and another camera needs to be attached. It is assumed that this will not cause problems mounting it on the gimbal, it will merely increase the UAV mass by 0.23 kg. The new mass then becomes 2.5 kg. For such a change, the airframe will not need to be altered. It is designed to be able to support a 5 kg UAV. However, the propulsion system is tailored to the actual design. Therefore, a 10% increase in mass cannot be compensated for if a thrust-to-weight ratio of 2:1 is to be maintained. This means that the design loop, explained in Section 5.3, will need to be done anew. This would cause a substantial amount of working hours. However, as explained in Section 3.3, the UAVs will return to the local command centre (LCC) after completing their photography routes to allow the SD card to be removed. This time can also be used to replace the batteries. The total time for a UAV to take off, fly its photomapping route, return to the LCC and perform a precision landing will be approximately 330 seconds, as can be determined from Section 3.3 by adding the execution times of the aforementioned elements. If the propulsion system is assumed to be running at full power over that period, this will require 178 Wh of power. This can be delivered by the larger of the two battery packs selected in Section 5.8. It is then better to use only that battery pack, and leave the smaller battery out. This will reduce the system mass by 380 grams, actually reducing the initial take-off mass.

Then it might seem logical to leave that battery out entirely. However, the battery packs are located in a fairly difficult position to reach, therefore it will take considerably more time to replace it and then continue, as compared to the current scenario. This is especially true since the system will need to be rebooted. Replacing its only battery pack means the system will need to shut down first and restart after the replacement. This will take an estimated three to four minutes, excluding the time actually used to replace the battery [1]. In total, replacing the battery can take more than five minutes, which is a quarter of the total mission time. This is a significant reduction, and its consequences need to be considered carefully.

Reduction of Time Available

Here, the consequences of a 25%, or five minute, reduction of the available mission time will be considered. This follows from the concept of changing batteries after the photomapping is completed. Since all available time is already being used, a reduction in mission time will mean that some mission elements cannot or can be only partially executed. Increasing flight velocity is not an option, since with a fixed mass, requirement *IMAV-SR-25* limits the flight velocity by placing a constraint on the maximum momentum, and this flight speed is already used at every stage in the mission where it is viable to do so. This means that either the roof landing or the house number inspection would be affected. Since the latter can be executed partially, it will simply not be completed before the end of the mission. However, since points are awarded per correctly identified house number, partial points will still be awarded. The total score would simply decrease for each house that cannot be visited anymore. Since this will apply to each of the four UAVs, the decrease per unvisited house is $4 \cdot 12 = 48 points$.

Increasing Costs

Of the project budget of €5000, construction of the UAVs and ground station takes up €4900. The remaining €100 will be spent on spare parts. The propellers can easily break during testing. Since six sets are needed, the remainder of the budget will be spent on replacements. Many parts were found on websites working with currencies other than euros. Unfavourable fluctuations in exchange rates could affect the budget, but these will not cause it to exceed the €5000 limit [188]. Overall, the system is insensitive to changes in the financial budget, compared to its sensitivity in other areas.

7.6. Market Analysis

The market analysis in this chapter is aimed towards a comparison between the design of the system presented in this report and existing multicopters. Furthermore, potential customers and other interested parties that may be interested in purchasing a Soteria UAV system are identified. This can be used when commercialising Soteria after the IMAV competition.

7.6.1. Comparison with Comparable Multicopters

The purpose of this section is to present a comparison between existing UAV and the one designed by Soteria. As the designed UAV is a multicopter, this comparison is done with other available multicopters already available on the market.

After some research, comparable multicopters that are already on the market have been found. These are shown in the list below.

- Microdrones MD4-1000[180]
- Microdrones MD4-200[189]
- Parrot AR.Drone 2.0[181]
- SteadiDrone QU4D[190]
- Aibot X6[113]
- Aeryon Scout[191]

The specifications of these UAVs are shown, along with the specifications of the designed UAV, in Table 7.2.

Table 7.2: Specifications of similar UAVs

Name	Mass	Flight time	Control	Cruise speed	Largest dimension	Cost
Microdrones MD4-1000	2650g	70 min.	Remote control or with GPS	15 m/s	1030mm	€34498,-
Microdrones MD4-200	800g	30 min.	Remote control or with GPS	8 m/s	540mm	€5872,-
Parrot AR.Drone 2.0	380g	12 min.	Autonomous flight with GPS and Paparazzi	18 m/s	451mm	€284,-
SteadiDrone QU4D	1500g	18 min.	Radio controlled	28 m/s	645mm	€1688,-
Aibot X6	3400g	30 min.	Remote controlled, automatic waypoints	11 m/s	1036.32mm	€22018,-
Aeryon Scout	1400g	25 min.	Radio controlled	14 m/s	800mm	€88079,-
Soteria	2300g	20 min.	Autonomous	17 m/s	830mm	€1150,-

In this table it can be seen that the Soteria UAV is among the smaller ones, average flight time and a lower price than most. However a big improvement over the other multicopters is that the Soteria UAV is designed to fly autonomously, as well as being able to perform some tasks without human interference.

7.6.2. Interested Parties

UAVs could have many applications in SAR mission, or they may provide an overview of a disaster area with the use of aerial photography. The focus in this section is on SAR missions, and related applications.

Search and rescue teams could have a UAV that can create a photomap of a disaster area, to determine the possible location of survivors, blocked roads and danger zones to allow for quicker, safer and more efficient survivor extraction. In order to understand the needs and opportunities for UAVs of SAR teams, it is necessary to familiarise oneself with their way of operations. This section gives some remarks on this topic.

The National Land Search Operations Manual of Australia [192] states that the chance of survival of injured persons decrease by 80 percent during the first 24 hours, and that it is therefore crucial to gather information as quickly as possible in order to:

- Locate, support and rescue persons in distress in the shortest possible time
- Use any contribution survivors may still be able to make towards their own rescue while they are still capable of doing so

In order to do this, a SAR operation encompasses multiple stages. The National Land Search Operations Manual of Australia mentions five, namely awareness, initial action, planning, operations and conclusion. These five stages include everything from getting to know about a possible distress situation to debriefing of personnel and completing documentation. For this UAV project, the stage of interest is Operations, which deals with the dispatching of SAR assets to the scene and conducting searches. The current scope of this project is urban areas.

The Urban Search and Rescue Response System Field Operations Guide of the United States of America [193] specifies the following initial reconnaissance operations:

- Area sketch/map and building Identifier
- Structural/Hazard evaluation and marking
- Building sketch/plan, including building cross section
- Building type/configuration, including size and stories
- Building occupancy type
- Collapse type
- Void locations
- Hazard locations
- Best access
- Hazard mitigation notes

For each of these tasks the use of a UAV system instead of, or in addition to personnel, might be of great value. At the current stage, the system has been designed to be able to assist in the tasks of area mapping and building identification, discovering hazard locations and determining best access routes (by identifying road blocks).

A network called "Search With Aerial RC Multirotor" (S.W.A.R.M.) exists, in order to inspire volunteers to assist

SAR organisations with their missions. This is done at no cost to the organisations or the families of those afflicted [194]. Furthermore, police departments may also be an interested party, as they could benefit from UAVs being able to create a photomap of a location of interest, as well as being able to aid in the search for missing persons.

7.7. System Characteristics and Design Analysis Conclusion

This chapter concludes the section of the report where the design has been analysed and finalised. The response of the UAV to a gust or control inputs such as full upwards thrust has been simulated and analysed. Furthermore, strengths of the structure and material of the UAV have been determined. Failure loads were calculated to determine whether the system can remain intact throughout its mission.

The reliability, availability, maintenance and safety aspects of the system have also been discussed. The sustainability of the design have been shown, in order to consider the impact of the design on the environment during production and throughout its lifetime. For the competition, a sensitivity analysis was performed, in order to quantify the impact of changes to the system to its performance. An analysis of the overall design has been done as well to compare it to similar UAVs already available on the market.

8

Post Design Synthesis Exercise Design and Development

The end of the design synthesis exercise (DSE) is not the end of the project. The system must still be built, tested and then compete in the international micro aerial vehicle (IMAV) 2014 competition in order to fulfil the project objective statement (POS). Due to this, an approach has to be developed for the post-DSE phase of the project. First, a logical order has to be established in which the activities need to be performed, this is presented in Section 8.1. With THE overall flow chart of the development process in mind, a production plan of the unmanned aerial vehicle (UAV) may be made. This production plan is provided in Section 8.2. During and after the construction of the UAVs, a number of tests have to be performed and subsystems will need further verification and validation. A strategy for these topics will be discussed in Section 8.3. Finally, for the competition day itself a plan for logistics is needed as well. These competition logistics are provided in Section 8.4. With the use of the design and development logic block diagram and aforementioned sections, a planning may be made for the post-DSE activities. The Gantt-chart in which this planning is visualised may be found in Section 8.5. The chapter wraps up with a conclusion in Section 8.6 of what needs to be done in the post-DSE phase of the project.

8.1. Project Design and Development Logic

As mentioned earlier, an overview should first be made of the activities that need to be performed in the post-DSE phase of the project, in order to be able to compete in the IMAV 2014 competition. Such an overview may be obtained with the use of Figure 8.1.

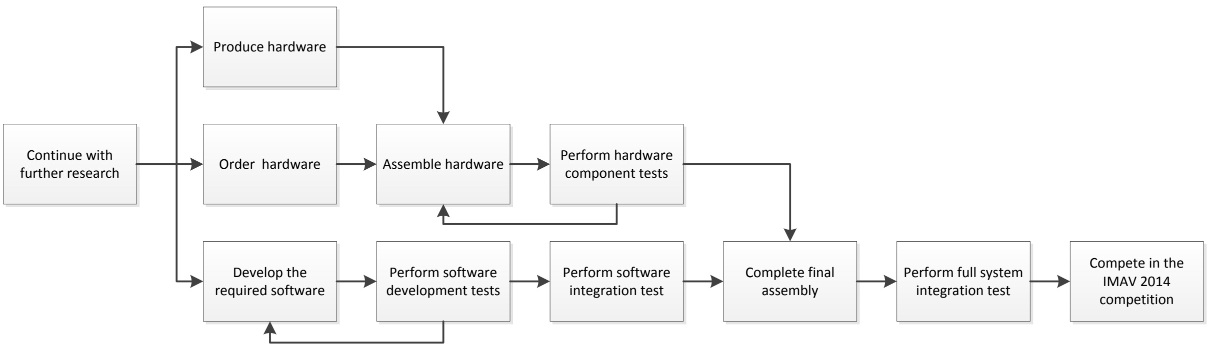

Figure 8.1: An overview of the activities that need to be performed in the post-DSE phases of the project

The following may be noted from Figure 8.1: first, further research should be done with respect to the design. From there on, the software may be developed and the required hardware may be produced or ordered. While the hardware is being produced or delivered, software development tests may be performed. The results of these tests will then be used as an input to further develop the required software. Once the software has been completed and the hardware has been obtained, the software may be integrated into the hardware. In the first stage of this process, a software integration test will be performed. The results of this integration test will also act as an input for the hardware assembly, as each subsystem will be assembled and verified to work separately. As soon as the software has been verified to work on the chosen hardware, the complete system may be assembled. The system may then be verified to work with the use of a full system integration test. Finally, the UAV may compete in the IMAV 2014 competition, once it has been completed. Each of these phases will be elaborated upon in the following sections.

8.2. Production Plan

As discussed in the previous section, the hardware may be produced once the research phase has finished. In order to produce the Soteria UAVs, a solid production plan is needed. This is done to ensure that the UAV will function properly and according to the design requirements. Some elements that were designed will be entirely made by the team, such as the airframe, payload platform, landings struts and damping connectors. Other parts will be bought off-the-shelve, for example the propellers, engines and the battery packs. For the parts that will be made by the team, an in-depth production plan is needed. The other parts will need to be ordered and shipped in time. When all different subsystem parts are present and/or produced the plan for the system integration, presented in Section 8.2.3, will be executed.

8.2.1. Airframe

The airframe will be made of carbon fibre, as was decided in Section 5.9. The cross sectional dimension were later derived in Section 7.2. A visualisation of the production process is presented by means of a flow diagram as shown in Figure 8.2. The carbon fibre needs to be laminated around a mould. This mould can easily be created from Styrofoam. This is a low-cost product which is easy to model in the desired mould dimensions. After the carbon fibre frame is finished, the Styrofoam can easily be removed. A total of 4 moulds will be created, one for the tripod connection point and three for the structural arms.

In the next step, the carbon fibre cloth will be wrapped around the moulds according to the thickness's specified in Section 7.2. When wrapping, one should make sure that no gaps are created and that parts are not overlapping where unnecessary. The tripod and three structural arms will be laminated while being joined together. This will create one integral frame.

Once the tripod and three structural arms have been laminated, the resin should be heated up to the temperature provided in the manual of this specific resin type. The carbon fibre may then be coated evenly with the resin by using a brush.

A bag made of polythene, which can be connected to a vacuum pump, should be present and ready for use. Once the carbon fibre has been coated with the resin, the whole structure should be inserted in the bag immediately. The bag should then be closed and the vacuum pump should be activated. The pump will then lower the pressure in the bag to approach vacuum conditions.

The bag should now be sealed and the vacuum pump should be taken off. Air may now get in and a constant pressure will then be applied. This ensures that the shape is preserved as the resin is curing. The package should be held at the curing temperature specified within the resin's manual.

When the resin has cured, the carbon with the mould will be taken out of the vacuum bag. The Styrofoam will then be taken out of the carbon fibre structure. A final inspection has to be made to ensure the product fulfils the pre-set strength requirements.

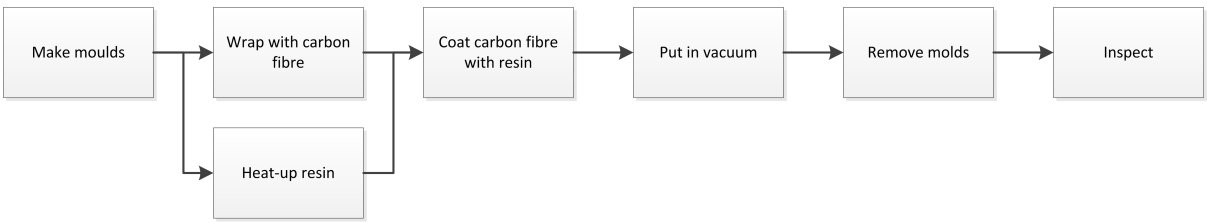

Figure 8.2: The production flow diagram for the production of the carbon fibre airframe.

8.2.2. 3D PRINTING

The payload platform, gimbal and landing struts will be 3D-printed. For this a 3D printer and the design file of the platform are needed. The design has already been done as was shown in Section 6.1. The file will be loaded into the 3D printer software and then the printer will start printing the input design. The material used was described in Section 8.2.1. The flow diagram of the production with the use of a 3D printer is given in Figure 8.3. The damping connectors with the function described in Section 7.2 will also be 3D printed. The material and technique for printing rubbers of this sort is already available [182]. The layout and design of the rubbers that will be printed is given in Figure 8.4.

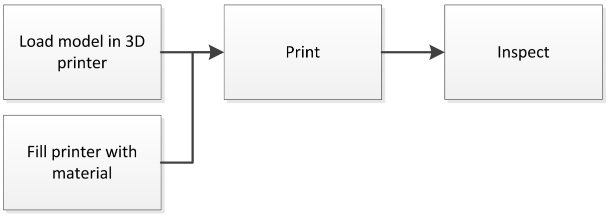

Figure 8.3: The flow diagram for the production of the parts with the use of a 3D printer.

Figure 8.4: A 3D visualisation of the damping connector that will be 3D printed.

8.2.3. INTEGRATION

As soon as all the components have either been produced or delivered, the system needs to be assembled into a functioning UAV. The different components will be attached mechanically as can be seen in Section 6.1 or by means of the Araldite glue discussed in Section 7.2. The integration order of the different components will be as follows, as is also visualised in the flow diagram that may be seen in Figure 8.5.

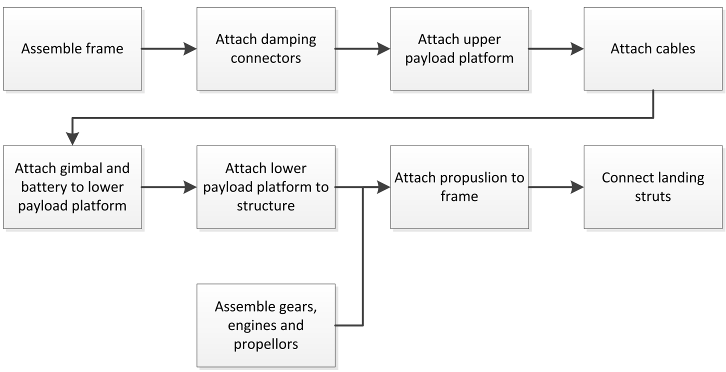

Figure 8.5: The integration flow diagram for the UAV assembly during production.

The damping connector rubbers can be pushed over the structural arms to the correct position. Once there, they can be glued as well. Now the upper payload platform can be attached to the rubbers via the mechanical locking mechanism and glued into place. On there, the different payload systems may be placed and the first cables can be attached to the frame. From this, the dome can be placed on top of the upper payload platform. On the lower payload platform the batteries will be attached as will the gimbal. This platform can now be attached to the bottom of the frame in a similar fashion as was done with the upper payload frame. The batteries can then be connected to the upper payload and the frame wiring. The engines, gearboxes and propellers need to be assembled. Once completed, they can be attached to the carbon frame by means of a connection shown in Section 6.1. Finally, the landing struts can be attached to the endings of the structural arms, they may be pushed into the end of these arms. For these parts the glue will be used to ensure proper bonding between the different elements.

8.3. FUTURE TEST PLANS, VERIFICATION AND VALIDATION

This section discusses the tests that have to be performed in order to ensure that Soteria can operate within the given design limits. The tests will be performed in the groups that were defined in Section 8.1. These groups are based on the completion of the system required in order for the test to be performed.

First, there are the software development tests, which will provide a proof of concept. These tests may be performed on a computer. This group requires the least amount of resources, as computers are readily available and most of the programs are freeware. These tests verify that software is capable of performing the tasks required. In the case that off-the-shelf software cannot handle the tasks demanded, new software will have to be developed by the team. Furthermore, the software (which does not directly interface with the UAV) of the ground-station is tested to verify that it works on the intended computer. An overview of these tests is given in Table 8.1.

Table 8.1: Software development tests on a computer of the software used on the UAV and ground station

Test ID	Test Description
ST-01	The possibility and duration of the stitching of a photo map with 99 photos with a resolution of 20 mega-pixel
ST-02	The automatic copying and preparation before the stitching of the photos, when the SD card with photos is inserted into the ground station
ST-03	The detection of blockades on a stitched photo map
ST-04	The use of software to detect an A4 sheet at different ranges
ST-05	The combination of sheet and number recognition to identify a number on an A4 paper

The tests presented in Table 8.1 are related to requirement *IMAV-CR-ME2* and underlying requirements as well as *IMAV-CR-ME4*. More specifically, tests *ST-04* and *ST-05* were developed to determine the 'to be discussed' specifications within requirements *IMAV-CR-ME4-9* and *IMAV-CR-ME4-10*. These test are necessary for the Soteria system as the tests verify and validate the yet unfulfilled requirements as described in the compliance matrix and feasibility analysis of Section 6.7.

The second group of tests are the software integration tests. These tests are performed on the on-board computer, the Raspberry Pi. For these tests the software developed is migrated to the Raspberry Pi to verify compatibility with the hardware used on the Raspberry Pi and the available processing power. This group requires a deeper understanding and optimisation of the software, as the Raspberry Pi has a less processing power than a laptop. Furthermore, unlike in the case of a computer, a lot of the programs still need to be written. The tests will also involve for instance, the Raspberry Pi camera Module, to verify its capability of detecting a sheet of A4 paper combined with the Raspberry Pi itself. An overview of these tests can be found in Table 8.2.

The tests presented in Table 8.2 are related to requirement *IMAV-CR-ME4* more specifically requirement *IMAV-CR-ME4-1*. These test are necessary for the Soteria system as the test verify and validate the yet unfulfilled requirements as described in the compliance matrix and feasibility analysis of Section 6.7.

The third group will be the hardware components tests. These tests will verify that the hardware components work as intended under simulated conditions. These tests require the purchase of the intended hardware used in the system and will be performed before and during the assembly. The hardware component tests may be

Table 8.2: Software integration tests of the developed software on the Raspberry Pi on-board computer

Test ID	Test Description
RT-01	The compatibility of the two ultrasonic range finders with the Raspberry Pi
RT-02	The compatibility of the sheet recognition software with the Raspberry Pi
RT-03	The integration of the Raspberry Pi camera module with the Raspberry Pi
RT-04	Performing number recognition on the Raspberry Pi
RT-05	The use of the sheet recognition to detect a sheet of A4 paper with the Raspberry Pi with the Raspberry Pi camera module
RT-06	Combining the sheet detection with the number recognition on the Raspberry Pi

found in Table 8.3.

Table 8.3: Hardware component tests of hardware used on the Soteria to verify component performance is as intended

Test ID	Test Description
CT-01	The range, stability and data rate of the XBee communication system
CT-02	The interference of the two ultrasonic range finders
CT-02	The connection between the Lisa/M v2.0 autopilot and the Raspberry Pi on-board computer
CT-03	The accuracy of GPS in an urban area
CT-04	The compatibility of the GPS with the Lisa/M v2.0 autopilot board
CT-05	The accuracy of GPS and the IMU in an urban area
CT-06	The propeller thrust on different RPM settings
CT-07	The effects of the pusher-puller propeller configuration
CT-08	The capacity of the battery
CT-09	The voltage drop of the battery when discharged
CT-10	The integration of the gimbal
CT-11	The accuracy of the gimbal
CT-12	The structural loads on landing legs
CT-13	The structural loads on the airframe
CT-14	Determination of the eigenfrequency of the airframe
CT-14	Autopilot integration within the propulsion system

The tests presented in Table 8.3 are related to requirement *IMAV-CR-ME2*, more specifically *IMAV-CR-ME2-8* and *IMAV-CR-ME2-9*. Furthermore, the hardware component test are related to requirement *IMAV-CR-ME4*, *IMAV-SR-26* and *IMAV-AU*. These test are necessary for the Soteria system as the test verify and validate the yet unfulfilled requirements as described in the compliance matrix and feasibility analysis of Section 6.7.

Lastly, the fourth group contains the full system tests. These tests require the full UAV to be assembled in order to test the integration of the entire system. Also part of these tests is the tuning of the autopilot to the characteristics of the UAV. These tests will verify that the entire system meets the set requirements and will validate that it can perform the intended mission. An overview of these tests can be found in Table 8.4

The tests presented in Table 8.4 are related to requirement *IMAV-CR*, more specifically *IMAV-CR-ME1-1*, *IMAV-CR-ME2-10* and *IMAV-CR-ME4-5*. Furthermore, these full system test relate to requirement *IMAV-SR*, more specifically *IMAV-SR-26*. These test are necessary for the Soteria system as the test verify and validate the yet unfulfilled requirements as described in the compliance matrix and feasibility analysis of Section 6.7.

Table 8.4: Full system tests of the UAV to tune the autopilot, verify that it meets the set requirements and validate that it can perform the intended mission

Test ID	Test Description
FT-01	A vibration test to determine vibrational integrity of the UAV
FT-02	A performance test of the propulsion system without the payload
FT-03	The ground station and UAV communication link
FT-04	The tuning of the autopilot
FT-05	Manual control range, stability and integrity
FT-06	Flight envelope determination (maximum range, flight time, altitude and weather conditions)
FT-07	Completion of the separate mission elements
FT-08	Completion of the entire mission
FT-09	Test flights at the competition area

8.4. Competition Logistics

A well thought-out plan for logistics issues surrounding the competition will be prove to be very useful to avoid running into what would otherwise be an unexpected problem. Transportation to the testing ground and the set-up of the equipment will be elaborated upon in this section.

8.4.1. Transportation

To consider transportation, it could already be useful to determine the route as well as transportation time ,from where the systems are stored to the competition grounds. This will avoid running into time shortages due to not leaving on time or not being sufficiently prepared. It is assumed that the travelling is done by car and the route is planned using Google Maps [195].

It is assumed that the UAVs and ground station, along with all other supporting equipment, are constructed, tested and kept on university grounds. The faculty of Aerospace Engineering, Kluyverweg 1, Delft, The Netherlands, is therefore used as the starting location. The route to the exact competition grounds cannot be calculated on Google Maps. Therefore, the nearest road to this location is being taken as the destination in order obtain a travelling time estimation. Kostverlorensteeg 27, Harskamp, the Netherlands is taken as this destination. The driving time is estimated to be roughly 1 hour and 30 minutes. Traffic jams or other unforeseen circumstances have not been taken into account. Therefore, a conservative time frame around this estimate should be taken as travel time.

Transportation Vehicle

For the competition, all team members, UAVs and equipment should be transported. It is likely that this requires a larger vehicle than the standard car. It is possible to rent a van to transport all the equipment. It can be assumed that for the most part, team members will be able to find their own transport. In order to protect the equipment, sufficient packaging should also be made for all the UAVs and ground station, such that they do not get damaged during transport.

8.4.2. Equipment

It is vital that a check-list is made to make sure no equipment for competition is forgotten. Running through the items on the check-list before travelling to the competition area can be incredibly useful. Bringing back-up equipment such as a secondary (and tertiary) computer to serve as ground stations in case the primary would experience problems, should also be considered. Additional cables and wires, with a tool-kit for quick repairs, would also be a good addition. At the competition location there is a 230V power supply available for the ground station.

8.4.3. Mission Start

As soon as the team is allowed to start, all equipment needs to be set up in the control zone. Computers will need to be assembled and turned on. Furthermore, the UAVs will need to be brought to the take-off zone and powered up. Preferably, to save UAV battery power, the UAVs are powered on at the end of the preparation phase such that the mission may start right after they are powered up.

8.4.4. During Mission

During the mission, team members can be divided among a variety of tasks to ensure the mission goes according to plan. An example task would the monitoring of the equipment, to ensure that the ground station does not overheat. Also making sure visual contact is maintained with as many UAVs as possible could be useful, in case there is a software failure and their location it not returned to the ground station. A flow diagram was constructed for the mission. This diagram is presented in Figure 8.6.

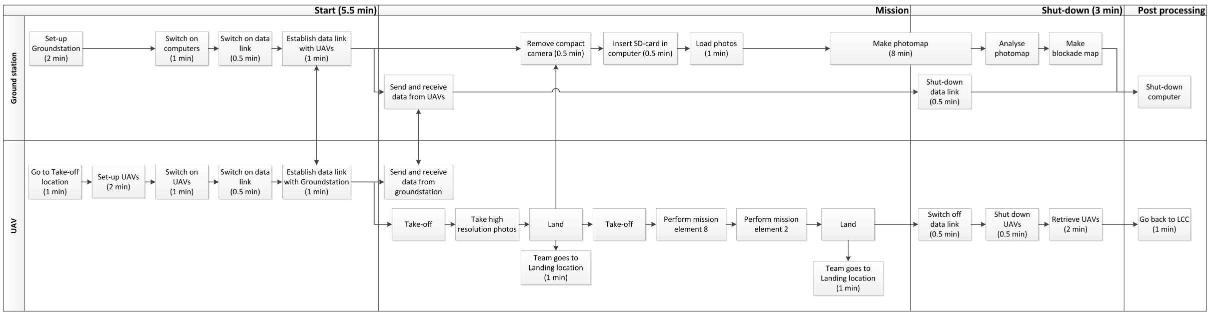

Figure 8.6: The Functional Flow Diagram of the operations during the competition day of the IMAV competition

First, the ground station needs to be initialised and the UAVs need to be brought to the take-off location. When the ground station and the UAVs are on-line, a communication link can be established. The UAVs can now start their mission as described in Section 3.3. During the mission, every UAV will return to the local command centre (LCC) once, this is done such that the Sony Cybershot camera may be detached and to secure the SD card with the photomap data. The UAVs will continue their mission and the ground station will start the photo stitching operations. When the photomap has been stitched, it will be analysed by means of software. The team will make a decision whether the blockade map parts will be done manually or automatically, as was already described in Section 3.3. At the end of the mission, the UAVs will land again at the LCC. The team will shut down the UAVs and retrieve them. The ground station is still allowed to run the photomap or blockade map operations until 10 minutes after the actual mission time. The maps will then be delivered to the IMAV jury.

8.4.5. Mission End

After the event, any lost UAVs will need to be recovered quickly. This may be done either by car or by a cyclist if the lost UAV is far from the LCC. Properly landed UAVs also need to be recovered from the landing site. The ground station needs to be shut down and dismantled. All equipment needs to be loaded in the transportation vehicle. Finally, any photomap sent to the ground station should also be sent to the IMAV jury digitally or physically for the determination of the score. Blockades should be drawn on a copy of the map as well.

8.5. Post Design Synthesis Exercise Time Scheduling

With the use of the elaboration that was done on the production and verification and validation of the UAV, a time schedule may be created. This time schedule was made using a Gantt Chart, which may be used to obtain an initial estimate for the schedule of the post-DSE activities. This Gantt Chart may be found in Figure 8.7. The development has been divided into the phases that have been discussed in Section 8.1.

It may be noted that a certain duration was predicted for each of the tasks. This duration has been based upon the importance, the current state and the expected duration of the task. An example would be Task 1.4, the further research on the detection of blockades. As the ability of the system to detect blockades is in an early development stage and as this ability is of great importance, three full days have been predicted to be needed in order to finish the research on this matter. The further research, hardware component tests and full system integration tests are the most time-consuming phases of the development. As mentioned earlier, time has been allocated to these phases according to their importance.

The Gantt Chart has been made such that the weekends are also taken into account as being working days, due to the need for extra development time. This results in a total of 37 days which may be used to complete the development of the UAV system.

ID	Task Name	Duration	Start	Finish
1	**1 Further research**	**5 days**	**Mon 07/07/14**	**Fri 11/07/14**
2	1.1 Aerodynamics model & characteristics	3 days	Mon 07/07/14	Wed 09/07/14
3	1.2 stability & control characteristics	2 days	Thu 10/07/14	Fri 11/07/14
4	1.3 Battery characteristics	2 days	Thu 10/07/14	Fri 11/07/14
5	1.4 blockade detection	3 days	Mon 07/07/14	Wed 09/07/14
6	1.5 Passive gimbal accuracy	1 day	Thu 10/07/14	Thu 10/07/14
7	**2 Order hardware**	**1 day**	**Fri 11/07/14**	**Mon 14/07/14**
9	**3 Produce hardware**	**3 days**	**Mon 14/07/14**	**Wed 16/07/14**
10	3.1 Airframe	3 days	Mon 14/07/14	Wed 16/07/14
11	3.2 3D printing	1 day	Mon 14/07/14	Mon 14/07/14
12	**4 Hardware assembly**	**3 days**	**Thu 17/07/14**	**Mon 21/07/14**
13	4.1 Assemble payload	3 days	Thu 17/07/14	Mon 21/07/14
14	**5 Develop software**	**3 days**	**Mon 14/07/14**	**Wed 16/07/14**
15	5.1 A4 sheet recognition	2 days	**Mon 14/07/14**	Tue 15/07/14
16	5.2 Number recognition	3 days	**Mon 14/07/14**	Wed 16/07/14
17	5.3 Blockade detection	3 days	**Mon 14/07/14**	Wed 16/07/14
18	5.4 Photomap stiching	2 days	**Mon 14/07/14**	Tue 15/07/14
19	**6 Software Development tests**	**4 days**	**Mon 14/07/14**	**Thu 17/07/14**
20	6.1 ST-01: Duration of stitching 99 photos	1 day	**Mon 14/07/14**	Mon 14/07/14
21	6.2 ST-02: Sticthing logistics	1 day	**Tue 15/07/14**	Tue 15/07/14
22	6.3 ST-03: Blockade detection	3 days	**Mon 14/07/14**	Wed 16/07/14
23	6.4 ST-04: A4 sheet detection	2 days	**Mon 14/07/14**	Tue 15/07/14
24	6.5 ST-05: Number & sheet recognition	2 days	Wed 16/07/14	Thu 17/07/14
25	**7 Software integration tests**	**4 days**	**Mon 21/07/14**	**Thu 24/07/14**
26	7.1 RT-01: Ultrasonic range finders & on-board processor	0.5 days	Mon 21/07/14	Mon 21/07/14
27	7.2 RT-02: Compatibility of A4 sheet detection with on-board processor	0.5 days	Mon 21/07/14	Mon 21/07/14
28	7.3 RT-03: Camera & on-board processor	1 day	Mon 21/07/14	Mon 21/07/14
29	7.4 RT-04: Number recognition & on-board processor	1 day	**Tue 22/07/14**	Tue 22/07/14
30	7.5 RT-05: A4 sheet detection	1 day	**Tue 22/07/14**	Tue 22/07/14
31	7.6 RT-06: A4 sheet detection & number recognition with on-board processor	2 days	**Wed 23/07/14**	Thu 24/07/14
32	**8 Hardware component tests**	**6 days**	**Wed 23/07/14**	**Wed 30/07/14**
33	8.1 CT-01: XBee communication system	1 day	Wed 23/07/14	Wed 23/07/14
34	8.2 CT-02: Ultrasonic range-finder interference	0.5 days	Thu 24/07/14	Thu 24/07/14
35	8.3 CT-02: Autopilot & On-board processor connection	1 day	Wed 23/07/14	Wed 23/07/14
36	8.4 CT-03: GPS accuracy within an urban area	0.5 days	Thu 24/07/14	Thu 24/07/14
37	8.5 CT-04: GPS with the Lisa/M v2.0 autopilot system	1 day	Fri 25/07/14	Fri 25/07/14
38	8.6 CT-05: GPS and IMU accuracy within an urban area	0.5 days	Thu 24/07/14	Thu 24/07/14
39	8.7 CT-06: Propeller thrust on different RPM settings	0.5 days	Sat 26/07/14	Sat 26/07/14
40	8.8 CT-07: Push-puller propeller configuration effects	1 day	Sat 26/07/14	Sat 26/07/14
41	8.9 CT-08: Battery capacity	0.5 days	Sun 27/07/14	Sun 27/07/14
42	8.10 CT-09: Battery voltage drop	0.5 days	Sun 27/07/14	Sun 27/07/14
43	8.11 CT-10: Gimbal integration	0.5 days	Sun 27/07/14	Sun 27/07/14
44	8.12 CT-11: Gimbal accuracy	0.5 days	Sun 27/07/14	Sun 27/07/14
45	8.13 CT-12: Structural load on landing legs	1 day	Mon 28/07/14	Mon 28/07/14
46	8.14 CT-13: Structural load on airframe	1 day	Mon 28/07/14	Mon 28/07/14
47	8.15 CT-14: Airframe eigenfrequency determination	0.5 days	Tue 29/07/14	Tue 29/07/14
48	8.16 CT-15: Autopilot & propulsion integration	1 day	Wed 30/07/14	Wed 30/07/14
49	**9 Final assembly**	**3 days**	**Thu 31/07/14**	**Sat 02/08/14**
50	9.1 Frame assembly	1 day	Thu 31/07/14	Thu 31/07/14
51	9.2 Payload assembly & integration	1 day	Fri 01/08/14	Fri 01/08/14
52	9.3 Engine assembly & integration	1 day	Sat 02/08/14	Sat 02/08/14
53	9.4 Landing gear assembly & integration	0.5 days	Sat 02/08/14	Sat 02/08/14
54	9.5 Wiring	3 days	Thu 31/07/14	Sat 02/08/14
55	**10 Full system integraiton test**	**7 days**	**Sun 03/08/14**	**Sun 10/08/14**
56	10.1 FT-01: Vibrational integrity of the UAV	1 day	Sun 03/08/14	Sun 03/08/14
57	10.2 FT-02: Propulsion performance test	1 day	Mon 04/08/14	Mon 04/08/14
58	10.3 FT-03: Command and communication test	1 day	Sun 03/08/14	Sun 03/08/14
59	10.4 FT-04: Autopilot tuning	2 days	Mon 04/08/14	Tue 05/08/14
60	10.5 FT-05: Manual control range , stability and integrity	1 day	Tue 05/08/14	Tue 05/08/14
61	10.6 FT-06: Flight envelope determination	1 day	Wed 06/08/14	Wed 06/08/14
62	10.7 FT-07: Mission element completion	2 days	Wed 06/08/14	Thu 07/08/14
63	10.8 FT-08: Full mission completion	2 days	Fri 08/08/14	Sun 10/08/14
64	**11 IMAV 2014 competition**	**3 days**	**Mon 11/08/14**	**Wed 13/08/14**
65	11.1 FT-09: Test flights at the competition area	1 day	Mon 11/08/14	Mon 11/08/14
66	11.2 Optimisation & final tests	1 day	Tue 12/08/14	Tue 12/08/14
67	11.3 Competition	1 day	Wed 13/08/14	Wed 13/08/14

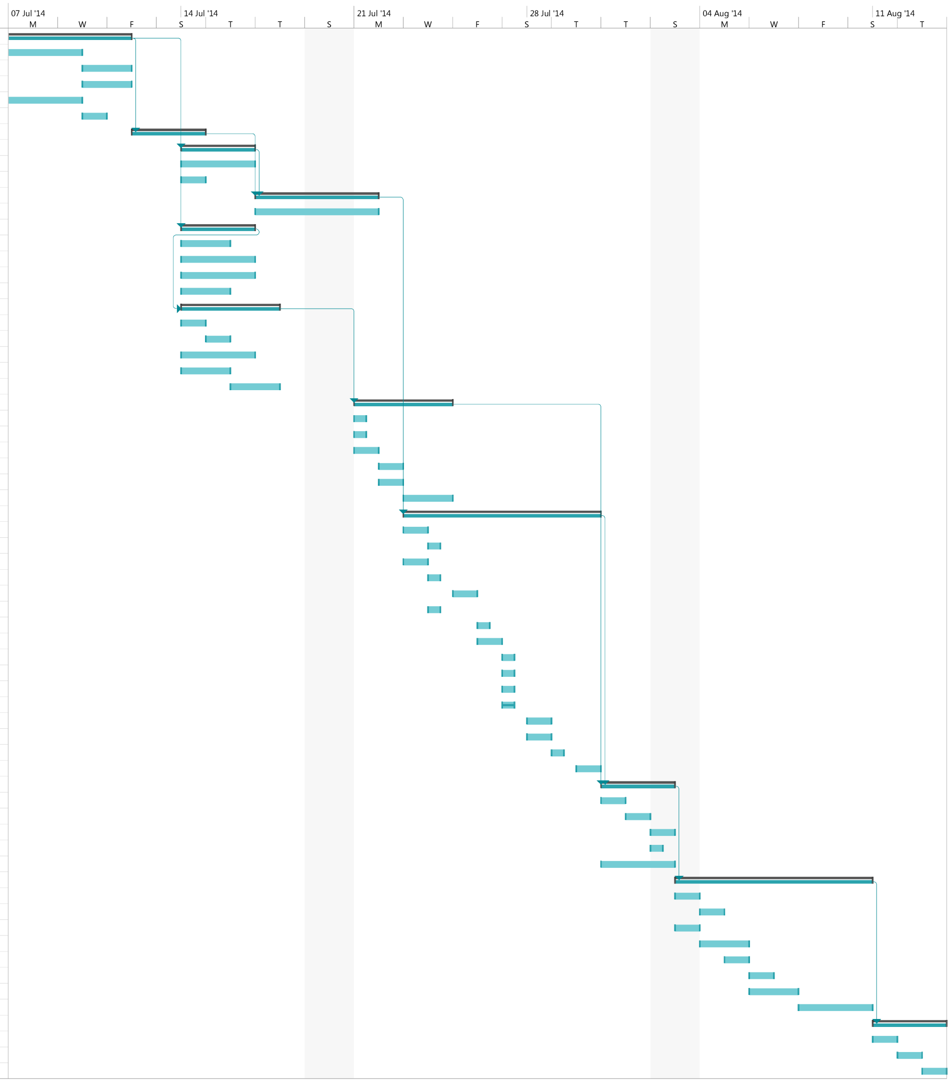

Figure 8.7: The Gantt Chart which will be used as a planning for the post-DSE activities

8.6. Post Design Synthesis Exercise design and Development Conclusion

This chapter presented a plan for the design and development after the conclusion of the DSE. This stage will involve simultaneous work on the production and ordering of components, assembly and testing. To streamline this process, a detailed production plan was made. Future verification and validation, along with other tests to ensure proper operation of the system, have also been included in the schedule.

The logistics of the competition were also analysed, to ensure no errors are made by the team during the competition. Part of this, is a detailed plan describing what the team must do during various stages of the mission.

Finally, a time planning of this phase was made to ensure all tasks are performed on time. With this, the team ensures optimal preparation for the IMAV 2014 competition and the fulfilment of the POS.

9

Conclusion & Recommendations

This project was initiated with the objective to design an autonomous multi-unmanned aerial vehicle (UAV) system that can be used to aid in search and rescue (SAR) missions after natural disasters, while keeping costs within a budget of €5000. The design, named Soteria, will be tested at the international micro aerial vehicle (IMAV) competition in August 2014. It is comprised of four UAVs and two laptops that act as ground station. To distinguish between UAVs, they are coloured red, magenta, cyan and yellow. At the competition, Soteria will perform a mission consisting of five elements. Starting with the take-off at the local command centre (LCC), the UAVs will create a photomap of the competition area. It will then return to the LCC to perform a precision landing, where the SD card containing the photos is retrieved. The ground station will then stitch these into one photomap, upon which it will detect and mark road blockades. Meanwhile, the UAVs will continue their mission, first performing a roof landing. Next, it will identify the numbers of all houses in a specified section of the competition area. Finally, they will again perform a precision landing at the LCC.

In order to perform the mission, the UAV design is split up in two parts: payload design and design of the airframe and propulsion. The airframe consists of three carbon beams in a Y-shape with a double-deck payload platform in the centre. Six propellers are mounted in counter-rotating pairs, with one pair on each beam. A small strut with a pressure sensor is mounted at the tip of each beam. Together, the three struts form the landing gear, and the pressure sensors allow the UAV to detect when it has landed. A double-deck payload platform is situated at the centre of the airframe. It is covered with a dome to protect it against weather influences and impacts. The payload will consist of one high resolution and one low resolution camera, a Raspberry Pi board computer, a transceiver module, and a navigation module composed of a global positioning system (GPS) receiver, autopilot board with built-in inertial measurement unit (IMU) and two ultrasonic rangefinders. The entire system will be powered by two battery packs.

The GPS, transceiver, board computer and autopilot are placed on the top deck. This is done to protect the sensitive circuits from the strong electric currents running from the battery pack to the other payload modules and the propulsion system. A rubber damper between the airframe and the top payload deck nullifies the vibrations induced by the propulsion.

The design process has been completed, so the project objective statement (POS) can now be evaluated:

With ten students in ten weeks, design a multi-UAV system with autonomous capabilities, which will prove itself to be useful in disaster scenarios in urban areas by winning the IMAV 2014 competition with a budget of €5000.

Since the IMAV competition has not yet taken place, the related top level requirements, *IMAV-CR* and *IMAV-SR*, cannot be met as of yet. However, the total system cost does not exceed €5000 (*IMAV-CO*) and the system is designed by ten students in ten weeks (*IMAV-TU*) to function autonomously (*IMAV-AU*, although this has not yet been physically demonstrated). The SAR applications (*IMAV-SAR*) of the payload are apparent. Soteria is will generate a high quality photomap of an area 277 m by 171 m and identify roadblocks on the map in less than 40 minutes. The only human interaction consists of activating the system, retrieving the SD card and camera upon return of each UAV and then starting the photomapping process on the ground station. Furthermore, the house number recognition can be used to determine which houses are destroyed and which aren't, if pre-disaster information is available for comparison. Lastly, a UAV can be told to land on any flat surface to monitor an area or building using the Raspberry Pi camera.

A production plan for the system and a logistics plan for the competition day have been made and the market analysis shows that Soteria offers a greatly reduced price in comparison with similar systems, and increased functionality in comparison with other systems in the same price category. However, it is recommended to perform additional verification and validation before the competition begins. The recommended tests can be divided into three categories: software compatibility, hardware compatibility and complete system tests.

Bibliography

[1] E. den Boer, J. T. Booms, H. J. A. Engwerda, A. P. Feenstra, C. R. Fonville, L. R. J. Hellenthal, R. H. Lenssen, R. C. van 't Veld, S. Verbist, and J. J. Vroom, "Multi-UAV Operations: Mid-term Report," Delft University of Technology, Delft, Tech. Rep., 2014.

[2] IMAV2014 [v1.3], "IMAV 2014 Micro Air Vehicle Competion rules," Dec. 2014.

[3] E. den Boer, J. T. Booms, H. J. A. Engwerda, A. P. Feenstra, C. R. Fonville, L. R. J. Hellenthal, R. H. Lenssen, R. C. van 't Veld, S. Verbist, and J. J. Vroom, "Multi-UAV Operations: Baseline Report," Delft University of Technology, Delft, Tech. Rep., 2014.

[4] IMAV2014 [v0.2], "IMAV 2014 Security and Safety Regulations," 2014.

[5] C. de Wagter, "AE3-200 Project Description," Apr. 2014.

[6] C. de Wagter, "Project Guide Design Synthesis Exercise IMAV 2014 - Multi - UAV Operations," Apr. 2014.

[7] J. Sutherland, "The Scrum Guide ™," p. 16, 2013.

[8] W. Verhagen and R. Curran, "AE3211-I Lecture 08 Risk & Reliability," 2014.

[9] Stanford University, "Risk and Weight Factors used in contingency assessment," 2010. [Online]. Available: http://www-glast.slac.stanford.edu/systemengineering/GAO/Contingencyfactors.pdf Accessed: 29/04/14

[10] OpenCv, "OpenCV." [Online]. Available: http://opencv.org/ Accessed: 22/05/14

[11] Parallax, "Parallax Ultrasonic Distance Sensor." [Online]. Available: http://www.parallax.com/product/28015 Accessed: 22/05/14

[12] DX.com, "EB-5631RE SiRF IV GPS Module." [Online]. Available: http://www.dx.com/p/eb-5631re-sirf-iv-gps-module-silver-white-green-189987 Accessed: 22/05/14

[13] Sparkfun, "9 Degrees of Freedom IMU Breakout - LSM9DS0." [Online]. Available: https://www.sparkfun.com/products/12636 Accessed: 12/05/2014

[14] Trust International B.V., "Trust - Digital Lifestyle Accessories - SpotLight Webcam." [Online]. Available: http://www.trust.com/nl-nl/all-products/16429-spotlight-webcam Accessed: 22/05/14

[15] Amazon.co.uk, "Edimax EW-7811UN 150Mbps Wireless Nano USB Adapter." [Online]. Available: http://www.amazon.co.uk/Edimax-EW-7811UN-150Mbps-Wireless-Adapter/dp/B003MTTJOY Accessed: 22/05/14

[16] Sony, "Sony CyberShot DSC-W810 specificaties." [Online]. Available: http://www.letsgodigital.org/images/artikelen/55/sony-cybershot-dsc-w810.pdf Accessed: 22/05/14

[17] Sony, "20.1 Mega Pixel W Series 6x Optical Zoom Cyber-shot (Black)," 2014. [Online]. Available: http://www.sony.co.in/product/dsc-w810 Accessed: 15/05/14

[18] Amped Wireless, "High Power 500mW Dual Band AC Wi-Fi USB Adapter." [Online]. Available: http://www.ampedwireless.com/products/aca1.html Accessed: 12/05/2014

[19] E. Gill, "AE3211-I Lecture 02 System Engineering Methods," 2014.

[20] S. Se, D. Lowe, and J. Little, "Mobile robot localization and mapping with uncertainty using scale-invariant visual landmarks," *The international Journal of robotics . . .*, vol. 21, no. 8, pp. 735–758, 2002.

[21] C. de Wagter, "Design synthesis excercise status meeting on outdoor to indoor flight transition," private communication, May 2014.

[22] Microsoft Research, "Image Composite Editor," 2008. [Online]. Available: http://research.microsoft.com/en-us/um/redmond/groups/ivm/ICE/ Accessed: 12/05/14

[23] T. L. Saaty, "Decision making with the analytic hierarchy process," *Int. J. Services Sciences*, vol. 1, no. 1, pp. 83–98, 2008.

[24] K. D. Goepel, "AHP Excel template with multiple inputs | BPMSG," 2014. [Online]. Available: http://bpmsg.com/new-ahp-excel-template-with-multiple-inputs/ Accessed: 22/05/14

[25] Google Inc., “Google Earth,” 2005

[26] Conrad, “Raspberry Pi model A 256 MB,” 2014. [Online]. Available: http://www.conrad.nl/ce/nl/product/399650/Raspberry-Pi-model-A-256-MB?ref=list Accessed: 08/05/14

[27] Conrad, “Raspberry Pi model B 512 MB,” 2014. [Online]. Available: http://www.conrad.nl/ce/nl/product/874675/Raspberry-Pi-model-B-512-MB?ref=list Accessed: 08/05/14

[28] Conrad, “Cubieboard A10 A8 1 GB,” 2014. [Online]. Available: http://www.conrad.nl/ce/nl/product/674155/Cubieboard-A10-A8-1-GB?ref=list Accessed: 08/05/14

[29] Conrad, “Cubieboard A20 A7 1 GB,” 2014. [Online]. Available: http://www.conrad.nl/ce/nl/product/674156/Cubieboard-A20-A7-1-GB?ref=list Accessed: 08/05/14

[30] Adafruit, “BeagleBone Black Rev C - 4GB Flash - Pre-installed Debian.” [Online]. Available: http://www.adafruit.com/products/1876 Accessed: 08/05/14

[31] Sparkfun, “Arduino Uno- R3 SMD,” 2014. [Online]. Available: https://www.sparkfun.com/products/11224 Accessed: 08/05/14

[32] Conrad, “Arduino Mega 2560 A000067 ATmega2560,” 2014. [Online]. Available: http://www.conrad.nl/ce/nl/product/191790/Arduino-Mega-2560-A000067-ATmega2560?ref=list Accessed: 08/05/14

[33] Sparkfun, “Arduino Pro Mini 328 - 3.3V/8MHz,” 2014. [Online]. Available: https://www.sparkfun.com/products/11114 Accessed: 08/05/14

[34] S. I. Siddiqui, “Raspberry Pi VS Arduino VS BeagleBoard VS PandaBoard VS Other Mini Computers,” 2014. [Online]. Available: http://realhackerspoint.blogspot.nl/2013/04/raspberry-pi-vs-arduino-vs-beagleboard.html Accessed: 20/06/14

[35] JENOPTIK, “IR-TCM HD 1024 Thermographic Infrared Cameras,” 2014.

[36] IMAV2014, “IMAV 2014 Schedule,” 2014. [Online]. Available: http://imavs.org/2014/schedule.html Accessed: 09/06/2014

[37] Dronespecialist, “KX-171 FPV camera 420TVL,” 2014. [Online]. Available: http://dronespecialist.nl/kx-171-fpv-cam-420tvl Accessed: 08/05/14

[38] Raspberry Pi Foundation, “FAQs | Raspberry Pi.” [Online]. Available: http://www.raspberrypi.org/help/faqs/ Accessed: 22/05/14

[39] Axis Communications, “Identification and Recognition: Required Resolution,” 2014. [Online]. Available: http://www.axis.com/academy/identification/resolution.htm Accessed: 30/06/2014

[40] Maxbotix, “High Performance Sonar Range Finder MaxBotix MaxBotix,” 2012. [Online]. Available: http://www.maxbotix.com/documents/MB1000_Datasheet.pdf Accessed: 08/05/14

[41] T. Lv-maxsonar, “LV-MaxSonar-EZ1 High Performance Sonar Range Finder,” 2012. [Online]. Available: http://www.maxbotix.com/documents/MB1010_Datasheet.pdf Accessed: 08/05/14

[42] Micropik, “Ultrasonic Ranging Module HC - SR04,” 2012. [Online]. Available: http://www.micropik.com/PDF/HCSR04.pdf Accessed: 08/05/14

[43] H. Performance and S. Range, “XL-MaxSonar - EZ ™ Series,” 2012.

[44] Raspberry Pi Foundation, “Camera Module Usage,” 2014. [Online]. Available: http://www.raspberrypi.org/documentation/usage/camera/README.md Accessed: 20/06/14

[45] D. Jones, “Python PiCamera Setup,” 2014. [Online]. Available: http://www.raspberrypi.org/learning/python-picamera-setup/ Accessed: 20/06/14

[46] Raspberry Pi Spy, “Ultrasonic Distance Measurement Using Python,” 2013. [Online]. Available: http://www.raspberrypi-spy.co.uk/2013/01/ultrasonic-distance-measurement-using-python-part-2/ Accessed: 10/06/14

[47] A. Greiner, F. Petrot, and M. Carrier, “Mapping an obstacles detection, stereo vision-based, software application on a multi-processor system-on-chip,” *Intelligent Vehicles Symposium*, p. 7, 2006

[48] T. G. McGee, R. Sengupta, and K. Hedrick, “Obstacle Detection for Small Autonomous Aircraft,” pp. 4679–4684, 2005.

[49] J.-i. Meguro, T. Murata, J.-i. Takiguchi, Y. Amano, and T. Hashizume, "GPS Multipath Mitigation for Urban Area Using Omnidirectional Infrared Camera," *IEEE Transactions on Intelligent Transportation Systems*, vol. 10, no. 1, pp. 22–30, Mar. 2009

[50] Paparazzi, "Paparazzi - System Overview." [Online]. Available: https://wiki.paparazziuav.org/wiki/Overview#Sensors Accessed: 22/06/14

[51] OpenPilot, "OpenPilot." [Online]. Available: http://wiki.openpilot.org/display/Doc/OpenPilot+Overview Accessed: 30/06/14

[52] ArduPilot, "APM Open source autopilot." [Online]. Available: http://ardupilot.com/ Accessed: 30/06/14

[53] Paparazzi, "Paparazzi - Flight Plans." [Online]. Available: http://wiki.paparazziuav.org/wiki/Flight_Plans Accessed: 30/06/14

[54] P. Brisset, M. Bronz, M. Gorraz, and J. Tyler, "Yet Another Paparazzi," 2008

[55] ArduPilot, "ArduPilot Mission Planner." [Online]. Available: http://planner.ardupilot.com/ Accessed: 30/06/14

[56] World Wide Web Consortium, "Extensible Markup Language (XML)." [Online]. Available: http://www.w3.org/XML/ Accessed: 21/06/14

[57] Paparazzi, "Paparazzi Autopilots." [Online]. Available: http://wiki.paparazziuav.org/wiki/Autopilots Accessed: 05/06/2014

[58] Paparazzi, "Paparazzi Autopilot Boards." [Online]. Available: http://wiki.paparazziuav.org/wiki/Category:Autopilots Accessed: 10/06/14

[59] Transition Robotics, "Transition Robotics Lisa/M v2.0." [Online]. Available: http://transition-robotics.com/products/lisa-m-v20-with-10-dom-aspirin-22 Accessed: 21/06/14

[60] 1 BIT SQUARED, "1 BIT SQUARED Lisa/S." [Online]. Available: http://1bitsquared.com/products/lisa-s Accessed: 21/06/14

[61] Paparazzi, "Paparazzi - Subsystem/Telemetry," 2012. [Online]. Available: http://wiki.paparazziuav.org/wiki/Subsystem/telemetry Accessed: 06/06/2014

[62] Hobbyking.com, "Turnigy 9XR - HobbyKing." [Online]. Available: http://hobbyking.com/hobbyking/store/__31544__turnigy_9xr_transmitter_mode_2_no_module_.html Accessed: 24/06/14

[63] Turnigy, "Turnigy 9XR Transmitter." [Online]. Available: http://turnigy9xr.com/ Accessed: 24/06/14

[64] Spektrum, "DX7s 7-Ch DSMX Radio System." [Online]. Available: https://www.spektrumrc.com/Products/Default.aspx?ProdId=SPM7800 Accessed: 24/06/14

[65] HobbyKing.com, "OrangeRX DSMX/DSM2 2.4Ghz Transmitter Module." [Online]. Available: http://www.hobbyking.com/hobbyking/store/__24656__orangerx_dsmx_dsm2_2_4ghz_transmitter_module_jr_turnigy_compatible_.html Accessed: 24/06/14

[66] Spektrum, "AR8000 8-Channel DSMX Receiver." [Online]. Available: https://www.spektrumrc.com/Products/Default.aspx?ProdID=SPMAR8000 Accessed: 24/06/14

[67] Spektrum, "DSMX Remote Receiver SPM9645." [Online]. Available: https://www.spektrumrc.com/Products/Default.aspx?ProdID=SPM9645 Accessed: 24/06/14

[68] Paparazzi, "Paparazzi - RC Receivers and Radios." [Online]. Available: https://wiki.paparazziuav.org/wiki/RC_Receivers_and_Radios Accessed: 22/06/14

[69] TU Delft, "AR Drone 2/getting started - PaparazziUAV," 2013. [Online]. Available: https://wiki.paparazziuav.org/wiki/AR_Drone_2/getting_started#TU_Delft_-_Autonomous_Quadrotor Accessed: 29/04/14

[70] Arduino, "What Is Degrees Of Freedom." [Online]. Available: http://playground.arduino.cc/Main/WhatIsDegreesOfFreedom6DOF9DOF10DOF11DOF Accessed: 23/06/14

[71] National Research Council's Committee on the Future of the Global Positioning System, "The Global Positioning System: A Shared National Asset," p. 284, 1995. [Online]. Available: http://www.nap.edu/openbook.php?record_id=4920&page=177 Accessed: 24/06/14

[72] U-blox, "LEA-6 Product Summary." [Online]. Available: http://www.u-blox.com/images/downloads/Product_Docs/LEA-6_ProductSummary_(GPS.G6-HW-09002).pdf Accessed: 23/06/14

[73] U-blox, "NEO-6 Data Sheet." [Online]. Available: https://www.u-blox.com/images/downloads/Product_Docs/NEO-6_DataSheet_(GPS.G6-HW-09005).pdf Accessed: 23/06/14

[74] CSG-shop, "U-blox NEO-M8N GPS/QZSS GLONASS BeiDou receiver with Antenna." [Online]. Available: http://www.csgshop.com/product.php?id_product=174 Accessed: 23/06/14

[75] Proto-pic.co.uk, "SparkFun COM-09190 Momentary Push Button Switch." [Online]. Available: http://proto-pic.co.uk/momentary-push-button-switch-12mm-square/ Accessed: 24/06/14

[76] Paparazzi, "Paparazzi - Sensors/GPS." [Online]. Available: http://wiki.paparazziuav.org/wiki/GPS Accessed: 23/06/14

[77] A. Elgammal, "CS 534: Computer Vision 3D Model-based recognition," 2014. [Online]. Available: http://www.cs.rutgers.edu/~elgammal/classes/cs534/lectures/3D_modelbasedvision.pdf Accessed: 26/05/14

[78] H. O. R. U. C. Receptive, "Object Recognition." [Online]. Available: ftp://ftp1.nada.kth.se/pub/documents/CVAP/reports/LinLin04-ICPR.pdf Accessed: 26/05/14

[79] MatlabTricks, "Understanding the Hough transform," 2014. [Online]. Available: http://matlabtricks.com/post-39/understanding-the-hough-transform Accessed: 20/06/14

[80] Google Project Hosting, "pytesser - OCR in Python using the Tesseract engine from Google." [Online]. Available: https://code.google.com/p/pytesser/ Accessed: 30/06/14

[81] Arindam Bose, "How to Detect and Track White Objects in Live Video in MATLAB | Arindam's Blog," 2013. [Online]. Available: http://arindambose.com/blog/?p=86 Accessed: 20/06/14

[82] A. L. Olly Andrade, Ed Jones and D. Bates., "Blob Detection - Physical Computing with Raspberry Pi." [Online]. Available: https://www.cl.cam.ac.uk/projects/raspberrypi/tutorials/robot/blob_detection/ Accessed: 30/06/14

[83] Teorex, "PhotoStitcher photo stitching software - Automatically create panoramic images," 2014. [Online]. Available: http://www.photostitcher.com/ Accessed: 23/05/14

[84] MonumentalTrees.com, "De hoogste bomen in Nederland," 2014. [Online]. Available: http://www.monumentaltrees.com/nl/hoogterecords/nld/ Accessed: 21/06/14

[85] Sandisk, "Number of pictures that can be stored on a memory device." [Online]. Available: http://kb.sandisk.com/app/answers/detail/a_id/69/~/number-of-pictures-that-can-be-stored-on-a-memory-device Accessed: 06/06/14

[86] I. Bluetooth SIG, "Bluetooth basics," 2014. [Online]. Available: http://www.bluetooth.com/Pages/Basics.aspx Accessed: 02-06-2014

[87] B. Mitchell, "No Title." [Online]. Available: http://compnetworking.about.com/od/homenetworking/g/bldef_infrared.htm Accessed: 02-03-2014

[88] M. connection, "Figuring out wireless transmission distance," 2008. [Online]. Available: http://www.moxa.com/newsletter/connection/2008/03/Figure_out_transmission_distance_from_wireless_device_specs.htm Accessed: 28-05-2014

[89] BENCOM, "Comparison mobile internet on the smartphone," 2014. [Online]. Available: http://www.bellen.com/mobiel/vergelijking-mobiel-internet-op-smartphone Accessed: 27/05/2014

[90] I. VIA Technologies, "Overview of USB." [Online]. Available: http://www.via.com.tw/en/products/peripherals/usb/overview.jsp Accessed: 05/06/2014

[91] K. B.V., "Computerland Kingston." [Online]. Available: http://www.computerland.nl/zkb-01opsl/20022770/kingston-sdhc-4gb-class-4/details.aspx?channel_code=17&product_code=40715855&utm_source=kieskeurig Accessed: 06-06-2014

[92] 4Gdekking.nl, "Coverage 4G," p. 1, 2014. [Online]. Available: http://www.4gdekking.nl/http://www.coveragechecker.nl/https://www.vodafone.nl/support/netwerk-en-dekking/dekkingskaart.shtmlhttp://www.t-mobile.nl/service-en-contact/bereik/dekkingskaarthttp://newsroom.tele2.nl/2012/05/tele2-start-4g-dienst-voor-consumenten/ Accessed: 22-05-2014

[93] Mouser Electronics, “XBee Transceiver,” 2014. [Online]. Available: http://au.mouser.com/Search/ProductDetail.aspx?qs=YPg7lQ8MWScuRYrdMeLImQ== Accessed: 22-05-2014

[94] M. Electronics, “XBee Pro1 UAV,” 2014. [Online]. Available: http://au.mouser.com/Search/ProductDetail.aspx?qs=YPg7lQ8MWSfV8kj5fH/Z+w== Accessed: 22-05-2014

[95] Agentschap Telecom, “National Frequency Register,” 2014. [Online]. Available: http://appl.at-ez.nl/nfr/main_nfr_uk.html Accessed: 01/07/2014

[96] DJI, “Zenmuse H3-3D - Specs,” 2014. [Online]. Available: http://www.dji.com/product/zenmuse-h3-3d/spec Accessed: 22/06/14

[97] Hobbyking.com, “DYS Smart3 3 Axis GoPro Gimbal with AlexMos Control Board (BaseCam),” 2014. [Online]. Available: http://www.hobbyking.com/hobbyking/store/__52136__dys_smart3_3_axis_gopro_gimbal_with_alexmos_control_board_basecam_.html Accessed: 22/06/14

[98] FlyCamHk.com, “LIBRAN 3-Axis Handheld E-Stabilizier for GoPro Hero 2/3+.” [Online]. Available: http://www.flycamhk.com/libran-3-axis-handheld-e-stabilizier-for-gopro-hero-2-3.html?___store=default&___from_store=chinese Accessed: 22/06/14

[99] XAircraftAmerica.com, “Stella 2-Axis Brushless Gimbal,” 2014. [Online]. Available: http://xaircraftamerica.com/products/stella-2-axis-brushless-gimbal Accessed: 22/06/14

[100] FPV Monkey, “Mobius Gimbal,” 2014. [Online]. Available: http://www.fpvmonkey.com/mobius-gimbal/ Accessed: 22/06/14

[101] Hobbyking.com, “2-Axis Brushless Camera Gimbal Stabilization Control Board w/IMU,” 2014. [Online]. Available: http://www.hobbyking.com/hobbyking/store/uh_viewitem.asp?idproduct=41386&aff=226716 Accessed: 22/06/14

[102] HobbyKings.com, “2206-140Kv Brushless Gimbal Motor,” 2014. [Online]. Available: http://www.hobbyking.com/hobbyking/store/uh_viewitem.asp?idproduct=43037&aff=226716 Accessed: 22/06/14

[103] Linux, “Linux.com | .Net Framework on Linux?” [Online]. Available: http://www.linux.com/learn/answers/view/910-i-have-just-switched-from-win7-to-zorin-ubuntu-i-have-been-working-with-an-ai-program-called-verbot-for-awhile-and-my- Accessed: 23/06/14

[104] R. Knoops, S. Hulsman, M. Milis, J. de Groot, J. Bouman, and D. Dokter, “ATMOS UAV B.V.” 2014. [Online]. Available: http://www.atmosuav.com/ Accessed: 23/06/14

[105] J. W. R. Taylor, *Jane’s All the World’s Aircraft 1965-66.* London: Sampson Low, Marston & Co, 1966.

[106] T. Mast, “Rotormast LLC V-22 Acrobatic Version,” 2014. [Online]. Available: http://www.rotormast.com/en/index.php/home Accessed: 03/06/14

[107] senseFly Ltd, “eBee Brochure,” Cheseaux-Lausanne, 2014.

[108] Lockheed Martin, “Desert Hawk III - Putting Capability in the Hands of the Warfighter,” 2014. [Online]. Available: http://www.lockheedmartin.com/content/dam/lockheed/data/ms2/documents/Desert_Hawk_III_brochure.pdf Accessed: 04/06/14

[109] Andreas, “The Silent Runner,” 2014. [Online]. Available: http://www.silent-runner.net/index.php/Main_Page Accessed: 05/06/14

[110] P. Nilaratna, “Ollie – a DIY autonomous robotic blimp,” 2014. [Online]. Available: http://meandollie.com/ Accessed: 05/06/14

[111] Rotomotion LLC, “SR5 Helicopter UAV Specifications,” 2014

[112] AUAVT Ltd, “AT-10 Ultra lightweight, short endurance VTOL UAV,” 2014. [Online]. Available: http://www.auavt.com/portfolio-item/111/ Accessed: 05/06/14

[113] Aibotix GmbH, “The new Aibot X6 V2,” 2014. [Online]. Available: http://www.aibotix.com/aibot-x6.html Accessed: 05/06/14

[114] DJI, “Phantom 2 - The Spirit Of Flight,” 2014. [Online]. Available: http://www.dji.com/product/phantom-2 Accessed: 05/06/14

[115] S. Odedra, “HALO Unmanned Aerial Vehicle (UAV) for the MoD,” 2012. [Online]. Available: http://www.sidodedra.com/halo-uav/ Accessed: 05/06/14

[116] MavLab, “DelFly,” 2014. [Online]. Available: http://www.delfly.nl/home.html Accessed: 23/6/2014

[117] WowWee Group Limited, “Flytech Dragonfly,” 2014. [Online]. Available: http://www.wowwee.com/en/products/toys/flight/flytech/dragonfly Accessed: 23/06/14

[118] N. Chronister, “Skybird RC Ornithopter,” 2014. [Online]. Available: http://www.glue-it.com/aircraft/gallery/ornithopter.html Accessed: 23/06/14

[119] M. Tayyab, “Design of a Blimp Based Unmanned Aerial Vehicle for Surveillance,” vol. 5, no. 1, pp. 519–530, 2013.

[120] Hobbyking.com, “Helicopters & Parts>Ready to Fly (RTF).” [Online]. Available: http://www.hobbyking.com/hobbyking/store/__986__196__Helicopters_Parts-Ready_to_Fly_RTF_.html Accessed: 23/06/14

[121] UnmannedMulticopter.nl, “Unmanned Multicopter: Building a Quadcopter.” [Online]. Available: http://unmannedmulticopter.blogspot.nl/2013/10/building-quadcopter.html Accessed: 23/06/14

[122] SPAWAR Systems Center Atlantic, “UAVForge Fly-off Competition,” 2012. [Online]. Available: http://www.uavforge.net/ Accessed: 03/06/14

[123] S. Hulsman, J. de Groot, and D. Dokter, “ATMOS UAV: High-tech startup with game-changing ideas,” pp. 8–11, 2014. [Online]. Available: http://issuu.com/vsv_leonardo_da_vinci/docs/lt_march_2014_website__2_/9?e=1505175/7420675 Accessed: 03/06/14

[124] S. Yanguo and W. Huanjin, “Design of Flight Control System for a Small Unmanned Tilt Rotor Aircraft,” *Chinese Journal of Aeronautics*, vol. 22, no. 3, pp. 250–256, Jun. 2009

[125] CTRM, “The ALUDRA SR-08,” 2014. [Online]. Available: http://www.ctrm.com.my/ps_alu_sr.php Accessed: 04/06/14

[126] Unmanned.co.uk, “Multirole M-011 Unmanned Aerial Vehicle (UAV) Specifications and Data Sheet,” 2012. [Online]. Available: http://www.unmanned.co.uk/autonomous-unmanned-vehicles/uav-data-specifications-fact-sheets/multirole-m-011-unmanned-aerial-vehicle-uav-specifications-and-data-sheet/ Accessed: 04/06/14

[127] Unmanned Vehicle Systems Association, “UAV Catalog,” 2014. [Online]. Available: http://en.ruvsa.com/catalog/category/uav/ Accessed: 05/06/14

[128] K. Masuko, I. Takahashi, S. Ogawa, M.-H. Wu, A. Oosedo, T. Matsumoto, K. Go, F. Sugai, A. Konno, and M. Uchiyama, “Autonomous takeoff and landing of an unmanned aerial vehicle,” *2010 IEEE/SICE International Symposium on System Integration*, pp. 248–253, Dec. 2010

[129] H. Saiki, T. Fukao, T. Urakubo, and T. Kohno, “A path following control method under wind disturbances for outdoor blimp robots,” *2011 IEEE/SICE International Symposium on System Integration (SII)*, pp. 978–984, Dec. 2011

[130] P. González, W. Burgard, R. Sanz, and J. L. Fernández, “Developing a Low-Cost Autonomous Indoor Blimp,” vol. 3, no. 1, pp. 43–52, 2009.

[131] HELIPSE, “HE 190 Electric version,” 2014. [Online]. Available: http://helipse.com/welcome-to-helipse/uav-world/he-190-ve/ Accessed: 05/06/14

[132] J. G. Leishman, *Principles of Helicopter Aerodynamics*. Cambridge University Press, 2006

[133] Microdrones GmbH, “Microdrones UAV,” 2014. [Online]. Available: http://www.microdrones.com/index.php Accessed: 05/06/14

[134] T. Carancho, “AeroQuad - The Open Source Multicopter,” 2014. [Online]. Available: http://aeroquad.com/content.php Accessed: 05/06/14

[135] MAVLab, “TU Delft: Micro Air Vehicle Laboratory,” 2014. [Online]. Available: http://mavlab.lr.tudelft.nl/ Accessed: 23/06/14

[136] J.-h. Lee, B.-m. Min, and E.-t. Kim, “Autopilot design of tilt-rotor UAV using particle swarm optimization method,” *2007 International Conference on Control, Automation and Systems*, pp. 1629–1633, 2007

[137] R. Beard, D. Kingston, M. Quigley, D. Snyder, R. Christiansen, W. Johnson, T. Mclain, and M. A. Goodrich, "Autonomous Vehicle Technologies for Small Fixed-Wing UAVs," *Journal of Aerospace Computing, Infromation, and Communication*, vol. 2, no. January, pp. 92–108, 2005.

[138] C. Anderson, "BlimpDuino home page," 2008. [Online]. Available: http://diydrones.com/profiles/blogs/blimpduino-home-page Accessed: 03/06/14

[139] R. Nieuwland, "Flybarless." [Online]. Available: http://www.rc-heli-zwartewaal.nl/flybarless.html Accessed: 10/06/14

[140] J. Salt, "Understanding Flybarless RC Helicopters." [Online]. Available: http://www.rchelicopterfun.com/flybarless.html Accessed: 10/06/14

[141] R. Baránek and F. Šolc, "Modelling and Control of a Hexa-copter," vol. 0, no. 2, pp. 19–23, 2012.

[142] C. a. Arellano-Muro, L. F. Luque-Vega, B. Castillo-Toledo, and A. G. Loukianov, "Backstepping control with sliding mode estimation for a hexacopter," *2013 10th International Conference on Electrical Engineering, Computing Science and Automatic Control (CCE)*, pp. 31–36, Sep. 2013

[143] Hobbyking.com, "Radio Control Planes, Helicopters, Cars, Boats, FPV and Quadcopters - Hobbyking." [Online]. Available: http://www.hobbyking.com/hobbyking/store/__19534__HobbyKing_Multi_Rotor_Control_Board_V2_1_Atmega168PA_.html Accessed: 10/06/14

[144] N. B. Knoebel, S. R. Osborne, D. O. Snyder, T. W. Mclain, R. W. Beard, and A. M. Eldredge, "Preliminary Modeling , Control , and Trajectory Design for Miniature Autonomous Tailsitters," no. August, pp. 1–12, 2006.

[145] R. Leishman, J. Macdonald, S. Quebe, J. Ferrin, R. Beard, and T. McLain, "Utilizing an improved rotorcraft dynamic model in state estimation," *2011 IEEE/RSJ International Conference on Intelligent Robots and Systems*, pp. 5173–5178, Sep. 2011

[146] A. Stepek and I. L. Wijnant, "Interpolating wind speed normals from the sparse Dutch network to a high resolution grid using local roughness from land use maps," 2011.

[147] H. B. Jiang, Y. R. Li, and Z. Q. Cheng, "Relations of Lift and Drag Coefficients of Flow around Flat Plate," *Applied Mechanics and Materials*, vol. 518, pp. 161–164, Feb. 2014

[148] G. Hoffmann, H. Huang, S. Waslander, and C. Tomlin, "Quadrotor Helicopter Flight Dynamics and Control: Theory and Experiment," *AIAA Guidance, Navigation and Control Conference and Exhibit*, pp. 1–20, Aug. 2007

[149] C. Powers, D. Mellinger, A. Kushleyev, and B. Kothmann, "Influence of Aerodynamics and Proximity Effects in Quadrotor Flight," *International Symposium on Experimental Robotics*, pp. 1–14, 2012.

[150] Hobbyking.com, "HobbyKing Forums - A guide for multi-rotor newbies - Page 1." [Online]. Available: http://www.hobbyking.com/hobbyking/forum/forum_posts.asp?TID=38561&PID=220353#220353 Accessed: 22/05/14

[151] J. B. Brandt and M. S. Selig, "Propeller Performance Data at Low Reynolds Numbers," *49th AIAA Aerospace Sciences Meeting*, vol. AIAA paper, no. January, pp. 1–18, 2011.

[152] G. Ananda, "UIUC Propeller Data Site." [Online]. Available: http://aerospace.illinois.edu/m-selig/props/propDB.html Accessed: 16/06/14

[153] Landing Products, "APC Propellers 11x4.7SF," 2009. [Online]. Available: http://www.apcprop.com/ProductDetails.asp?ProductCode=LP11047SF Accessed: 20/06/14

[154] M. Mueller, "eCalc - Multicopter Calculator," 2014. [Online]. Available: http://www.ecalc.ch/xcoptercalc.php?ecalc&lang=en Accessed: 17/06/14

[155] dr. Kiwi, "RC BRUSHLESS MOTOR PERFORMANCE TEST DATA," 2014. [Online]. Available: http://www.geocities.ws/dr.kiwitn/ Accessed: 17/06/14

[156] Hobbyking.com, "Gear Box 3mm - 22T - 64T," 2014. [Online]. Available: http://hobbyking.com/hobbyking/store/__15244__Gear_Box_3mm_22T_64T.html Accessed: 24/06/14

[157] Hobbyking.com, "Gear Box 3mm - 10T - 40T," 2014. [Online]. Available: http://hobbyking.com/hobbyking/store/__15245__Gear_Box_3mm_10T_40T.html Accessed: 24/06/14

[158] D. Walton, A. B. Cropper, D. J. Weale, and P. K. Meuleman, “The efficiency and friction of plastic cylindrical gears Part 1: Influence of materials,” *Proceedings of the Institution of Mechanical Engineers, Part J: Journal of Engineering Tribology*, vol. 216, no. 2, pp. 75–78, Jan. 2002

[159] RC Groups, “Gearbox efficiency,” 2003. [Online]. Available: http://www.rcgroups.com/forums/showthread.php?t=170387 Accessed: 24/06/14

[160] Society of Robots, “How to Build a Robot Tutorials,” 2014. [Online]. Available: http://www.societyofrobots.com/mechanics_gears.shtml#gearefficiency Accessed: 24/06/14

[161] Stock Drive Products/Sterling Instrument, “Plastic Spur Gears Catalog,” 2014. [Online]. Available: https://sdp-si.com/eStore/Catalog/Group/338# Accessed: 24/06/14

[162] T-motor, “MN1806 - Navigator Series Motors,” 2013. [Online]. Available: http://www.rctigermotor.com/html/2013/Navigator_0910/34.html Accessed: 20/06/14

[163] Cobra Motors, “Cobra C-2204/32 Brushless Motor,” 2014. [Online]. Available: http://www.cobramotorsusa.com/2204-32.html Accessed: 23/06/14

[164] T-Motor, “MN2206 - Navigator Series Motors,” 2013. [Online]. Available: http://www.rctigermotor.com/html/2014/Navigator_0309/197.html Accessed: 23/06/14

[165] RC Models Wiz, “Electronic Speed Control (ESC) | Information & Guide to Electronic Speed Controllers System.” [Online]. Available: http://www.rcmodelswiz.co.uk/electronic-speed-controllers-esc/ Accessed: 20/06/14

[166] Paparazzi, “Paparazzi Lisa/M v2.0.” [Online]. Available: http://wiki.paparazziuav.org/wiki/Lisa/M_v2.0 Accessed: 05/06/2014

[167] Hobbyking.com, “Radio Control Planes, Helicopters, Cars, Boats, FPV and Quadcopters - Hobbyking.” [Online]. Available: http://www.hobbyking.com/hobbyking/store/__42551__Afro_Slim_20Amp_Multi_rotor_Motor_Speed_Controller_SimonK_Firmware_.html Accessed: 20/06/14

[168] Wholesale Solar, “Solar Panels.” [Online]. Available: http://www.wholesalesolar.com/solar-panels.html Accessed: 13/06/14

[169] P. Horowitz and W. Hill, “The Art Of Electronics.”

[170] Panasonic, “Panasonic Li-Ion Batteries - Technical Handbook,” Tech. Rep., 2007

[171] Nitroplanes, “Batteries at Nitroplanes.” [Online]. Available: http://www.nitroplanes.com/batteries.html Accessed: 20/05/14

[172] MaxAmps.com, “MaxAmps Battery Packs.” [Online]. Available: http://www.maxamps.com/categories.php?cat=358 Accessed: 11/06/2014

[173] BuddyRC, “iCharger 206B 300W 20A 6S Balance Charger.” [Online]. Available: http://www.buddyrc.com/icharger-206b.html Accessed: 19/06/14

[174] J. Salt, “Understanding RC Battery Chargers.” [Online]. Available: http://www.rchelicopterfun.com/rc-battery-chargers.html Accessed: 16/06/14

[175] C. P. Coleman, “A Survey of Theoretical and Experimental Coaxial Rotor Aerodynamic Research A Survey of Theoretical and Experimental Coaxial Rotor Aerodynamic Research,” *NASA Technical Paper 3675*, no. March, 1997.

[176] Cambridge University Engineering Department, *Materials Data*, 2003.

[177] K. Uusitalo, “Designing in Carbon Fibre Composites,” 2013.

[178] University of Cambridge, “Physical computing with Raspberry Pi - Buttons and Switches,” 2013. [Online]. Available: https://www.cl.cam.ac.uk/projects/raspberrypi/tutorials/robot/buttons_and_switches/ Accessed: 13/06/14

[179] Raspberry Pi Foundation, “Raspberry Pi • View topic - FTDI USB Serial Hangs,” 2012. [Online]. Available: http://www.raspberrypi.org/forums/viewtopic.php?t=8010 Accessed: 30/06/14

[180] Microdrones GmbH, “md4 - 1000 Flyer,” Siegen.

[181] Parrot SA, “AR.Drone 2.0. Parrot new wi-fi quadricopter- Specifications,” 2012. [Online]. Available: http://ardrone2.parrot.com/ardrone-2/specifications/ Accessed: 29/04/14

[182] I.materialise, "No Title," 2014. [Online]. Available: http://i.materialise.com/materials/rubber-like/technical-specifications Accessed: 16-06-2014

[183] Araldite, "No Title," 2014. [Online]. Available: http://www.go-araldite.com/ Accessed: 18-06-2014

[184] V. Bistrovs and A. Kluga, "Combined Information Processing from GPS and IMU using Kalman Filtering Algorithm," vol. 5, no. 5, 2009.

[185] U.S. Environmental Protection Agency, "eCycling." [Online]. Available: http://www.epa.gov/epawaste/conserve/materials/ecycling/index.htm Accessed: 01/07/14

[186] U.S. Environmental Protection Agency, "Plastics Recycling

[187] DSM, "DSM demonstrates significant carbon footprint reduction in composite recycling through cement co-processing," 2013. [Online]. Available: http://www.dsm.com/corporate/media/informationcenter-news/2013/02/2013-02-19-dsm-demonstrates-significant-carbon-footprint-reduction-in-composite-recycling-through-cement-co-processing.html Accessed: 18/06/2014

[188] Bloomberg L.P., "Euro to USD Exchange rate." [Online]. Available: http://www.bloomberg.com/quote/EURUSD:CUR Accessed: 01/07/2014

[189] Microdrones GmbH, "md4 - 200 Flyer," Siegen.

[190] SteadiDrone, "2014 SteadiDrone QU4D," 2014. [Online]. Available: http://www.steadidrone.com/index.php/drones/2014-steadidrone-qu4d.html Accessed: 01/07-2014

[191] Aeroyon Labs Inc., "Aeryon Scout™," 2014. [Online]. Available: http://www.aeryon.com/products/avs/aeryon-scout.html Accessed: 01/07/2014

[192] Australian National Search and Rescue Council, "National Land Search Operations Manual," 2014.

[193] DHS and FEMA, "National Urban Search & Rescue (US & R) Response System RESCUE FIELD OPERATIONS GUIDE," 2006.

[194] SWARM, "SAR Drones | UAV Search And Rescue Drones." [Online]. Available: http://sardrones.org/ Accessed: 29/04/14

[195] Google Inc., "Google Maps," 2005. [Online]. Available: maps.google.com Accessed: 26/05/2014

A

Technical Drawings

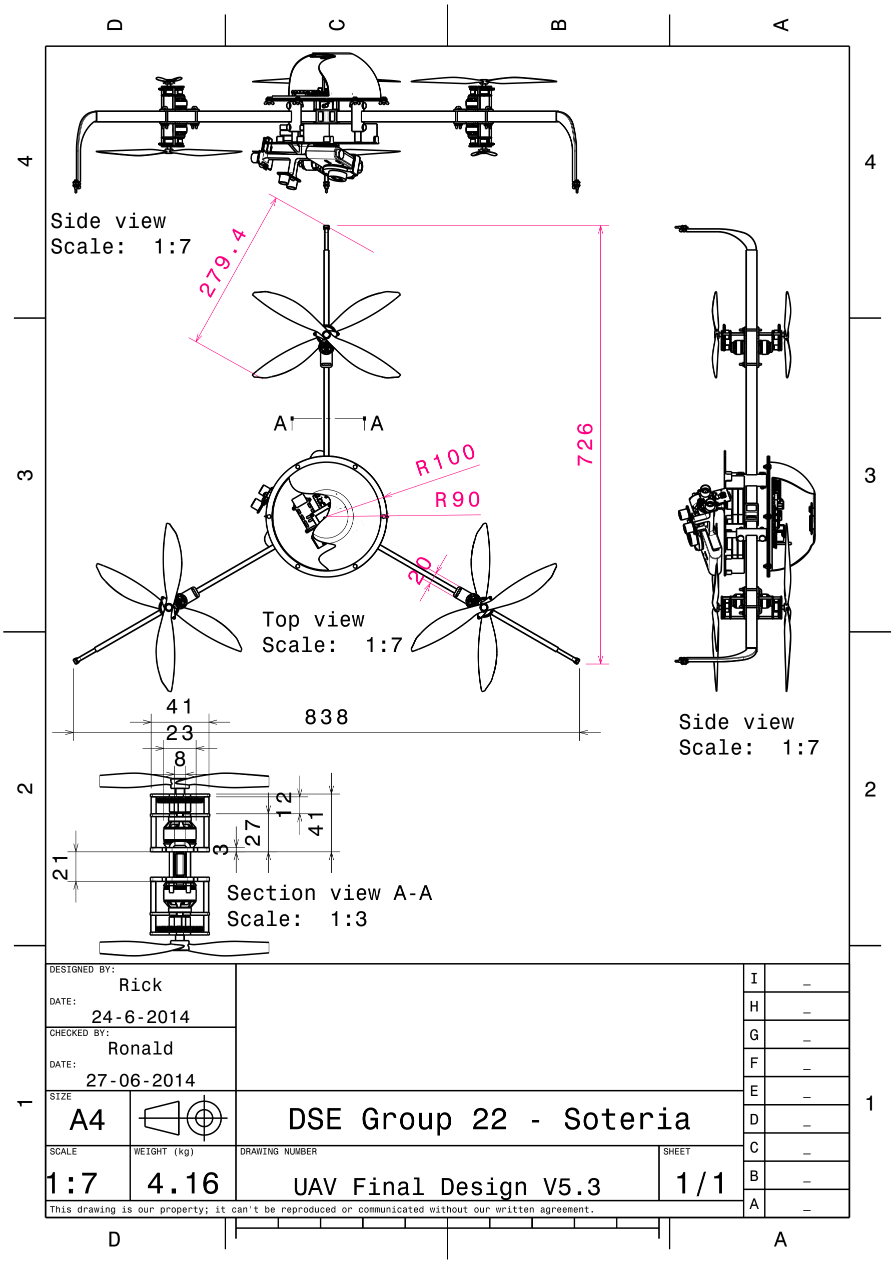

Figure A.1: Technical drawing of the UAV

B

Overview of Writers and Reviewers

This report has been written by 10 people. Figure B.1 shows which section of the report have been written by which team member. Also indicated is the person that has processed all the feedback that was given by other team members or tutors. Attention should be given to the fact that every team member has reviewed every section; the name put in the *Content Review* column is merely the person responsible for processing any comments. The text reviewer is responsible for removing any mistakes in grammar. The persons stated in blue rows are responsible for the overall content and text review of the corresponding chapter.

Section	Name	Writer	Content Review Processing	Text Review
	Summary	Stephen	Erik	Erik
	Changelog	Joris	Erik	Erik
	Preface	Joris	Erik	Erik
	List of Deliverables	AP	Erik	Erik
	List of Tables / List of Figures	-	Joris	Joris
	Glossaries	-	Erik	Joris
	List of Symbols	Stephen	Erik, Stephen	Erik
1	**Introduction**	**Erik**	**Erik**	**Luuk**
1.1	Desciption of the IMAV 2014 Competition	Erik	Erik	Luuk
1.2	Design Requirements	Erik	Erik	Luuk
1.3	Report Content	Erik	Erik	Luuk
2	**Project Management**	**Joris**	**Joris**	**Heiko**
2.1	Team Organisation	Rick	Joris	Heiko
2.2	Project Management Tool: Scrum	Rick	Joris	Heiko
2.3	Team Optimisation	Rick	Joris	Heiko
2.4	Resource Allocation	Joris	Joris	Heiko
2.5	Project Management Conclusion	Joris	Joris	Heiko
3	**Mission Design**	**AP**	**AP**	**Luuk**
3.1	Generating Mission Concepts	AP	AP	Luuk
3.2	Trade-off Between Mission Concepts	Heiko	AP	Luuk
3.3	Mission Strategy	Chris	AP	Luuk
3.4	Mission Design Conclusion	AP	AP	Luuk
4	**Payload Design**	**Stephen**	**Luuk**	**Aram**
4.1	On-board computer	Aram	Aram, Luuk	Aram
4.2	Object detection	Aram	Aram, Luuk	Aram
4.3	Navigation	Luuk	Luuk	Aram
4.4	Location	Luuk	Luuk	Aram
4.5	Number recognition	Heiko	Heiko	Aram
4.6	Data transmission	Rick	Rick	Aram
4.7	Map stitching	Rick	Rick	Aram
4.8	Blockade mapping	Heiko, Rick	Heiko	Aram
4.9	Attitude control	Rick	Heiko	Aram
4.10	Ground Station	Luuk	Luuk	Aram
4.11	Payload Design Conclusion	Rick, Stephen	Luuk	Aram
5	**Propulsion and Airframe Design**	**Joris**	**Ronald**	**Erik/Luuk**
5.1	Requirement Analysis	Ronald	Ronald	Erik
5.2	Flying Concept Selection	Ronald	Ronald	Erik
5.3	Design Process Description	Ronald	Ronald	Erik
5.4	Required Thrust to Weight Ratio	Ronald	Ronald	Erik
5.5	Propeller	Joris	Ronald	Luuk
5.6	Motor	Ronald	Ronald	Luuk
5.7	Electronic Speed Controller	Joris	Ronald	Luuk
5.8	Power Supply	Erik	Erik	Luuk
5.9	Airframe	AP	Ronald, AP	Erik
5.10	Propulsion and Airframe Design Conclusio	Ronald, Joris	Ronald	Luuk

Section	Name	Writer	Content Review Processing	Text Review
6	**System Interfacing**	**Erik**	**Joris**	**Stephen**
6.1	Configuration and Lay-out of Aerial Vehicles	Rick	Joris	Stephen
6.2	Mission Functions	Chris	Joris	Stephen
6.3	Communication and Data Handling	Rick	Joris	Stephen
6.4	Electrical Diagrams	Heiko+Aram	Joris	Stephen
6.5	System Failure Analysis	Aram	Joris	Stephen
6.6	Budget Breakdown	Joris	Joris	Stephen
6.7	Compliance Matrix & Feasibility Analysis	Ronald	Joris	Stephen
6.8	System Integration Conclusion	Erik	Joris	Stephen
7	**System Characteristics and Design Analysis**	**Stephen**	**Stephen**	**Aram, Stephen**
7.1	Performance Analysis	Stephen	Stephen	Aram
7.1.1	Performance Analysis Program	Stephen	Stephen	Aram
7.1.2	Verification and Validation of the Performance Analysis Program	Stephen	Stephen	Aram
7.1.3	Aerodynamics characteristics	Stephen	Stephen	Aram
7.1.4	Performance Characteristics	Stephen	Stephen	Aram
7.1.5	Stability and Control Characteristics	Stephen	Stephen	Aram, Stephen
7.2	Material and Structural Characteristics	AP+Chris	Stephen, AP	Stephen
7.3	Reliability Availibility Maintanability and Safety	Erik	Stephen, Erik	Stephen
7.4	Sustainability Considerations	Erik	Stephen, Erik	Stephen
7.5	Sensitivity Analysis	Erik	Stephen, Erik	Stephen
7.6	Market Analysis	Stephen	Stephen	Aram
7.7	System Characteristics and Design Analysis Conclusion	Stephen	Stephen	Aram
8	**Post Design Synthesis Exercise Design and Development**	**Joris**	**Aram**	**Aram**
8.1	Project Design and Development Logic	Aram	Aram	Aram
8.2	Production Plan	Chris	Aram	Aram
8.3	Future Test and Future Verification and Validation	Joris	Aram, Ronald, Heiko	Aram
8.4	Competition Logistics	Chris	Aram	Aram
8.5	Post Design Synthesis Exercise Time Scheduling	Aram	Aram	Aram
8.6	Post Design Synthesis Exercise Design and Development Conclusio	Joris	Aram	Aram
9	**Conclusion**	**Erik**	**Erik**	
	Bibliography	Joris	Heiko	Heiko
A	Technical Drawings	Rick		-
B	Overview of Writers and Reviewers	Luuk		

Figure B.1: Overview of writers and reviewers per section of the report